Faculty of Engineering and Science

Enhanced Synthesis and Delivery of
Magnesium Oxide Nanoparticles for
Reverse Insulin Resistance in Type 2 Diabetes Mellitus

Jaison Jeevanandam

This thesis is presented for the Degree of
Doctor of Philosophy
of
Curtin University

November 2017

DECLARATION

To the best of my knowledge and belief, this thesis contains no material previously published by any other person except where due acknowledgement has been made.

This thesis contains no material which has been accepted for the award of any other degree or diploma in any university.

Signature:

Jaison Jeevanandam
Date: 30-11-2017

ABSTRACT

Diabetes mellitus has emerged as a major threat to human health. The past two decades have seen a tremendous increase in the number of people diagnosed with diabetes worldwide. Significant changes in the human environment, behavior and lifestyle have led to an escalation in the number of patients diagnosed with diabetes. Clinical data show that about 90% of diagnosed diabetes cases worldwide relate to type 2 diabetes. Type 2 diabetes is caused by the inability of the human pancreas to produce sufficient insulin, or insulin resistance resulting from a blockage or malfunction of insulin receptors. Conventional type 2 diabetic treatments are based on the administration of insulin supplements. However, such supplements may lead to hypoglycemia, weight gain and associated ailments. Hence the search for effective treatments for type 2 diabetes has become a major research endeavor.

Magnesium is an essential trace element in the human body and its deficiency has proven to increase insulin resistance in diabetic patients. Administration of magnesium sulphate is the conventional approach to address insulin resistance. However, high concentrations of $MgSO_4$ can lead to hypermagnesaemia and other side effects. The current study focuses on the development of a new and improved magnesium based formulation as a potential drug to reverse insulin resistance in adipose cells. The development of magnesium oxide nanoparticles through chemical and green synthesis was conducted to generate different morphologies and sizes of MgO nanoparticles. Sol-gel method was used for the chemical synthesis approach and plant extract based nanoparticle formation method used for green synthesis. The results showed that the chemical synthesis generated MgO nanoparticles with 30-80 nm size and different morphologies while the green synthesis generated MgO nanoparticles with size ranging from 15-25nm. The physicochemical characteristics of the nanoparticles were studied using UV-Visible spectrometer, Dynamic Light scattering technique, Thermogravimetry, X-ray diffraction, Fourier Transform Infrared spectroscopy and Transmission electron microscope. The chemically synthesized MgO nanoparticles yielded spherical, hexagonal and rod-like morphologies whereas green synthesized MgO nanoparticles

mostly yielded spherical shaped nanoparticle with various sizes. MgO nanoparticles generated from *Amaranthus tricolor* leaf extract resulted in mixed morphologies including spherical and hexagonal shapes with pH being an influential factor in driving morphological transformations.

Six MgO nanoparticles uniquely selected from the chemical and green synthesis approaches were analyzed for cytotoxicity using 3T3-L1 (diabetic) and VERO (non-diabetic) cell lines via MTT assay. The results showed that hexagonal MgO nanoparticles were less toxic towards diabetic cell lines. Comparative cytotoxicity analysis between diabetic and non-diabetic cells shows that at 600 μl/ml dosage of hexagonal chemically synthesized nanoparticles and 400 μl/ml dosage of hexagonal green synthesized nanoparticle, both were less toxic. Thus, they were used for insulin resistant reversal studies. Glucose assay showed that the nanoparticles reversed ~35% of insulin resistance compared to control cells, with time dependent analysis showing stability after 24 h. GLUT4 protein was identified by western blot to validate insulin resistance reversal. Fluorescent microscopy was used to investigate cellular interactions with the nanoparticles in order probe the mechanism of insulin resistance reversal ability of MgO nanoparticles. Overall, the present work successfully generated unique transformational morphologies of MgO nanoparticles with promising biophysical and performance indicators for insulin resistance reversal based on the foundational work covered in this thesis. However, more work involving further *in vivo* testing is essential to fully validate efficacy.

ACKNOWLEGMENT

This work would never have been completed without the support of several people for which I will always be deeply grateful for all the help they gave me through the course of my PhD studies.

First of all, I would like to thank my supervisors for their guidance and valuable advice throughout the course of my studies. I would like to give my sincere acknowledgement to my thesis committee, especially to Dr. Stephanie Chan Yen San for giving me the opportunity to work under her guidance and for her support in shaping up my article writing skills, data analysis and thesis. I am grateful towards her endless guidance, advice and motivation throughout my PhD candidature. Most importantly, I have learned so much, in both technical knowledge and philosophy, from her that I consider priceless throughout this journey.

Secondly, I would like to thank, Prof. Michael Danquah who continue to provide valuable supports and inspiration throughout my PhD candidature. I am especially grateful to his continuous supervision and help in preparing manuscripts for journal publications. Also, I would like to extend my gratitude to Prof. Marcus Lee and Prof. Clem Kuek, Dean of Research and Development, Curtin University, Malaysia, my thesis chairperson Associate Professor Dr. Chua Han Bing and my associate supervisors, Dr. Venkata Srikanth Meka from International Medical University, Kuala Lumpur and Dr. Clarence M. Ongkudon from University Malaysia Sabah, for their useful advice and assistance that have critically improved the quality of my work. I would like to extend my thanks to Dr. Santhanalakshmi, and all the staffs of Life Teck Research Centre, Chennai, India for their kind help for performing cell line studies in their lab.

Next, I would like to thank all my HDR friends, lab manager and lab technicians for their supports and encouragements throughout my PhD candidature. This journey will not be such delightful without them. I gratefully acknowledge the financial support by Curtin Malaysia Postgraduate Research Scholarship (CMPRS) from Curtin Malaysia Graduate

School. Last but not least, I would like to thank my parents, relatives and friends for their endless support and encouragement during my study. Thank you all!

Jaison Jeevanandam

Publications from this thesis

Journal publications included as Chapters

Jeevanandam, Jaison, Michael K Danquah, Sujan Debnath, Venkata S Meka, and Yen S Chan. (2015). "Opportunities for nano-formulations in type 2 diabetes mellitus treatments." *Current pharmaceutical biotechnology* 16 (10):853-870. DOI - https://doi.org/10.2174/1389201016666150727120618 (Part of Chapter 1 and 2)

Jeevanandam, Jaison, Yen San Chan, and Michael K Danquah. (2016). "Biosynthesis of metal and metal oxide nanoparticles." *ChemBioEng Reviews* 3 (2):55-67. DOI - https://doi.org/10.1002/cben.201500018 (Part of Chapter 2)

Jeevanandam, Jaison, Yen San Chan, and Michael Kobina Danquah. (2017). "Biosynthesis and characterization of MgO nanoparticles from plant extracts via induced molecular nucleation." *New Journal of Chemistry* 41:2800-2814. DOI - https://doi.org/10.1039/C6NJ03176E. Reproduced by permission of the Royal Society of Chemistry. (Part of Chapter 3 and 4)

Jeevanandam, Jaison, Yen San Chan, and Michael Kobina Danquah. (2017). "Calcination dependent morphology transformation of sol-gel synthesized MgO nanoparticles." *Chemistry select* 2 (32): 10393 - 10404. DOI - https://doi.org/10.1002/slct.201701911 (Chapter 3 and 4).

Jeevanandam, Jaison, Yen San Chan, and Michael Kobina Danquah. (2017). "Effect of gelling agent and calcination temperature in sol-gel synthesized MgO nanoparticles." *Bulletin of Korean Chemical Society*. Submitted. (Chapter 3 and 4).

Jeevanandam, Jaison, Yen San Chan, and Michael Kobina Danquah. (2017). "Effect of pH variations in morphology transformation of biosynthesized MgO nanoparticles." *Journal of Biological Inorganic Chemistry*. Submitted. (Chapter 4).

Jeevanandam, Jaison, Yen San Chan, and Michael Kobina Danquah. (….). "Cytotoxic analysis of morphologically different sol-gel synthesized MgO nanoparticles and their insulin resistance reversal ability in adipose cells." To be submitted. (Chapter 3 and 5)

Jeevanandam, Jaison, Yen San Chan, and Michael Kobina Danquah. (….). "Cytotoxic analysis of biosynthesized MgO nanoparticles and their insulin resistance reversal ability in adipose cells." To be submitted. (Chapter 3 and 5)

Table of contents

List of Figures

List of Tables

Abbreviations

Magnesium oxide	MgO
Dynamic light scattering	DLS
Thermo gravimetric – differential scanning calorimetry	TG-DSC
X-ray diffraction	XRD
Fourier transform – infrared spectroscopy	FTIR
Transmission electron microscopy	TEM
3, 5 – dinitrosalicylic acid	DNS
Glucose transporter 4	GLUT4
Up-converted persistent luminescence	UCPL
Continuous subcutaneous insulin infusion	CSII
Daily multiple injections	MDI
Zinc oxide	ZnO
Titanium oxide	TiO_2
Daunorubicin	DNR
Photodynamic therapy	PDT
Isoelectric point (pI)	IEP
Bovine serum albumin	BSA
Rabbit – immunoglubin antibodies	r-IgGs
Deoxyribonucleic acid	DNA
Ultraviolet	UV
Adenosine triphosphate	ATP
Nuclear magnetic resonance	NMR
3-[4, 5-dimethylthiazol-2-yl]-2, 5 diphenyl tetrazolium bromide	MTT
Polydispersity index	PDI
Fetal bovine serum	FBS
Dulbecco's modified eagle medium	DMEM
Ethylenediaminetetraacetic acid	EDTA
Phosphate buffered saline	PBS
Dimethyl sulfoxide	DMSO

Half maximal inhibitory concentration	IC_{50}
Sodium dodecyl sulfate	SDS
Sodium chloride	NaCl
Hydrochloric acid	HCl
Polyvinylidene difluoride	PVDF
Semi-denaturating detergent – Polyacrylamide gel electrophoresis	SDD-PAGE
Joint committee on powder diffraction standards	JCPDS
Crystallography open database	COD

CHAPTER 1

INTRODUCTION

1.1. Background

Diabetes mellitus has developed into a major menace for human health in the 21st century (Zimmet, 2000). A tremendous rise in the number of people diagnosed with diabetes worldwide has been observed (Amos et al., 1997; King et al., 1998; WHO, 2016). The International Diabetes Federation (IDF) has estimated that 366 million people were diagnosed with diabetes in the year 2011, and the figure is predicted to increase to 552 million by 2030 (Petrak et al., 2013). IDF recently reported that there were 415 million people with diabetes in 2015, representing an escalation in the number of diabetes cases in the global community. The report also alerts that diabetes caused 5 million deaths in 2015 at a rate of one person per every six seconds (Atlas, 2015). World Health Organization (WHO) has projected that diabetes would be the seventh fatal disease in humans by 2030 (Mathers et al., 2006). Diabetes mellitus is generally known to be a syndrome of anarchic metabolism relating to high level of glucose in the blood (hyperglycemia) (Tierney, 2002). Diabetes can be categorized into type 1 (destruction of insulin producing β-cells that leads to autoimmune diabetes) and type 2 (β-cell dysfunction which results in reduced response to insulin) as shown in Figure 1.1. Alzheimer's disease and gestational diabetes are sometimes termed as type 3 diabetes (Abdullah et al., 2014; Buchanan et al., 2005), and both are different from type 1 and 2 diabetes. There is no insulin production in the body of type 1 diabetes patient, thus, daily insulin injections are required. Type 1 diabetes cases represent one in six hundred children across the world. Hence, it is usually diagnosed during childhood (Stang et al., 2005). Type 2 diabetes results from insufficient insulin production by the pancreas or physiological mechanisms resulting in insulin resistance through the blockage or malfunction of insulin receptors (Rosenbloom et al., 1999). Both types of diabetes are responsible for hyperglycemia, compensatory thirst, excessive production of urine, mysterious weight loss, distorted vision, increased fluid intake, variations in energy

metabolism and lethargy (Lin et al., 2010). However, type 2 diabetes relates to the malfunction of a more complex metabolic condition that leads to an upsurge in blood glucose levels, resulting from impairments in the secretion and activity of insulin (Das et al., 2006). WHO reported that type 2 diabetes is the most common among diabetic patients, and obesity, smoking and unhealthy lifestyle contribute to the epidemicity of diabetes (Surugue, 2016). Diminished secretion of insulin, impairment in the action of insulin and increased production of hepatic glucose are the three crucial blemishes in the onset of hyperglycemia in type 2 diabetes (DeFronzo, 1992; DeFronzo, 1999; Stumvoll et al., 2005).
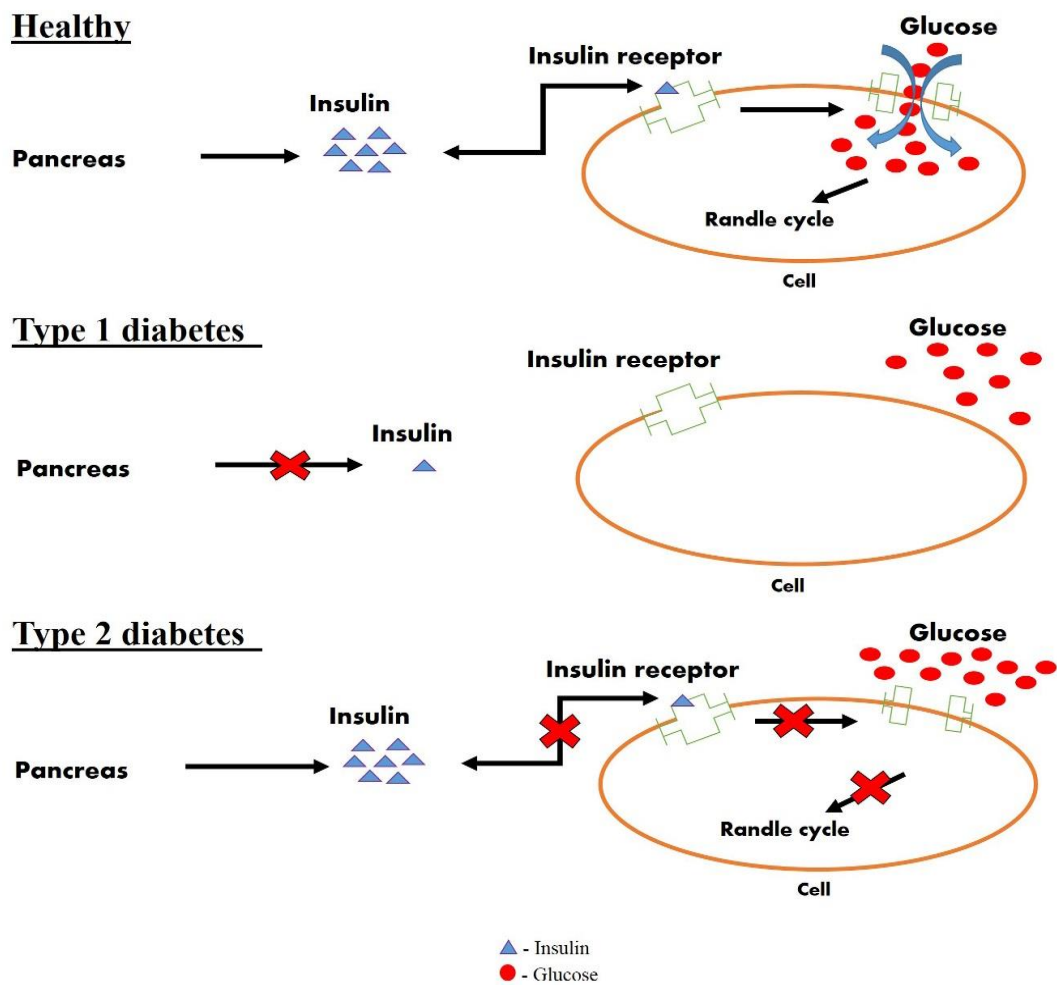
Figure 1.1: Insulin secretion and activity pathways of healthy, type 1 and 2 diabetes patients (Jeevanandam et al. 2015). Reproduced with permission of Bentham Science Publishers Ltd.

Diabetes and its associated relationship with obesity has become a major concern to public health as these can be life-threatening, result in co-morbidity, and put huge economic burdens on societies. WHO defines obesity as a condition where the Body Mass Index (BMI) is equivalent or higher than 30 Kg/m^2. Type 2 diabetes and obesity are strongly associated based on several research reports (Fagot-Campagna et al., 1998; Fu et al., 2017). Obesity is considered the threatening aspect for type 2 diabetes, and in many cases, acts as a precursor for type 2 diabetes followed by resistance to insulin (Mitropoulos et al., 1992; Frayn, 1996; Hussain, 2010). The pervasiveness of obesity and overweight (BMI in the range of 25 and 30 kg/m^2) has become a major concern (Yaturu, 2011). The comparative risk of type 2 diabetes rises as BMI escalates above 23 (Colditz et al., 1990; Ollila et al., 2016). In a study conducted with adults aged between 18 to 74 years, it was reported high that BMI and waist circumference can independently lead to type 2 diabetes (Qiao et al., 2010). The key link between type 2 diabetes and obesity is insulin resistance. Resistance to insulin in diabetes is demonstrated by reduced stimulation of glucose transporters, diminished adipocyte, skeletal muscle metabolism, and hepatic suppression of glucose output (Reaven, 1995; Yaturu, 2011). Initial deposition of triglycerides in obesity arises in the adipose tissue present in the subcutaneous region and this intensifies insulin resistance above auxiliary lipid accumulation limit in the subcutaneous region. Triglycerides are then dissuaded to the depot of visceral fat, leading to visceral obesity (Ali et al., 2011). A large number of research have established the relationship between insulin resistance, fat accumulation and type 2 diabetes in intra-abdomen (visceral obesity) (Frayn, 2000; Merino-Ibarra et al., 2005; Hayashi et al., 2008; Shi et al., 2017). Thus, type 2 diabetic patients face premature deaths as they are prone to numerous forms of long and short term complications (Azevedo et al., 2008; Rossi et al., 2017).

1.1.1. Treatment of type 2 diabetes mellitus

The three main abnormalities involved in type 2 diabetes, which are extreme production of hepatic glucose, reduced secretion of pancreatic insulin, and marginal insulin action resistance, occur mainly in the muscle and liver tissues (DeFronzo, 1992). In early stages, type 2 diabetic patients compensate increased resistance to insulin at the tissue level by amplifying the secretion of pancreatic beta-cell insulin (Weyer et al., 1999). Reduced

insulin secretion is the predominant weakness in lean and thin type 2 diabetic patients, hence resistance to insulin is less severe than in obese patients. Instead, hyper-insulinemia and insulin resistance are the conventional anomalies of type 2 diabetic patients suffering from obesity (Caro, 1991). Extreme secretion of insulin is often observed more with type 2 diabetic patients than non-diabetic patients, but it is still inadequate to overcome insulin resistance (Hales et al., 2013). This results in significant complications in insulin therapy for type 2 diabetes treatment (Genuth, 1990; Davis et al., 2004). DeFranzo (1999) suggested a treatment strategy for type 2 diabetes based on the natural diabetes history of the patient. The strategy of treatment is as follows.

- Initiation of a pharmacological therapy with metformin or insulin oral agents.
- Adequate glycemic control (under 9 mmol/L, 2 hours after meals) achieved by increasing the oral agent or insulin dosage.
- Administration of a drug with glucose-lowering potency as a monotherapeutic agent to achieve the desired glycemic control level for diabetic patients treated with oral agents.
- Administration of a secondary oral agent at rapid dose levels to control glycemic concentrations for diabetic patients with improper glycemic control under an individual oral agent.
- Administration of additional bedtime insulin doses to switch to a third oral agent, or splitting insulin regimen and mixed combination especially for diabetic patients with unsuccessful glucose control using combined oral agent therapy (DeFronzo, 1999).

Numerous studies have revealed that intensive insulin therapy can efficiently control glucose levels in patients with type 2 diabetes (Abraira et al., 1995; Henry et al., 1993; DeFronzo, 1999; Association, 2016). The most conventional and universal insulin regimen is a single dose of 80 U/d (Harris, 1996; DeFronzo, 1999). Since most type 2 diabetes patients require a dosage of 80 to 100 U/d insulin, a multiple dosage in split regimen is applied (Abraira et al., 1995; Henry et al., 1993; DeFronzo, 1999). Hence, the reason why blood glucose levels in most type 2 diabetic patients are inadequately controlled (Hayward et al., 1997; DeFronzo, 1999). Other insulin therapies include insulin pump therapy (Raskin et al., 2003) and insulin pen therapy (D'Eliseo et al., 2000).

Diabetes therapies relying on insulin pumps for treatment have been in practice for ~25 years and continues to be favorite amongst type 2 diabetes patients due to its flexibility and precise insulin delivery (Raskin et al., 2003). The recently available commercial Paradigm Veo continuous glucose monitoring insulin pump system manufactured by Medtronic Diabetes, USA, is equipped with the function of low glucose suspension. This modification halts insulin delivery when hypoglycemia is noted (Ly et al., 2013; Abdullah et al., 2014). Severe hypoglycemia with wide fluctuations of glucose levels are the main drawbacks of insulin pumps in diabetic patients (Jennings et al., 1991; Saudek et al., 1996; DeWitt et al., 2003).

Insulin pen therapy has been available for over 20 years. It is convenient, more accurate in dosage administration, and well adapted for visually impaired patients (D'Eliseo et al., 2000). Recently, advanced insulin pens with memory functions have been designed to program insulin dosage delivery depending on the insulin history of the patient (Venekamp et al., 2006). The memory functions in insulin pens enhance blood glucose normalization and reduce insulin overdose in diabetic patients (Guo et al., 2017). However, these types of insulin pen therapies cannot be used as insulin supplements for pre-meal hyperglycemia, as they possess premixed insulin with limited capacity to provide prolong insulin action (Hirsch, 2005). Other than insulin pen and insulin pump, U-500 insulin, an injectable liquid form of insulin is also used in treating minority of diabetic patients. U-500 insulin is quite uncommon in type 2 diabetes treatment as it contains a higher insulin dosage (500 U/mL); 5 fold highly concentrated than U-100 insulin. It is used for the treatment of severe insulin resistance patient to achieve required glycemic levels (Cochran et al., 2008). U-500 are currently available in insulin pen formulations to reduce insulin concentrations in the blood steam after medication. U-500 administration has been reported to cause insulin stacking and increased hypoglycemia risk (Olin et al., 2017).

1.1.2. Role of magnesium in glucose metabolism and diabetes

Magnesium controls glucose metabolism in cells, the coupling of stimulus-contraction secretion, transduction of peptide hormone receptor signal, and translocation of ion

channel directly at the biochemical level (Barbagallo et al., 2003). Magnesium is important in the formation of activated MgATP complex to regulate the enzymes that limit the rate of glycolysis cycle (Heaton, 1990). MgATP complexes also regulate the activity of the enzyme kinase, which is associated with phosphate transfer of CaATPases in the plasma membrane ATP and endoplasmic reticulum (Barbagallo et al., 1996; Paolisso et al., 1997). A major decrease in the activities of these enzymes are observed with low magnesium levels (<0.75 mmol/L) in diabetic and hypertensive patients (Laughlin et al., 1996; Gibson, 2005). Insulin resistance in fat tissues and skeletal muscles are found to be due to the suppression of cellular magnesium concentration (Barbagallo et al., 2003). Studies have revealed that supplementing magnesium daily for elderly diabetic patients helps in improving insulin response and glucose uptake (Paolisso et al., 1992). A recent study investigated and identified that magnesium supplement improves metabolic profile in obese and pre-diabetic patients with chronic kidney disease (Toprak et al., 2017). It has also been reported that magnesium participates directly in human glucose metabolism disorders and provides validation for insulin resistance control through effective magnesium supplementation (Morais et al., 2017). Morais et al., 2017 further discussed the benefits of magnesium supplement in patients with hypomagnesaemia mediated insulin resistance and revealed that magnesium possess the ability to improve insulin sensitivity. The promising therapeutic effects of magnesium supplements present a unique opportunity to formulate and deliver different magnesium based supplements with enhanced biological properties to reverse insulin resistance and improve cellular glucose metabolism.

1.1.3. Nanoparticles and Nanomedicine

Nanoparticles have dimensions of less than 100 nm, and have attracted significant attention due to their exclusive advantages and functionalities over their bulk counterparts. There are a large number of physical, chemical, biological, and hybrid methods that are available for synthesizing different types of nanoparticles such as nanorods, nanotubes, and nanoflowers (Rahaman et al., 2017; Ozkan et al., 2017; Mourdikoudis et al., 2016; Oluwafemi et al., 2016). Nanoparticles are finding importance in biomedical and pharmaceutical applications due to their amenability to biological

functionalization, enhanced permeability and retention effects (Parak et al., 2003; Ravishankar Rai et al., 2011). For example, nanoparticles of PLGA, which is a copolymer formed by poly (lactic acid) (PLA) and poly (glycolic acid) (PGA) (Bala et al., 2004), lipid (Maia et al., 2000) and gold (Dreaden et al., 2012) have been investigated extensively and reported to have excellent drug carrier and drug delivery performance. It has also been reported that size/shape, solubility, and targeting potential are the three main criteria important for bio-application of nanoparticles (Chan et al., 2011). Conventional drugs have limitations of antagonistic effects such as non-specific action and low efficiency due to ineffective or inappropriate dosages (Jeevanandam et al., 2016c). Nanoscience and nanotechnology offer the opportunity for new drug designs with superior cell specificity and interactive drug release dynamics to act precisely on desired targets (Sheikhpour et al., 2017). This permits the administration of reduced but effective doses with minimal hostile effects. Nanotechnology and nanocarriers (Langer et al., 2004; Nishiyama, 2007; Peer et al., 2007) can function to increase drug solubility, optimize drug formulations and alter pharmacokinetics in order to prolong bioavailability and drug release ability (Freitas, 2005b; S Rahiman, 2012a; IS, 2008).

Nanomaterials of different structures and functionalities are being manufactured for medical applications (Chan, 2017). These include nanoparticles, nanocapsules, nanofilms, nanotubes, nanocarriers (Moghimi et al., 2005) and complex nano molecules such as fullerenes (Rašović, 2017). Nanomedicine can relate to (a) nano-analytical devices for measuring small concentrations of analytes or detection of defects (Lin et al., 2017), (b) therapy using artificial bio nano-materials such as artificial nanopancreas (Hwang et al., 2016), and (c) nano-formulations for effective drug delivery including multidrug carriers (Torchilin, 2012), smart drugs and nanorobots that propel independently around the body as a replacement for red blood cells, immune system, and many other biological systems (Report, 2013; Woldu et al., 2014). Over the next 5-10 years, biotechnology would advance in molecular medicine to enable the development of engineered organisms or biobotics-microbiological systems. Modern nanorobots and molecular machine systems may be incorporated in medical armamentarium to serve as the most potent tool for physicians to combat human diseases (Freitas, 2005a). The emergence of nano-formulation of biopharmaceutical ingredients and the promising applications in the

development of smart drugs has driven research interests into the creation of new and improved nanomedicines to address a wide range of disease conditions. Hence the objective of the present work focuses on the synthesis and characterization of MgO nanoparticles as a potential nanomedicine formulation to reverse insulin resistance characteristics in diabetic cell models.

MgO nanoparticles can possess biological functionalities including antibacterial activity, bone regeneration, and heartburn treatment (Bertinetti et al., 2009a). (Martinez-Boubeta et al., 2010) and (Chalkidou et al., 2011) have demonstrated the potential of MgO nanoparticles in breast cancer treatment. Recent studies by (Di et al., 2012) described the superior functionality of MgO nanoparticles in nano-cryosurgery for tumor treatment. MgO nanoparticles demonstrate higher mammalian bioactivity and lower toxicity than most metal oxides (Krishnamoorthy et al., 2012), hence, it can be a potential ingredient in drug formulation. According to section 184.1431 in Food and Drug Administration (FDA), magnesium oxide is listed under food for human consumption and as a direct food substance generally recognized as safe. Also, FDA approved MgO supplements such as Mag-200, MagGel, Mag-Ox 400 and Uro-Mag, and are available on the market (Karosanidze, 2014). However, most MgO based formulation are in clinical trials for use in drug formulation to treat several diseases (Chow et al., 2010; Quaresma et al., 2017). It has been established in a recent study that acute administration of MgO nanoparticles prevents convulsion in diabetic male mice (Jahangiri et al., 2014a). It is hypothesized that the high bioactivity and surface-to-volume ratio of MgO nanoparticles (Rahiman et al., 2012b) would facilitate improved molecular interaction and entry into cells in order to activate enzymes such as AMPK (5' adenosine monophosphate-activated protein kinase) and reverse insulin resistance in diabetic patients.

1.2. Problem statement

Insulin therapy is the most common therapy for type 2 diabetes, providing an insulin supplement essential to overcome resistance to insulin. Severe cases of hypoglycemia and unexpected weight gain have been reported to be the result of insulin therapy (Sanne G. Swinnen, 2009). Reasons including difficulties in the control of glycemic levels, insulin therapy intervals, and prior hypoglycemic history contributes towards hypoglycemic

conditions (Cryer, 1994). Total urine triglyceride formation (Law et al., 2017), homozygous phosphoenolpyruvate carboxykinase 1 (PCK 1) mutation (Vieira et al., 2017) and intake of drugs such as Ginseng (Carella et al., 2017) have been reported to be closely linked to hypoglycemia. Intensive glucose-lowering therapies are administered to type 2 diabetic patients to reduce the risk of cardiovascular diseases. It has been reported that intensive glucose-lowering therapy can lead to escalations in hypoglycemia levels (Elam et al., 2017; SBU, 2009). Although insulin therapy has been successful in lowering the concentration of blood glucose to normalcy, exogenous insulin in large doses are required to achieve it. For type 2 diabetic patients, these elevated dosages result in weight gain and hyperinsulinemia. Several studies have confirmed that exogenous insulin based diabetes treatment leads to 3-9% increase in the average body weight (Mudaliar et al., 2001). The observed weight gain associated with insulin therapy has been conventionally elucidated when glycemic control is improved by decreasing glucosuria and resting energy expenditure (Nathan et al., 2009; Yki-Jarvinen, 2001). A previous study reported 1.8 kg increase in the weight of type 2 diabetic patients under insulin therapy over six months period. This was not attributed to resting energy expenditure, change in glucosuria or physical activity but rather the insulin therapy agents (Ryan et al., 2008). In a recent study, 412 individuals with type 2 diabetes were treated with metformin insulin therapy for 18 months and the results showed a 2.4 kg median weight gain increase (Cichosz et al., 2017). This demonstrates one of the several possible side effects of insulin therapy agents. The drawbacks associated with current insulin therapies for type 2 diabetes have triggered interests in the development of new and improved curative and preventive technologies.

Magnesium deficiency is a common problem found in insulin and non-insulin dependent diabetes. Magnesium reduction associated with intracellular resistance to insulin conditions has been ascribed to decreasing cellular entry of Mg ions through simulation of insulin (Huerta et al., 2005; Devaux et al., 2016; Sales et al., 2014). Conversely, association of ketoacidosis mediated insulin resistance leads to hypomagnesaemia. Thus, low magnesium level and hypomagnesaemia in the intracellular region can be attributed to insulin resistance (Nadler et al., 1993). It has been reported that the administration of magnesium sulfate (MgSO$_4$) supplements successfully reversed insulin resistance, though

high concentrations resulted in hypermagnesaemia (Kandeel et al., 1996). In order to overcome this issue, nano-formulations of magnesium supplements exhibiting high surface to volume ratio is proposed. It has been proven that MgO nanoparticles are less toxic with high biocompatibility and bioavailability towards various human cells (Krishnamoorthy et al., 2012; Mangalampalli et al., 2017; Mahmoud et al., 2016). Moreover, MgO is more stable compared to other magnesium oxide metastable compounds such as MgO_4 and Mg_3O_2 (Wang et al., 1992; Zhu et al., 2013). This strongly positions MgO nanoparticles as useful magnesium based supplements in terms of molecular stability under various storage conditions. However, to date, there is limited research into the applications of MgO nanoparticles in diabetes treatment.

1.3. Research gap

Insulin is widely used to manage type 2 diabetes. A number of conventional therapies increase insulin production to reduce glucose uptake in insulin resistant cells. The number of reported therapies relying on the use of nutrient supplements to reverse insulin resistance is limited. Magnesium has been identified as an important nutrient in reversing insulin resistance. Previous research reports indicate that chemically synthesized magnesium supplements such as magnesium sulphate are capable of reversing insulin resistance (Kandeel et al., 1996; Fleming et al., 1999; Martins, 2016). However, they can be toxic to human cells and their efficacy in reversing insulin resistance requires improvement. In 1989, it was demonstrated that dietary magnesium supplements improve beta cell response to glucose and arginine in elderly non-insulin dependent diabetic patients (Paolisso et al., 1989). Since then, several reported findings have also revealed that oral magnesium supplements improve glycemic control, insulin sensitivity and metabolic control in type 2 diabetic subjects (Song et al., 2006; Rodríguez-Morán et al., 2003; Naik et al., 2017). Most of these research reports used high concentrations (more than 3-5 g/day) of magnesium supplements including magnesium pidolate, magnesium chloride and magnesium citrate (Eibl et al., 1995). Also, magnesium oxide (41.4 mmol/day) was used as a magnesium supplement to increase insulin sensitivity in diabetic patients (Maria et al., 1998). The major drawback associated with these regimens is the extended time required (almost a month) for pharmacokinetic impact and the high concentrations needed to establish insulin sensitivity, glycemic and metabolic control.

Thus, the present work aims at the utilization of MgO nanoparticles with engineered biophysical characteristics, including enhanced surface to volume ratio, biocompatibility and bioavailability, to reduce the concentration and time required to reverse insulin resistance in mammalian cells. Several chemical and physical methods are available for MgO nanoparticles synthesis with most of them applying high temperatures and/or toxic chemicals for the nanoparticle formation. Thus, sol-gel synthesis method which uses less toxic chemicals and yields highly stable MgO nanopowders has been successfully demonstrated (Kumar et al., 2008; Mastuli et al., 2012). The morphology of MgO nanoparticles has been reported to influence its bioactivity for insulin resistance reversal (Albanese et al., 2012; Agarwal et al., 2013). For example, it has been demonstrated that hexagonal shaped nanoparticles possess enhanced cellular activity (Kittitheeranun et al., 2015) and insulin resistance reversal ability. Understanding the relationship between sol-gel synthesis conditions of MgO nanoparticles and the physicochemical features of nanoparticles is critical to engineer and introduce specific features and functionalities to the nanoparticles. Calcination temperature mediated morphological transformation of MgO nanoparticles represents a significant opportunity to create unique architectures of MgO nanoparticles with specific functional capacities, and this is not well exploited in the literature. Whilst sol-gel synthesized MgO nanoparticles possess high stability and their cellular activity can be enhanced through morphological transformation, the cytotoxicity of the nanoparticle formulation may increase due to the use of toxic chemicals in the sol-gel synthesis process. This creates an opportunity to implement green synthesis technologies using aqueous plant leaf extract to generate less toxic MgO nanoparticles. To date, there is no previously reported work on the synthesis of MgO nanoparticles using aqueous plant leaf extract. The present project focuses on the synthesis of MgO nanoparticles generated from plant leaf extract with further investigations into morphological transformations through variations in synthesis process conditions.

1.4. Research questions

The following research questions are developed based on intended novel contributions and existing research gaps in the literature in order to drive the specific objectives of this project. These are critical research questions necessary to establish the scientific and theoretical basis for successful development and formulation of pharmaceutical-grade

MgO nanoparticles supplements at desired dosages for enhanced insulin resistance reversal potential in type 2 diabetes.

➢ What is the level of efficacy of MgO nanoparticles as a potential nutrient supplement for reversing insulin resistance in type 2 diabetes? How does morphological and size transformations of MgO nanoparticles affect insulin resistance reversal ability?

➢ What process strategies are important to trigger different morphological transformations of MgO nanoparticles during sol-gel synthesis?

➢ What is the potential of synthesizing MgO nanoparticles using plant leaf extracts with high flavonoid to address cytotoxicity issues associated with sol-gel synthesis method?

➢ What process parameters are critical to trigger morphological and size transformations during green synthesis of MgO nanoparticles using plant leaf extract? How specific is MgO nanoparticles in terms of cytotoxicity towards diabetic cells and impacts on normal cells?

1.5. Objectives

The specific objectives of this project are formulated based on identified research gaps and questions.

➢ To develop optimized processes for the preparation of MgO nanoparticles through chemical and green synthesis approaches.

➢ To determine key process variables driving morphological and size transformation in MgO nanoparticles synthesis using chemical and green synthesis approaches.

➢ To determine the relationship between type and dosage of MgO nanoparticles and cytotoxicity in normal and 3T3-L1 adipocytes diabetic cell lines.

➢ To investigate the efficacy of insulin resistance reversal of MgO nanoparticles in adipose cell lines.

1.6. Scope of the work

The scope of this project relates to the preparation of a novel MgO nanomedicine to reverse insulin resistance in type 2 diabetes. It is hypothesized that MgO nanoparticles

can be molecularly engineered to offer desirable biophysical characteristics for effective insulin resistance reversal. Moreover, MgO nanoparticles are comparatively less toxic than other metal oxides. Two synthesis routes, chemical and bio-based green synthesis approaches, are used for the preparation of MgO nanoparticles. Sol-gel technique is used for chemical synthesis whereas plant leaf extract mediated green synthesis is used for the bio-based approach. Two different magnesium precursors along with three gelling agents and various calcination temperatures are used in sol-gel synthesis to investigate their impacts on morphological and size transformation. Three different plant sources with high leaf extract flavonoid contents are used for the green synthesis approach, and the synthesis parameters necessary to achieve desirable biophysical characteristics of MgO nanoparticles are determined. Various material characterization techniques, including Dynamic Light Scattering (DLS), Thermogravimetric analysis, UV-Visible spectroscopy, X-Ray diffraction (XRD), Fourier Transform – Infrared (FTIR) spectroscopy and Transmission electron microscope (TEM), are used to determine the physicochemical characteristics of MgO nanoparticles.

MgO nanoparticles with various shapes and sizes generated from the two synthesis approaches were subjected to cytotoxic analysis to investigate dose requirements on the viability of both diabetic and non-diabetic cells. The cytotoxic analysis is conducted using 3T3-L1 (diabetic) and VERO (non-diabetic) cells. MgO nanoparticles with low cytotoxicity are investigated for their insulin resistant reversal capability. Colorimetric glucose assay using 3, 5 – dinitrosalicylic acid (DNS assay) is used to determine the amount of glucose after incubating the drug for 24 h in the diabetic cell. DNS analysis at regular time intervals is carried out to establish the kinetics of time dependent glucose conversion in both the control and cells incubated with MgO nanoparticles. Reversal of insulin resistance results in the expression of GLUT4 protein, and this was analyzed by western blot. Finally, fluorescent microscopy is used to probe the mechanism of MgO nanoparticles to reverse insulin resistance in diabetic cells.

1.7. Significance of the study

The statistics provided by WHO in 2016 revealed an alarming estimation that one in eleven of global adult population is suffering from diabetes. Generally, diabetes inhibits

the pathway of energy formation mechanism required for the cells to perform their regular activities, and this could subsequently leads to critical complications such as cardiovascular diseases, neuropathy, nephropathy, retinopathy and Alzheimer. Hence, effective diabetes treatments would eventually help prevent these disease complications. According to American Diabetes Association, the total estimated cost involved in treating diabetes in the US is $245 billion as of 2012, and this number is expected to increase due to the increasing numbers of diabetes cases and cost of diabetes drugs. It can be appreciated that a significant amount of economic resources is spent on treating diabetes. However, most of these treatment strategies focus on controlling and managing diabetes complications rather than curing it with minimal or no side-effects. Thus, it is critical to develop new and improved drugs which are efficient, stable and inexpensive to make and can be distributed globally.

Insulin therapy is one of the well-known treatment method for type 2 diabetes. Even though, it helps in maintaining glucose levels in patients, it may also lead to side effects such as weight gain. As insulin is secreted in type 2 diabetic patients, researchers are trying to reverse insulin resistance with the help of novel treatment methods. The significance of the present work relates to the development of novel MgO nanoparticles as magnesium supplement to reverse insulin resistance in diabetic cell model. The utilization of MgO nanoparticles is anticipated to reduce the time and concentration required to reverse insulin resistance. A chemical synthesis method via sol-gel is used to synthesize distinct morphologies of MgO nanoparticles whereas plant leaf based green synthesis approach is used to synthesize MgO nanoparticles with various size/shape ranges. Since green synthesis uses phytochemicals from plant leaf extract, it can be significant in yielding less cytotoxic MgO nanoparticles whilst enhancing insulin resistance reversal ability. Further, the plants selected in the present study are widely available and can be cheap sourced for scale-up production. The development of MgO nanoparticles from plant materials to effectively treat diabetes represents a significant advancement in current diabetes treatment strategies and could potentially revolutionize current treatment modalities whilst delivering lasting economic benefits.

1.8. Thesis layout

Chapter 1 gives a brief introduction to diabetes, various treatment methods for diabetes and problems associated with conventional treatment methods such as insulin therapy to identify existing research gaps that drive the objectives of this study. The chapter also covers research questions, objectives, project scope and significance.

Chapter 2 critically reviews various nanomedicines used in different diabetes treatment strategies and describes how MgO nanoparticles may serve as a potential nanomedicine to reverse insulin resistance.

Chapter 3 covers the research methodology, detailing the experimental methods for the synthesis of MgO nanoparticles by chemical (sol-gel) and green (leaf extract) approaches, nanoparticle characterization, cell culture, cytotoxic analysis, DNS assay, western blot and fluorescent microscopic studies.

Chapter 4 covers the results and discussions relating to the synthesis and characterization of MgO nanoparticles.

Chapter 5 discusses cytotoxicity and insulin resistance reversal efficacy data generated using diabetic cell line model treated with MgO nanoparticles.

Chapter 6 covers the conclusion of this thesis which includes summary of research findings, reflections on research questions and objectives, and recommendations for future work.

CHAPTER 2

LITERATURE REVIEW

2.1. Nanomedicine for diabetes treatment

Nanomedicines are designed and developed using nanoparticles and nanomaterials for therapeutic and diagnostic applications (Sanna et al., 2014). The field of nanomedicine is gaining interest among researchers due to their superior ability as diagnostic agents and delivery vehicles with exceptional efficiency and safety. The current standards of intracellular uptake, biodistribution and dosing efficacy of a drug can be improved by using encapsulation and target specific controlled delivery properties of nanoparticles (Farokhzad et al., 2009). The solubility of drug compounds can also be improved by nanomedicine encapsulation ability (Chrastina et al., 2011). Biodegradability, large volume to surface area ratio, low toxicity and modifiable external shell are the additional advantages in using nanomedicines in treatment and disease diagnosis (Davis et al., 2008). All these advantages of nanomedicines gives immense promises for making personalized medicine in reality (Xu et al., 2015). As nanomedicine shows potential in biomedical applications, it has been used to identify and diagnose certain issues related to continuous blood glucose monitoring and insulin delivery in diabetes. In blood glucose monitoring, the conventional treatment procedures lack continuity due to stable implanted enzyme electrodes and non-invasive monitoring. This was solved using biocompatible nanofilms and smart tattoos of glucose nanosensors respectively. Conventional drug lack targeted molecular imaging during diagnosis or monitoring diabetes which makes it complicated to understand mechanism and solve problems during therapy. These complications were solved through single-molecule detecting near infrared quantum dots, gold nanoparticles and nanotherapeutic solutions. Moreover, conventional drugs used to improve insulin delivery face problems during islet cell transplantation, oral insulin delivery and closed-loop insulin delivery. Nanomedicines has solutions to these problems via islet nanoencapsulation, insulin nanoparticles and 'artificial nanopancreas' (Pickup et al., 2008; Hassan et al., 2016). The recent advancements in the field of nanomedicine leads

to the upsurge of orally administered nanoformulations such as carbon nanotubes, quantum dots, microsphere, artificial pancreas and nanopumps which are under extensive research for diabetes treatment.

2.1.1. Carbon nanotubes

Carbon nanotubes (CNTs) are seamless layers of cylindrical graphene either with open or close ended (Iijima, 1991; Harris et al., 2009). Generally, CNTs have bonded carbon atoms in a hexagonal lattice excluding their ends. The single-walled carbon nanotubes (SWNT) and multi-walled nanotubes (MWNTs) will have a typical diameters of about 0.8 to 2 nm and 5 to 20nm, respectively (De Volder et al., 2013). SWCNTs show fluorescence behavior in the near infra-red (NIR) spectral area. Since, SWCNTs are mostly suitable in *in vivo* glucose sensors as fluorophore (FL) probes as they don't exhibit photobleaching (Barone et al., 2005; Rahiman et al., 2012a). In a recent review, the uses of CNTs as an electrochemical glucose measurement system and optical glucose measurement system in diabetes treatment has been listed (DiSanto et al., 2015). The major drawback of using CNT in diabetes treatment is their lack of solubility in aqueous media and its non-biodegradability (Eatemadi et al., 2014).

2.1.2. Quantum dots

Nanosized crystals called as quantum dots, have been extensively examined by researchers for many applications. Typically, quantum dots sizes range between 2-20 nm (Kluson et al., 2007), though diameters below 10 nm is more recommended (Ferancová et al., 2008; Kral et al., 2006; Drbohlavova et al., 2009). Quantum dots are used in biomedical applications as a diagnostic material and also a tool for various disease therapies (Rahiman et al., 2012a). Quantum dot as a fluorescence donor and gold nanoparticle as an acceptor was used to build a glucose sensor based on Fluorescence Resonance Energy Transfer (FRET). In this setup, glucose gets displaced by concanavalin A- labeled quantum dots from gold-labeled cyclodextrin that reduces FRET and increases fluorescence (Tang et al., 2008; Rahiman et al., 2012a).The fluorescence of these quantum dots are quenched by the enzyme generated hydrogen peroxide in the existence of glucose. Direct enzyme tethering of quantum dot allows the glucose detection through rapid optical

analysis (Cao et al., 2008; Cash et al., 2010). Recently, graphene quantum dots has been established to be useful as glucose sensor (Shehab et al., 2017). However, the difficulties in measuring and identifying time-resolved fluorescence, blinking of quantum dots in single-molecule spectroscopic applications (Resch-Genger et al., 2008) and challenges in presenting weaker blue signal and up-converted persistent luminescence (UCPL) (Shen et al., 2012) are the drawbacks of utilizing quantum dots as glucose sensor.

2.1.3. Microspheres

Microspheres are spherical small particles, with micrometer sized diameter range (typically 1µm to 1000µm). Hollow and solid microspheres differ extensively in density and, hence, are utilized for distinct purposes. Polystyrene microspheres possesses capacity to ease procedures in cell sorting and immuno precipitation and are used in biomedical applications (Sahil et al., 2011). A combination approach with microsphere system has been used as a better strategy to accomplish oral insulin. Microspheres also protects the insulin from enzymatic degradation by encapsulation and enables active epithelial layer crossing after oral administration. Thus, they act as protease inhibitors and permeation enhancers for the encapsulated drug (Carino et al., 1999). In a study by Senthil et al., (2011) an anti-diabetic drug, Glipizide, was entrapped in a mucoadhesive microsphere to observe the capacity for sustained drug delivery efficiency. The results indicated that the mucoadhesive microspheres sustained the release of the drug for more than 12 hours (Senthil et al., 2011). Similarly, Glucagon-like peptide-1 (GLP-1) agonist exenatide was formulated into a product called Bydureon[TM] using Medisorb microspheres to provide a controlled release of exenatide that activates GLP-1 receptors and induces glucose-dependant stimulation of insulin secretion over a 7-day period (Painter et al., 2013). Recently, mucoadhesive microsphere formulation of repaglinide was utilized in the type 2 diabetes treatment as it shows increased drug absorption rate (Parmar et al., 2015). Microsphere can be used only as formulation to deliver conventional drugs which is a limitation in diabetes treatment as the current study focuses on nanoparticle drug materials.

2.1.4. Artificial pancreas

Artificial pancreas (automated subcutaneous closed-loop insulin delivery system) is a technological innovation that enables diabetic patients to spontaneously regulate their glucose level in blood by mimicking the activities of a healthy pancreas (Pareta et al., 2012). The development of artificial pancreas has become a closer-to-permanent solution for patients with diabetes. The concept of artificial pancreas is similar to nanorobots where an electrode with sensor constantly measures the blood glucose level and the information is fed into a computer to activate an infusion pump which administers the required insulin units from a small reservoir into the bloodstream (Hanazaki et al., 2001; S Rahiman, 2012b). Recently, the results presented at the 76th scientific session of American Diabetes Association (ADA) showed that artificial pancreas are effective, feasible and safe to manage hyperglycemic condition in hospitalized type 2 diabetes patients (Thabit et al., 2016). Other than artificial pancreas, transplantation of Islets were also becoming popular for the diabetes treatment (Shapiro et al., 2000). Ramiya et al (Ramiya et al., 2000) used islets from pancreatic stem cells that are produced in *in vitro* condition, implanted them in diabetic mouse and succeeded in decreasing level of glucose in blood after a week of time. Recent reviews portrays with strong evidences that islet transplantation can be safe and least invasive transplant procedure to avoid diabetic complications in patients (Shapiro et al., 2017). However, extensive research in these two techniques will identify challenges involved in medical implications and thereby finds solution to overcome those challenges.

2.1.5. Nanopumps

The nanopump is a versatile device that has potential uses in DNA analysis, drug screening, clinical and forensic analysis (Thorsen et al., 2002). It was first introduced by Debiotech for insulin delivery (Sasank et al., 2016). Continuous subcutaneous insulin infusion (CSII), regarded as an insulin pump system, is an approach to stimulate daily insulin secretion physiology (Yaturu, 2013). Insulin pump is a disk shaped infusion systems implanted in the abdominal subcutaneous tissue (Selam et al., 1990), and injects insulin at a constant rate through a free-moving peritoneal catheter to the patient (Saudek

et al., 1989) to balance blood sugar concentration. Many studies have reported improved glycemic control in patients using insulin pumps related to those on daily multiple injections (MDI) (Ramchandani et al., 2012). In an experiment performed by Kesavadas et al (Kesavadev, 2011), 48 out of 52 patients showed improved glucose control after using insulin pumps and amongst them, 42 patients experienced significantly lowered blood glucose level. However, resistance to insulin in cells will be a major problem in improving glucose control while using nanopumps. Thus, all these nanomedicines have pros and cons which promotes the need for an alternate or enhanced nanomedicine for the treatment of diabetes.

2.2. Metal oxide nanoparticles in biomedical applications

Oxide nanoparticles display exceptional chemical and physical properties due to their relatively small size and densely edge or corner surface sites (Ayyub et al., 1995). Existing knowledge shows that the physicochemical properties of oxide materials show critical size dependence (Iravani, 2017). A cluster of unique oxide nanoparticle applications dependents on the size of its optical, transport, mechanical and surface-chemical properties (Rodríguez et al., 2007; Yadavalli et al., 2017). Amongst the different oxide nanoparticles, metal oxides are exceptionally significant for their use in chemical, mechanical or electronic industries (Fierro, 2005). Metal oxide have been utilized in electronic and electrical systems such as varistor, surge protection devices and photo anode for solar cells due to their outstanding low, non-linear coefficient of current leakage (Kanade et al., 2006; Abdulmajeed et al., 2013). Also, the biocompatibility and biodegradability of metal oxides make it an important material in biological applications. Certain metal oxide nanoparticles such as zinc oxide (ZnO), magnesium oxide (MgO) and titanium oxide (TiO$_2$) have been found to be toxic towards cancer cells, with further potential applications in treating chronic diseases (Krishnamoorthy et al., 2012; Yadavalli et al., 2017).

2.2.1. ZnO nanoparticles

Zinc oxide possesses exclusive physicochemical properties such as high electrochemical coupling coefficient, wide range of radiation absorption increased chemical stability and

great photostability, making it a material with multifunctional ability (Segets et al., 2009; Lou, 1991). ZnO is usually used in converters, sensors, photocatalysts and energy generators in the production of hydrogen due to its piezo- and pyroelectric properties (Wang, 2008; Chaari et al., 2012). Its low toxicity, antibacterial, disinfecting and drying properties (Liu et al., 2013; Mirhosseini et al., 2013; Ng et al., 2017), biodegradability and biocompatibility makes it a superior material for pro-ecological and biomedical systems (Bhattacharyya et al., 2008; Ludi et al., 2013; Mirzaei et al., 2017). This oxide material is also utilized in several diet supplements and nutritional products to deliver necessary dietary zinc (Kołodziejczak-Radzimska et al., 2014; Liu et al., 2017).

The physicochemical properties of ZnO nanoparticles are often determined by the synthesis methods and functionalization chemistry. For example, ZnO nanocrystals prepared by sol-gel methods usually exhibit strong visible fluorescence due to its broad energy band (3.37 eV). Such products are mostly useful for bio-imaging (Xiong, 2010). Furthermore, biocompatible ZnO nanocrystals degrade readily in moderately acidic environment, making them suitable for pH-responsive systems as nanocarriers. The extracellular acidic environment of tumour tissues and its intracellular compartments such as endosomes and lysosomes provide ideal conditions for drug-ZnO nanocarriers (Zhang et al., 2013). Zhang et al. (Zhang et al., 2011) combined ZnO nanorods, which has theragnostic ability, along with daunorubicin (DNR) which is an anticancer drug and applied them in a photodynamic therapy (PDT). The results demonstrated that the combined system improved the anti-tumour activity remarkably with UV illumination.

Many investigations have reported that the size of ZnO nanocrystals contributes to their toxicity (Baek et al., 2011; Kang et al., 2013; Najim et al., 2014). However, some reports found that under UV irradiation, the effect of size is significant (Zhang et al., 2013). Palanikumar and co-workers (Palanikumar et al., 2013) used ZnO nanoparticles as a carrier for the delivery of amoxicillin drug. The amoxicillin-loaded 15nm ZnO nanoparticles demonstrated virtuous antibacterial activities against gram-negative and gram-positive bacteria. Semiconductor ZnO nanocrystals are one among the capable material with biosensing ability, not only because of their good photochemical and electrochemical properties, but also for their biocompatibility and low production cost

(Zhang et al., 2013). As ZnO has a high isoelectric point (IEP) of about 9.5, ZnO is appropriate for the adsorption of low IEP enzymes or proteins such as glucose oxidase (Zang et al., 2007), tyrosinase (Li et al., 2006), transferase (Sudhagar et al., 2011), bovine serum albumin (BSA) and rabbit-immunoglubin antibodies (r-IgGs) (Ansari et al., 2010) in the appropriate buffer solutions. Chakraborti et al. (Chakraborti et al., 2009) showed that ZnO nanoparticles are proficient in disrupting protein-protein interactions such as signal transduction between proteins as they are smaller in size. Nano-sized ZnO materials may exhibit different toxicity level because of their smaller size and larger surface to volume ratio. Studies on the cytotoxicity of ZnO nanoparticles have been conducted and the results demonstrated that ZnO nanocrystals are more toxic than aluminium oxide (Al_2O_3), TiO_2 nanoparticles and silica (SiO_2), and are mostly employed in the medical field as antibacterial agents and disinfectants (Zhang et al., 2013). Moreover, ZnO nanocrystals may cause cell death as well as carcinogenic effect by damaging DNA molecular structures (Hackenberg et al., 2011; Sharma et al., 2009; Yin et al., 2010; López-Moreno et al., 2010; Huang et al., 2010). In diabetes, ZnO nanoparticles shows promising results as therapeutic agent to cure diabetes in combination with certain antibiotics due to their drug loading capability (Alkaladi et al., 2014; Umrani et al., 2014). However, many literatures shows ZnO nanoparticles are toxic to certain types of cells, which makes them unfit to be used for diabetic treatments (Zhang et al., 2013; Hackenberg et al., 2011; Sharma et al., 2009; Yin et al., 2010; López-Moreno et al., 2010; Huang et al., 2010).

2.2.2. TiO_2 nanoparticles

Recently, TiO_2 nanoparticles have been extensively exploited in industries and consumer products compared to TiO_2 micro particles due to their strong catalytic activity (Tsuji et al., 2006; Shi et al., 2013a; Chibac et al., 2017). TiO_2 has unique properties such as brightness and high refractive index (ORTLIEB, 2010). Currently, TiO_2 nanoparticles are synthesized in abundance and are broadly used due to their photocatalytic, anticorrosive properties and high stability (Shi et al., 2013a; Alrobayi et al., 2017). In medical applications, TiO_2 nanoparticles are used in advanced imaging and nanotherapeutics (Shi et al., 2013a; Wang et al., 2017). For instance, TiO_2 nanoparticles are being estimated as

possible photosensitizer in photodynamic therapy (PDT) (Szacilowski et al., 2005). TiO_2 nanoparticles formulations are under investigation as an innovative method to treat and cure acne vulgaris at present (Bangale et al., 2012), recurrent condyloma accuminata (Nasir, 2010), atopic dermatitis (Yanagisawa et al., 2009), hyper-pigmented lesions in skin and other non-dermatologic diseases (Wiesenthal et al., 2011; Shi et al., 2013a) as well as drug delivery systems (Ensafi et al., 2017). TiO_2 nanoparticles also possess UV light mediated antibacterial properties (Montazer et al., 2011; Shi et al., 2013a; Senarathna et al., 2017). The doping of metal oxides or metals on the TiO_2 nanoparticle surface escalates the value of electron–hole pair charge separation by reducing the band-gap energy which leads to a recombination rate delay. When UV light falls on TiO_2 nanoparticle, it absorbs the light and acts as a photocatalyst to kill the bacterial colonies (Gupta et al., 2013). This information clearly articulates that TiO_2 nanoparticles are extensively used in biological applications.

Titanium (Ti) is found to be present in all animal tissues but only in trace amounts (Schkroeder et al., 1963; Shi et al., 2013a). However, titanium has never been reported as an essential element for humans or animals (Shi et al., 2013b). The increased growth in the number of publications portrays the interest among researchers in studying the safety and toxicity of TiO_2 nanoparticles (Shi et al., 2013b). Traditionally, TiO_2 fine particles are sparingly soluble with lower cytotoxicity (report, 1992; Borm et al., 2000). However, this is disproved after the development of lung tumors in rats, when high concentrations of fine TiO_2 particles are exposed for two years (Lee et al., 1985; Shi et al., 2013a). Studies have also shown that TiO_2 nanoparticles are highly toxic than micro or larger particles (Zhao et al., 2009; Fabian et al., 2008; Oberdörster, 2000). Oberdorster et al. (Oberdörster et al., 1994) described that TiO_2 nanoparticles (21nm) is responsible for pulmonary inflammatory response than TiO_2 fine particles at the same mass burden, with larger number of TiO_2 nanoparticles entering the lung alveolar interstitium. Sager et al. (Sager et al., 2008) stated similar results in rats after intra-tracheal instillation of well-dispersed TiO_2 nanoparticle suspensions. Recent *in vitro* assessment of TiO_2 nanoparticles in human plasma revealed that they are toxic to humans due to their difference in antioxidant enzyme machinery, DNA repair capabilities and metabolic rate (Ganapathi et al., 2017). Wide applications of TiO_2 nanoparticles confer substantial potential for environmental

release and human exposure, leading to a possible health hazard in livestock, eco-system and humans (Long et al., 2007; Kuku et al., 2017). However, in diabetes, TiO_2 nanoparticles are still extensively used in Bio MEMS to detect glucose in blood due to their semiconductor property (Subramani et al., 2012; Makaram et al., 2014) and as a carrier for drug (Moreno-Vega et al., 2012; Kulkarni, 2008) to delivery diabetic drugs. Recently, TiO_2 coated smart medical socks were developed to prevent bacterial growth in diabetic foot ulcer patients (Elsayed et al., 2017). However, due to their cytotoxicity and probability to develop tumor, it is still under research to use these nanoparticles as an anti-diabetic agent (Lee et al., 1985; Zhao et al., 2009; Relier et al., 2017).

2.2.3. MgO nanoparticles

Magnesium oxide (MgO), or magnesia, is a solid, white mineral that is present naturally as periclase. It is indeed hygroscopic and are formed by a magnesium and an oxygen atom connected through an ionic bond. MgO can be solubilized into their ionic state using water and ammonia, however they are poorly or insoluble in alcohols. It is an inimitable basic oxide with perfect crystal structure, simple stoichiometry, and high ionic character (Choudhary et al., 1994; Rajagopalan et al., 2002; Utamapanya et al., 1991; Morris et al., 1983; Sundrarajan et al., 2012b). It is an important material for industrial applications due to their high thermal stability, high melting point (2850°C), low heat capacity and high boiling point (3600°C) (Shand, 2006; Ropp, 2012). Currently, it is extensively used in reflecting and anti-reflecting coatings, lithium ion batteries, electroluminescence/ liquid crystal / fluorescent/ plasma displays, ferroelectric and superconductor thin films as a substrate (Shen et al., 2007; Zhou et al., 2004; Haraguchi et al., 2007; Boeuf, 2003; Zhang et al., 2006; Liu et al., 2005; Phillips, 1996; Hamet et al., 1992; Duyar et al., 2004; Davini et al., 1985; Jeevanandam et al., 2002; Stark et al., 1996; Kakkar et al., 2004; Qingwen et al., 2002; Gu et al., 2007; Kumar et al., 2008).

MgO in nano-form will help in enhancing their properties to a large extent because of their high surface to volume ratio. MgO has gained significant consideration due to its unique properties such as wide band gap, which is an important feature for enhanced catalytic properties (Schönberger et al., 1995), low heat capacity and high melting point

(Shukla et al., 2004). MgO nanoparticles have found applications in the production of refractories, insulating materials, paints, superconductors, and toxic waste remediation (Zhan et al., 2004; Kawaguchi, 2000; Shukla et al., 2004). Other than industrial applications, MgO nanoparticles were also used in antimicrobial applications. MgO nanoparticles exhibit high bioactivity against bacteria (Mirhosseini, 2016), spores (Sawai et al., 2004) and viruses because of its large surface area (Koper et al., 2002). The positively charged MgO nanoparticles interact strongly with the negatively charged bacterial cellular membrane. As a proof to this phenomenon, (Stoimenov et al., 2002) suggested that MgO nanoparticles can take up halogen gases due to its surface defect. This results in a robust interaction with bacteria having negative surface charge and damages them due to Reactive Oxygen Species (ROS) production by MgO nanoparticles. Compared with titanium oxide, silver, copper and other solid bactericides, MgO nanoparticles has the advantage of being synthesized from readily available, cheaper solvents and precursors.

Magnesium is an important ion of the human body though its concentration in the serum is low (0.3% of total body magnesium). It occurs as protein bound (33%), ionized (62%) and attachments to complexes to anions and albumin. Due to these attachments, MgO nanoparticles are used as a cure for heartburns and in bone regeneration (Bertinetti et al., 2009b). In addition, MgO nanoparticles have become a suitable candidate in pharmaceutical industries as anticancer agents (Krishnamoorthy et al., 2012; Bertinetti et al., 2009b), nanocryosurgery medium (Di et al., 2012) and biosensors platforms (Lu et al., 2010) due to their high thermal and bioactive properties. At different voltage-gated channels, it acts as a physiological calcium antagonist, and sometimes they have sheer importance in the antinociception mechanisms (Fawcett et al., 1999). For instance, magnesium and NMDA receptors have been demonstrated by Begon et al (Begon et al., 2001) and Hasanein et al (Hasanein et al., 2007) to be a key player in the modulation of pain. Likewise, the combination of ketamine with conventional MgO in mice revealed the effect of nano – MgO as an anti – inflammatory and analgesic agent (Jahangiri et al., 2013). Furthermore, many literatures have also revealed that MgO nanoparticles are non-toxic in low concentrations towards different cell lines with concentration-dependent and time-dependent cytotoxicity profiles (Ge et al., 2011; Sun et al., 2011; Lai et al., 2008).

However, limited research focus has been given to the uses, behavior and functions of MgO nanoparticles in the treatment and cure of diseases such as diabetes, pneumonia, and cholera.

2.3. MgO nanoparticles for type 2 diabetes treatment

The significance of magnesium relates to the physiology enzyme system functions and its effect on membrane properties (Fawcett et al., 1999; Jahangiri et al., 2014b). Magnesium directly controls cellular glucose metabolism (Swaminathan, 2003), signal transduction of peptide hormone receptors (Resnick, 1997), coupling of stimulus-contraction (Michailova et al., 2004), stimulus-secretion coupling (Mooren et al., 1994) and ion channel translocation (Fujita-Becker et al., 2005), at the biochemical level. Magnesium is crucial in activating magnesium-adenosine triphosphate (MgATP) complex essential for limiting the rate of glycolysis and kinase enzyme activity. MgATP complex is needed for all phosphate transfers and ATP-associated enzymes, such as endoplasmic reticulum and CaATPases in the plasma membrane (Barbagallo et al., 1996; Paolisso et al., 1997). Substantial decrease in the activities of enzymes at low magnesium concentrations has been reported by Laughlin et al (1996) for hypertension and diabetes cases via nuclear magnetic resonance (NMR) analysis. Insulin resistance is the anticipated consequence of suppressed cellular magnesium in fat tissues and skeletal muscles. Barbagallo et al (2003) explained in his review that oxidative stress in skeletal and fat tissues are due to low cellular magnesium level and this leads to insulin resistance.

Magnesium deficiency is a common problem in insulin and non-insulin dependent diabetes (Sjogren et al., 1988a; Velayutharaj et al., 2016). Reduction in intracellular magnesium content under insulin resistant conditions has been ascribed to a reduction in the entry of magnesium ions stimulated by insulin into the cell (Paolisso et al., 1990; Paolisso et al., 1986; Paolisso et al., 1989). Conversely, hypomagnesaemia has been found to be involved in ketoacidosis-associated pathogenesis of insulin resistance. This was reported by Ponder et al (1990) after evaluating the medical case history of 220 diabetic children (Ponder et al., 1990). Thus, both low intracellular magnesium and hypomagnesaemia can be a consequence (Sjogren et al., 1988a; Paolisso et al., 1990;

Alzaid et al., 1995) and cause insulin resistance (Lostroh et al., 1973; Sanui et al., 1978). A recent research on 42 recently diagnosed patients with type 2 diabetes also revealed that reduced magnesium level in serum is strongly related to insulin resistance. The researchers also suggested that serum magnesium level can be used as an indicator of diabetic complications (Jayaraman et al., 2017). Thus, supplementing magnesium to improve serum magnesium level will help in reversing insulin resistance. In the experiment conducted by (Kandeel et al., 1996), magnesium sulphate ($MgSO_4$) supplemented fat cells (adipocytes) taken from Male Sprague-Dawley rats successfully reversed insulin resistance. However, high concentrations of $MgSO_4$ were required for the reversal of insulin metabolic path, suggesting the need for an improved formulation.

Another clinical study, conducted by (Maier et al., 2004) showed that low magnesium concentrations can lead to endothelial cell dysfunction. They reported that that low concentrations of magnesium impede endothelial proliferation reversibly, resulting in down-regulation of CDC25B. Dysfunction of endothelium can result in a number of diseases including atherosclerosis (Cines et al., 1998), hypertension (Epstein et al., 1999), diabetes (Lifton et al., 2001) and thrombosis (Lifton et al., 2001). A recently reported research showed that combined perioral supplementation of both chromium and magnesium effectively reversed insulin resistance (Dou et al., 2016). The research was conducted on 120 individuals between the age of 45-59 and they discussed that insulin resistance reversal may be due to increased repression of *GSK3β* and induction of *GLUT4* expression. As magnesium supplements can lead to reversal of insulin resistance in patients with type 2 diabetes, MgO nanoparticles is proposed in this research as a potential agent in supplementing magnesium to reverse insulin resistance as shown in Figure 2.1. It is hypothesized to be a more effective insulin resistance reversing agent than $MgSO_4$ and $MgCl_2$, as it is a metal oxide nanoparticle with high edge surface site density (Ayyub et al., 1995). Since nanoparticles are known for their superior surface to volume ratio, a lower dosage of MgO nanoparticles would be required for effective insulin resistance reversal (Rahiman et al., 2012b). The present project aims at probing the relationship between the biophysical characteristics of MgO nanoparticles and insulin resistance reversal efficiency. Sol-gel and aqueous leaf extract mediated bio-based green synthesis would be used to generate 2 different types of MgO nanoparticles. The screening of MgO

nanoparticles toxicity would be performed using 3T3-L1 cell lines as a diabetic cell model and VERO cell line as a non-diabetic normal cell model via MTT assay. Bio-assay analysis on insulin resistance reversal ability would be conducted to investigate the efficacy of the nanoparticles.
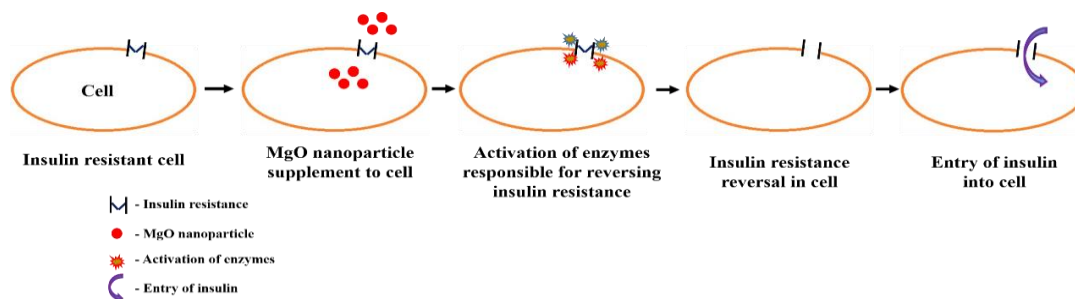
Figure 2.1: Proposed mechanism for MgO nanoparticle to reverse insulin resistance (Jeevanandam et al. 2015)

2.4. Synthesis of MgO nanoparticles

The surface properties of MgO nanoparticles affect its functional properties. MgO nanoparticle synthesis methods and process parameters (Liang et al., 1985; Klabunde et al., 1996; Morales et al., 1995) play a significant role in defining their characteristic features and functional properties Jeevanandam et al., (2016b). Thus, the synthesis method is critical in generating MgO nanoparticle with distinct surface properties and morphology necessary to promote insulin resistance reversal. MgO nanoparticles can be synthesized either by a physical, chemical or biological method.

2.4.1. Physicochemical synthesis of MgO nanoparticles

MgO nanoparticles can be prepared using a variety of synthesis approaches, including vapor phase oxidation (Itatani et al., 1997), hydrothermal synthesis (Sōmiya et al., 2000; Su et al., 2011), high temperature solid state synthesis (Myagkov et al., 2004), alkoxide based preparation (Zhang et al., 2002), microwave irradiation (LI et al., 2007) and sol-gel synthesis (Cosentino et al., 2006; Athar et al., 2012). Table 2.1 summarizes the merits and limitations of each physicochemical synthesis method. Sol-gel method is recognized as a promising method for biomedical applications as it results in smaller nanoparticle with

comparatively low toxicity than other chemical methods (Ibrahim, 2010; Hyun et al., 2003). This method is considered superior to other synthesis methods due to its simplicity, cost-effectiveness and the ability to generate nanoparticles with high purity and surface area-to-volume ratio (Jiu et al., 2004; Chadwick et al., 1998; Bokhimi et al., 1999; Subramania et al., 2007). Sol-gel synthesis requires comparatively low temperature conditions compared to other chemical methods (Mastuli et al., 2014), offers sufficient control over metal oxide composition (Yoshimura et al., 1999), and facilitates the generation of nanoparticles with controlled chemical structure (Lind et al., 2010) and particulate size (Athar et al., 2012).

It is known that the size and shape of nanoparticles significantly affect their properties (Cao, 2004; Giri et al., 2011). Conventional sol-gel synthesis technique has been used extensively to produce spherical shaped MgO nanoparticles (Athar et al., 2012; Suresh, 2014) for unique applications (Athar et al., 2012; Makhluf et al., 2005). However, in pharmaceutical delivery, spherical nanoparticle may result in ineffective attachment to target cells, resulting in reduced functionality or activity (Kolhar et al., 2013) compared to other morphologies. Shapes of nanoparticles such as hexagon (Lu et al., 2009) and rods (Gratton et al., 2008) can promote better bioactivity on target cells. Synthesis process conditions strongly influence the stability, morphology and size of nanoparticles (Ghorbani et al., 2011). Process investigation of sol-gel synthesis through variations in the concentration of gelling agent (Zhang et al., 2003; Kareiva et al., 1994; Thirunakaran et al., 2005) and precursors (Mirzaei et al., 2012; Ouraipryvan et al., 2009) have been performed, and different sizes and shapes of nanoparticles were generated. Niederberger (2007) reported that various shapes such as cube, cone, multipods and nanorods can be generated by specific process variation strategies (Niederberger, 2007). (Mastuli et al., 2014) synthesized diverse shapes of MgO nanoparticles such as cube, sphere and cuboid through sol-gel process by altering the gelling agents. However, a major drawback to sol-gel synthesis is the requirement for high calcination temperatures for prolonged durations (950°C for 36 hours) to yield MgO nanoparticles with distinct morphology. Since, sol-gel method has the capability to yield spherical, hexagon and rod shaped nanoparticles, it is used to investigate the particle formation process necessary to engineer morphological characteristics. The present work utilizes a simple sol-gel synthesis method modified from

(Kumar et al., 2008) to synthesize spherical, hexagonal and rod shaped MgO nanoparticles. Kumar et al (2008) utilized nitrate precursor and oxalic acid as gelling agent to form agglomerated spherical MgO nanoparticles that are less than 100 nm after calcinating at 1000°C for 2 hours. The present work introduces variations in precursor and gelling agent to reduce the calcination temperature and to synthesize stable, small size nanoparticles with varying morphology.

Table 2.1: Summary of various physicochemical methods for MgO nanoparticle synthesis

Synthesis method	Description	Advantages	Disadvantages	References
Hydrother-mal	A crystal synthesis procedure that uses high-pressure water conditions and high temperature from substances that are insoluble in normal temperature and pressure.	Used for synthesis of multi metal oxide compounds	Cost of the equipment is high and monitoring of crystals in their growth process is impossible.	(Hayashi et al., 2010)
Vapour phase oxidation	This technique uses vapor phase precursors that are brought into a hot-wall reactor under favorable nucleation condition of	Promising method for producing continuous layers of high quality metal oxide	Difficult to control hydrolysis rate of precursors, resulting in the formation of aggregates	(Swihart, 2003; Bhattacharyya et al., 2012; Mattevi et al., 2011;

	particles in the vapor phase.			Ali et al., 2014)
Sol-gel synthesis	It is a colloidal synthesis method with an intermediate sol and/or gel state which is utilized extensively to produce ceramics.	Offers a low temperature method to synthesize metal oxide, and doping can readily be introduced.	Formation of covalent linkages between the glass slide and chemicals leads to weak coating resistant.	(Ibrahim, 2010; Hyun et al., 2003; Pudukudy et al., 2017)
High temperature solid state synthesis	A synthesis procedure that produces nanoparticles step-by-step in a reactant solution in which molecules are bound on a bead.	Easy to remove by-product. Can be used for the synthesis of peptides and DNA.	Large grain size, poor chemical homogeneity, undesirable phases	(John et al., 2010; Gordon et al., 1999)
Alkoxide based preparation	A method used for the preparation of oxide materials in a single step using alkoxide and their derivatives	Easy to remove alkoxide ligands via thermal treatment	Undesirable phases, micrometre grain size	(John et al., 2010)

Microwave irradiation	It is a method in which microwave is applied to chemical reactions to sufficiently heat thin objects throughout their volume.	It heat the target compound without heating the entire furnace. Thus saving time and energy	Non uniform and localized superheating occurs that affects the formation of nanoparticles	(Loupy, 2006; de la Hoz et al., 2005; Strauss et al., 1995; Kappe et al., 2012)

2.4.2. Green synthesis of MgO nanoparticles

Green methods are widely used for nanoparticle synthesis. Biomaterials such as plant extracts, fungi and bacteria can be used for metal oxide nanoparticle synthesis through green synthesis approaches. Amongst green synthesis methods, plant extract facilitated synthesis possesses significant advantages in terms of toxic byproduct reduction and the capacity to engineer the nanoparticle size using embedded phytochemicals (Malik et al., 2014). Table 2.2 gives a summary of plant extracts that have been used for metal oxide nanoparticle synthesis. Phytochemicals such as aldehydes, ketones, amides, terpenoids, carboxylic acids and flavonoids present in plant extracts play an major role in nanoparticle synthesis (Terenteva et al., 2015).

In the present work, MgO nanoparticles is synthesized by adopting the synthesis procedure reported by (rao Pasupuleti, 2013) for silver nanoparticles synthesis using *Rhinacanthus nasutus* extract. The synthesis procedure uses plant leaf extracts from *Amaranthus tricolor*, *Amaranthus blitum* and *Andrographis paniculata* as feedstock. *Amaranthus tricolor Linn* is a tropical annual plant that belongs to the *Amaranthaceae* family (Rao et al., 2010). It has traditionally been used for the treatment of piles, bladder distress, blood disorders, tooth ache and dysentery (Madhava Chetty et al., 2008). The leaves of *A. tricolor* typically consists of unsaturated linolenic fatty acid (42%) and saturated palmitic fatty acid (18-25%) (Fernando et al., 1984). Mature leaves of *A. tricolor*

contains betacyanins, red-violet pigments, isoamaranthin and amaranthin (Rao et al., 2010; Piattelli et al., 1969) along with other phytochemicals. *Amaranthus blitum L.*, a wild amaranth and native to the Mediterranean region (Walshaw, 2005), contains a high percentage of carotene, thiamine, riboflavin, niacin and ascorbic acid (Alegbejo, 2014; Achigan-Dako et al., 2014). The leaves are commonly utilized as poultice and febrifuge to treat lung disorders, boils and inflammations (Walshaw, 2005). *Andrographis paniculata* is an eminent plant native to Asia that belongs to the *Acanthaceae* family. Diterpene and lactones are the active components present in the aerial part of *A. paniculata* plant, collectively called andrographolides (Akowuah et al., 2008; Hossain et al., 2014). The leaves are also reported to have diterpenoids, flavonoids and steroids (Siripong et al., 1992), and are used as medications for several diseases in Asia and Europe (Siripong et al., 1992; Burkill, 1966; Akbar, 2011a; Jarukamjorn et al., 2008). These three plants were selected for the present work because of their high flavonoid contents (Amin et al., 2006; Gupta et al., 1983) as flavonoids have been reported as an essential phytochemical for plant leaf based biosynthesis of nanoparticles (Ahmad et al., 2010; Jeevanandam et al., 2016a).

Table 2.2: Biosynthesis of metal oxide nanoparticles using various organisms.

Copyright Wiley-VCH Verlag GmbH & Co. KGaA. Reproduced with permission

Nanoparticle	Bacteria	Size	Reference
Manganese oxide	*Shewanella loihica*	18-202nm	(Jiang et al., 2015)
Iron oxide	*Aquaspirillium magnetotacticum, Magnetaspirillum magnetotacticum*	47nm	(Philipse et al., 2002; Mann, 1985)
Uranium oxide	*Desulfosporosinus sp., Shewanella oneidensis*	1-5nm	(Marshall et al., 2006; Cunningham et al., 1993)

Nanoparticle	Fungi	Size	Reference
Titanium dioxide	*Aspergillus flavus TFR 7*	12-15nm	(Raliya et al., 2015)
Zinc oxide	*Aspergillus terreus*	55-83nm	(Baskar et al., 2013)
Bismuth oxide	*Fusarium oxysporum*	5-8 nm	(Uddin et al., 2008)
Nanoparticle	Plant leaf extract	Size	Reference
Iron oxide, Zinc oxide	*Camellia sinensis* (Green tea extract)	5-20nm	(Hoag et al., 2009; Shahwan et al., 2011; Senthilkumar et al., 2014)
Iron oxide	Bran extract from *Sorghum sp.,* Plantain peel extract, Grape seed proanthocyanidin*,* Grape marc, Fruit pericarp of *Terminalia chebula,* Banana peel ash extract, Leaf extracts of *Eucalyptus globulus,* Pomegranate*, Dodonaea viscosa, Tridax procumbens,* Vine leaf, *Eucalyptus tereticornis, Melaleuca nesophila, Rosmarinus officinalis*	20-80nm	(Njagi et al., 2010; Venkateswarlu et al., 2013; Narayanan et al., 2011; Machado et al., 2013; Thakur et al., 2014; Madhavi et al., 2013; Wang, 2013; Rao et al.,

			2013; Daniel et al., 2013; Senthil et al., 2012; Wang et al., 2014)
Zinc oxide	Aloe leaf broth extract, Milky latex of *Calotropis procera,* Leaf extracts of *Coriandrum sativum, Calotropis gigantean, Acalypha indica, Hibiscus rosa-sinensis*	25-40nm	(Gunalan et al., 2012a; Anastas et al., 2000; Clark et al., 2008; Devi et al., 2014; Gnanasangee tha, 2013)
Titanium dioxide	Latex of *Jatropha curcas,* Leaf extracts of Neem, *Eclipta prostrate*	25-100nm	(Hudlikar et al., 2012; Rajakumar et al., 2012; Shilpa Hiremath et al., 2014)
Copper oxide	*Malva sylvestris, Aloe barbadensis Miller*	14-30nm	(Awwad et al., 2015; Gunalan et al., 2012b)
Magnesium oxide	*Nephelium lappaceum* leaf peels	60-70nm	(Suresh et al., 2014; Jeevanandam

| | *Andrographis paniculata*, *Amaranthus tricolor*, *Amaranthus blitum* aqueous leaf extract | | et al., 2017; Karthik et al., 2017) |

2.5. Cytotoxic analysis

Cytotoxic analysis of metal oxide nanoparticles for pharmaceutical applications can be performed using MTT assay. MTT (3-[4, 5-dimethylthiazol-2-yl]-2, 5 diphenyl tetrazolium bromide) assay determines the activity of mitochondria in the conversion of tetrazolium MTT salt into formazan crystals. Since the total activity of mitochondria can be correlated to the quantity of living cells in a population, this method is widely used to quantify the effects of drug *in vitro* cytotoxicity on cell lines (van Meerloo et al., 2011). Different concentrations of nanoparticles are prepared and subjected to a two-stage cytotoxic study. In the current study, the cytotoxic analysis is performed using 3T3-L1 adipocyte cell lines and VERO cell lines. 3T3-L1 is widely accepted as a model for diabetic studies (He et al., 2007), therefore cytotoxicity analysis using these cell lines will help to screen toxic nanoparticles before further formulation. The selected nanoparticles is subjected to further cytotoxic analysis using VERO cells, being the normal cell model in the present study. Table 2.3 shows MTT based cytotoxicity analysis of different nanoparticles using 3T3-L1 and VERO cell lines.

Table 2.3: MTT based cytotoxic analysis of various nanoparticles using diabetic and non-diabetic cell models

Cell line	Nanoparticle	Reference
	Mesoporous silica nanoparticles	(Huang et al., 2005)
	Amorphous silica nanoparticles	(Uboldi et al., 2012)
	Nanodiamond-insulin complex	(Shimkunas et al., 2009)

3T3-L1 adipose cell line (diabetic cell model)	Zinc oxide nanoparticles	(Pandurangan et al., 2015)
VERO cell lines (non-diabetic cell model)	Gold nanoparticles	(Chueh et al., 2014)
	Gold nanoshells	(Su et al., 2007)
	Pristine coated non-biodegradable graphene	(Sasidharan et al., 2011)
	Zirconia nanoparticles	(Balaji et al., 2017)
	Iron oxide nanoparticles	(Szalay et al., 2012)

2.6. Insulin resistance reversal analysis

The diabetes study includes glucose assay, western blot assay and adhesion analysis. These tests are necessary to provide evidence that MgO nanoparticles possess insulin resistance reversal ability. The reversal of insulin resistance due to MgO nanoparticle and the conversion of glucose into fatty acid is measured using DNS colorimetric glucose assay (Rivers et al., 1984). 3, 5 – Dinitrosalicylic acid (DNS) is a compound that binds and reacts with reducing sugar molecules due to their aromatic nature to form 3-amino-5-nitrosalicylic acid which absorbs visible light at 540 nm (Lide et al., 2009; Miller, 1959). This assay can help in measuring the quantity of insulin intake reflected by the amount of glucose converted and the efficiency of MgO nanoparticles in reversing insulin resistance. It has been reported that the glucose transporter protein (GLUT-4) is critical during reversal of insulin resistance in adipose tissues (Slot et al., 1991). Elaborate further in 2 sentences on the importance of GLUT-4. Hence, western blot assay is used to analyze the expression of GLUT-4 protein to indicate the insulin resistant reversal and insulin entry into the cell. Western blot is used to identify and separate proteins using gel electrophoresis. Results are obtained by transferring the electrophoresized gel to a nitrocellulose membrane which generate bands corresponding to each protein. The

membrane is then incubated with the precise antibody labels to determine the presence of protein (Mahmood et al., 2012). This protein separation technique is to reveal the presence of GLUT4 protein, thereby confirming the insulin resistance reversal ability of MgO nanoparticles. Fluorescence microscopic analysis can be used to test and check nanoparticles-cell adhesion (Balasundaram et al., 2006; Gupta et al., 2004). Fluorescent microscopic images of the cell is generated using acridine orange and propidium iodide in order to differentiate several cell components. This analysis gives information about the adhesion and entry of nanoparticles into the adipose cells (Burmeister et al., 1998). Hence, this analysis will be helpful in probing possible mechanisms of MgO nanoparticles in reversing insulin resistance.

2.7. Research novelty

The novel aspects of the current project relate to strategies to generate multi-functional less toxic MgO nanoparticles with diverse morphologies and sizes to improve insulin resistance reversal ability in type 2 diabetes cases. Previously reported studies mostly focus on spherical shaped MgO nanoparticles synthesized via chemical based sol-gel method (Kumar et al., 2008). Even though spherical nanoparticles possess high surface to volume ratio, ease of endocytosis remains a major challenge (Panariti et al., 2012). Hexagonal and rod shaped morphologies have been reported to have an improved cell penetration capacity for activating intracellular enzymes (Xu et al., 2008). Thus, a new and improved approach with the capacity to generate transformational morphologies of MgO nanoparticles is critical to enhance therapeutic effects. The effect of calcination temperature and gelling agent is explored in sol-gel technique to generate three different morphologies (spherical, hexagonal and rod-like shapes) of MgO nanoparticles. Bio-based green synthesis approach has been used to yield several shapes of MgO nanoparticles. To date, only two literatures have reported green synthesis of MgO nanoparticles using peels of *Nephelium lappaceum* (Rambutan fruit) and leaves of *Swertia chirayaita* (Sharma et al., 2017; Suresh et al., 2014). The nanoparticles were spherical and in the size range 40-60 nm. To further reduce MgO nanoparticles size and cytotoxicity compared to chemically-synthesized MgO nanoparticles, a green synthesis method using three plant leaf extracts; *Amaranthus tricolor*, *Amaranthus blitum* and *Andrographis*

paniculata is developed and characterized. A novel pH-mediated technique is used to control morphological transformations in MgO nanoparticles.

Another important novel aspect of the project relates to the generation of hexagonal MgO nanoparticles to improve insulin resistance reversal capacity due to its high edge surface density. The edge surface atoms of metal oxide nanoparticles can be highly influential in facilitating the entry of nanoparticle into cell and enhancing their bioavailability (Ayyub et al., 1995). The effect of metal oxide nanoparticle morphology on the efficacy of insulin resistance reversal is not well reported in the literature. Also, as nanoparticles are known for their high surface to volume ratio, low dosage of MgO nanoparticles may be effective for reversing insulin resistance. The current study hypothesized that morphologically engineered magnesium supplement in the nano-form can be an alternative to insulin supplement with high biocompatibility and bioavailability to reverse insulin resistance. This constitutes a novel addition to the field of study and would enhance capacity to develop new and improved nanomedicines for diabetes treatment.

CHAPTER 3

RESEARCH METHODOLOGY

3.1. List of chemicals, materials, reagents and cell lines used

Magnesium precursors such as magnesium acetate tetrahydrate and magnesium nitrate hexahydrate, ethanol as solvent along with gelling agents such as oxalic, tartaric and citric acid was used for the chemical (sol-gel) synthesis process. Similarly, the same magnesium precursors along with leaf extracts were used for green synthesis and pH modifications were performed using chemicals as mentioned in Table 3.1. No further purification of chemicals and reagents were carried out and are used directly in the experiment. The chemicals, reagents and cell lines used for cytotoxic and biological assays were also mentioned in Table 3.1.

Table 3.1: Chemicals and their specifications used for chemical synthesis of MgO nanoparticles

Purpose	Chemicals and specifications	Brand
Chemical synthesis of MgO nanoparticles (sol-gel)	Magnesium acetate tetrahydrate Molecular weight – 214.45 g/mol Purity – 98%	Alfa Aesar (USA)
	Magnesium nitrate hexahydrate Molecular weight – 256.41 g/mol Purity – 98%	Alfa Aesar (USA)
	Oxalic acid Molecular weight – 126.06 g/mol Purity – 99.5%	Merck (USA)
	Tartaric acid Molecular weight – 150.08 g/mol Purity – 99.5%	Acros organics (Belgium)
	Citric acid Molecular weight – 192.12 g/mol	Fisher scientific (Singapore)

	Purity – 99.9%	
	Ethanol Molecular weight – 46.06 g/mol Purity – 99.4%	Fisher scientific (Singapore)
Green synthesis of MgO nanoparticles	*Andrographis paniculata* *Amaranthus blitum* (green spinach) *Amaranthus tricolor* (red spinach)	Local market in Miri, Sarawak, Malaysia
	Magnesium acetate tetrahydrate Molecular weight – 214.45 g/mol Purity – 98%	Alfa Aesar (USA)
	Magnesium nitrate hexahydrate Molecular weight – 256.41 g/mol Purity – 98%	Alfa Aesar (USA)
	Concentrate hydrochloric acid Molecular weight – 36.45 g/mol Purity – 30%	Merck Millipore (Singapore)
	Sodium hydroxide Molecular weight – 39.99 g/mol Purity – 97%	Merck Millipore (Singapore)
Cell lines for biological assays	3T3-L1 (diabetic) adipocytes from mouse	National Cell Culture Society (NCCS), Pune, India
	VERO kidney epithelial cells from African green monkey	National Cell Culture Society (NCCS), Pune, India
	Fetal Bovine Serum (FBS)	Sigma Aldrich (USA)
	Dulbecco's Modified Eagle's Medium (DMEM)	Sigma Aldrich (USA)

Reagents for cell culture	Penicillin	Thermo Fisher scientific company (USA)
	Streptomycin	Thermo Fisher scientific company (USA)
	Phosphate buffered saline (PBS) 10X with pH 7.4	Thermo Fisher scientific company (USA)
	Dimethyl sulfoxide (DMSO)	Thermo Fisher scientific company (USA)
	Trypsin-Ethylene di amine tetra acetic acid (EDTA)	Thermo Fisher scientific company (USA)
Biological assays	3-(4,5 – dimethylthiazol-2-yl)-2, 5-diphenyltetrazolium bromide (MTT) dye for cytotoxic assay	Sisco Research Labs Pvt. Ltd. (SRL-India)
	Anti-GLUT4 antibody for western blot	Krishgen biosystems (India)
	Anti-mouse IgG for western blot	Krishgen biosystems (India)
	3, 5-Dinitrosalicyclic acid for DNS assay Purity – 98%	Acros organics (India)
	Anhydrous D(+)-glucose	Acros organics (India)
	Propidium iodide dye for fluorescent microscope studies	Sigma Aldrich (USA)

	Acridine orange dye for fluorescent microscope studies	Sigma Aldrich (USA)
	Other common chemicals for western blot and glucose assay	Sigma Aldrich (USA)

3.2. Experimental methodology

3.2.1. Synthesis of MgO nanoparticle

Equimolar ratio of precursor and gelling agents were separately dissolved in ethanol. Later both solutions were mixed together and the formation of gel starts immediately after mixing. Addition of gelling agent leads to a three dimensional magnesium network formation with molecules from gelling agent and ethanol. Later, the gel was subjected to age for 12 hours followed by drying for 24 hours at 100°C in a hot air oven (***Memmert GmbH VO400cool***) (Kumar et al., 2008). In the present work, two precursors such as magnesium acetate and magnesium nitrate were used. Four combinations of gelling agent such as oxalic acid, tartaric acid, citric acid and mixture of three gelling agents with precursors were used for the synthesis. The complete synthesis process was summarized in the Figure 3.1. The sample names for sol-gel product obtained from different precursors and gelling agents were shown in Table 3.2. The obtained sol-gel product in powder form were characterized using Thermogravimetry-Differential Scanning Calorimetry (TG-DSC) and X-Ray diffraction studies to analyze the crystallinity and thermal behavior of the powder. This analysis will help to select the calcination temperature to form pure MgO nanoparticles. The obtained sol-gel product in the powder form after drying was then calcinated at different temperatures for two hours for MgO nanoparticles formation from the sol-gel product. The calcinated samples were analyzed using Dynamic Light Scattering (DLS) technique to study the average particle size. Later, the selected samples were subjected to XRD to study the phase formation, Fourier Transform-Infra Red (FT-IR) spectroscopy (***Thermo scientific NICOLET iS10***) to identify functional groups and Transmission Electron Microscopy (TEM) analysis to analyze MgO nanoparticles morphology.
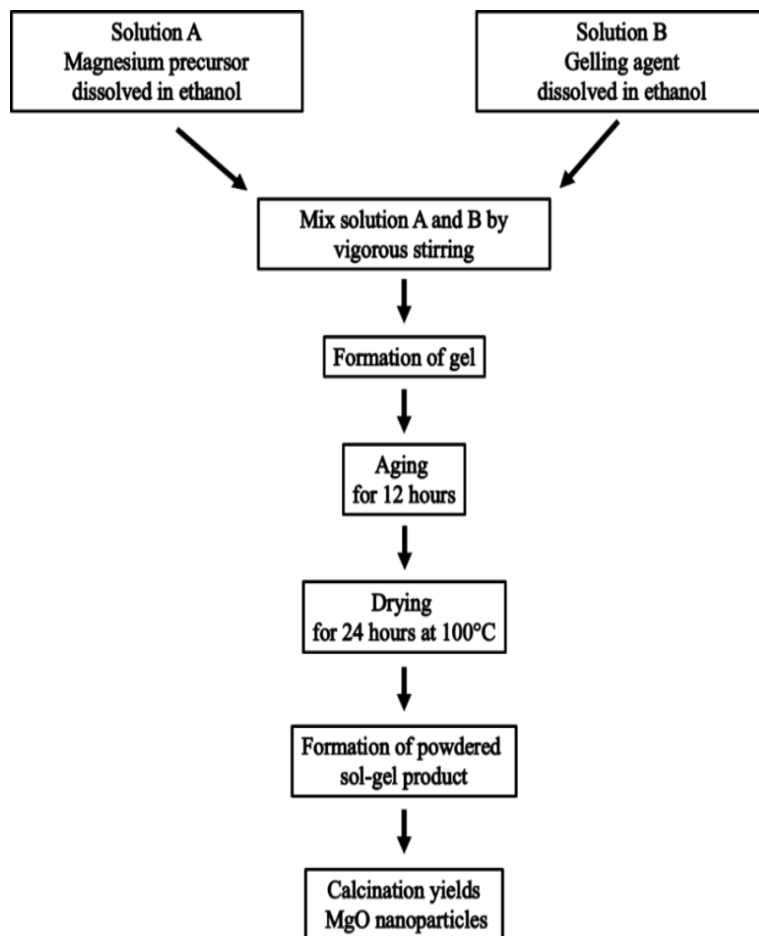
Figure 3.1: Sol-gel synthesis of MgO nanoparticles

Table 3.2: Sol-gel product from different precursor and gelling agent

Sample name	Magnesium precursor	Gelling agent
Sample AO	Magnesium acetate	Oxalic acid
Sample AT	Magnesium acetate	Tartaric acid
Sample AC	Magnesium acetate	Citric acid
Sample AM	Magnesium acetate	Mixture of oxalic, tartaric and citric acid
Sample NO	Magnesium nitrate	Oxalic acid
Sample NT	Magnesium nitrate	Tartaric acid
Sample NC	Magnesium nitrate	Citric acid
Sample NM	Magnesium nitrate	Mixture of oxalic, tartaric and citric acid

Note – A-Magnesium acetate, N-Magnesium nitrate, O-Oxalic acid, T-Tartaric acid, C-Citric acid, M-Oxalic+Tartaric+Citric acid

3.2.2. Green synthesis of MgO nanoparticles

Aqueous plant extract was prepared by adding boiling distilled water into the fresh leaves in the ratio of 10:1 for 20 minutes (Pasupuleti et al., 2013). Later, the extract was allowed to cool in room temperature. The leaves were filtered by using a filter mesh and then by using Whatman No: 1 filter paper to eliminate dust particles. The extract that are filtered and purified, is stored in refrigerator at 4°C for further use. 5, 10 and 15ml of aqueous leaf extracts were added separately to 1mM, 5mM and 10mM concentrations of magnesium precursors that are dissolved in distilled water, for the synthesis of MgO nanoparticles. This mixture was then heated for 5, 10 and 15min at a temperature of 40°C, 60°C and 80°C for MgO nanoparticle synthesis (rao Pasupuleti, 2013). Figure 3.2 shows the methodology for the MgO nanoparticle formation using different leaf extracts. There are six combinations of magnesium precursor and leaf extracts that are used to synthesize smaller MgO nanoparticles as mentioned in Table 3.3. Optimization of nanoparticle synthesis was obtained by using one-factor-at-a-time method. The obtained nanoparticles

were further characterized with UV-Visible spectrophotometer and Zeta sizer to confirm the presence of MgO nanoparticles and its size.
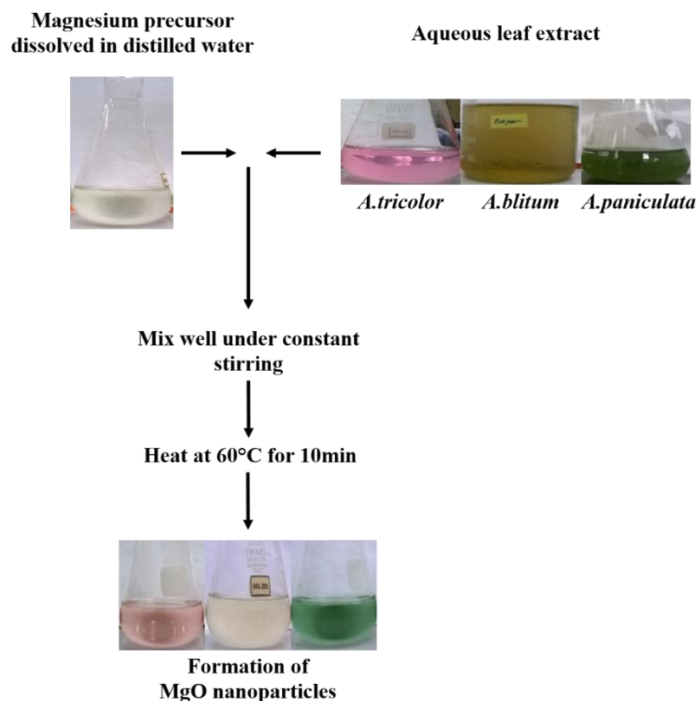
Figure 3.2: Leaf extract mediated MgO nanoparticle synthesis. Reproduced by permission of the Royal Society of Chemistry.

Table 3.3: MgO nanoparticle synthesis with different magnesium precursors and leaf extracts

Sample	Precursor	Leaf extract
Sample AT	Magnesium acetate	*Amaranthus tricolor*
Sample AB	Magnesium acetate	*Amaranthus blitum*
Sample AP	Magnesium acetate	*Andrographis paniculata*
Sample NT	Magnesium nitrate	*Amaranthus tricolor*
Sample NB	Magnesium nitrate	*Amaranthus blitum*
Sample NP	Magnesium nitrate	*Andrographis paniculata*

Note: A-Magnesium acetate, N-Magnesium nitrate, T-*Amaranthus tricolor*, B-*Amaranthus blitum*, P-*Andrographis paniculata*

3.2.3. Characterization of nanoparticles

The crystallinity and thermal behavior of sol-gel product from chemical synthesis were analyzed using X-ray diffraction (XRD) method and Thermogravimetry-Differential Scanning Calorimetry (TG-DSC) to understand MgO nanoparticles formation. Later, calcination of the sol-gel product were performed in a box furnace *(Carbolite 1200°C heavy duty box furnace)*. The MgO nanoparticles, formed using leaf extracts, were initially characterized by UV-Visible spectrophotometer and Dynamic Light Scattering method. Later, the optimized parameters were used to form MgO nanoparticles which are freeze dried into powder using *LABCONCO 2.5 L refurbished freeze dryer/lyophilizer* at -40°C with 0.133mBar vacuum pressure. The freeze dried powder samples were studied using XRD and Fourier transform-Infra Red spectroscopy (FT-IR) to analyze its phase formation and chemical composition respectively. The MgO nanoparticles in its colloidal form was used in Transmission Electron Microscopy (TEM) studies to observe their morphology. The images of instruments that are used for characterization of nanoparticles were given in the appendices.

3.2.3.1. Thermal analysis

TG-DSC measures weight change as a function of temperature and helps in determining chemical and physical changes that leads to mass fluctuations, when a material undergoes heating process. Modern TG-DSC equipment has a sensitive microbalance for continuous sample weight measurement, sample holder surrounded by a furnace, and an inert or reactive atmosphere purge gas system. The furnace and the data (weight vs. sample temperature) is controlled, collected and processed by a computer. Intelligent auto samplers are accessible for several instruments that allows the unattended study of samples. Decomposition, desorption, absorption, reduction, vaporization or sublimation are the reason for mass change in the sample and these can be measured in TG-DSC (Haines, 2012; Le Parlouër, 1987). In the present study, the instrument used for TG-DSC analysis was *Thermal Gravimetric Analyzer, Mettler Toledo* (Plate A.1). 15-20mg of samples were heated from 30-1000°C for the thermal analysis under nitrogen atmosphere at 20°C/min of heating rate.

3.2.3.2. Dynamic light scattering technique

Dynamic light scattering (DLS) is a method used to determine the average particle size and their distribution profile of colloidal nanoparticles. The Brownian movement of nanoparticles leads to the scattering of laser light at diverse intensities in a colloidal suspension (Berne et al., 2000). The particle size distribution of nanoparticle was established using the Stokes-Einstein relationship via the analysis of intensity fluctuations which gives information on the Doppler shift velocity and Brownian motion of the particle (Instruments, 2004). The instrument used for particle size distribution, polydispersity and zeta potential analysis in the present study was *Malvern® Zetasizer Nano ZS* (Plate A.2). Water as dispersant and laser light backscattering at an angle of 173° was used for the analysis. In the sample holder of the instrument, disposable folded capillary tube was placed with 1ml of sample. Three sets of analysis for particle size distribution and zeta potential measurements were performed for each samples.

3.2.3.3. Surface plasmon resonance studies

UV-Visible spectrophotometer uses visible and adjacent near-UV light to detect the presence of colloidal particles. It is a method used to measure the absorption of light by a sample. The absorbance of the sample are scanned for a wavelength range (250-800nm) which helps to identify the optical properties of nanoparticle (Förster, 2004). Optical properties of nanoparticles are sensitive to concentration, shape, agglomeration and size, which makes this technique, a valuable tool for studying, characterizing and identifying nanoparticles (Haiss et al., 2007). *Perkin Elmer® Lambda 25 UV-Vis spectrophotometer* (Plate A.3) was utilized to analyze the optical property of MgO nanoparticles in this present work. A glass cuvette which contains 1ml of sample was used for the optical analysis and the MgO nanoparticle absorbance was analyzed through scanning the sample from 800-300nm.

3.2.3.4. Crystallinity studies

X – Ray Diffraction (XRD) is a broadly used method to reveal information regarding distribution of elements, chemical bonds, crystal structure, and strains in the crystals by

analyzing the crystals. The main principle of XRD is that electrons in the material scatter X-rays, when the electromagnetic field of the incoming X-rays interact with the negatively charged electrons. The applied X-ray flux field respond to the electrons in the crystal and oscillates with the X-rays beam. These charged accelerated particles then release their individual electromagnetic field, which propagates radially from every scattering source as the scattered waves. These scattered waves can generate both destructive as well as constructive interference to produce a diffraction pattern. Diffraction at an incident angle equal to the Bragg law: $n\lambda = 2d_{hkl} \sin\theta$ where n is the diffraction order, λ is the wavelength, d_{hkl} is the spacing and θ is the diffraction angle (Warren, 1969). ***Bruker® Advanced D8 XRD*** (Plate A.4) was used in the current study to examine the crystallinity and phase formation of sol-gel product and MgO nanoparticles.

3.2.3.5. Functional group identification studies

Radiation interference between two beams yield an interferogram which is the principle of Fourier – Transform Infrared (FTIR) spectroscopy. The interferogram is a signal produced between two beams as a function of path length alteration. Frequency and distance domains are inter-convertible by the *Fourier – transformation* method. The elementary FTIR spectrometer components are sample, interferometer, detector, analog to signal converter, radiation source, amplifier, and computer (Greenstreet et al., 1957). The sample receives the radiation from the source before reaching the detector through an interferometer. A filter is used to eliminate high frequency contributions upon signal amplification and the data are converted to digital form and transferred to the computer by an analog – to – digital converter for Fourier- transformation (Friese et al., 1995). The potassium bromide (KBr) powder is mixed with the sample for the analysis in order to measure the infrared spectrum up to low-wavenumber region (250cm^{-1}). Approximately 0.1-1% sample is well mixed into 250mg of KBr and are made into pellets using a vacuum pelletizer. Later, the sample pellets were scanned from higher to lower wavenumber in order to recognize the functional groups in the sample. The functional group present in the nanoparticles are identified in the current study using ***Thermo scientific NICOLET iS^{TM}10*** (Plate A.5).

3.2.3.6. Size and morphology study

Transmission Electron Microscope (TEM) is utilized for studying and imaging of smaller nanoparticles. The electrons in TEM can pass through the samples and interact with their atoms, in contrast to other microscopes. The electrons are being scattered due to this electron-atom interaction. The final output image is a highly confound interference pattern of diffracted and incident beams. The principle setup of TEM is similar to one of light microscope. The sample is irradiated with the light (in case of TEM with electrons). The sample image is then magnified by means of projection lenses and epitomized on a screen. However, in HRTEM electromagnetic lenses are used in case of glass lenses to guide the electron beam through the microscope (Williams et al., 1996). In our study, ***Tecnai^{TM} G^2 Spirit BioTWIN, FEI Company*** (Plate A.6) was used with a resolution of about 0.34 nm. This instrument has a magnification of 18x-300000x to enlarge and capture smaller sized nanoparticles. For the analysis, the sample is water dispersed and coated in a copper grid which has 100 mesh. The grid is then fixed over the stage of TEM in order to analyze the electron micrograph.

3.2.4. Biological studies

3.2.4.1. Cell culture

The cells that are cryopreserved in liquid nitrogen were thawed for 5 minutes at 37°C in water bath. The medium was eliminated and the cells were conserved in a fresh DMEM medium with streptomycin (100 μg/ml), penicillin (100 U/ml) and 10% FBS in an incubator at 37°C with 50 μg/ml of CO_2 that act as a humidified atmosphere in a T75 flask. Each day, the cells were rinsed with 1X PBS and Trypin-EDTA solution to peel the cells from the sides of the T75 flask and fresh medium was added. The cells achieved 60% of confluence in 3 days. After 3rd day, the cells were passaged into a T25 flask for secondary culture and further analysis, following a similar PBS and Trypsin-EDTA washing. Compound microscope (***OMAX 40X-2000X digital lab LED binocular compound microscope***) was used to analyze and capture image of the cell morphology and cell count.

3.2.4.2. Cytotoxic analysis

The toxicity of MgO nanoparticles towards cell lines were determined based on the mitochondrial dehydrogenase mediated conversion of 3-(4, 5 – dimethylthiazol-2-yl)-2, 5-diphenyltetrazolium bromide (MTT) dye into formazan crystals (Carmichael et al., 1987; Mosmann, 1983). The cells ($1x10^5$ / well) were cultured in 24-well plates in 37°C under 5% CO_2 condition. The nanoparticle samples were added at different concentration and incubated for 24 h along with the cell culture. The sample with medium was detached from the well and the cells were rinsed with PBS (pH 7.4) after incubation. Later, 100 μl/well (5mg/ml) of 0.5% MTT dye was added to the cell and incubated for 4 h. The MTT dye was eliminated and 1 ml of DMSO was added in each wells after incubation of cells for 4 hours. The absorbance at 570 nm was measured with microplate reader using DMSO as blank. The formula for calculating percentage cell viability was mentioned in Equation 1. Absorbance measurements were performed and the required concentration for 50% cell inhibition (IC_{50}) was evaluated from the assay.

$$\% \text{ cell viability} = \frac{\text{Absorbance of nanoparticle treated cells at 570 nm}}{\text{Absorbance of control cells (without nanoaprticle treatment) at 570 nm}} \times 100$$

(Equation 1)

3.2.4.3. Glucose assay

The standard graph with known quantity of glucose was obtained prior to the experiment as mentioned in literature (Mohamed et al., 2009). The standard glucose stock solution was prepared with 450 mg (0.025 M) of glucose in 100 ml of distilled water. 0.2 – 1 ml of standard glucose solutions were added in a test tube and the final volume was made upto 2 ml with distilled water. 1 ml of orange yellow color DNS reagent was added along with the diluted standard glucose solution. The mixture was incubated for 5 minutes in a boiling water bath. The mixture was cooled down and its optical density was observed at 540 nm using portable UV-Visible spectrometer (***Hitachi U-3900H UV-Visible spectrometer***). The same procedure was carried out to measure the glucose present in the medium as well as inside the cells. The 60% confluent 3T3-L1 cells were plated in a 6-well plate and DMEM medium with 10% FBS in an incubator at 37°C and 50 μg/ml CO_2 as humidified atmosphere. The DNS assay was performed using DMEM medium for control (without loading nanoparticle) and cells loaded with nanoparticle (selected

concentration) after every 5 hours of incubation. The medium was washed away after 24 hours of incubation and the cells were lysed by using 1x PBS, 10% SDS and the lysed cells were moved to a corner of the plate by using cell scraper. The contents were centrifuged and the glucose present in the supernatant was measured using DNS assay procedure. The total glucose was calculated by adding the glucose present in DMEM medium after 24 hours of incubation and glucose present inside the cell. This total glucose present in control sample was compared with nanoparticle loaded cell sample to study the insulin resistant reversal ability of MgO nanoparticles.

3.2.4.4. Western blot

After incubating the cells ($1x10^5$ cells/ml) with nanoparticle sample for 24 hours, the cells were gathered and rinsed twice with 10xPBS. The cells were then lysed in lysis buffer which consists of, pH 8, 0.5% Nonidet P-40, 250 mM NaCl, 1x cocktail of protease inhibitor and100 mM Tris-HCl, disrupted by sonication and extracted after 30 min at 4°C. The lysates were then centrifuged at 13000x rpm for 25 min at 4°C. The supernatant was stored as protein sample for further use. The aliquots of cell lysates (supernatant) were separated by 12-15% SDD-PAGE and transferred onto the PVDF membrane. The proteins were blocked with 5% non-fat dried milk and the membrane was incubated for 2 hours with primary Anti-GLUT4 antibody followed by incubation for 30 minutes with anti-mouse IgG secondary antibody. The protein bands were detected at a molecular weight range of ~54 kDa using the ***ChemiDoc^{TM} MP*** Western Blot Detection system (Moon et al., 2011).

3.2.4.5. Fluorescent microscope studies

After incubating cells ($1x10^5$ cells/ml) with nanoparticle sample for 24 hours in a 6 well plate, the cells were collected and rinsed with 1xPBS. 70% ethanol purchased from ACROS organics was used to fix the cells to the cover slip. 0.2 ml of 10 μg/ml propidium iodide was added to the cells and maintained for 15 to 30 minutes. The cover slip containing the stained cells was eliminated from the 6-well plate and positioned on a clean grease free glass slide. The glass slide with stained cells was placed in a fluorescent microscope (***40X-1000X infinity plan EPI Fluorescent microscope FM800TC***) to obtain the microscopic images of the cells and their nucleus. Similarly, the cells were incubated with the nanoparticle sample for 24 hours in a 6 well plate and 0.2 ml of acridine orange

(10 µg/ml) was added to the cells after fixing the cells to the cover slip using 70% ethanol. The fluorescent microscope was used to image the stained cells which gives color to the cell organelles inside the cells such as liposomes depending on their acidity.

CHAPTER 4:

SYNTHESIS AND CHARACTERIZATION OF MgO NANOPARTICLES

4.1. Chemical synthesis

Precursor and the gelling agent that are dissolved in ethanol were first mixed and a white color gel formation was observed immediately. The gel, thus formed, has to be under stirring for 2 hours for the complete formation of rigid gel. Later, the obtained gel was allowed to age for 12 hours in room temperature and dry in oven for 24 hours at 100°C before formation of MgO. After drying process, a pure white powder is obtained as sol-gel product. However, a pale yellow sol-gel powder was obtained when magnesium nitrate is used as precursor as shown in Plate 4.1.
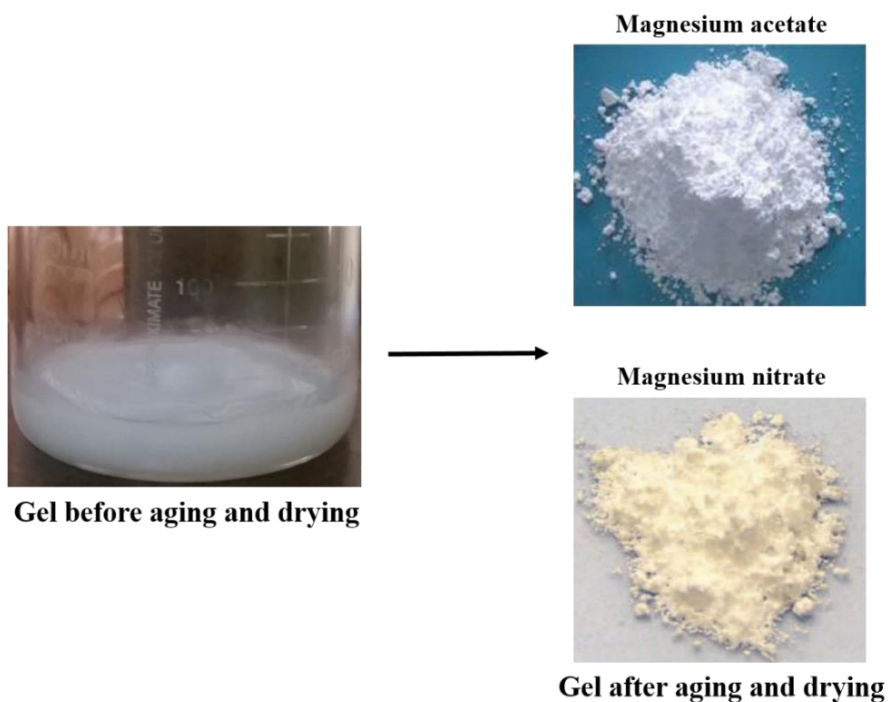
Plate 4.1: Gel before and after aging and drying

4.1.1. Crystallinity of sol-gel product

The crystallinity of sol-gel products were analyzed by using X-ray diffraction (XRD) method. Figure 4.1. shows the XRD peaks of sol-gel samples prepared by using magnesium acetate as precursor. The characteristic peaks for perfect crystals were observed in sample AO (Figure 4.1 A), while in sample AT, AC and AM (Figure 4.1 B, C and D), the characteristic peaks were absent. In sample AO, the atoms are arranged in a perfect crystalline order which makes the x-ray to diffract in order to give characteristic peaks (Warren, 1969). However, in amorphous solids, the atoms are randomly arranged because of which the X-ray diffracts randomly according to Bragg's law and hence no characteristics were observed (Guinier, 1994). Therefore, the three samples (AT, AC and AM) were categorized as amorphous powders. The XRD peaks of sample AO was compared with JCPDS (Joint Committee for Powder Diffraction Standards) to identify the crystallinity of the sample and gave magnesium malonate crystal according to JCPDS file no: PDF 24-1794 (Jaison et al., 2015). Some additional peaks and peak shifts were observed due to the presence of impurity in the sample (Golovchenko et al., 1974).

Figure 4.2 shows the crystallinity and phase formation of sample NO, NT, NC and NM prepared by using magnesium nitrate as precursor. The presence of characteristic crystal peak can be observed in all the samples except sample NT. The presence of additional peaks and peak shifts can also be observed in these four samples due to the presence of impurities (Golovchenko et al., 1974). All the four samples were compared with JCPDS file identify its phase formation and crystallinity from the standard peaks. As there is no characteristic XRD peak for crystals was observed in sample NT (Figure 4.2 F), it is categorized as amorphous powder. XRD peaks of sample NO (Figure 4.2 E) and NC (Figure 4.2 G) were matching with the JCPDS files – PDF 26-1223 and PDF 14-101 corresponding to magnesium oxalate dihydrate (Kumar et al., 2008) and nitromagnesite (Braibanti et al., 1969) respectively. As no JCPDS files were matching with the peaks observed in sample NM (Figure 4.2 F), those data were matched with COD (Crystallography Open database) file which yields a complex crystal ($C_{16} H_{34} Mg N_4 O_{14}$) with the COD file no: 96-151-9079 (Simonsen et al., 1999) along with impurity peaks and

peak shifts. The crystals that are formed as sol-gel product for each sample along with their reference JCPDS and COD file numbers is summarized in Table 4.1.

Table 4.1: Crystallinity of sol-gel products

Sample	Crystallinity	Reference
Sample AO	Magnesium malonate	PDF 24-1794
Sample AT	Amorphous	-
Sample AC	Amorphous	-
Sample AM	Amorphous	-
Sample NO	Magnesium oxalate dihydrate	PDF 26-1223
Sample NT	Amorphous	-
Sample NC	Nitromagnesite	PDF 14-101
Sample NM	$C_{16} H_{34} Mg N_4 O_{14}$	COD file no: 96-151-9079
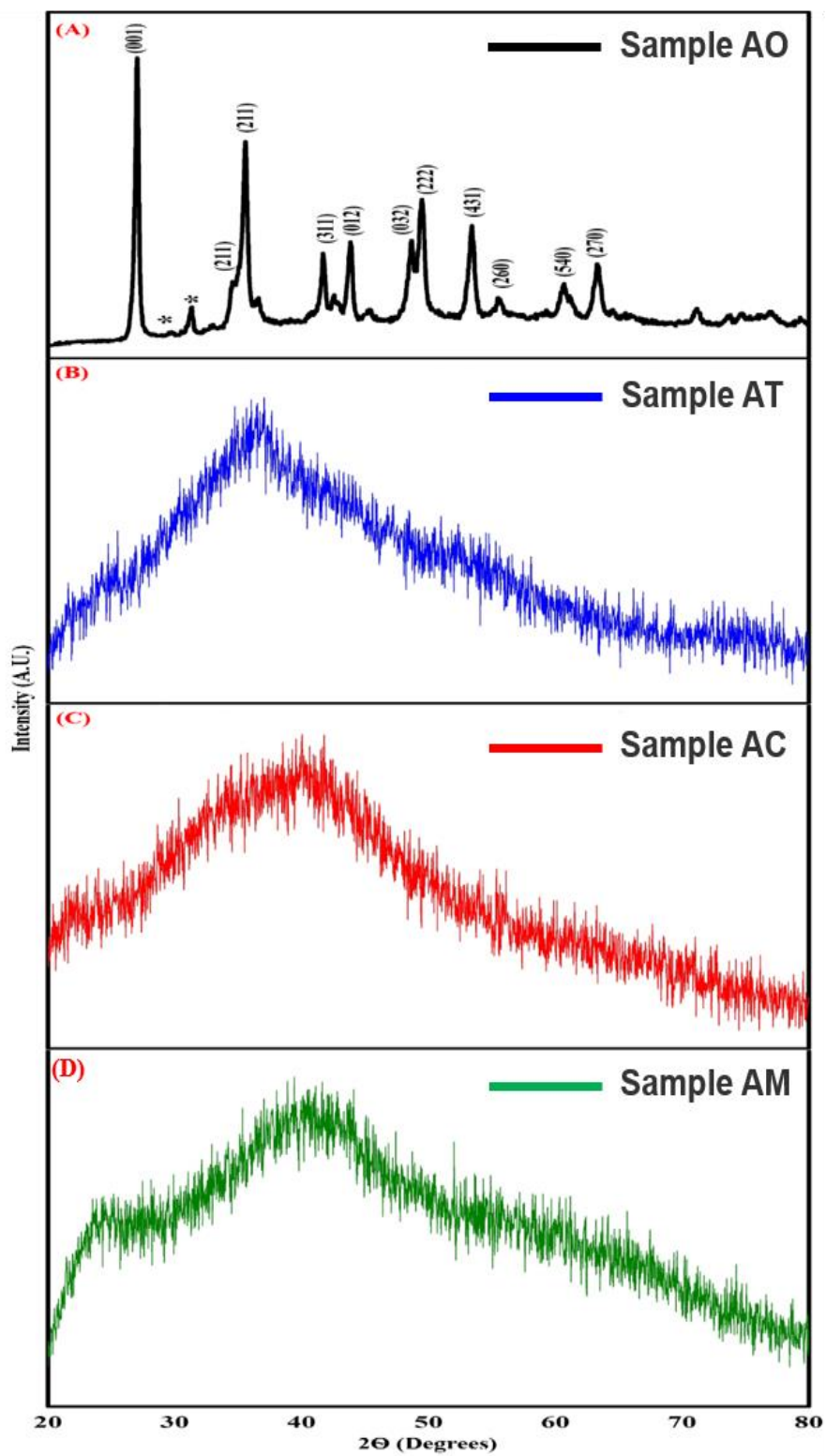
Figure 4.1: XRD analysis of sol-gel product with magnesium acetate as precursor
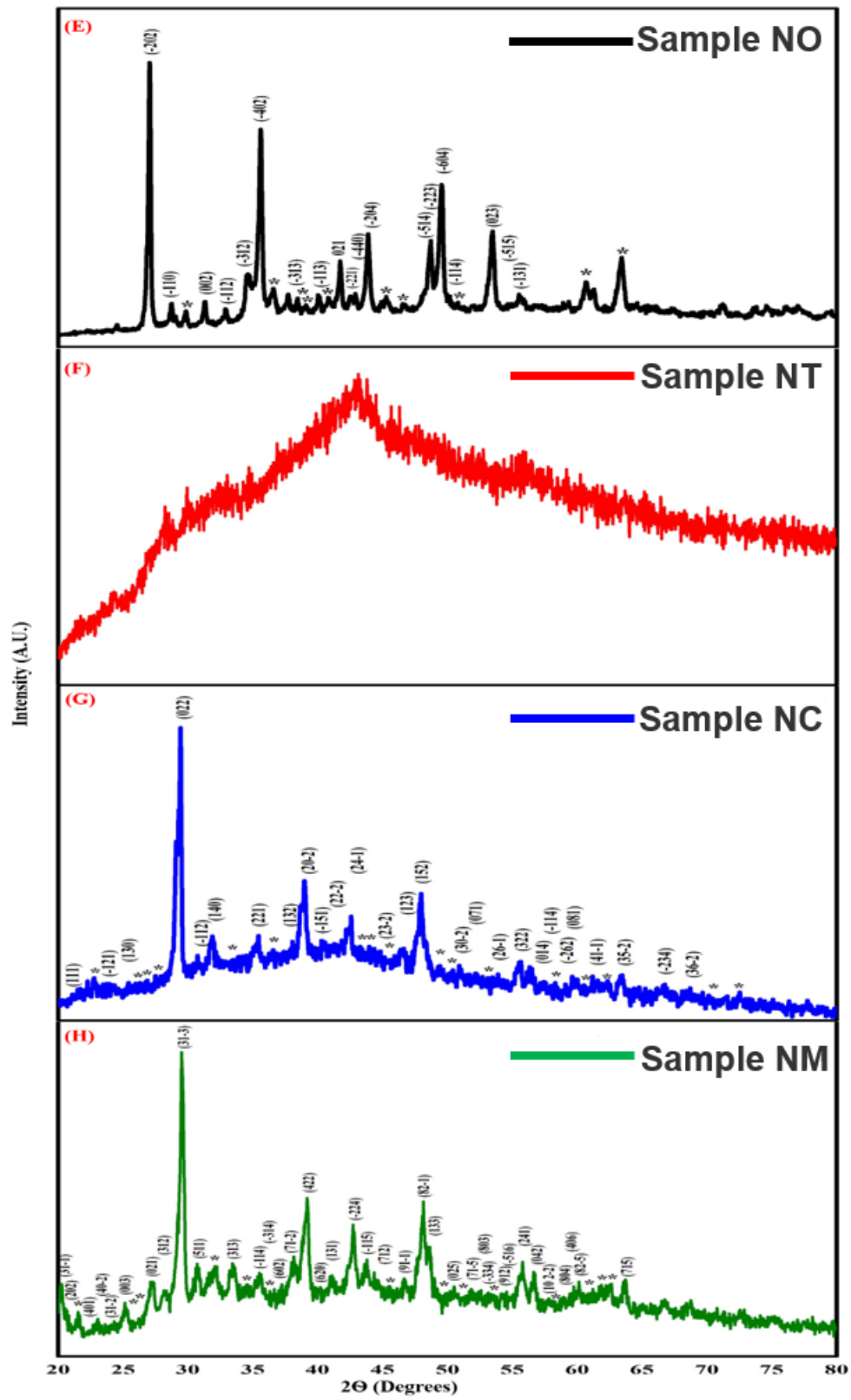
Figure 4.2: XRD analysis of sol-gel product with magnesium nitrate as precursor

4.1.2. Thermal analysis:

Thermal analysis were conducted using TGA to identify the weight loss in sample due to increase in temperature and DSC to identify the heat flow pattern (exothermic or endothermic) of the sample. The thermal analysis that shows the weight loss and the heat flow of samples with magnesium acetate and magnesium nitrate as precursor were shown in Figure 4.3 and Figure 4.4 respectively. By correlating weight loss and heat flow, the molecules that thermally degrade from the sample can be identified. From the thermal analysis of sample AO (Figure 4.3A), the magnesium malonate formed as a sol-gel product undergo two stage degradation to form stable magnesium oxide. Likewise, the amorphous samples AT (Figure 4.3B) and AC (Figure 4.3C) also experience a two stage thermal degradation to form magnesium oxide. But, for the amorphous sample AM (Figure 4.3D) prepared with the mixture of oxalic acid, tartaric acid and citric acid as gelling agent, a three stage degradation was observed with a lower melting transition temperature compared to other three samples. This may be due to the reaction between three gelling agents which is responsible for forming a weak amorphous sol-gel product decreased the melting transition temperature to form stable MgO at low temperature (Wang et al., 2000).

For the samples AO, AT and AC, the first degradation was due to decarboxylation (Doreswamy et al., 2005; Sato et al., 2004), and/or degradation of crystallizing water (Kumar et al., 2008). The second degradation was due to the melting transition of unstable magnesium complex to form stable MgO (Wriedt, 1987; Jaison et al., 2015). However, due to the reaction of three gelling agent in sample AM, the first and second degradations were due to endothermic thermal degradation of crystallizing water and decarboxylation respectively. The third degradation was found to be responsible for yielding stable MgO from unstable magnesium complex (Wriedt, 1987; Jaison et al., 2015). The sol-gel products prepared from magnesium acetate as precursor undergo ~58-78% of weight loss for the formation of pure MgO as mentioned in Figure 4.3. The degradation and melting transition temperatures for all the samples were summarized in Table 4.2. The melting transition of the four samples from the Table 4.2, indicates that the presence of tartaric

acid in the reaction mixture may be responsible for lowering melting transition temperature.
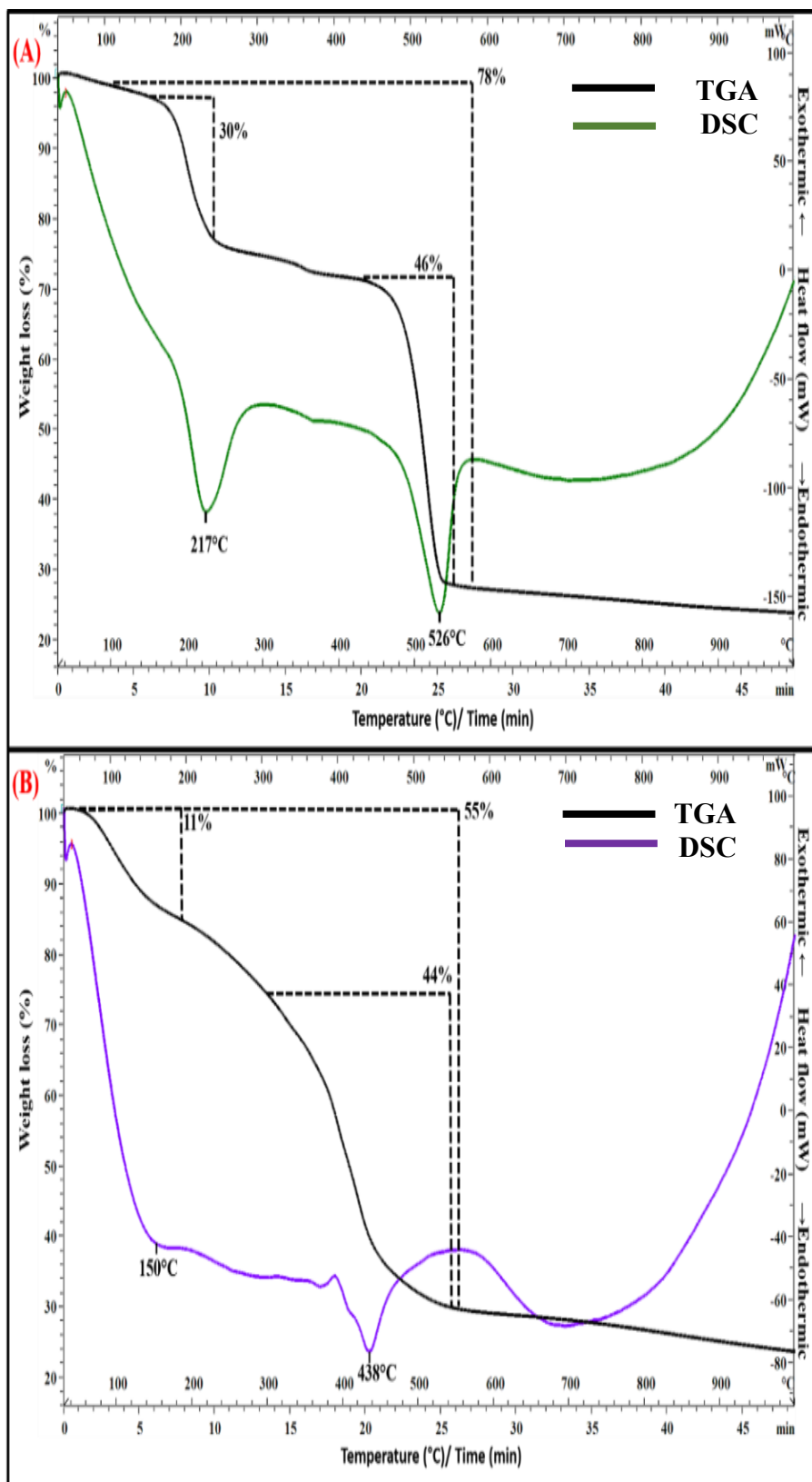
Figure 4.3: Thermal analysis of samples AO (A) and AT (B)
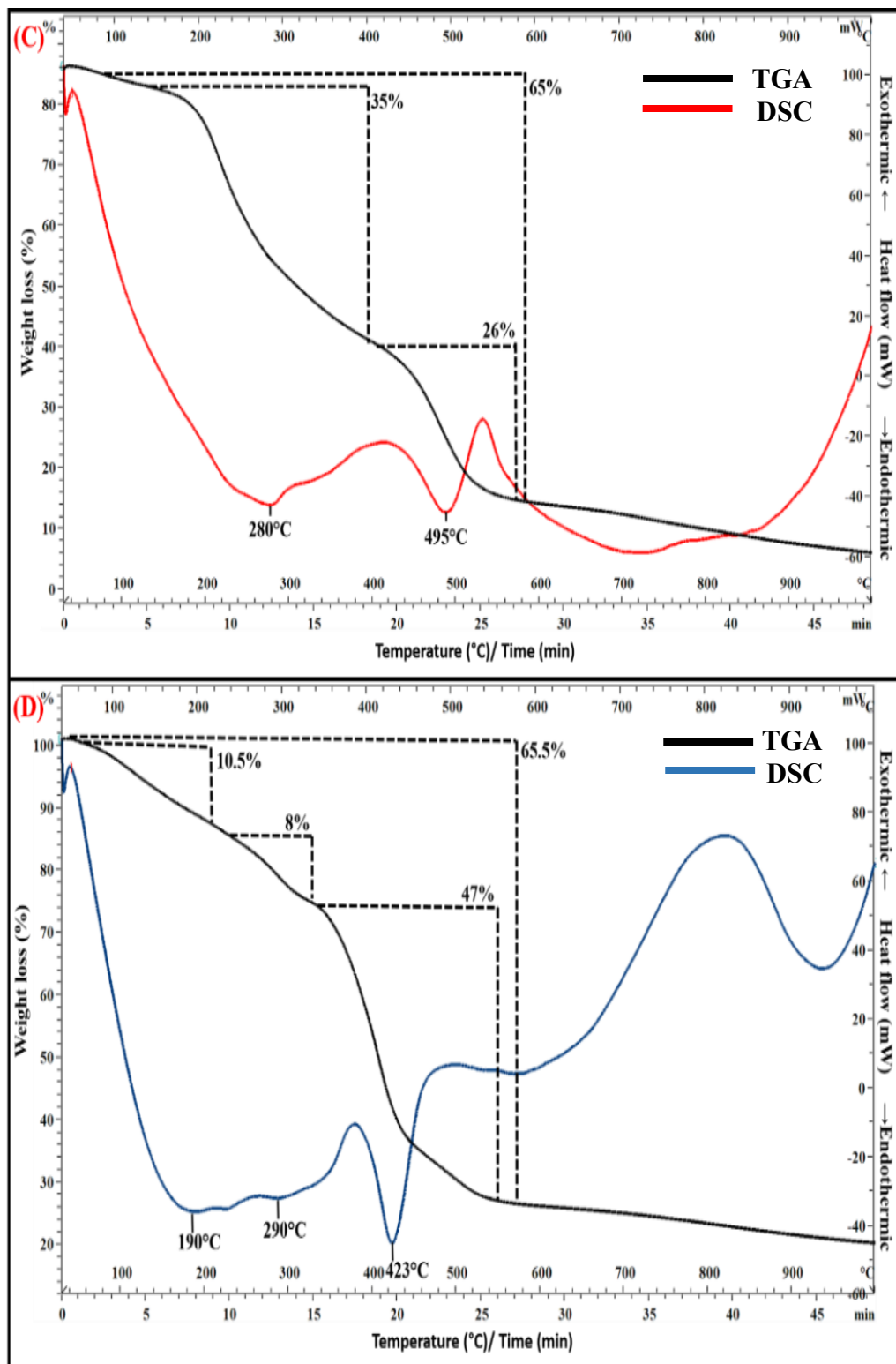
Figure 4.3: Thermal analysis of samples AC (C) and AM (D)
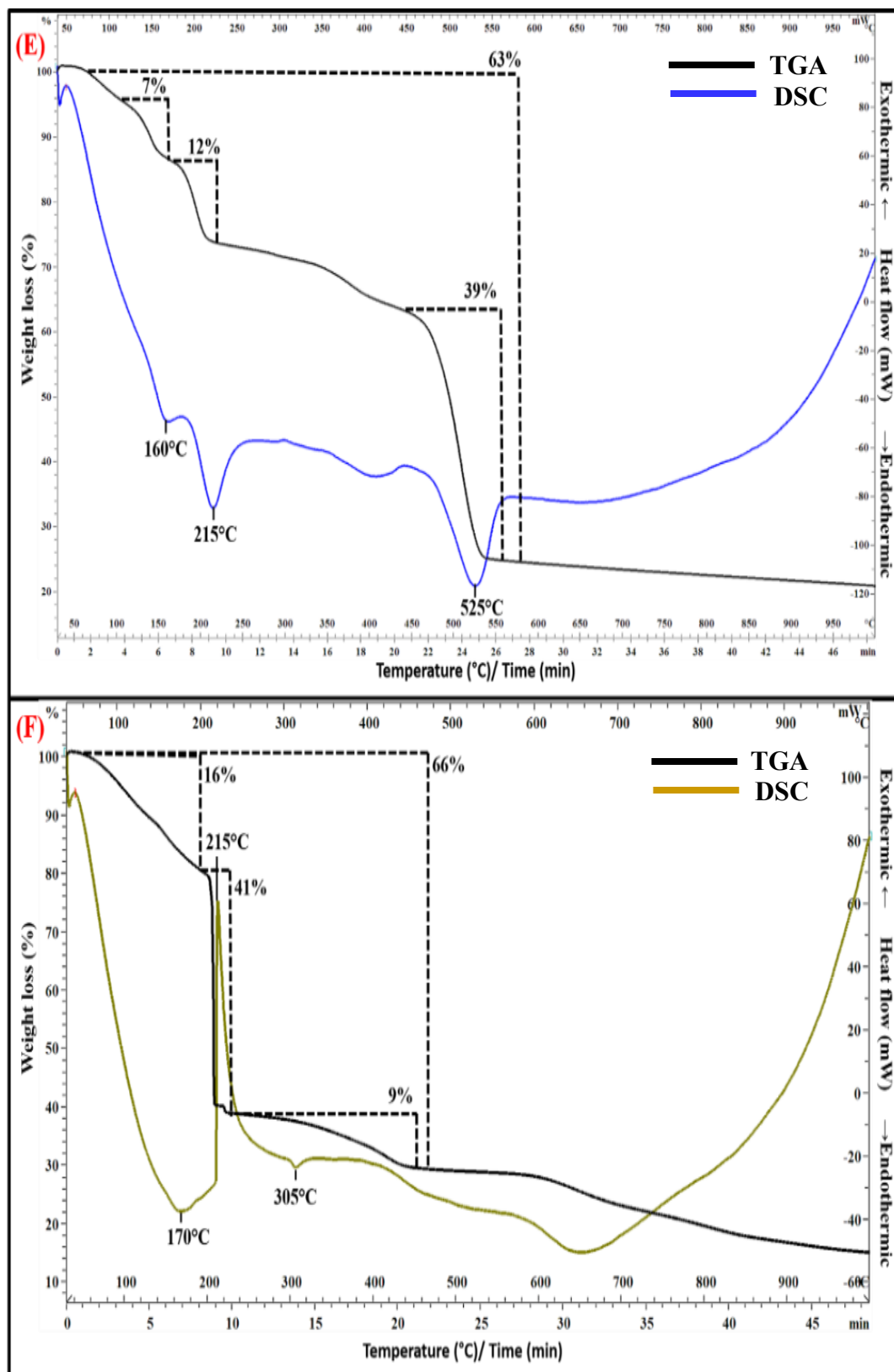
Figure 4.4: Thermal analysis of samples NO (E) and NT (F)
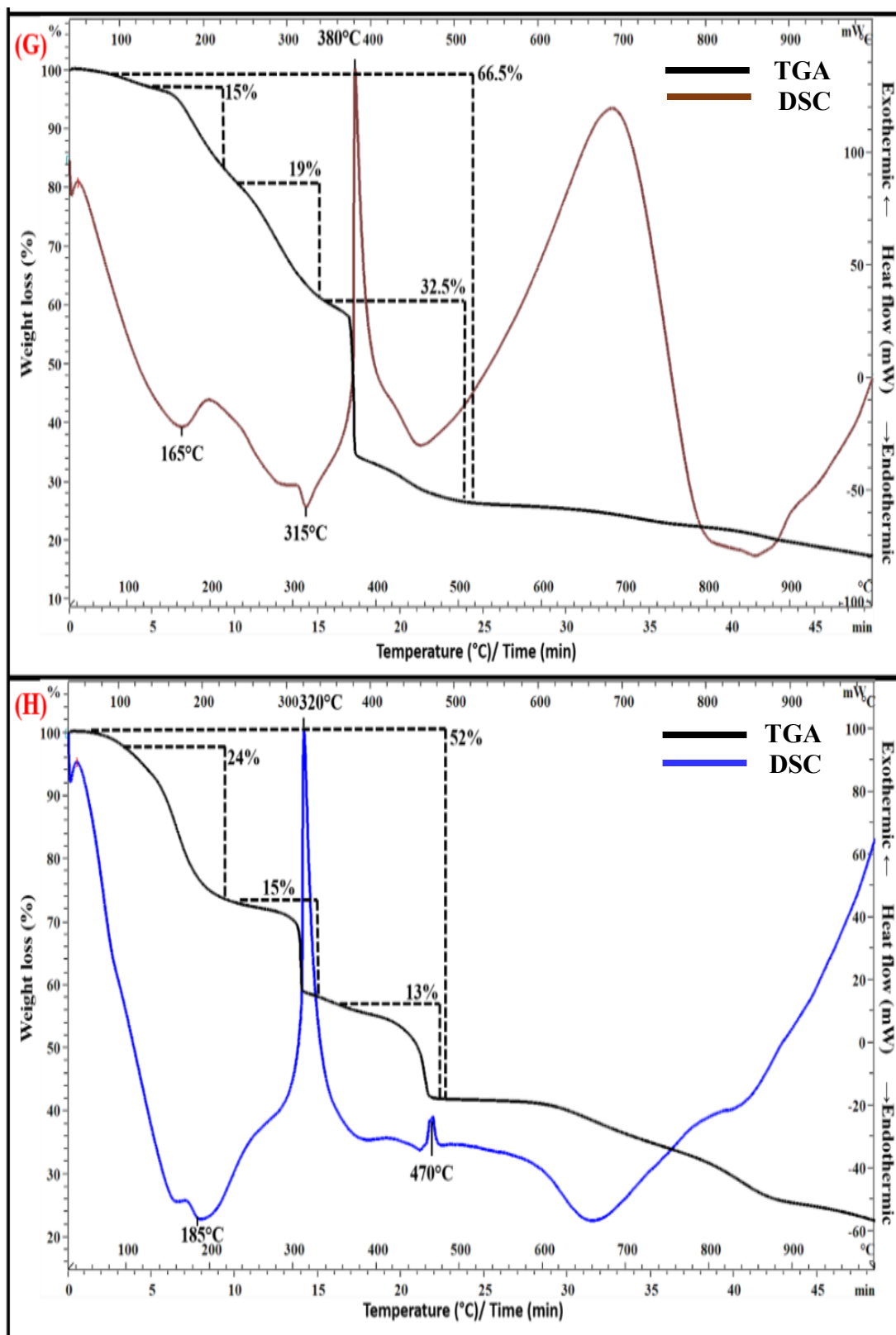
Figure 4.4: Thermal analysis of samples NC (G) and NM (H)

Table 4.2: Degradation and melting transition temperatures of sol-gel products

Sample	1st degradation (From TGA) (°C)	2nd degradation (From TGA) (°C)	3rd degradation (From TGA) (°C)	Melting transition (From DSC) (°C)
Sample AO	140-220°C	430-530°C	-	526°C
Sample AT	70-190°C	300-540°C	-	438°C
Sample AC	120-390°C	400-580°C	-	495°C
Sample AM	80-120°C	230-330°C	340-540°C	423°C
Sample NO	105-165°C	165-220°C	440-560°C	525°C
Sample NT	70-190°C	200-230°C	250-450°C	305°C
Sample NC	130-210°C	220-320°C	340-510°C	380°C
Sample NM	100-210°C	240-330°C	360-475°C	470°C

The thermal analysis of sol-gel products prepared by using magnesium nitrate are different probably due to the presence of nitrate in the reaction mixture. All the samples (NO, NT, NC and NM) show a three stage thermal degradation irrespective of their crystallinity. The first degradation is due to the endothermic thermal decomposition of crystallizing water (Kumar et al., 2008). The second degradation is due to an endothermic decarboxylation in sample NO (Doreswamy et al., 2005; Sato et al., 2004; Kumar et al., 2008), exothermic melting transition of unstable magnesium complex in sample NT, endothermic removal of nitrogen dioxide in sample NC (Keely et al., 1963), exothermic degradation of nitrogen dioxide, carbon, hydrogen, nitrogen and oxidation in sample NM (Tanaka et al., 1991; Yu et al., 2003). The third degradation in sample NO, NC and NM is due to the melting transition of unstable magnesium complex to form MgO and in sample NM oxygen binds to the sample during melting transition (Zhang et al., 2007).

Whereas in sample NT, the third degradation leads to the endothermic formation of MgO as the second degradation yields unstable magnesium peroxide (Golberg et al., 2003). All these four samples experienced ~52-67% of weight loss to form pure stable MgO.

From DSC analysis, the melting transition for amorphous sample NT is observed to be lower compared to other samples. Irrespective of the precursors, sample with tartaric acid as gelling agent yielded MgO at low temperature. Correspondingly, the presence of tartaric acid in sample NM is minimum compared to other samples which makes the sol-gel product from this sample to be a complex crystal rather than amorphous. Hence, it is evident that the gelling agent-tartaric acid in the sol-gel reaction is responsible for reducing melting transition temperature. Furthermore, it is clear that crystallinity plays a significant role in forming stable MgO at lower temperature. The atoms in the crystal are uniformly arranged, due to which high temperature is essential to transform crystalline sol-gel product into MgO crystals. But, the atoms in amorphous powders are randomly arranged due to which low temperature is sufficient to transform it into an MgO crystal. Therefore, it is clear from the melting transition of all the 8 samples that presence of tartaric acid in the reaction mixture helps in lowering melting transition.

4.1.3. Calcination of sol-gel products

The calcination temperature for the formation of MgO nanoparticles were determined from the TG-DSC analysis. Literatures (Yu et al., 2006; Haruta et al., 1989; Meshkani et al., 2009) suggested that the calcination temperatures of nanoparticles were selected at a higher melting transition temperature. In order to modify the shape of the MgO nanoparticles, three calcination temperatures were selected. In this study, all the samples were calcinated for 2 hours (Athar et al., 2012; Mirzaei et al., 2012). Table 4.3 summarizes three selected calcination temperatures for each sample and their average particle size.

4.1.4. Average particle size of all calcinated samples

Average particle size of the calcinated MgO samples were analyzed using Dynamic Light Scattering technique. Various range of nanoparticle sizes were observed as shown in Table 4.3. Most of the average size of calcinated samples were observed to be above

100nm. This may be due to the pre-assumption of DLS technique that all particles of different morphologies are spherical (Lim et al., 2013; Khlebtsov et al., 2011). Despite the pre-assumption, DLS technique can be helpful for preliminary analysis of average nanoparticle size. From these DLS results, three small size nanoparticle with different calcination temperatures will be selected for further characterization.

Table 4.3: Average particle size of calcinated samples from each sample

Sample	Calcination temperature ($^{\circ}$C)	Average particle size (nm) ± PDI
Sample AO	550	141.8±0.611
	650	164.2±0.664
	750	220.2±0.684
Sample AT	500	47.9±0.706
	600	825±0.845
	700	458.7±0.0.697
Sample AC	550	342±0.762
	650	43.8±0.615
	750	91.2±0.547
Sample AM	500	122.4±0.780
	600	122.4±0.790
	700	91.2±0.708
Sample NO	550	105.7±0.559
	650	122.4±0.614
	750	141.8±0.810
Sample NT	400	105.7±0.805
	500	58.7±0.343
	600	105.7±0.332

Sample NC	450	342±0.684
	550	105.7±0.770
	650	122.4±0.436
Sample NM	500	190.1±0.470
	600	141.8±0.623
	700	531.2±0.568

4.1.5. Selection of calcinated samples:

The sol-gel powders calcinated at 500°C from sample AT, 650°C and 750°C from sample AC showed the presence of smaller particles with sizes 47.9±0.706, 43.8±0.615 and 91.2±0.547nm from DLS technique respectively and the graph was included in Appendix D1. As reported by Kim et al (2002), increasing calcination temperature will influence the shape transformation of nanoparticles (Kim et al., 2002). The detailed justification for selecting the calcination temperatures were reported in Table 4.4. Thus, these three calcinated samples were selected for further characterization with the aim of obtaining smaller nanoparticle with different morphology of MgO nanoparticle.

Table 4.4: Calcinated samples selected for further analysis

Sample	Description	Size (nm)	Justification
Sample A	Sample AT calcinated at 500°C	47.9±0.706	Among three calcination temperature, the probability of yielding spherical nanoparticles are higher for first calcination temperature (50-100°C after melting transition) and the smaller size for first calcination temperature was observed in this sample.

Sample B	Sample AC calcinated at 650°C	43.8±0.615	The second calcination (100-200°C after melting transition) was performed with the aim of yielding hexagonal nanoparticles and the smaller size for first calcination temperature was observed in this sample.
Sample C	Sample AC calcinated at 750°C	91.2±0.547	The third calcination (300-400°C after melting transition) was performed with the aim of yielding rod shaped nanoparticles and the smaller size for first calcination temperature was observed in this sample.

4.1.6. Phase formation, chemical composition and morphology of calcinated samples

The XRD analysis of selected calcinated samples A, B and C were shown in Figure 4.5. The characteristic XRD peaks in the calcinated samples were matched with JCPDS files and all the peaks were exactly matching with the file PDF 45-0946 corresponding to magnesium oxide with periclase phase. The increase in peak intensity of samples were directly proportional to the increase in calcination temperature, which indicates morphology change in samples respective to increase in temperature (Mclaren et al., 2009; Yubao et al., 1994).
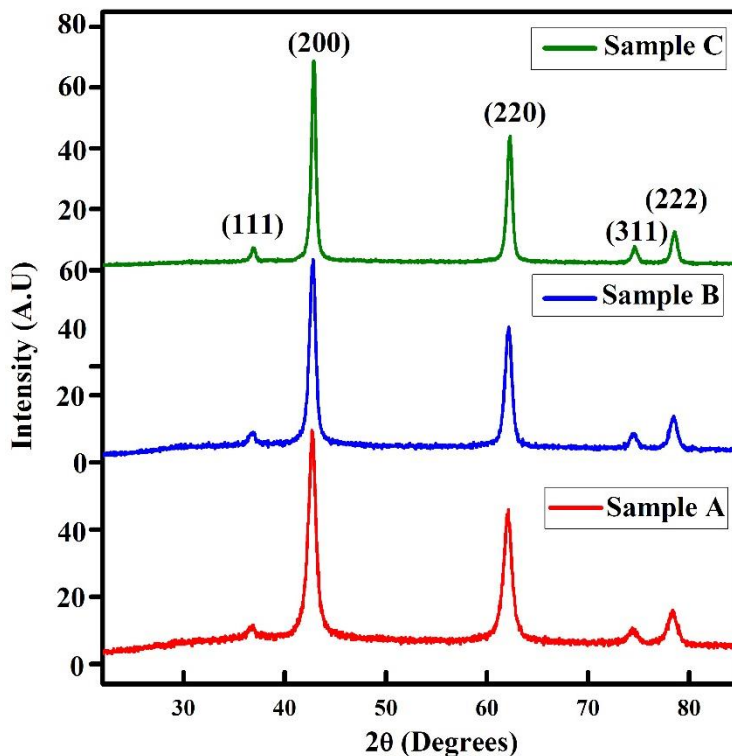
Figure 4.5: XRD analysis of selected calcinated samples

4.1.7. Functional group identification

The functional groups in the calcined samples were characterized using FTIR spectroscopic analysis and the results are shown Table 4.5 and Figure 4.6. The FTIR spectra showed peaks at 3305.5 cm^{-1}, 3246.4 cm^{-1} and 3245.6 cm^{-1}, indicating O-H stretch vibrational mode for the presence of carboxylic acids in all the three samples. The peaks at ~1425 cm^{-1} and ~1083 cm^{-1} which are due to C-O-H bending and C-O stretch vibrations support the presence of carboxylic acid in the samples. The peak at 2359 cm^{-1}, which is only present in sample A does not correspond to any particular peak in the FTIR spectral chart. The presence of peak at 2164 cm^{-1} is due to -CΞC- stretch vibration, representing the presence of alkyne in the sample. The peaks at 856, 583 and 546 cm^{-1} are due to MgO vibrations (Kumar et al., 2008; Tamilselvi et al., 2013; Rezaei et al., 2011; Song et al., 2010). The slight shift in peak wavenumbers between the samples supports potential calcination-mediated shape transformations of the particles (Yu et al., 2003). Previously reported MgO nanoparticles synthesized under different conditions have shown similar functional groups peaks for MgO vibrations (Meshkani et al., 2009; Kumar et al., 2008;

70

Chowdhury et al., 2015). The unique peak of Mg-O vibration at 856 cm^{-1} was only reported by Kumar et al (Kumar et al., 2008), and this peak is due to the formation of periclase MgO phase. The present work, supported by literature, shows the presence of peaks corresponding to carboxylic acid and alkyne, emerging from the reaction between acetate and the gelling agents. These functional groups may act as capping agents to control the size of nanoparticles (Vignesh Subramanian., 2015).

Table 4.5: FTIR spectral chart showing functional groups in calcined samples

Peak position (cm^{-1})			Vibrational mode	Functional group
Sample A	**Sample B**	**Sample C**		
3305.5	3246.4	3245.6	O-H stretch	Carboxylic acid
2359.5	-	-	-	Additional/Impure peak
2164.3	2164.4	2164.8	-C≡C- stretch	Alkynes
1425.8	1426.2	1427.9	C-O-H bending	Carboxylic acid
1083.1	1084.2	1085.5	C-O stretch	Alcohol, carboxylic acid, ester, ether
856.7	857.2	857.2	δ (O-C=O) + v (Mg-O)	Magnesium oxide
583.6	585.2	589.4	Mg-O	Magnesium oxide
546.1	553.8	556.1	Mg-O	Magnesium oxide
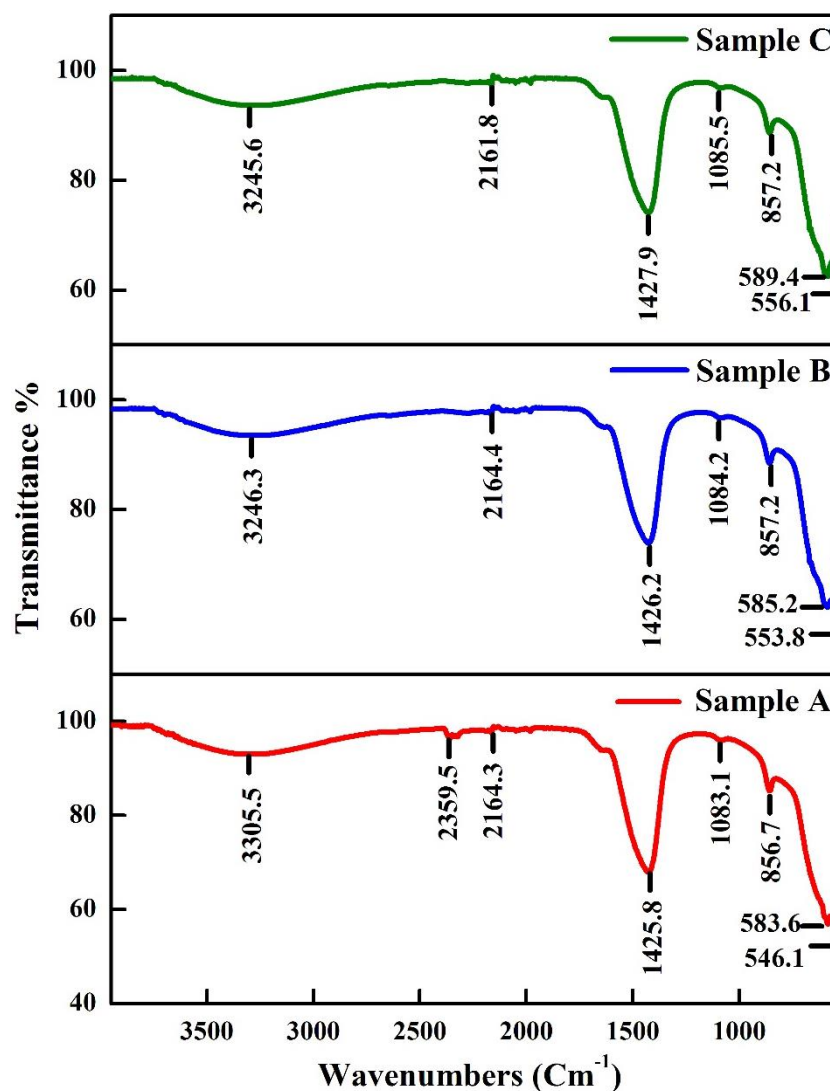
Figure 4.6: FTIR spectra of calcined samples

4.1.8. Morphology analysis

Figure 4.7 shows transmission electron micrograph of MgO nanoparticles from the calcined samples. The images show agglomeration in all the three samples, potentially due to the low dispersant capacity of the solvent used to suspend the samples (Tso et al., 2010). The particles from sample A were more agglomerated with a spherical shape as shown in Figure 4.7 (A). The micrograph at 18500 magnifications shows a wide size distribution of the particles and this is in agreement with the DLS studies. The crystallite size obtained from the XRD analysis is also in agreement with the particle size determined from TEM analysis. According to Demir et al., nanoparticles are formed from crystallites

hence crystallite size should be smaller than the particle size obtained from TEM (Demir et al., 2004). From the measurements, the crystallite sizes obtained are smaller than the nanoparticle sizes for samples A and B. However, the size of the crystallites are larger than the width of rod-like nanoparticles in sample C as the arrangement of crystallites varies with different particle shapes (Liu et al., 2004). The sample size ranges were 25-79 nm for A and 60-67nm for B. The rod-like nanoparticles in C showed a width of ~12nm. It can also be noted that the particles in samples B and C are in transformation phases, from spherical to hexagonal and hexagonal to rod-like shapes respectively. Hence, optimization of the calcination time and the properties of the solvent to suspend the powder samples are critical to establish uniform particle morphology and size.
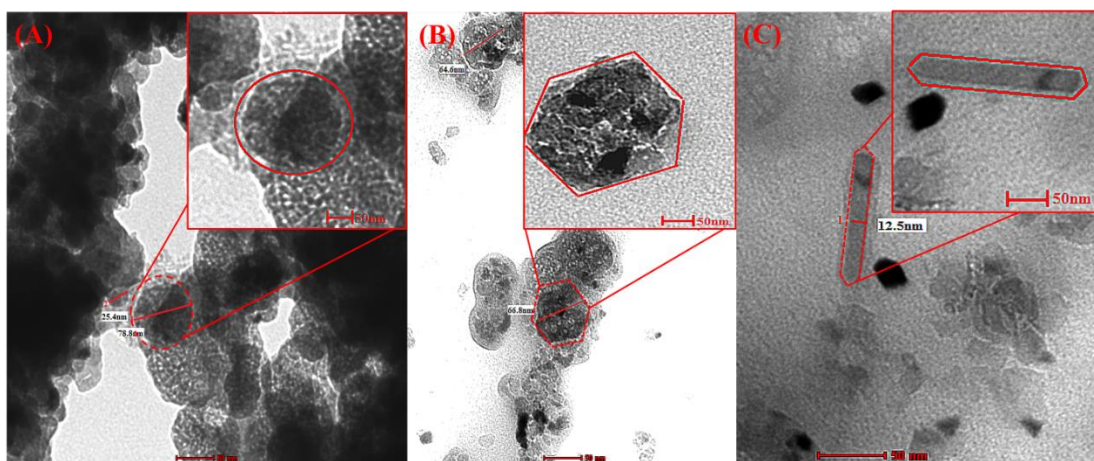
Figure 4.7: TEM micrograph of MgO nanoparticles at 18500 magnification for (A) Sample A - spherical, (B) Sample B - hexagonal and (C) Sample C – rod-like.
Inset: Close up micrographs of individual particles

4.1.9. Calcination mediated morphological evolution of MgO nanoparticles

The inset micrographs of individual particles at 18500 magnification for all the three samples were shown Figure 4.7. The images show that the particles evolve in morphology as a function of increasing calcination temperature. It can be noted that sample A calcined at a low temperature (500°C) generated spherical nanoparticles (Figure 4.7 A) whereas samples B and C calcined at 650°C and 750°C yielded hexagonal (Figure 4.7 B) and rod shaped nanoparticles (Figure 4.7 C) respectively. Increasing the calcination temperature enlarges the particle size and modify their shape. Calcination under elevated temperatures

results in high frequency molecular formation in the lattice assembly, impacting the emergence of regularly shaped nanoparticles. Kim el al., used sol-gel dip coating method to prepare TiO_2 thin films and examined their properties by calcinating them at various temperatures. They reported increased crystallite size with increasing calcination temperature (Kim et al., 2002). Similarly, wet precipitation of magnesium hydroxide nanoparticles by Lv et al., showed that that increasing calcination temperature resulted in the formation of needle-like and lamellar shaped nanoparticles. It can be observed from the reported data that a mild increase in temperature from 2-30°C could facilitate a morphological change (Lv et al., 2004). Apart from temperature driven morphological changes, morphological evolution of iron oxide nanocrystals has also been reported by Cheon et al (Cheon et al., 2004). The work explained the formation of iron oxide nanocrystals into different morphologies such as diamonds, triangles and spheres via a thermolysis process and portrayed the crystallographic differences between the varied morphologies. Moreover, Mastuli et al., 2014, achieved different shapes of MgO nanoparticles, including sphere, cube and cuboid by using oxalic and tartaric acid as gelling agents in sol-gel synthesis. Spherical nanoparticles have a high probability of penetrating into cell membranes (Chithrani et al., 2006) and are highly beneficial in targeted drug delivery systems. Similarly, hexagonal and rod shaped nanoparticles have demonstrated advantageous applications in cell marking (Lin et al., 2005) and biosensing (Lee et al., 2006; Jain et al., 2007). Hence, the present work is significant in synthesizing MgO nanoparticles with different morphologies under comparatively lower temperature conditions and reduced synthesis time for beneficial in biomedical applications.

4.1.10. Stability analysis

The stability of the calcined samples was studied using the DLS technique to determine the zeta potentials of the samples. The data for the zeta potential of the samples at neutral pH are shown in Figure 4.8 (A). The zeta potentials of the samples under neutral pH conditions were negative, indicating a negative surface charge. The electronegative zeta potential is typical for most metal oxides (Patil et al., 2007; Zhang et al., 2008). The MgO nanoparticles contain Mg^{2+} (metal) and O^{2-} on its surface. The samples are incipiently stable with a negative zeta potential below -10mV (áO'Brien, 1990; Hanaor et al., 2012).

According to Atalay et al (Atalay et al., 2014) and Qian (Qian, 2014), surface charge of the nanoparticles depend on the size and morphology of the particles. The zeta potentials of samples A and B in deionized water at neutral pH are almost the same due to their similar average particle sizes of - 47.9 nm and 43.8 nm respectively. However, the zeta potential of sample C at neutral pH is highly negative compared to A and B, and this is due to their rod-like morphology. The larger contact area of rod shaped nanoparticles compared to spherical (Chithrani et al., 2006) and hexagonal shapes as well as their high charge density of lattice points is the reason for their high electronegativity.

Additionally, the calcined samples were suspended in distilled water under pH variations as shown in Figure 4.8 (B) in order to identify their isoelectric points (pI) and stability of the nanoparticles. The pH values of the media were adjusted to pH 3, 5, 7, 9 and 11 using 1M HCl or NaOH. Sample A showed a pI of 3 while samples B and C did not demonstrate charge neutrality in this region. Further increase in acidity may help reach the pI point. Samples A and B achieved electronegative stability at pH 9 (-28.7mV) and 11 (-27.1mV) respectively. The increase in electronegativity with increasing pH is due to deprotonation (replacement of hydrogen ions with hydroxide ions) of the metal oxide. However, the maximum zeta potential value of sample C was obtained at pH 9 (-12.9mV), which is lower than accepted electronegativity for stable colloidal systems (-30mV) (Greenwood et al., 1999). This could mean that nanoparticles generated from sample C does not possess surface charge quantum property to be regarded as colloidally stable and further formulation is necessary to increase its stability. Reported data suggest that the isoelectric point of nanoparticles depends on the nanoparticle size where pI at low pH (1-3) is achievable for smaller nanoparticle (Finnegan et al., 2007; Tso et al., 2010).
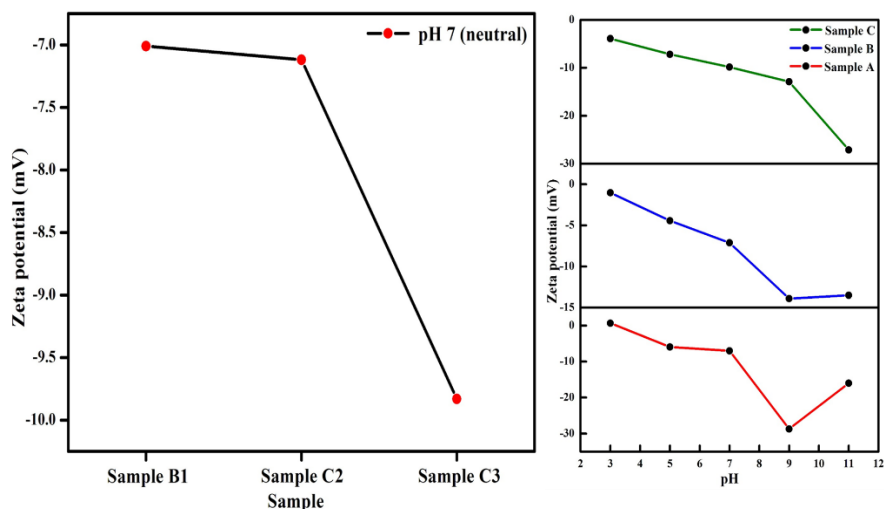
Figure 4.8: Zeta potential of MgO nanoparticles samples at (A) Neutral pH (B) different pH

4.2. Green synthesis

The aqueous leaf extracts were prepared by using water as solvent in 1:10 (w/v) ratio. The water mediated extraction process yields most of the phytochemicals and are non-toxic and hence highly recommended for biological studies (Cork et al., 1991). In green synthesis of MgO nanoparticles, the precursor is dissolved in distilled water in which leaf extract were added under constant stirring and the mixture was heated at different temperature. A color change from dark (color of extract) to pale color was observed after heating process. This indicates that the phytochemicals in the mixture degrades to act as a reducing agent and stabilizing agent (Iravani, 2011) in the formation of MgO nanoparticles. Synthesis parameters such as precursor concentration, extract concentration, time and temperature of heating were optimized to obtain smaller sized nanoparticles.

4.2.1. Optimization of process variables

4.2.1.1. Effects of extract concentration on nanoparticle synthesis

The UV-Vis absorbance and the average particle size were analyzed for each sample to select the extract concentration that yields smaller nanoparticles. Mie theory states that light absorbance is directly proportional to the size of metal nanoparticles, as they are

conductors and possess surface plasmon resonance (Kelly et al., 2003). But, Metal oxide nanoparticles do not obey Mie theory as it is a semi-conductor in which a gap is exist in between the valence and conduction band (Nicollian et al., 1982). This is the reason behind the absorbance of metal oxide nanoparticle in UV region (320nm) (Alwan et al., 2015; Umar et al., 2011) and the reason behind using X-ray photoelectron spectroscopy to analyze metal oxide nanoparticles (Lanje et al., 2010; Bora et al., 2013). Therefore, for the optimization of extract concentration, nanoparticle formed with lower average size and higher absorbance is desirable. The graph correlating average particle size and absorbance with different synthesis parameters for optimizing the extract concentration for sample AT, AB, AP, NT, NB and NP were mentioned in Figures 4.10-4.14 respectively.
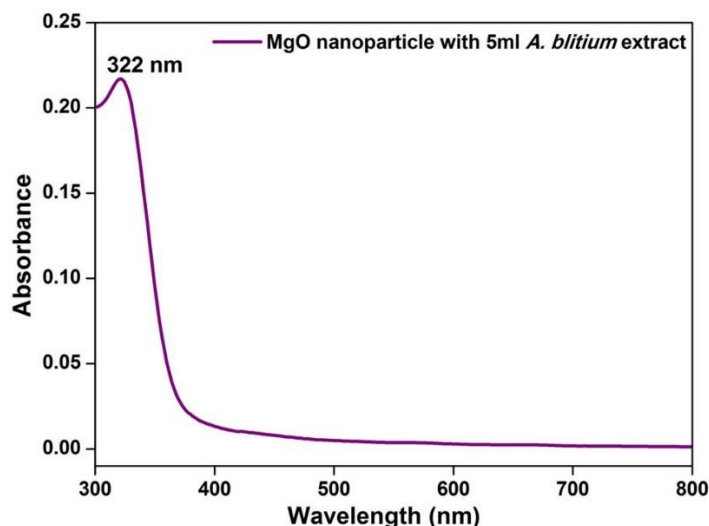
Figure 4.9: Absorbance of MgO nanoparticle at 320nm

The absorbance at 320nm from Figure 4.9 shows the formation of metal oxide nanoparticle (Alam et al., 2006; Arefi et al., 2012; Yu et al., 2012). For sample AT, the absorbance for 5ml of *A. tricolor* extract concentration is found to be lower compared to 10 and 15ml of extract concentration as in Figure 4.10. According to Shankar et al (2005), the lower absorbance indicates lower concentration of nanoparticles is formed with uniform size (Shankar et al., 2005). The yield of nanoparticle is low for 5ml of *A. tricolor* extract in sample AT with smallest size of nanoparticles formed, compared to other extract concentrations. Similar results were observed by varying parameters such as temperature

and time for heating. Therefore, 5ml extract concentration was selected as the optimum extract concentration for sample AT. Sample AB in Figure 4.11 showed that the absorbance for 15 ml of *A. blitum* extract was observed to be higher with average size higher compared to 10ml and 5 ml extract concentration. According to Iravani (2011), higher concentration of extract may increase size of nanoparticles (Iravani, 2011). Nanoparticles prepared with 5ml of extract is undesirable because the absorbance is low with high average size. Hence, 10ml of *A. blitum* extract is selected as the optimum extract concentration for sample AB.
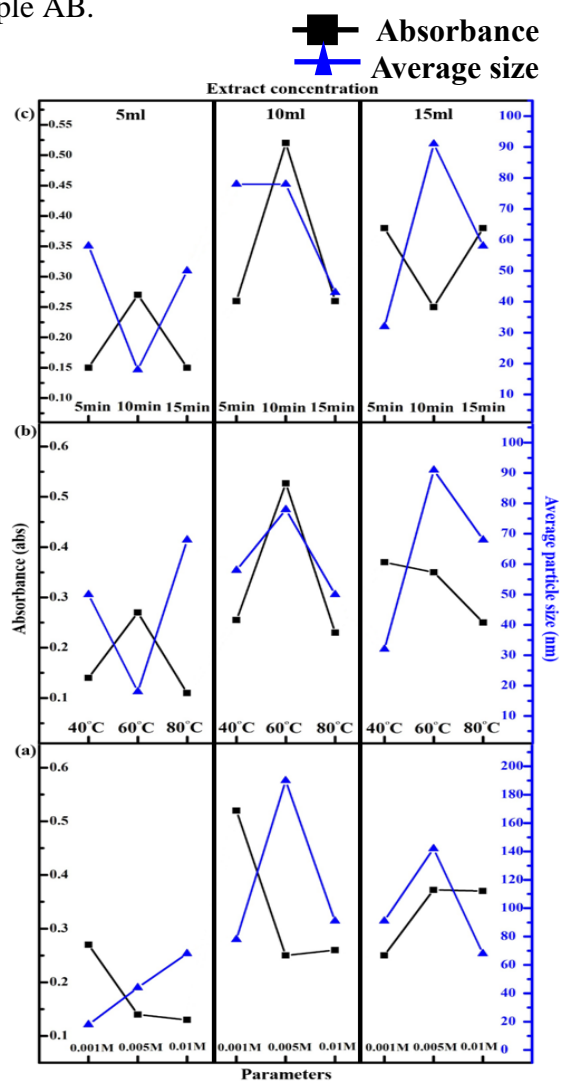
Figure 4.10: Average size and absorbance at 320nm for different extract concentration with different parameters (a) Precursor concentration, (b) Temperature, (c) Time in sample AT
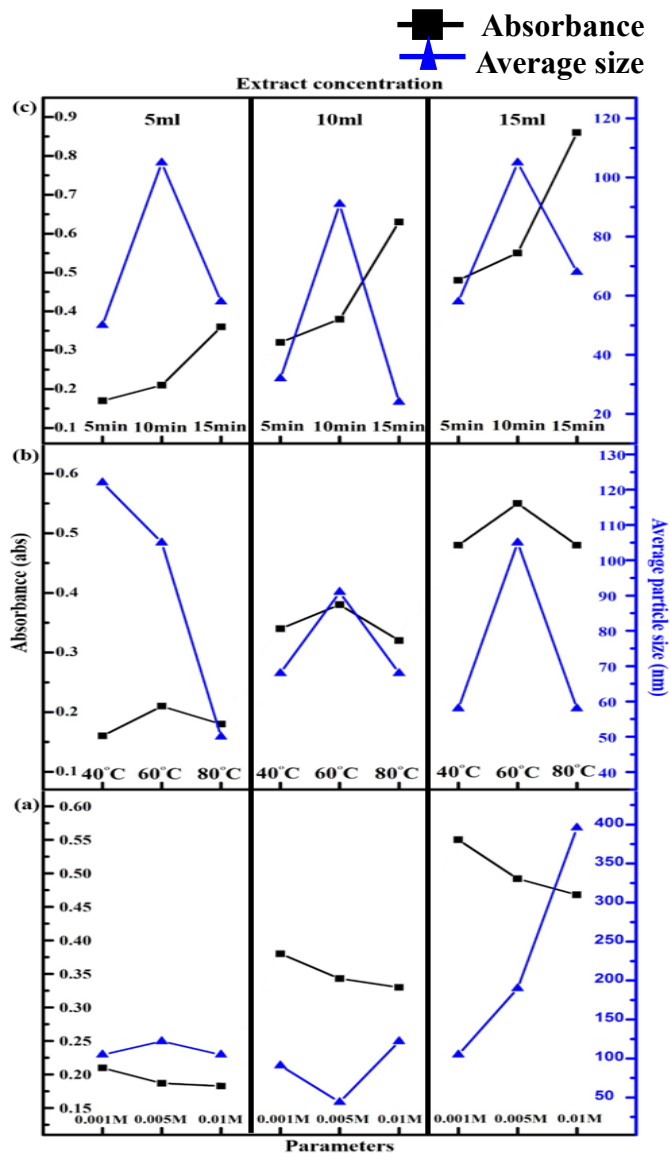
Figure 4.11: Average size and absorbance at 320nm for different extract concentration with different parameters (a) Precursor concentration, (b) Temperature, (c) Time in sample AB

For sample AP, 15ml of extract concentration is selected for the synthesis of smaller nanoparticle. According to Bar et al (2009), higher concentration of extract can also yield smaller nanoparticles, as the threshold concentration to form nucleation is higher (Bar et al., 2009). From Figure 4.12, it is clear that the nanoparticle prepared with 10ml of *A. paniculata* extract acts as a threshold point whereas 15ml of extract yields smaller particles with higher absorbance. The extract concentration for synthesizing smaller MgO

nanoparticle with magnesium acetate as precursor is different for three different plant species. This is due to the difference in the quantity of phytochemicals in plant species (Park et al., 2011; Nune et al., 2009) and the yield of phytochemicals through water mediated extract method as shown in Table 3.2 (Zuas et al., 2014).
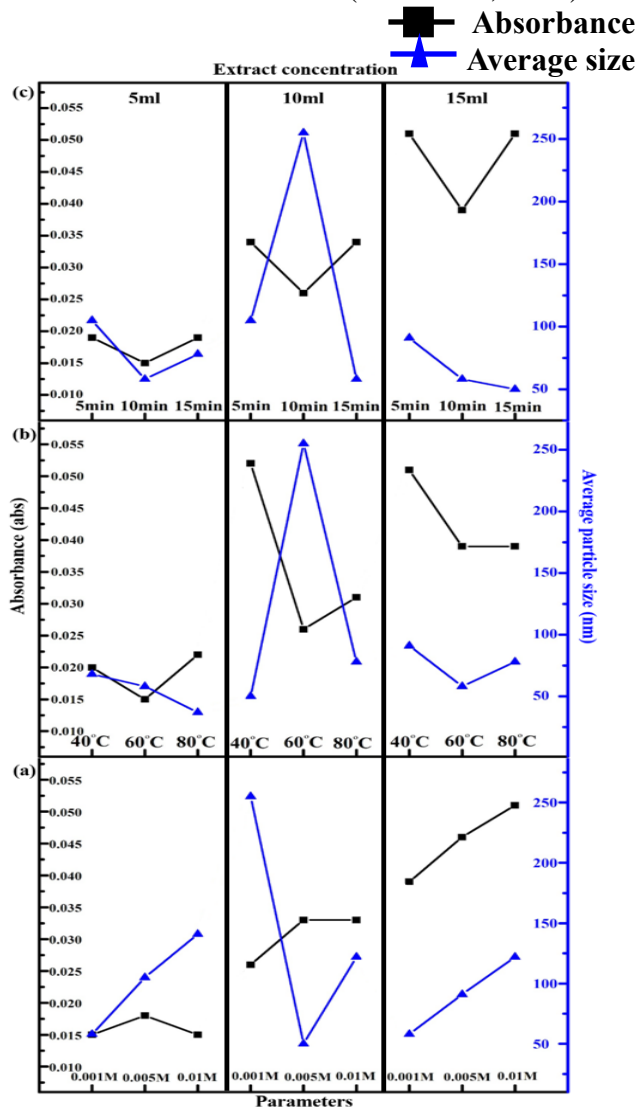
Figure 4.12: Average size and absorbance at 320nm for different extract concentration with different parameters (a) Precursor concentration, (b) Temperature, (c) Time in sample AP

Similar to MgO nanoparticles prepared with magnesium acetate, different extract concentration were selected as optimum concentration based on their ability to yield smaller sized nanoparticles. In both sample NT and NB, 10ml of plant leaf extracts were

selected for further optimization as it is observed from Figure 4.13 that the higher and lower concentration yields bigger sized nanoparticles. 5ml of *A. paniculata* extracts were selected in sample NP as shown in Figure 4.14 for further optimization as the lower concentration extract yielded smaller nanoparticles compared to high concentrations. Based on the size and absorbance analysis obtained from different extract concentration and synthesis parameters, mechanism of nanoparticle formation has been proposed and discussed in section 4.2.1.2.
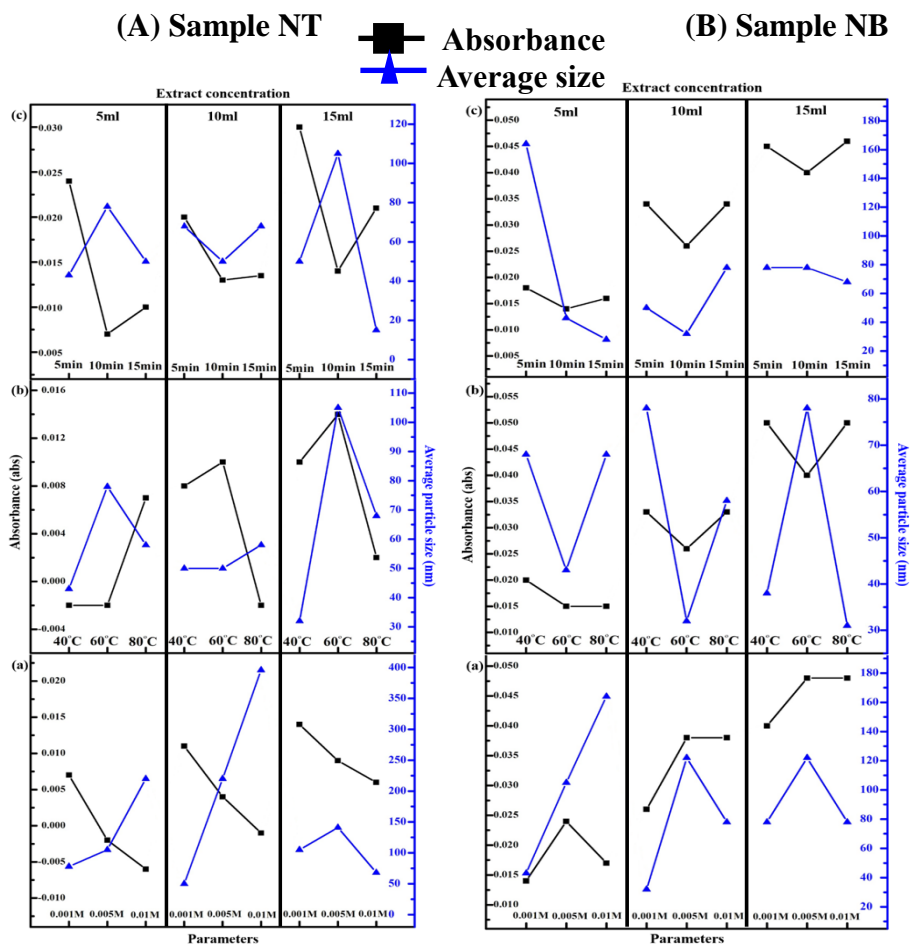
Figure 4.13: Average size and absorbance at 320nm for different extract concentration with different parameters (a) Precursor concentration, (b) Temperature, (c) Time in sample NT and NB
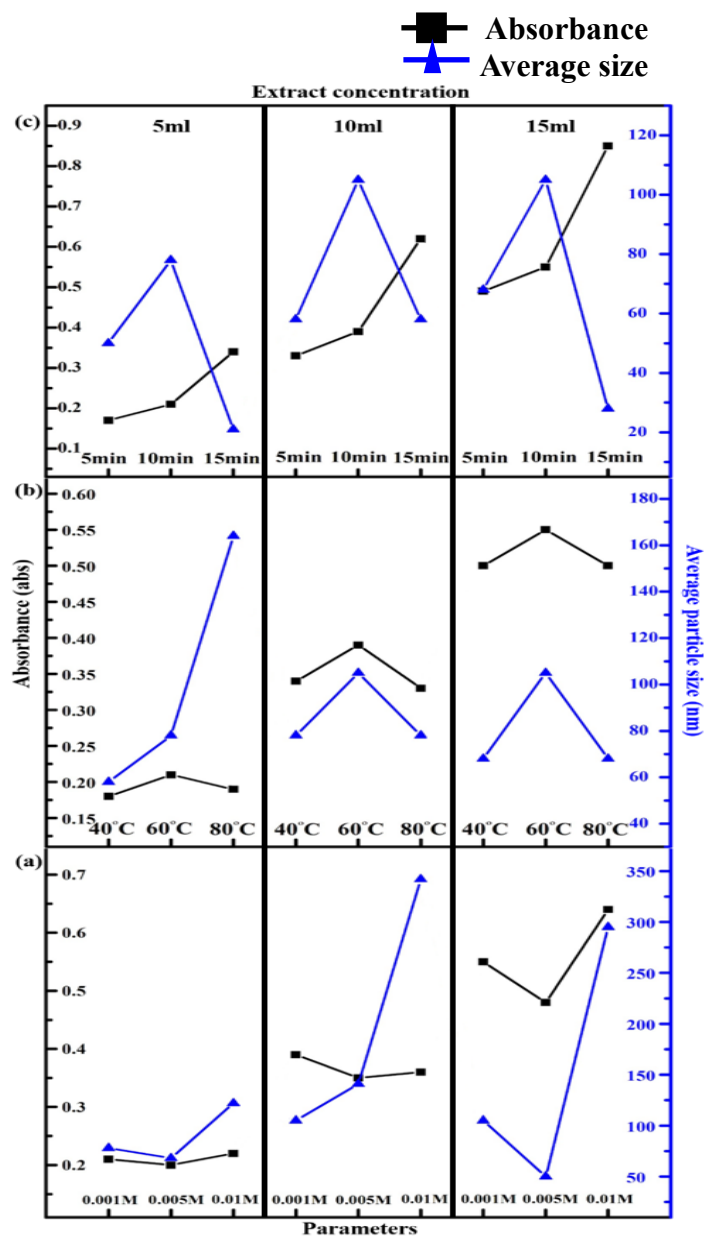
Figure 4.14: Average size and absorbance at 320nm for different extract concentration with different parameters (a) Precursor concentration, (b) Temperature, (c) Time in sample NP

4.2.1.2. Mechanism of action in green synthesis of MgO nanoparticles

The proposed mechanism in Figure 4.15 explains how the extract concentration influences the particle size. Figure 4.15 (A) showed the mechanism of MgO nanoparticles formation whereby 5ml extract concentration is selected for optimization. The nanoparticle size was noticed to increase as the extract concentration increases. However Figure 4.15 (B) clearly shown that the 10ml extract concentration yields smaller sized nanoparticles than 5 and

15ml. This may be resulted from the action of high extract concentration in interrupting the formation of larger nanoparticles. However, it was showed that 10ml of extract has been the threshold concentration for nanoparticle formation, higher concentration will lead to larger particle formation. The stability of the particle will decrease as the concentration increases which affect the size. The Figure 4.15 (C) is the proposed mechanism whereby 15ml of extract yielded smallest nanoparticle size. The threshold concentration for the nanoparticle formation may be higher in this reaction. Different mechanism with different extract concentration is observed as the phytochemicals and their composition in each plant species that are responsible for nanoparticle formation are different. For example, certain literatures suggests that flavonoids are responsible for leaf extract mediated nanoparticle formation (Huang et al., 2011; Krishnaraj et al., 2010). If the presence of flavonoids are higher in extract, low concentration is sufficient to convert dissolved precursor into smaller nanoparticles and vice versa. From the literatures (Noori et al., 2015; Gupta et al., 1983), it is proved that all the three plants used in this current study contains 30-35% of flavonoids and showed that flavonoid plays a significant role in determining the extract concentration and nanoparticle formation. After evaluating and selecting the optimized extract concentration to be used for synthesizing smaller MgO nanoparticles, the effect of precursor concentration, temperature and time of heating to be used in the reaction was evaluated and optimized by using absorbance from UV-Vis spectrometer. The absorbance helps in determining the nanoparticle yield through which the best parameter can be optimized.
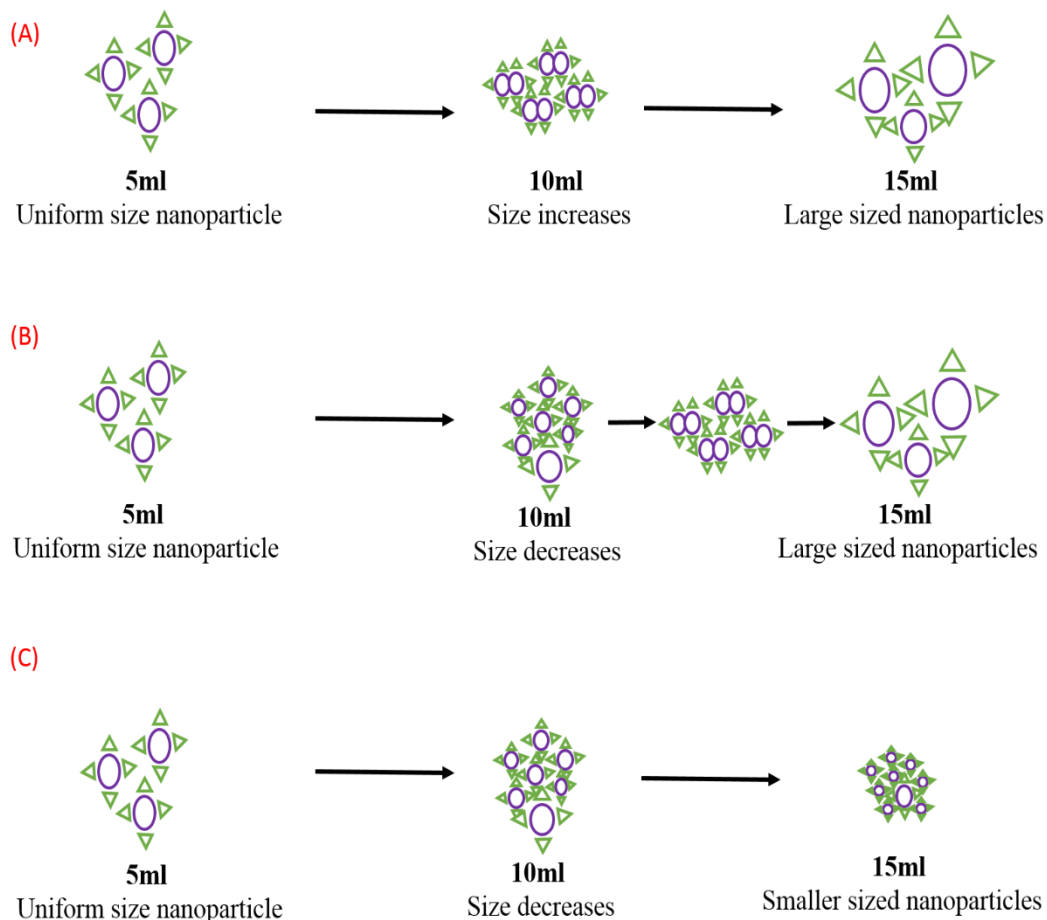
Figure 4.15: Proposed mechanism for MgO nanoparticle formation with (A) 5ml, (B) 10ml and (C) 15ml

4.2.1.3. Effect of precursor concentration

Three precursor concentrations namely 0.001M, 0.01M and 0.1M were used to study the effect of precursor concentration in MgO nanoparticle synthesis. When magnesium acetate was used as the precursor, the absorbance were observed to be high in 0.001M of precursor concentration as shown in Figure 4.16 (A, B, C). While, the characteristic absorbance at 320nm for metal oxide was observed only for 0.001M of precursor concentration when magnesium nitrate is used as precursor as shown in Figure 4.16 (D, E, F). This shows that lower magnesium acetate concentration is able to produce higher yield of nanoparticles, while the nanoparticle formation is observed only at lower magnesium nitrate concentration.
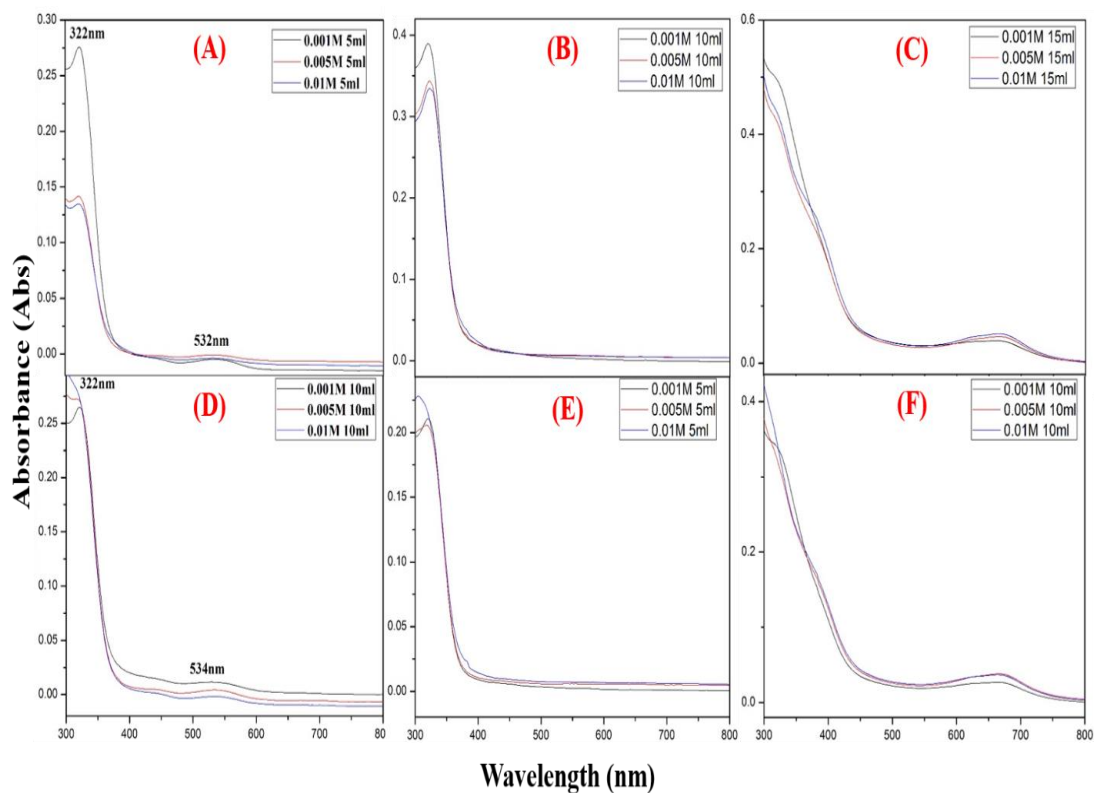
Figure 4.16: UV-Visible absorbance for nanoparticles formed with selected extract concentration of (A) sample AT, (B) sample AB, (C) sample AP, (D) sample NT, (E) sample NB, (F) sample NP with different precursor concentration

4.2.1.4. Effect of temperature

The magnesium precursor and extract mixture was heated for 40°C, 60°C and 80°C to study the effect of heating temperature on nanoparticle formation. It was observed that the absorbance at 320nm was higher for all samples heated at 60°C as shown in Figure 4.17. This shows that the optimum temperature for higher yield of MgO nanoparticle is 60°C. The temperatures lower and higher than 60°C leads to lower yield of MgO nanoparticles as the low temperature is not sufficient for the particle formation and high temperature degrades the active phytochemicals respectively (Alighourchi et al., 2009).
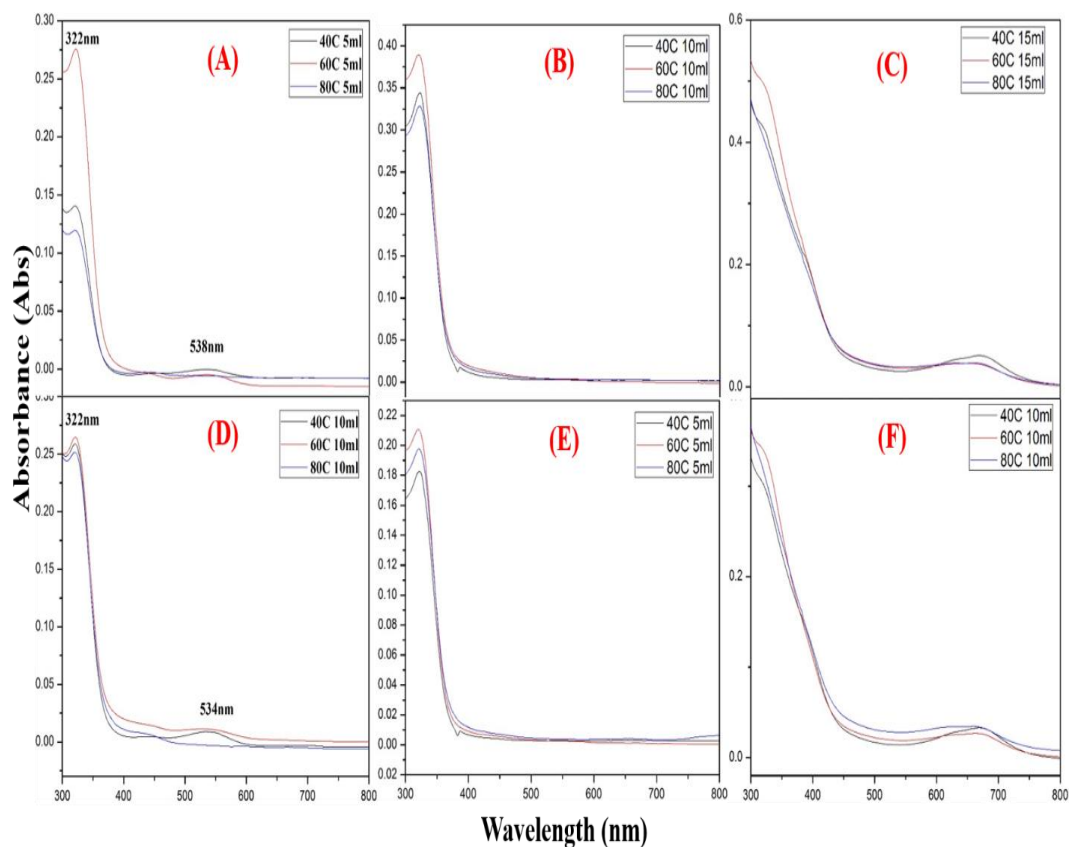
Figure 4.17: UV-Visible absorbance for nanoparticles formed with selected extract concentration of (A) sample AT, (B) sample AB, (C) sample AP, (D) sample NT, (E) sample NB, (F) sample NP with different temperature

4.2.1.5. Effect of heating time

In order to study the effect of heating time, all the samples were heated at 60°C for 5, 10 and 15 minutes. The absorbance at 320nm was highest when the samples are subjected to 10min of reaction time as shown in Figure 4.18 (A, C, F). While, higher absorbance was observed in 15min of reaction time for sample AB and NB (Figure 4.18 (B and E)). Ahn et al (2007) reported in their experiment that the size of nanoparticle will increase after the threshold time of heating (Ahn et al., 2007). From the Figure 4.11 (c), the size of nanoparticle with 15min of heating time is larger than the nanoparticles obtained from 10min of heating time. The Figure 4.18 (D) shows that the absorbance for reaction with 5min of heating is higher than 10min of heating for sample NT. Despite, the 10min of heating time is selected as optimum as they yield smaller nanoparticles as in Figure 4.13

(A, c). In summary, 0.001M of precursor concentration, 60°C of temperature and 10min of heating time was selected as the optimum reaction condition for all the samples. The presence of additional absorbance peaks at ~530nm and ~660nm in the samples are due to the presence of phytochemicals in the reaction mixture that absorbs UV light (Sahaya et al., 2012; Antony et al., 2013). The optimized parameters for the synthesis of smaller MgO nanoparticles from each of six samples were mentioned in Table 4.6.
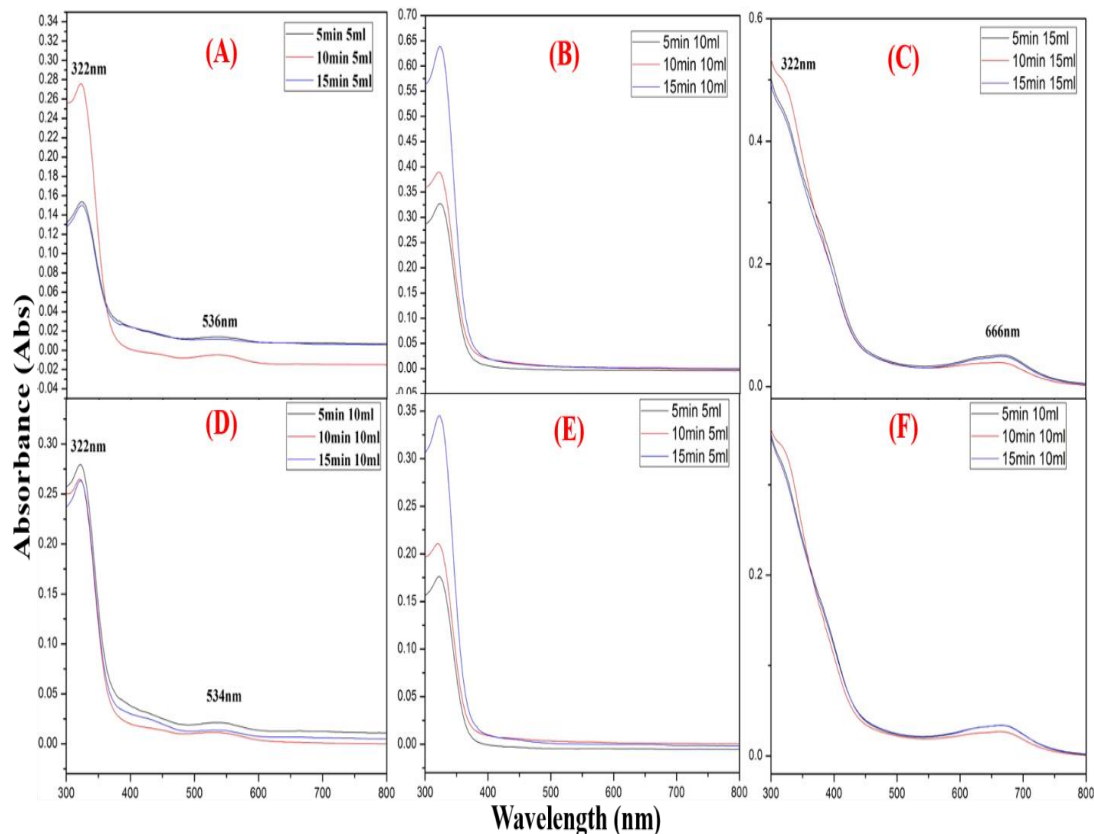
Figure 4.18: UV-Visible absorbance for nanoparticles formed with selected extract concentration of (A) sample AT, (B) sample AB, (C) sample AP, (D) sample NT, (E) sample NB, (F) sample NP with different time of heating

Table 4.6: Optimized parameters for leaf extract mediated synthesis of smaller MgO nanoparticles

Sample	Extract	Precursor	Temperature	Time
Sample AT	5ml	0.001M	60°C	10min
Sample AB	10ml	0.001M	60°C	10min
Sample AP	15ml	0.001M	60°C	10min
Sample NT	10ml	0.001M	60°C	10min
Sample NB	5ml	0.001M	60°C	10min
Sample NP	10ml	0.001M	60°C	10min

4.2.2. Characterization of green synthesized nanoparticles

4.2.2.1. Dynamic light scattering studies for optimized samples

The average particle size, polydispersity index (PDI) and zeta potential of the MgO nanoparticles synthesized using optimized parameters were studied using dynamic light scattering technique and the results were summarized in Table 4.7 and the graph was included in Appendix D2. All of the average size were observed to be below 100nm. The smallest size of 18nm was observed for sample AT and the average size for sample AB is larger compared to other samples. The PDI at a range of 0.2-0.6 is acceptable (Gaumet et al., 2008). It is observed that the PDI for all the samples are below 0.6 with a lower PDI of 0.276 for sample AB and a higher PDI of 0.558 was observed for sample NP. The zeta potential for all the samples are in the range -10 to -20mV. A negative zeta potential indicates the presence of negative surface charge which in the case of magnesium oxide is acceptable as the metal is positive charge which attracts the negative oxygen on its surface (Patil et al., 2007; Zhang et al., 2008). Range of zeta potential above -10mV also indicated that the particles are incipiently stable (áO'Brien, 1990; Hanaor et al., 2012). The highest (-21.4mV) zeta potential was observed for sample NT whereas sample NP shows low (-11.4mV) zeta potential compared to others. This analysis indicates that

among the samples, the MgO nanoparticles in sample NT are most stable and the particles in sample NP are least stable (Kumar et al., 2016).

Table 4.7: Average size and zeta potential of all samples with optimized parameters

Sample	Average size ±PDI (nm)	Zeta potential (mV)
Sample AT	18±0.4	-11.6
Sample AB	91 ± 0.276	-15.4
Sample AP	58 ±0.495	-11.7
Sample NT	50±0.379	-21.4
Sample NB	78±0.351	-15.4
Sample NP	32±0.558	-11.4

4.2.2.2. Crystallinity, chemical composition and morphology of MgO nanoparticles

The colloidal MgO nanoparticles synthesized from three plant species after optimization of synthesis parameters were dried using freeze dryer. The powders were analyzed with XRD, FT-IR and TEM to study their chemical and morphological characteristics. Figure 4.18 shows the XRD peaks for all the six green synthesized MgO samples. The characteristic XRD peaks for MgO were not observed for any sample. Due to the presence of phytochemicals that are bound with MgO, Figure 4.19 showed certain peaks are found that are interrupted by phytochemicals and hence cannot be categorized as amorphous solids.
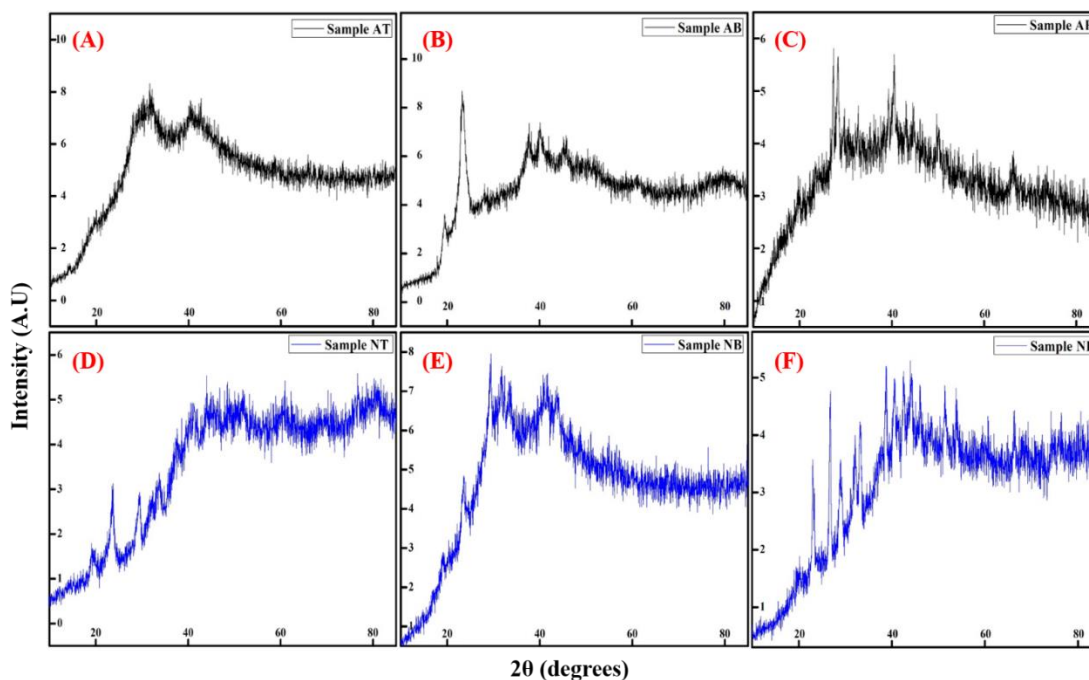
Figure 4.19: XRD analysis of six MgO nanoparticle samples prepared with leaf extract

4.2.2.3. Functional group analysis of MgO samples

The functional groups present in the leaf extracts and potential chemical modifications due to the formation of MgO nanoparticles were studied using FT-IR spectroscopic analysis, and the results are summarized in Table 4.8. The FTIR spectra of the three leaf extracts are shown in Figure 4.20 (a), 4.21(a) and 4.22(a). The FTIR spectral chart for functional groups identified the presence of alcohol, phenol, amines, alkanes, alkynes and carboxylic acid in the leaf extracts. These functional groups indicate the presence of alkaloids, flavonoids, polyphenols, terpenes and terpenoids in all the three leaf extracts (Were P S, 2015). In samples AT and AB as shown in Figure 4.20 (b) and Figure 4.21 (b), N-H bend (primary amine), and C-H (alkanes) rock bonds from extracts were derivatized into NH_2, CH_2 bending and C-H "oop" (aromatic) bond respectively to form MgO nanoparticles as confirmed by the peaks between 660-540 cm^{-1} (Rezaei et al., 2011; Song et al., 2010; Tamilselvi et al., 2013). Similarly, Figure 4.20 (c) and 4.21 (c) show the degradation of primary amine, alkanes and aromatics during MgO nanoparticles synthesis for samples NT and NB. The peak at 897-820 cm^{-1} shows the presence of MgO along with δ (O-C=O) due to the usage of magnesium nitrate as the precursor (Kumar et

90

al., 2008). As shown in Figure 4.22 (b) and (c), FTIR spectra for samples AP and NP synthesized from *A. paniculata* extract are different from the others. Similar to sample AT and AB, suppression of peaks attributed to N-H bond and C-H bond resulted in the formation of MgO nanoparticles as indicated by a peak at 660-540 cm^{-1} for sample AP. These changes resulted in the formation of O-H bond as an alcoholic compound along with MgO nanoparticles in sample AP as shown in Figure 4.22 (b). Similarly, alkynes and alkanes in the extract degrade and form aromatic amines during the formation of MgO nanoparticles in sample NP as shown in Figure 4.22 (c). The aliphatic compounds (Alkynes and alkanes) present in *A. paniculata* (Akbar, 2011b) transforms into aromatic amine groups due to the presence of nitrate from the magnesium precursor in the reaction mixture for preparing sample NP. This transformation can be attributed to the changes such as oxidation, reduction or degradation of phytochemical compounds occur during the nanoparticle formation (Makarov et al., 2014). The presence of MgO nanoparticles in sample NP was confirmed by a peak at 897-820 cm^{-1}, similar to samples NT and NB. As reported by Tamilselvi et al (Tamilselvi et al., 2013), the presence of peak at 660-540 cm^{-1} strongly confirms the presence of MgO and this is in keeping with findings for sample NP. The aqueous extracts yielded phytochemicals with different functional groups. These functional groups play an important role in the formation of MgO nanoparticles (Vignesh Subramanian, 2015). The difference between the presence and absence of δ (O-C=O) + v (Mg-O) vibrational mode in the samples demonstrates the effect of precursor in determining the oxidative-reductive reactions of the phytochemicals (Kumar et al., 2008).

Table 4.8: FTIR spectral chart showing functional groups in plant extract and MgO samples.

A. blitum					
Frequency cm^{-1}	Vibrational modes	Functional group	Plant extract	Sample AB	Sample NB
3500-3200	O-H stretch, H-bonded	Alcohol, phenol	+	+	+
1650-1580	N-H bend	Primary amine	+	-	-
1650-1550	NH$_2$ scissoring	Primary amine	-	+	-
1680-1640	-C=C-stretch	Alkenes	-	-	+
1370-1350	C-H rock	Alkanes	+	-	-

Frequency cm^{-1}	Vibrational modes	Functional group			
1400-1450	αCH$_2$ bending	Aldehyde & Ketone	-	+	-
1335-1250	C-N stretch	Aromatic amine	+	+	+
1320-1000	C-O stretch	Alcohol, carboxylic acid, ester, ether	+	+	+
900-675	C-H "oop"	Aromatics	+	-	-
897-820	δ (O-C=O) + v (Mg-O)	MgO	-	-	+
660-540	Mg-O	MgO	-	+	+

A. tricolor

Frequency cm^{-1}	Vibrational modes	Functional group	Plant extract	Sample AT	Sample NT
3500-3200	O-H stretch, H-bonded	Alcohol, phenol	+	+	+
1650-1580	N-H bend	Primary amine	+	-	-
1650-1550	NH$_2$ scissoring	Primary amine	-	+	-
1370-1350	C-H rock	Alkanes	+	-	-
1400-1450	αCH$_2$ bending	Aldehyde & Ketone	-	+	-
1335-1250	C-N stretch	Aromatic amine	+	+	+
1320-1000	C-O stretch	Alcohol, carboxylic acid, ester, ether	+	+	+
900-675	C-H "oop"	Aromatics	+	-	-
897-820	δ (O-C=O) + v (Mg-O)	MgO	-	-	+
660-540	Mg-O	MgO	-	+	+

A. paniculata

Frequency cm^{-1}	Vibrational modes	Functional group	Plant extract	Sample AP	Sample NP
3500-3200	O-H stretch, H-bended	Alcohol, Phenol	-	+	+
3300-2500	O-H stretch	Carboxylic acid	+	+	+
2260-2100	-C≡C-stretch	Alkynes	+	-	-
1760-1665	C=O stretch	Carbonyls	+	+	+
1650-1580	N-H bend	Primary amine	+	-	+
1650-1550	NH$_2$ scissoring	Primary amine	-	+	-

1370-1350	C-H rock	Alkanes	+	-	-
1400-1450	αCH$_2$ bending	Aldehyde & Ketone	-	+	-
1335-1250	C-N stretch	Aromatic amine	-	-	+
1320-1000	C-O stretch	Alcohol, carboxylic acid, ester, ether	+	+	+
830-820	δ (O-C=O) + v (Mg-O)	MgO	-	-	+
900-675	C-H "oop"	Aromatics	+	-	-
660-540	Mg-O	MgO	-	+	+
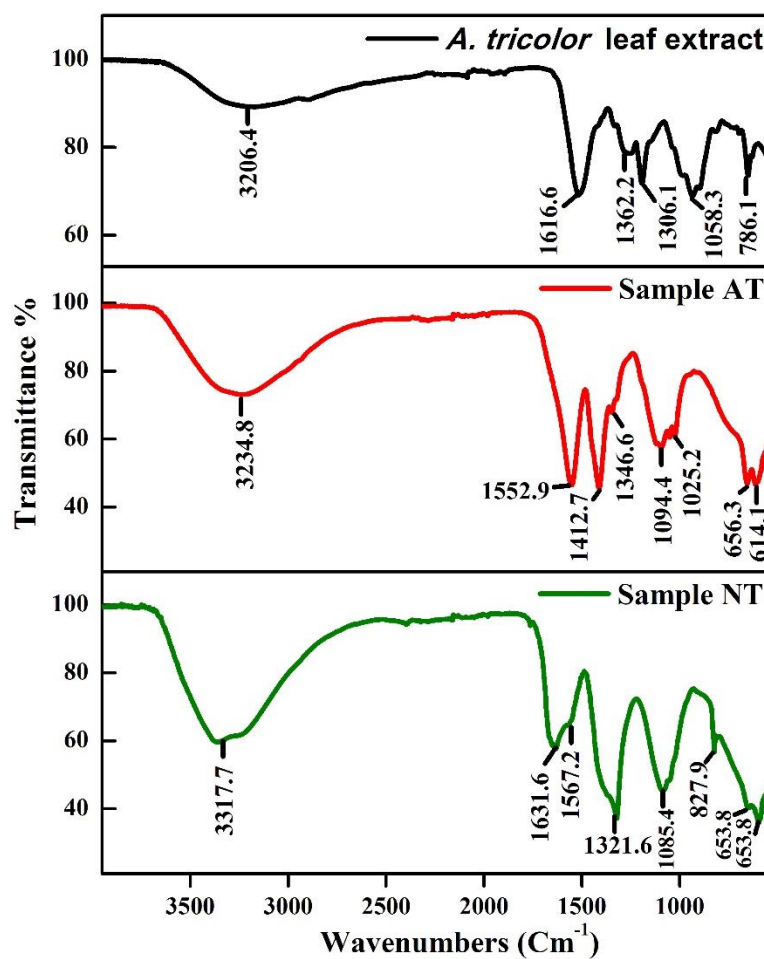
Figure 4.20: FTIR spectra of *A. tricolor* leaf extract, Sample AT and Sample NT
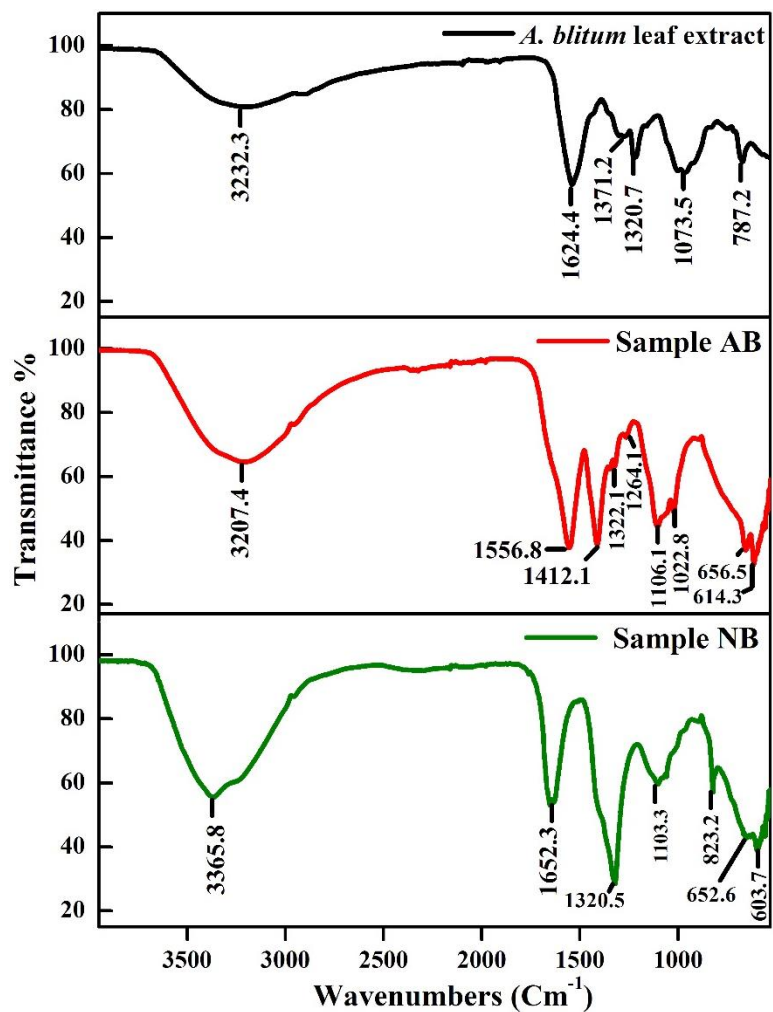
Figure 4.21: FTIR spectra of *A. blitum* leaf extract, Sample AB and Sample NB
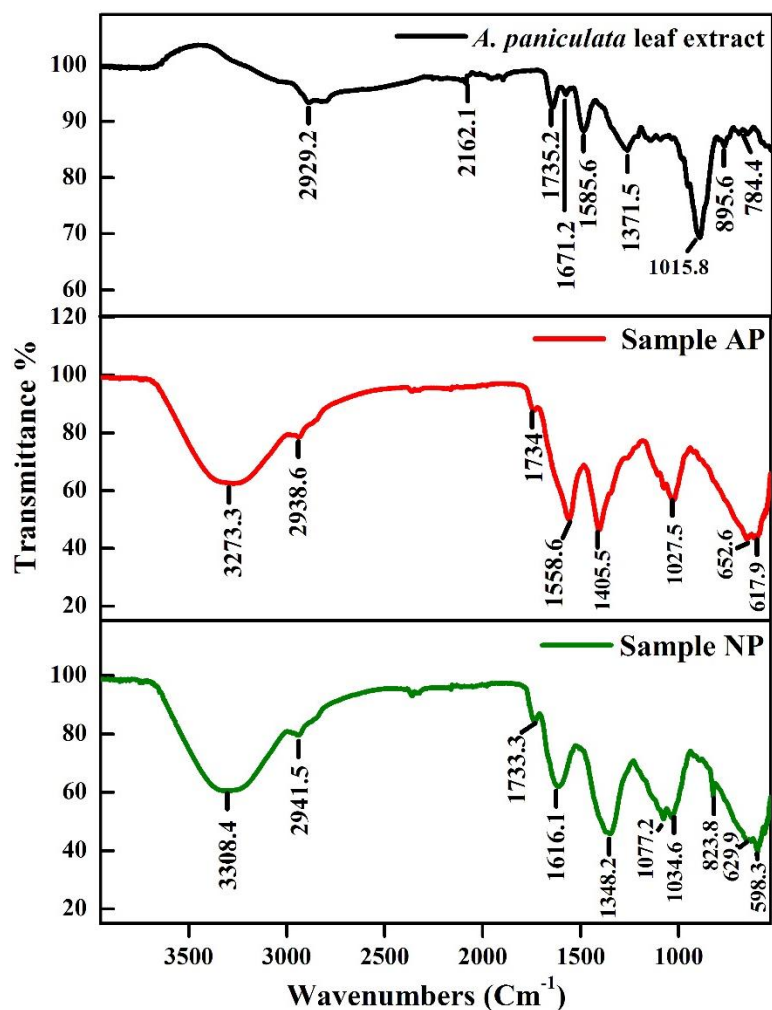
Figure 4.22: FTIR spectra of *A. paniculata* leaf extract, Sample AP and Sample NP

4.2.2.4. Morphology of green synthesized nanoparticles

Transmission electron micrographs of the synthesized MgO nanoparticles are shown illustrated in Figure 4.23. All the samples showed a spherical morphology except sample NT (Figure 4.23 D) where some of the nanoparticles appears to be hexagonal in shape. This deviation is potentially due to the reaction between nitrate and phytochemical composition of *A. tricolor* which forms as a capping as well as reducing agent and transforms nanoparticle shape from spherical to hexagonal (Ghodake et al., 2010). Hexagonally shaped nanoparticles have edge surface atoms (Ayyub et al., 1995) which promotes biological interactions and activity (Shaban et al., 2014), potentially offering useful benefits in pharmaceutical applications. The average particle sizes for the different

samples were within the range of 18-28nm except sample AT which showed a larger particle size in the range 50-80nm. Most reported studies on chemical synthesis of MgO nanoparticles yield particles with average size in the range 30-50nm. Mastuli et al (2014) synthesized MgO nanoparticles with an average crystallite size of 30 nm and 68 nm using oxalic acid and tartaric acid respectively as gelling agents along with high calcination temperatures (Mastuli et al., 2014). Similarly, Sundrarajan et al (2012) prepared 30-130 nm sized MgO nanoparticles by annealing at 300-700°C (Sundrarajan et al., 2012a). Also, Tamilselvi et al (2013) produced 30-50 nm sized MgO nanoparticles using ammonia and NaOH as reducing agent at 500°C calcination temperature (Tamilselvi et al., 2013). Hakimeh Mirzaei et al (2012) used microwave irradiation in a sol-gel method to synthesize 30-50nm sized MgO nanoparticles after calcination at high temperature (Mirzaei et al., 2012). Stengl et al (2003) used ultrasound radiation and prepared ~10nm MgO nanoparticles (Štengl et al., 2003). However, for most chemical based methods, reagents such as Magnesium methoxide and toluene are used as solvents, and these are regarded as toxic and not suitable for pharmaceutical, agricultural, biological and food applications. Hence, this work is significant to the development of small size MgO nanoparticles at low temperatures using non-toxic leaf extracts and simple mixing process. Based on the present work, Karthick et al produced MgO nanorods using *A. paniculata* extract with the assistance of microwave mediated synthesis procedure (Karthik et al., 2017). From Figure 4.23, it is also be observed that the size of the nanoparticles measured from TEM is slightly different from the average particle size from the DLS technique. This is because DLS measure average particle size (particle size distribution) which includes entrapped phytochemicals on the particles surface (Helfrich et al., 2006). The varying PDI for each sample is also a factor that could affect the size distribution profile (Mahl et al., 2011). From the images, it is also evident that the samples are agglomerated due to low stability. Agglomeration of particles can be reduced by altering the pH of the sample to improve charge electronegativity (Jiang et al., 2009; Berg et al., 2009).
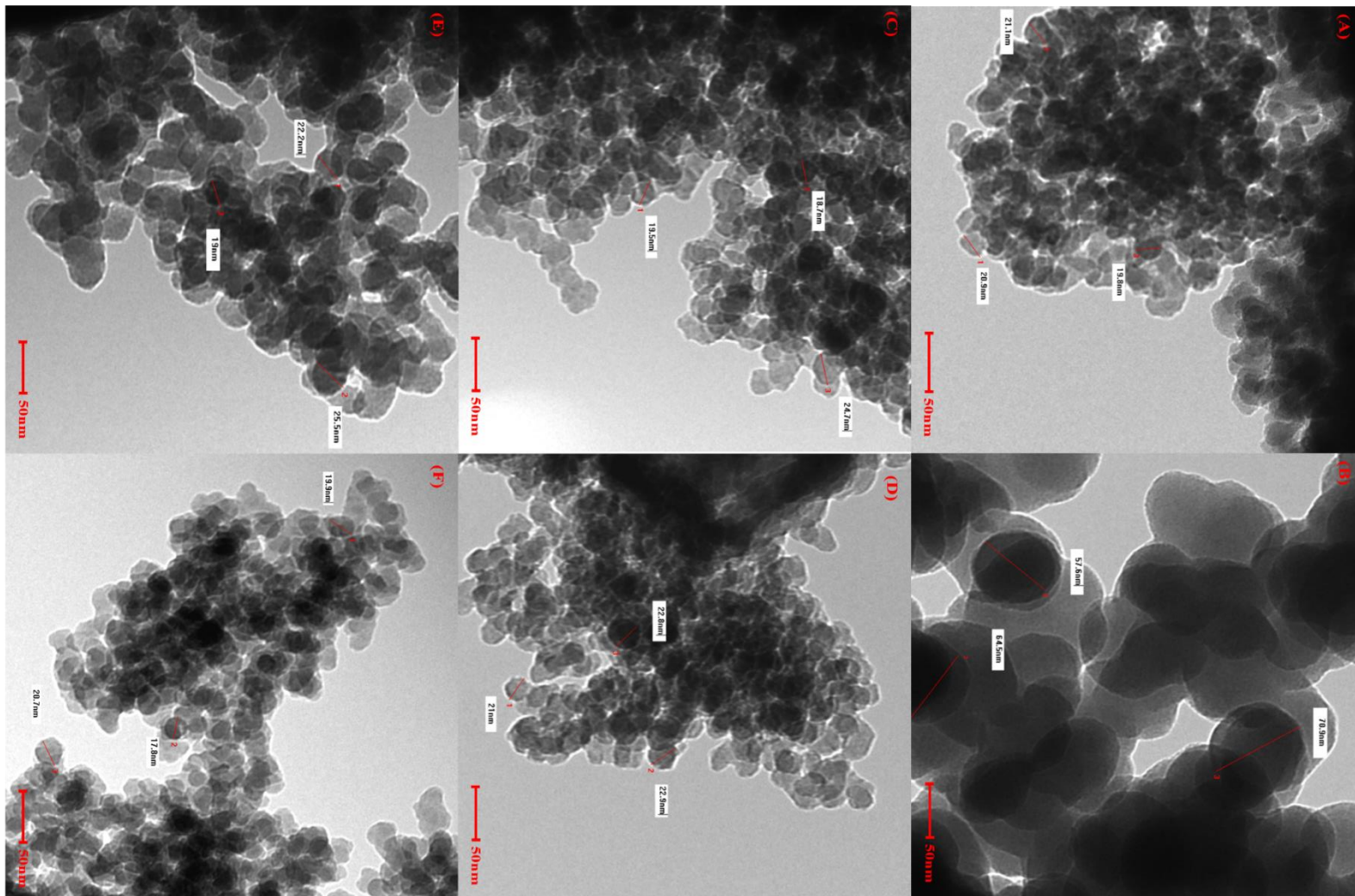
Figure 4.23: TEM images of MgO nanoparticles formed in green synthesized samples

4.3. Morphological changes during green synthesis

Since, sample NT was found to consist of hexagonal shaped nanoparticles, it was subjected to pH optimization. The aqueous leaf extract obtained from *A. tricolor* plant was mixed with the magnesium precursor using a magnetic stirrer at 350 rpm and 60°C for 10 min. The intensity of the extract color reduced as an indication of nanoparticle formation due to degradation of phytochemicals acting as reducing and stabilizing agent for MgO nanoparticle formation. The original pH of the synthesized nanoparticles was 7 as represented by sample C. The pH of the colloidal nanoparticles was lowered to 3 and 5 (as in samples A and B respectively) using 1M hydrochloric acid and increased to 9 and 11 (as in samples D and E respectively) using 1M sodium hydroxide. The color of the colloidal nanoparticles solution in the acidic pH remained unchanged while the basic pH altered the color to yellow as shown in Figure 4.24.
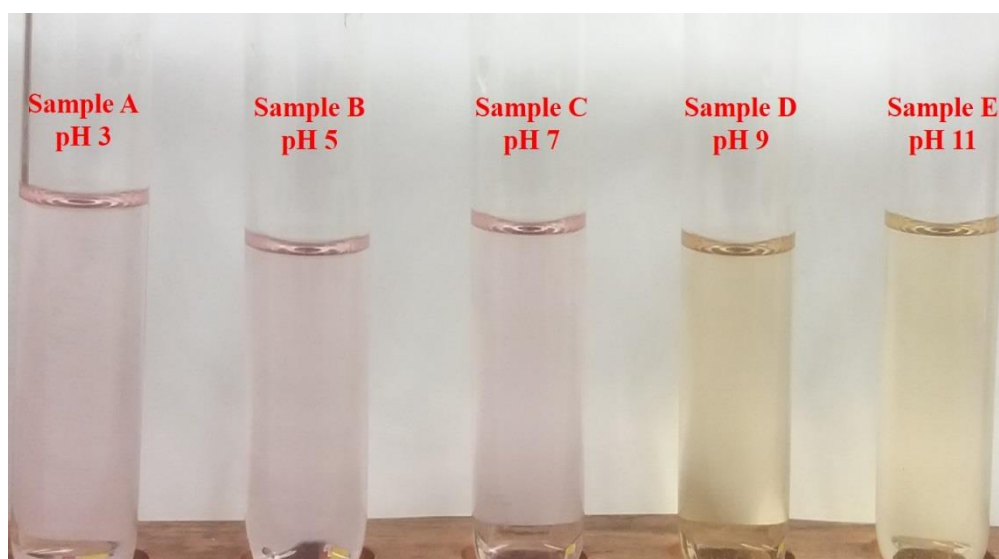
Figure 4.24: Effect of pH on the colour of MgO nanoparticles

4.3.1. Optical absorbance

The UV-visible absorbance of MgO nanoparticles at different pH conditions is shown in Figure 4.25. The peak at 322 nm, observed for the samples with pH 3, 5 and 7, indicates the presence of MgO nanoparticles (Alwan et al., 2015; Umar et al., 2011). The highest absorbance value, indicating the highest nanoparticle concentration, was observed in

sample A, followed by sample B and C. Mg peak for samples D and E was observed at 380 nm, and this is due to the color change from pale red to yellow under NaOH alkaline condition. It was inferred that magnesium hydroxide was present in sample D and E. Another peak was observed between 522-532 nm in samples A, B and C but absent in samples D and E. This is due to the presence of visible light absorbing phytochemicals (Antony et al., 2013; Sahaya et al., 2012). The phytochemicals present in the extracts of samples D and E may have been degraded due to increasing alkalinity.
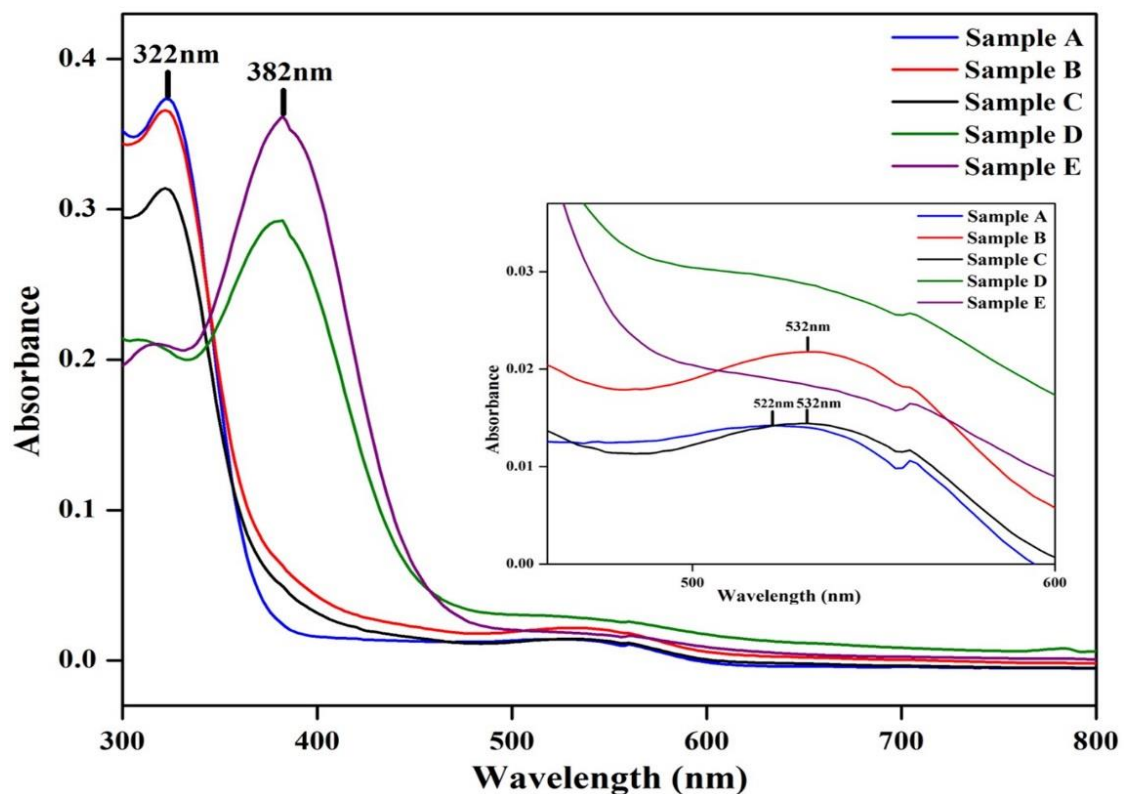
Figure 4.25: Absorbance scanning of MgO nanoparticles from 300-800nm under varying pH conditions. Inset: Absorbance scanning of MgO nanoparticles from 400-600nm under varying pH conditions

4.3.2. Thermal analysis

Samples D and E are expected to form magnesium hydroxide, instead of magnesium oxide, due to the addition of sodium hydroxide to modify the pH. The samples were freeze dried to perform thermal analysis and identify their calcination temperatures in order to transform them into magnesium oxide nanoparticles. The thermal analysis was carried out

using TGA to study the temperature mediated weight loss, and DSC was used to identify the heat flow pattern of the sample. The thermal analysis data showing the weight loss and heat flow patterns of samples D and E are shown as Figure 4.26 (a) and 4.26 (b) respectively. Both samples D and E show a two-stage weight loss mechanism as summarized in Table 4.9. The first degradation stage is due to the decomposition of crystallizing water (Kumar et al., 2008) observed from 70 to 290°C for sample D and from 60 to 260°C for sample E. Similarly, the second degradation stage was observed from 340 – 510°C for sample D and 280 – 500°C for sample E, and this was due to the melting transition of magnesium hydroxide to magnesium oxide (Rezaei et al., 2011; Tang et al., 2012; Mirzaei et al., 2012). The thermal degradation equation for the formation of magnesium oxide from freeze dried magnesium hydroxide is shown by equations 1a and 1b.

Stage 1: $Mg(OH)_2 . H_2O \longrightarrow Mg(OH)_2 + H_2O$ (Equation 1a)

Stage 2: $Mg(OH)_2 \longrightarrow MgO + H_2O$ (Equation 1b)
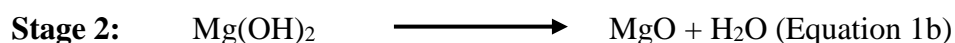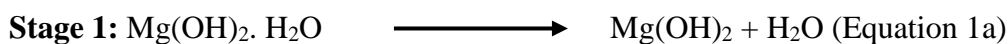
In the first degradation stage, endothermic DSC peaks at 190°C for sample D and 170°C for sample E were observed, confirming the degradation of crystallizing water from the samples. Likewise, exothermic DSC peaks were observed at 390°C for sample D and 420°C for sample E, confirming the melting transition of the samples. From Table 4.9, it can be seen that 27% and 44% by mass of freeze dried samples D and E respectively were degraded to form MgO. It was determined that the percentage weight loss for each stage of sample D thermal profile is lower compared to sample E, and this may be due to the presence of lower concentrations of hydroxide ions in sample D than sample E. The DSC analysis explain further that the freeze dried samples absorb heat energy in stage 1 to remove water of crystallization (equation 1a). The resultant magnesium hydroxide in stage 1 transforms into magnesium oxide by releasing heat from the sample in stage 2. At this point, water molecules from magnesium hydroxide degrade, potentially being the reason for the peak deflection observed for both samples (Figure 4.26 a). Further, it can also be noted from Table 4.9 that the degradation of water molecules increases with increasing alkalinity of the samples. The increase in alkalinity of the sample increases the

magnesium hydroxide formation along with crystalline water (Mg(OH)$_2$. H$_2$O) which decomposes in stage 1 excessively in sample E than sample D.

Table 4.9: Stage-wise thermal degradation analysis of samples D and E

Sample	Degradation stages	TGA	Weight loss	DSC
Sample D	Stage 1	70-290°C	9%	190°C
	Stage 2	340-510°C	13%	390°C
Sample E	Stage 1	60-260°C	14%	170°C
	Stage 2	280-500°C	30%	420°C
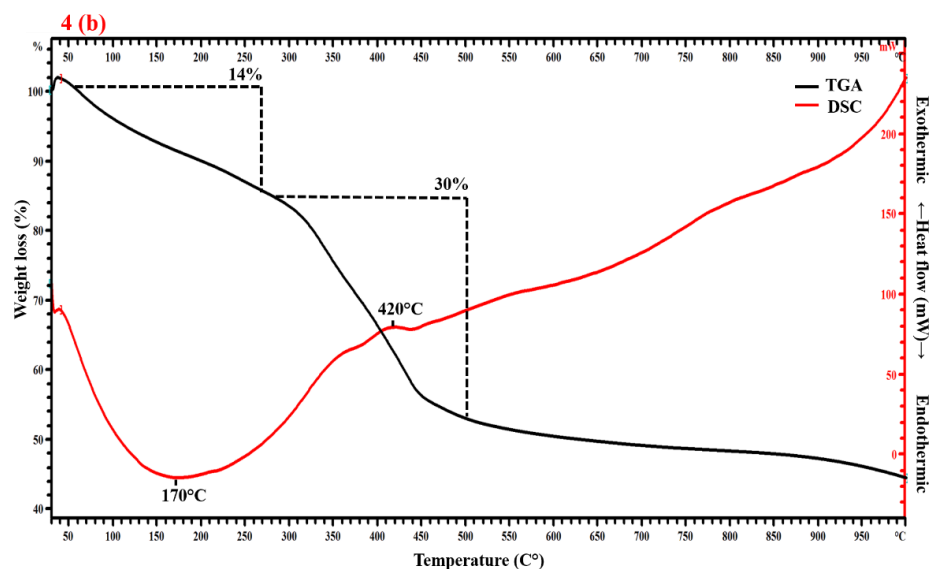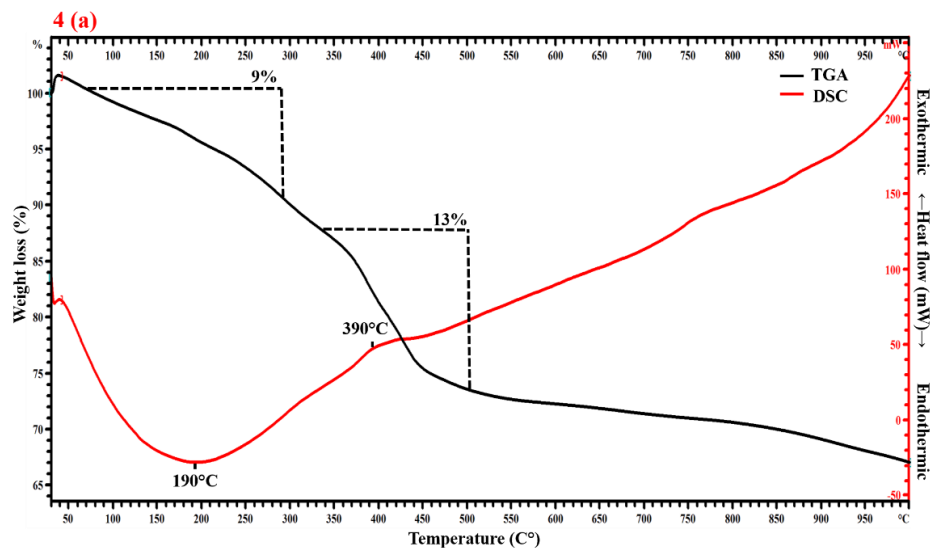
Figure 4.26: TG-DSC analysis of sample D (4a) and sample E (4b)

4.3.3. Calcination and absorbance of calcined samples

The calcination temperature of the alkaline treated samples D and E was determined to be 500°C based on the melting transition temperature obtained from the TG/DSC analysis. The freeze dried samples were subjected to calcination in a *Carbolite 1200°C heavy duty box furnace* for 2 h at a heating rate of 5°C/min. Figure 4.27 shows the color and nature of the sample before (Figure 4.27 a) and after calcination (Figure 4.27 b).
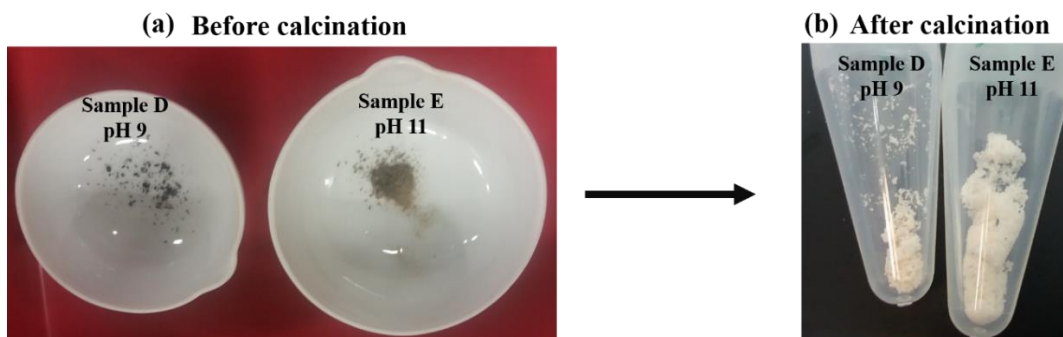
Figure 4.27: Samples D and E (a) before and (b) after calcination

The absorbance profiles of the calcined samples are shown in Figure 4.28. A weak peak at 324 nm and a strong peak at 586 nm with absorbance below zero was observed for both samples. The peak at 324 nm confirms the presence of metal oxide nanoparticles (Alam et al., 2006; Arefi et al., 2012; Yu et al., 2012). Generally, it was difficult to analyze water dispersed powder particles that reflect light with UV-Visible absorbance spectroscopy as the absorbance may differ from that of colloidal particles (Klaas et al., 1997; Morales et al., 2007). This may be the reason for the presence of a peak at 586 nm below zero absorbance. However, the analysis is helpful in demonstrating the presence of metal oxide in the calcined samples.
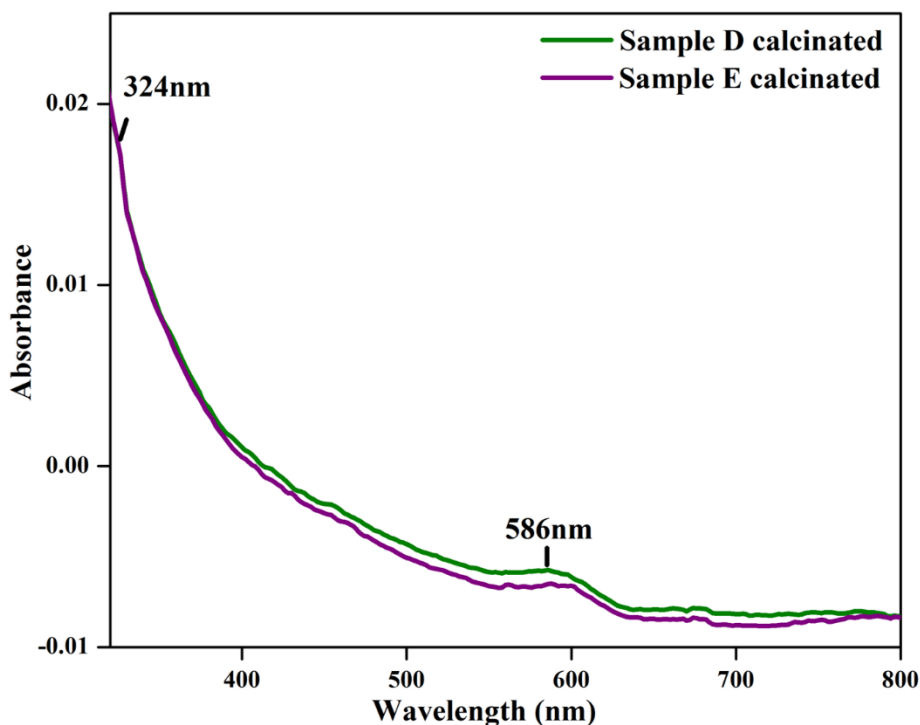
Figure 4.28: Absorbance spectra of the calcined samples D and E from 300-800 nm

4.3.4. Dynamic Light Scattering analysis

The samples of MgO nanoparticles were analyzed by dynamic light scattering to investigate the effects of pH on average particle size, polydispersity index (PDI) and zeta potential. The results are summarized in Table 4.10. The polydispersity index of all the samples were within 0.4 – 0.6, and this is an acceptable range for stable particles (ISO13321, 1996; Gaumet et al., 2008). It can be noted that the particle size decreases with decreasing pH. Also, zeta potential, which is an indicator of colloidal stability, decreases with pH decrement. Figure 4.29 shows the graphs of average particle size (Figure 4.29 a) and zeta potential (Figure 4.29 b) at different pH. Sample A with pH 3 resulted in a lower surface charge (-3.39 mV), and a further increase in acidity of the sample would arrive at the isoelectric focusing point due to protonation. The calcined samples (Samples D and E) were also dispersed in de-ionized water and subjected to DLS analysis. The results, as reported in Table 4.10, show that calcination of sample D resulted in a larger average particle size (190.1 nm) with an electronegative surface charge whereas sample E resulted in smaller particles (58.7 nm) with a stable electronegative surface charge. Thus, it can be concluded that MgO nanoparticles under highly acidic pH

conditions forms neutral stable particles with smaller particle sizes whilst MgO nanoparticles under alkaline pH conditions hydroxide particles which can be converted into MgO nanoparticle using calcination, and further increments in alkalinity may yield smaller particles with neutral stability via calcination.

Table 4.10: Average particle size and Zeta potential of MgO nanoparticles under different pH conditions

Sample	Average size ± PDI (nm)	Zeta potential (mV)
Sample A – pH 3 (MgO)	43.82 ± 0.454	-3.39
Sample B – pH 5 (MgO)	50.75 ± 0.592	-5.19
Sample C – pH 7 (MgO)	58.77 ± 0.599	-12.6
Before calcination		
Sample D – pH 9 (MgOH)	68.06 ± 0.625	-14.4
Sample E – pH 11 (MgOH)	220.2 ± 0.631	-18.2
After calcination		
Sample D (MgO)	190.1 ± 0.404	-23.2
Sample E (MgO)	58.7 ± 0.537	-15
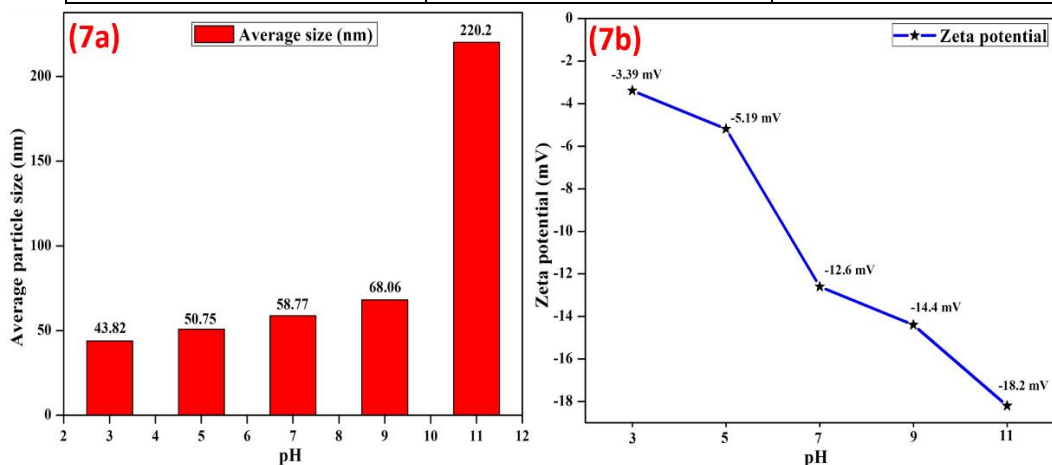
Figure 4.29: Effect of pH on the average particle size (7a) and zeta potential (7b) on MgO nanoparticles

4.3.5. Proposed mechanism for pH-mediated formation of stable hexagonal shaped MgO nanoparticles

From the DLS analysis, pH variation through the addition of hydrogen and hydroxide ions affects the particle size and stability. For the alkaline treated samples (D and E), magnesium hydroxide ($Mg(OH)_2$) was initially formed before conversion to MgO during calcination. The surface charges of the calcined samples were observed to be more electronegative, potentially due to the addition of hydroxide ions that contribute to the net surface charge of the nanoparticles as shown in Figure 4.30 A. The atomic weight of magnesium hydroxide (58.321 g/mol) is higher compared to magnesium oxide (40.299 g/mol). It can be noted that as the atomic weight of the molecule increases, its particle size and surface also increase (Liu et al., 2007; Chithrani et al., 2006). As the surface of magnesium hydroxide particles increases, the surface charge also increases and this is the reason for its high electronegative zeta potential. However, calcination of magnesium hydroxide generated magnesium oxide which is negatively charged, more stable, and larger sized particles as reported in Table 4.10.
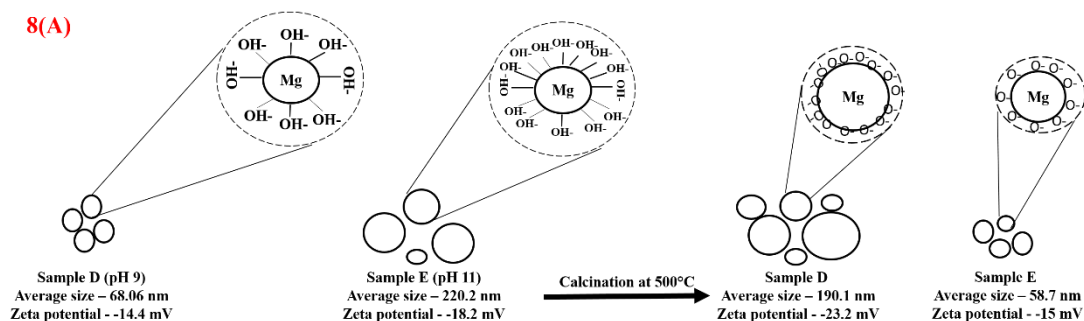
Figure 4.30 (A): Proposed molecular mechanism for the formation of Mg(OH)₂ and MgO from samples D and E

Magnesium oxide was generated from samples A, B and C under acidic pH conditions. The reduction in pH of the samples generates smaller nanoparticles with decreasing electronegativity. Spherical shaped MgO nanoparticles were formed from sample C at neutral pH and a further addition of hydrogen ions to decrease pH leads to the formation of hexagonal MgO nanoparticles as shown in Figure 4.30 B. The addition of hydrogen ion acts as a capping agent to modify and stabilize the shape of nanoparticles (Badawy et al., 2010; Mohanpuria et al., 2008; Armendariz et al., 2004; Gardea-Torresdey et al.,

2002) due to electrostatic force of attraction (Ju-Nam et al., 2008). The capping agent reduces the particle size and the positive surface charge of hydrogen ions to enhance attraction towards O^{2-} ion present in MgO nanoparticles. This leads to the formation of hexagonal shaped MgO nanoparticles as shown in Figure 4.30 (B). The hexagonal shaped nanoparticles possess high edge surface site (Ayyub et al., 1995) with oxygen atoms and this has been hypothesized to allow strong capping/attraction of hydrogen ions over MgO nanoparticles. Hence, the capping agent (hydrogen ions) gets attached strongly at the edge surface positions, further reducing the size of nanoparticles by hindering growth without deforming morphology as in the case of sample B. As more hydrogen ions are added in sample A, most of the O^{2-} ions in MgO nanoparticles are attached with hydrogen ions to reduce its electronegativity and make it more neutral.
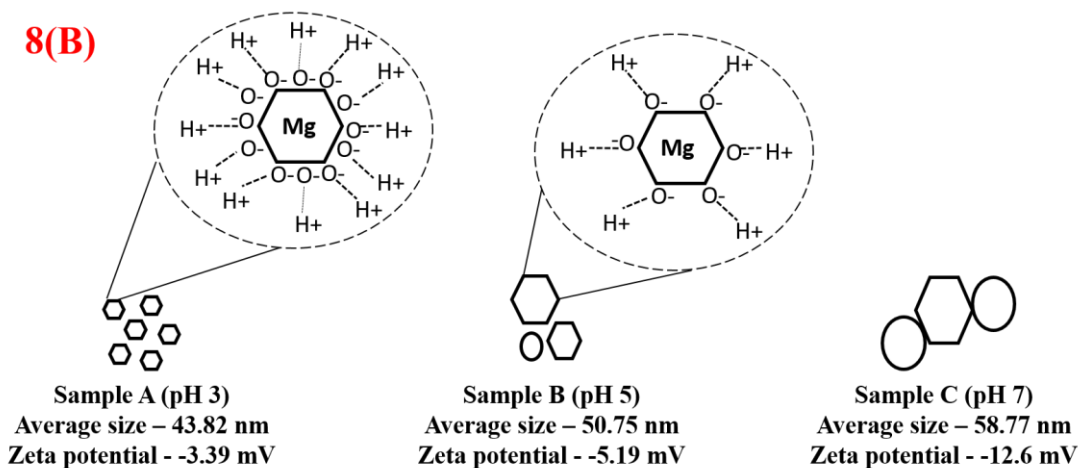
Figure 4.30 (B): Proposed molecular mechanism for the formation of hexagonal shaped MgO from samples A, B and C

4.3.6. Functional group and morphological analysis of MgO nanoparticles

Sample A was selected for morphological imaging using TEM to validate its anticipated hexagonal shape structures. Sample A was further subjected to FT-IR spectroscopy to identify key functional groups within the particulate system.

4.3.6.1. Functional group analysis

The compounds present in the leaf extracts and potential chemical modifications resulting from the formation of MgO nanoparticles were studied using FT-IR spectroscopy. The

results are summarized in Table 4.11. The FTIR spectra of *A. tricolor* leaf extract is shown as Figure 4.31 (A) whereas FTIR spectra of samples C and A are shown as Figures 4.31 (B) and 4.31 (C) respectively. The functional groups identified show the presence of alcohol, phenol, aromatic amines, carboxylic acid, ester and ether, directly indicating the presence of alkaloids, flavonoids, polyphenols, terpenes and terpenoids in the *A. tricolor* leaf extract (Were P S, 2015). The peaks indicating the presence of alcohol, phenol, aromatic amine, carboxylic acid, ester and ether in the phytochemical profile of *A. tricolor* leaf extract were also present in sample C and A. In addition, peaks showing functional groups such as carboxylic acid, alkanes, esters, saturated aliphatic and primary amine are present only in sample A. It can be noted that vibrational modes of carboxylic acid, alkanes and primary amine possess hydrogen molecules, confirming the addition of hydrogen ions to alter pH and bind with degraded phytochemicals to form new functional groups that may act as capping agents (Mohanpuria et al., 2008; Badawy et al., 2010; Gardea-Torresdey et al., 2002; Armendariz et al., 2004). Functional groups indicating esters and saturated aliphatic compounds are not present in the leaf extract and sample C. This shows that excess hydrogen ions can function to act a reducing agent (Philip, 2010; Halliwell, 1994) of phytochemicals during MgO nanoparticles formation. The peak showing Mg-O vibration along with δ (O-C=O) is found between 900-820 cm^{-1} (Kumar et al., 2008). The percentage transmittance is lower for most of the vibrational modes, and this indicates the presence of higher concentrations of the relevant functional groups (Ee et al., 2008) in sample A compared to sample C. This supports that more functional groups act as capping agents in sample A to transform the shape and size of MgO nanoparticle. However, the percentage transmittance for Mg-O vibrational mode is almost similar in both samples (sample A and C) with a slight shift in the peak due to the presence of additional functional groups after pH alterations.

It has been reported that that pH alterations influence the structural modification of nanoparticles. Shang et al (2007) investigated pH-dependent protein conformational changes in albumin-gold nanoparticle bioconjugates and reported using FTIR spectra that pH of the medium highly influenced the structural conformation of the bioconjugate (Shang et al., 2007). Bian et al (2011) studied the dissolution of 4 nm ZnO nanoparticle in different pH solutions and explained changes in particle stability and dissolution via

FTIR analysis. They reported that pH mediated protonation and deprotonation of nanoparticles can lead to surface complexation. Similarly, Alias et al (2010) examined the FTIR spectra of ZnO nanoparticles at pH 6-11 and found that the intensity of functional groups invariably change as the pH of the medium changes, indicating that the particle size is affected by the medium pH. These reports give ample evidence that addition of hydrogen ions through pH variation lead to changes in the FTIR spectra, indicating functional group modifications.

Table 4.11: FTIR spectral chart showing functional groups in plant extract and sample C and A

A. tricolor					
Frequency cm^{-1}	Vibrational modes	Functional group	Leaf extract	Sample C (pH 7)	Sample A (pH 3)
3500-3200	O-H stretch, H-bonded	Alcohol, phenol	+	+	+
3300-2500	O-H stretch	Carboxylic acid	-	-	+
3000-2850	C-H stretch	Alkanes	-	-	+
1750-1735	C=O stretch	Esters, saturated aliphatic	-	-	+
1650-1580	N-H bend	Primary amine	+	-	+
1650-1550	NH$_2$ scissoring	Primary amine	-	-	+
1370-1350	C-H rock	Alkanes	+	-	+
1335-1250	C-N stretch	Aromatic amine	+	+	-
1320-1000	C-O stretch	Alcohol, carboxylic acid, ester, ether	+	+	+
900-675	C-H "oop"	Aromatics	+	-	+
897-820	δ (O-C=O) + v (Mg-O)	MgO	-	+	+

Figure 4.31: FTIR spectra for (A) *A. tricolor* **leaf extract, (B) Sample C (pH 7) and (C) Sample A (pH 3)**

4.3.6.2. Morphology analysis

Figure 4.32 (a), (b) and (c) are the transmission electron micrographs of MgO nanoparticles in sample A. Figure 4.32 (a) shows that the particles in sample A (pH 3) are not agglomerated compared to sample C (pH 7). This is be due to the capping ability of hydrogen ions present in sample A. The particles are either hexagonal or a shape with edge atoms such as triangle and pentagon. Figure 4.32 (B) and (C) show the morphology of a single particle with a certain degree of agglomeration. The shape of the nanoparticles was observed to be hexagonal with some particles undergoing transformations into hexagonal forms. Literature suggests that protonation and deprotonation may lead to nanoparticle shape transformations (Jones et al., 2011). The size of the particles determined from the TEM analysis is ~40 nm, similar to that obtained from DLS analysis. Thus, the TEM analysis further demonstrates that pH variations can prevent agglomeration between particles, and transform the shape. Nanoparticles with neutral or slightly negative surface charge possess more bioavailability and bioactivity (Xiao et al., 2011; Blanco et al., 2015). Hence, the particles prepared in the present work can find significant biomedical applications.
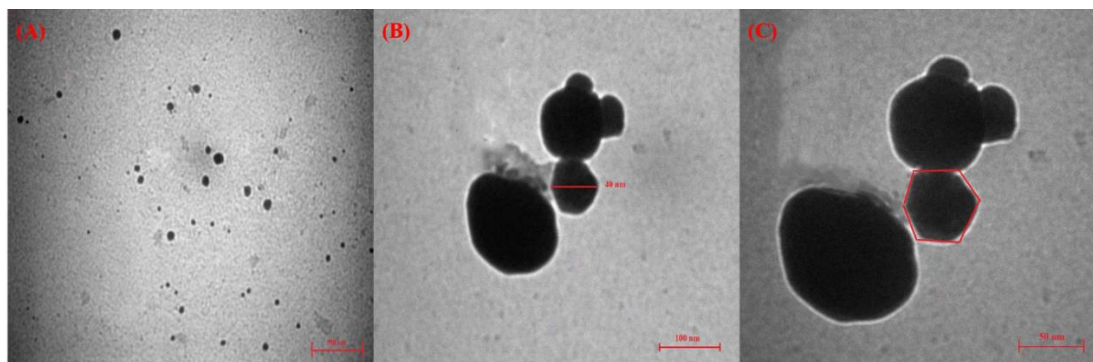
Figure 4.32: **TEM micrograph of MgO nanoparticles (A) At 200nm scale (B) Single particle at 100nm scale and (C) A closer look at the particles at 50nm scale showing hexagonal shaped nanoparticles**

4.4. MgO nanoparticles for *in vivo* cell line studies

Features of selected MgO nanoparticles used *in vivo* cell line studies to investigate cytotoxicity and insulin resistance reversal ability are described in Table 4.12. MgO nanoparticles were selected based on size and distinct morphology. The selected MgO

nanoparticles were subjected to cytotoxic studies and biological assays to test their toxicity towards diabetic and non-diabetic cells as well as to study their ability to reverse insulin resistance in a diabetic cell model.

Table 4.12: Selected MgO nanoparticle samples for cell line studies

Sample	Size (nm)	Morphology
Chemical synthesized MgO nanoparticles		
Sample A	47.9 ±0.706	Spherical
Sample B	43.8 ±0.615	Hexagonal
Sample C	91.2 ±0.547	Rod
Green synthesized MgO nanoparticles		
Sample NT at pH 3	43.82 ± 0.454	Hexagonal
Sample NB	78 ±0.351	Spherical
Sample NP	32 ±0.558	Spherical

CHAPTER 5:

INSULIN RESISTANCE REVERSAL EFFICIENCY AND CYTO-TOXICITY ANALYSIS OF MgO NANOPARTICLES

Synthesized MgO nanoparticles with various morphologies and sizes were characterized based on their insulin resistance reversal capacity and cytotoxicity. The cytotoxicity of selected MgO nanoparticles was analyzed using 3T3-L1 adipose cell line. 3T3-L1 cell lines are derived from mouse and possess characteristics such as fibroblast-like morphology, the capacity to increase the synthesis and accumulation of triglycerides. They are also sensitive to lipogenic and lipolytic hormones and insulin (Green et al., 1975; Moreno-Navarrete et al., 2017). MgO nanoparticles that are less toxic to the diabetic cell model is further subjected to a cytotoxic analysis using normal epithelial cell lines to help determine the action of MgO nanoparticles in both diabetic and normal cell lines. Further, less toxic and optimal dosage levels of MgO nanoparticles determined from chemical and green synthesis were subjected to biological assays such as glucose assay, western blot and fluorescent microscopy to analyze the insulin resistance reversal ability of MgO nanoparticles.

5.1. Nanoparticle dosages for cytotoxic analysis

Low concentrations of chemically synthesized MgO nanoparticles (0.001M) was selected for this test as they have been reported to be toxic towards cells (Lima et al., 2012; Mal et al., 2017). 0.001M of chemically synthesized MgO nanoparticle samples were suspended in distilled water using vortex mixing (***VX-200 Lab Vortexer***) at 3400 rpm. The colloidal MgO nanoparticles from the green synthesis approach were used without any further suspensions. The concentration of green synthesized colloidal MgO nanoparticles present in each dosage are measured as mentioned in Appendix B and are mentioned in Table 5.1.

Table 5.1: Dosages and concentration of MgO nanoparticles for cytotoxic analysis

Dosage (µl)	Green synthesis (mg)		
	Sample GA	Sample GB	Sample GC
200	0.19	0.22	0.16
400	0.39	0.43	0.32
600	0.58	0.64	0.49
800	0.78	0.86	0.65
1000	0.98	1.08	0.82

5.2. Cytotoxic analysis of MgO nanoparticles in diabetic cell lines

The cytotoxicity analysis of MgO nanoparticles towards 3T3-L1 cell lines was performed to identify the biocompatibility of different MgO nanoparticles morphologies synthesized through chemical and green synthesis approaches. During 3T3-L1 cell line culturing, it was found that a thin oily layer was formed in the DMEM medium as 3T3-L1 cells differentiate into adipocyte cells which restricts the flow of carbon-dioxide and oxygen into the cells, eventually inhibiting cell growth. The cell culture achieved 60% confluence after the third day and the medium was replenished daily. Figure 5.1 shows the micrograph of completely grown 3T3-L1 adipose cells with 60% confluence. The cells were sub-cultured for cytotoxic analysis after the third day in a 24-well plate along with nanoparticle treatment for 24 h (Mosmann, 1983; Präbst et al., 2017). The cells were treated with nanoparticles at different dosages in triplicates at rates of 200, 400, 600, 800 and 1000 µl/ml to identify maximal inhibitory concentration (IC_{50}).
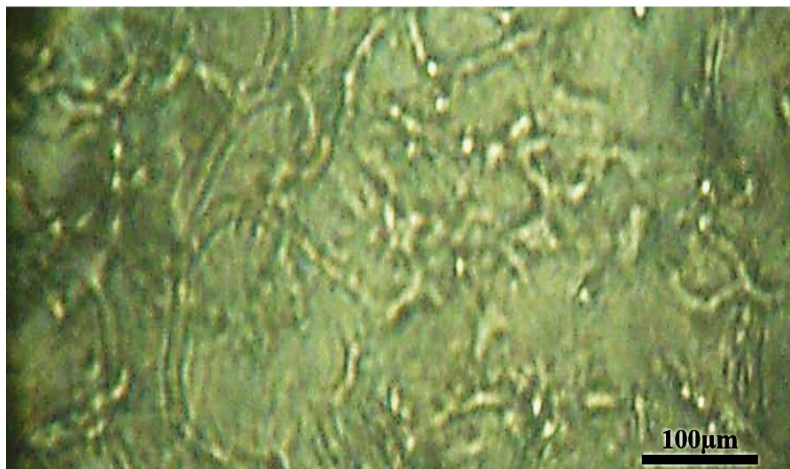
Figure 5.1: 3T3-L1 cell lines after 60% confluence without nanoparticle treatment

5.2.1. Cytotoxicity of chemical synthesized MgO nanoparticles

Purple and yellow colors from cell proliferation MTT assay represents live and dead cell respectively. The absorbance of the color change and the intensity represent the percentage of viable cells after treatment with chemically synthesized MgO nanoparticles. The percentage of viable cells were obtained by measuring the live cells at the absorbance of 570 nm, and the values are recorded in Appendix E1. Figure 5.2 shows the percentage of viable cells with standard error (SE) after the treatment of different MgO nanoparticles for 24 h. The absorbance is observed to be directly proportional to the viability of cells, and 50% inhibition of cells (IC_{50}) can be obtained from the absorbance/viability graph.
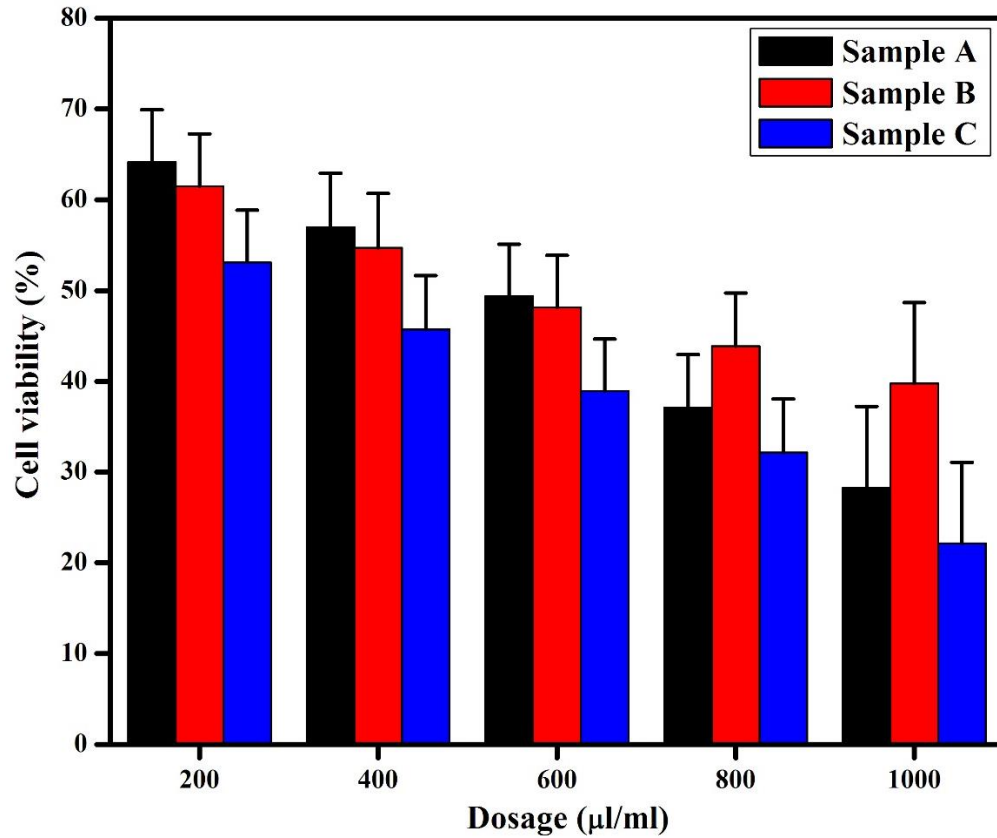
Figure 5.2: Cell viability of spherical (sample A), hexagonal (sample B) and rod (sample C) shape nanoparticles at different dosages of treatment
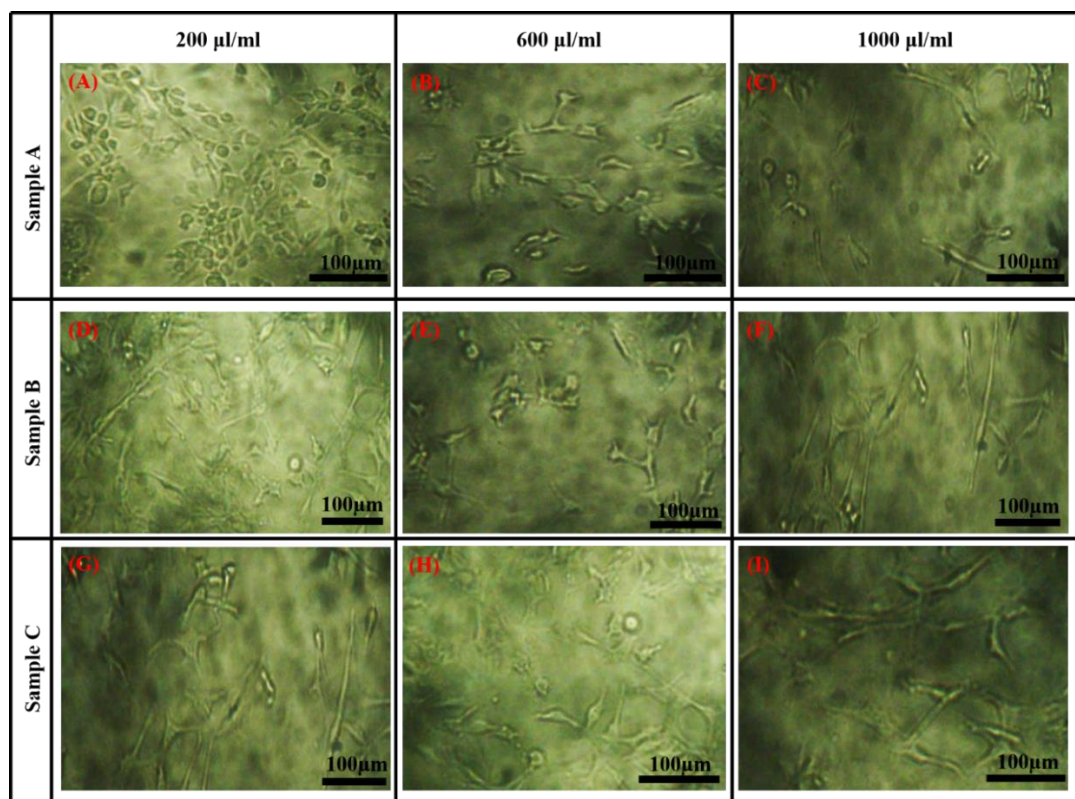
Figure 5.3: Micrographs of 3T3-L1 cells after treatments with different morphologies of MgO nanoparticles such as spherical (sample A), hexagonal (sample B) and rod (sample C)

Figure 5.2 shows that lower MgO nanoparticles dosage, irrespective of their morphology, supported the growth of adipose cells, and cell mortality increased with increasing dosage of nanoparticles. The graph shows that 600 µl/ml dose of samples A and B resulted in 50% inhibition of cell growth (IC_{50}) whereas IC_{50} for sample C was obtained at a comparatively lower dosage of 200 µl/ml. This shows that spherical (sample A) and hexagonal (sample B) shapes of MgO nanoparticles demonstrated comparative cytotoxic effect. However, rod (sample C) shaped MgO nanoparticles showed higher toxicity, potentially due to their relatively higher electronegative surface charge (-9.83 mV). The micrograph in Figure 5.3 shows morphologies of 3T3-L1 cells after treatment with nanoparticle samples at various dosages: 200, 600 and 1000 µl/ml. Samples A and B treatments resulted in similar morphological changes in the adipose cells. Lower dosage treatments of MgO nanoparticles (sample A and B) did not change the fibroblast morphology whereas mid and high dosages led to elongation of fibroblast shape and the

formation of spherical morphology. For rod shape nanoparticles (Sample C), the morphology of cells started deforming and elongating even for lower dosages. Cellular morphological alterations are indicative of cytotoxic effects resulting from nanoparticle interactions with cellular structures (Mao et al., 2015; Duan et al., 2013). To date, there is no reported work on the cytotoxicity profile of MgO nanoparticle towards 3T3-L1 adipose cell lines. Hence, the results from this work are compared with the literature data relating to nanoparticle cytotoxicity on adipose cells.

Huang et al (2005) conducted cell viability studies to analyze the toxicity of 110 nm size, hexagonal shaped fluorescein isothiocyanate – conjugated mesoporous silica nanoparticles towards adipose cells. Concentrations of 20, 40 and 80 μg/ml were added and studied after an hour of nanoparticle incubation with the cells. After 24 h and 78 h, the 20 and 40 μg/ml nanoparticle dosages did not show any effect on cell growth whereas 80 μg/ml dosage increased growth (Huang et al., 2005). Another study by Uboldi et al (2012) subjected amorphous, spherical shape silica nanoparticles of various sizes ranging from 25 to 100 nm to MTT assay in 3T3-L1 adipose cells at concentrations 1, 10 and 100 μg/ml. The results showed the influence of particle size on cell viability, and that smaller size nanoparticle showed more viability at high concentrations (100 μg/ml) (Uboldi et al., 2012). Similarly, cytotoxicity of ~10nm sized, hexagonal shaped nanodiamond-insulin complexes were analyzed in adipose cells via MTT assay by Shimkunas et al (2009). The cytotoxic analysis showed no trend in cell viability with increasing nanoparticle concentration (Shimkunas et al., 2009). The cell viability assay of zinc oxide nanoparticles conducted by Pandurangan et al (2015) using adipose cells also supported the current study. Cell viability decreased with increasing nanoparticle concentration in the range of 10-30 μg/ml (Pandurangan et al., 2015). All these studies demonstrate that cell viability is a function of nanoparticle size, shape, and concentration.

Figure 5.2 shows that sample A supports higher cell growth than sample B and C. However, concentration after IC_{50} reduced the cell viability significantly. It has been reported that the surface charge of 3T3-L1 adipose cells is positive due to the presence of fat and lipid on its surface (Chung et al., 2007). In this study, the surface charge of samples A, B and C were determined as -7.01 mV, -7.21 mV and -9.83 mV respectively at neutral pH. The similarity in the surface charges of samples A and B at neutral pH could explain

their comparable cytotoxicity levels before IC_{50}. On the other hand, the morphology of nanoparticles plays a major role in understanding e the cytotoxicity levels of these two samples. For spherical shape nanoparticles (sample A) with size within the range $25 - 71$ nm, smaller particles (<30nm) enter into the cells and larger particles (>30 nm) disrupt the cell surface (Verma et al., 2010; Hussain et al., 2005). This is possibly the reason behind the higher cytotoxicity of sample A after IC_{50}. Also, the hexagonal shaped particles (sample B) possess edge surface atoms which facilitate cellular entrance without disrupting them (Ayyub et al., 1995; Helveg et al., 2000; Jeevanandam et al., 2015). This was reflected on the graph as only 22% of cells were dead after treatment with nanoparticles at $200 - 1000$ μl/ml. Since sample C has relatively a higher electronegative surface charge than sample A and B, it was inferred that rod-shaped nanoparticles interacted with the positively charged cell surface (The adipose cells are positively charged due to the presence of lipids in their cell surface), resulting in the disruption of cells. This was evident as IC_{50} was observed at 200 μl/ml for sample C and only 22% of cells were alive at 1000 μl/ml of nanoparticle concentration. Hence, the current study shows that surface charge and morphology of nanoparticles play a major role in inhibiting cell growth. Sample B has the less toxic MgO nanoparticle morphology from the cytotoxicity analysis in diabetic cell lines.

5.2.2. Cytotoxicity analysis of green synthesized MgO nanoparticles

Similarly, the green synthesized MgO nanoparticle samples were treated with 3T3-L1 cells for 24 hours. The percentage of viable cells are presented in Appendix E2. Figure 5.4 shows the percentage of viable cells along with standard error (SE) after the treatment of different green synthesized MgO nanoparticles dosages for 24 hours.
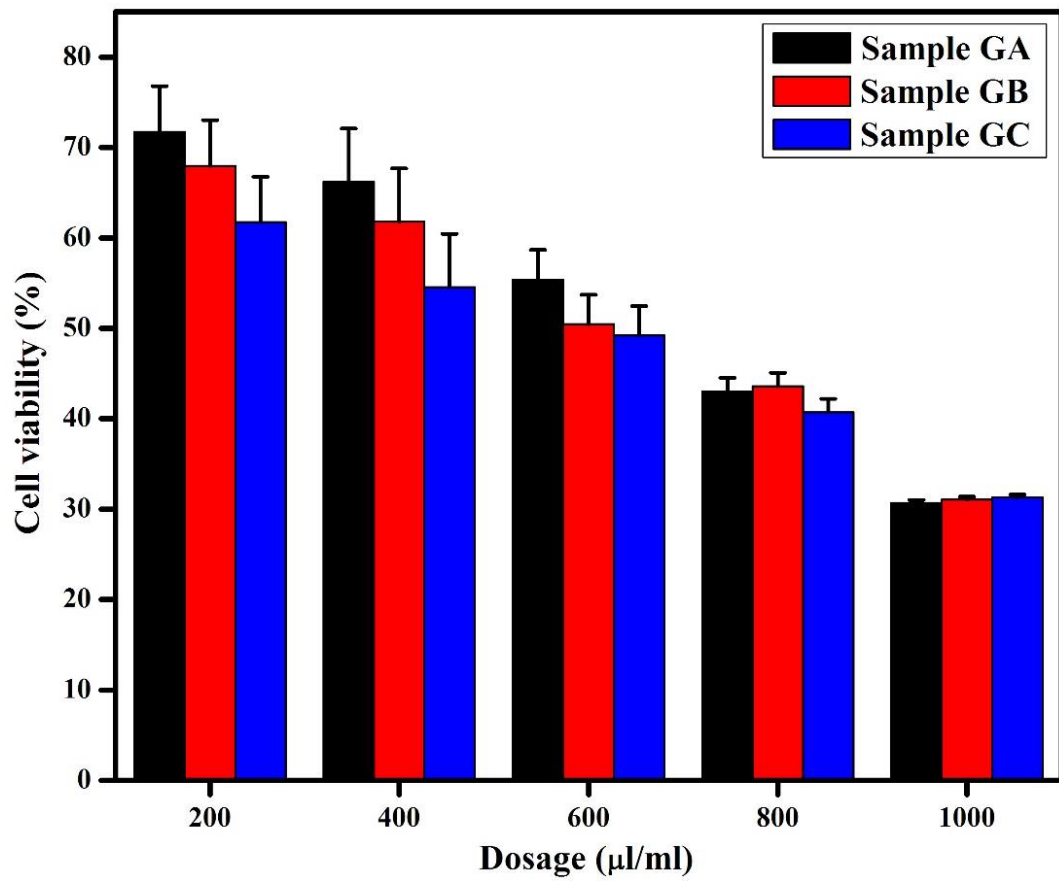
Figure 5.4: Cell viability of sample GA, GB and GC at different dosage treatment
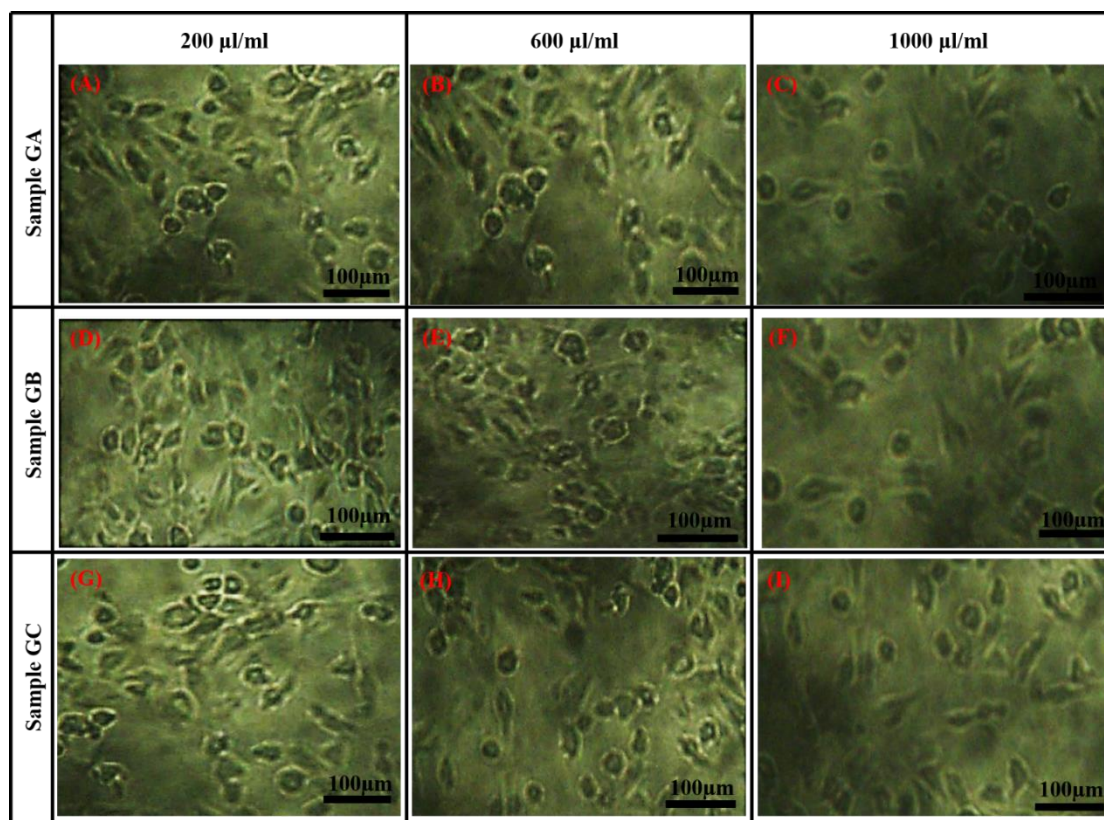
Figure 5.5: Micrograph of 3T3-L1 cells after MgO nanoparticle treatments with Samples GA, GB and GC.

Similar to the chemically synthesized samples, MgO nanoparticles with different morphologies supported the growth of adipose cells, and cell mortality increased with increasing dosage of MgO nanoparticles as shown in Figure 5.4. 600 μl/ml dose of samples GA, GB and GC led to 50% inhibition of cell growth (IC_{50}). At 600 μl/ml dosage, sample GA showed slightly more viability (55%) than sample GB and GC, and this may be due to the edge surface atoms present in hexagonal shaped nanoparticles (Van Hardeveld et al., 1969; Zuo et al., 2017) that enhances more cellular reactivity. Hence, hexagonal shaped green synthesized nanoparticle give better support to cell growth than spherical shaped MgO nanoparticles. The micrograph in Figure 5.5 shows the morphologies of 3T3-L1 cells after treatment with green synthesized MgO nanoparticles at low (200 μl/ml), mid (600 μl/ml) and high dosages (1000 μl/ml). All the treatments resulted in similar morphological changes to the adipose cells. Even at lower dosage, the fibroblast morphology of adipose cells started transforming into a spherical shape. Cell viability was visible in 200 and 600 μl/ml dosages, whereas in 1000 μl/ml dosage, very

few cells were observed to be present due to severe cytotoxicity of the nanoparticles at high dosages.

Figure 5.4 shows that sample GA supported a higher cell growth than samples GB and GC, and IC_{50} was determined at 600 μl/ml dosage. The cell viability of sample GA at IC_{50} dosage was higher compared to samples GB and GC, hence sample GA with hexagonal morphology was selected for further analysis. Moreover, the surface charge of sample GA was -3.39 mV which is closer to neutral stability compared to other two samples (sample GB = -15.4 mV and sample GC = -11.4 mV). Xiao et al (2011) reported that slightly negative or neutral surface charge particles have a longer circulation period and lower accumulation in cells (Xiao et al., 2011) due to their low adsorption towards proteins (Alexis et al., 2008; Yamamoto et al., 2001). Comparatively, lower toxicity at IC_{50} dosage is due to hexagonal morphology and slightly electronegative / close-to-neutral surface charge stability which supports low adsorption towards cellular proteins, making sample GA, a better candidate for further biological analysis.

5.3. Cytotoxic analysis of MgO nanoparticles in non-diabetic (normal) cell lines

The cytotoxicity analysis of MgO nanoparticles with distinct morphology using VERO cells was performed to study biocompatibility towards normal (non-diabetic) cells. VERO cells were cultured based on the procedure reported in Section 3.2.4.1 to attain 60% confluency after 48 hours as mentioned in Figure 5.6.
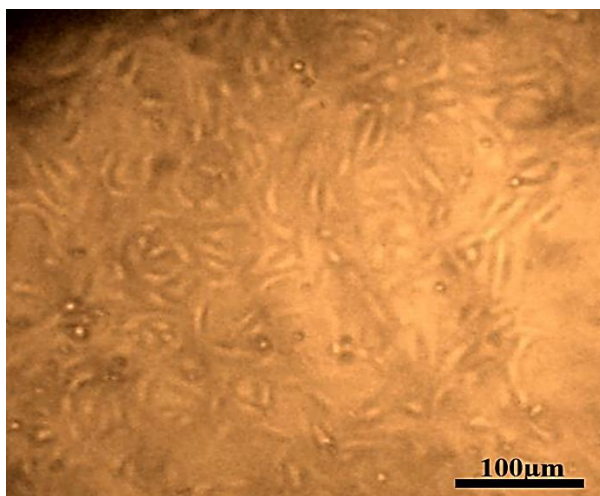
Figure 5.6: VERO cell lines after 60% confluence without nanoparticle treatment

Appendix E3 shows the percentage of viable VERO cells in comparison to 3T3-L1 cell viability, after treating different dosages of MgO nanoparticle samples B and GA. Figure 5.7 is the micrograph of the cellular morphology after treating MgO nanoparticles of sample B and GA at low (200 µl/ml), mid (600 µl/ml) and high (1000 µl/ml) dosages.
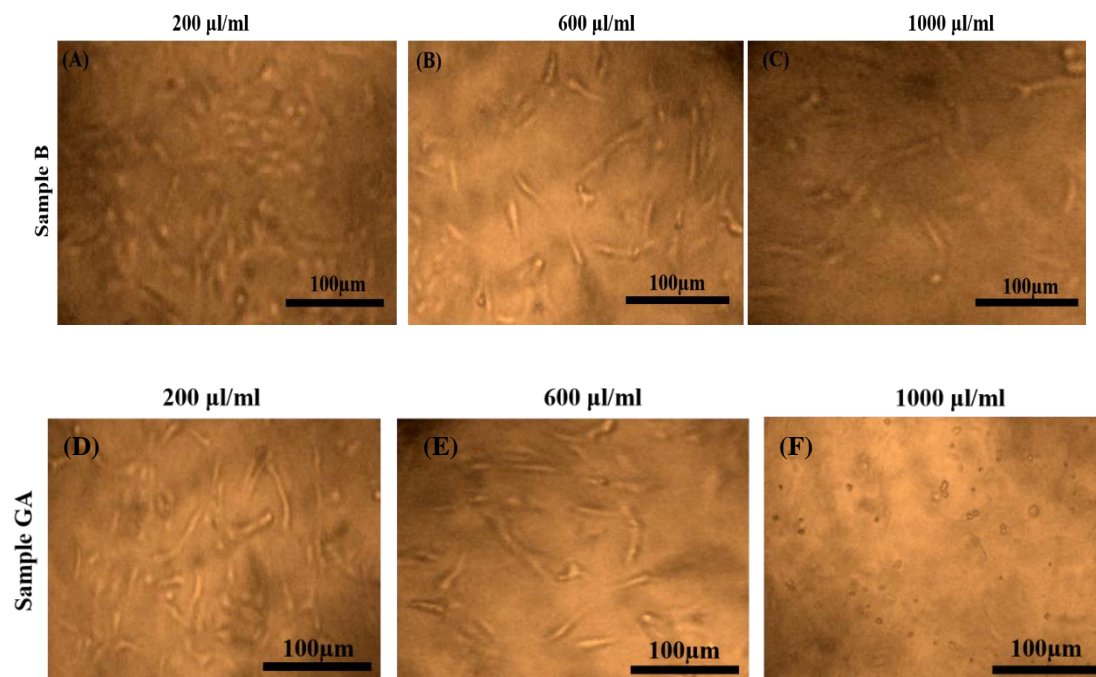
Figure 5.7: Micrograph of VERO cells after 24 h of samples B and GA treatment at dosages (A, D) 200 µl/ml, (B, E) 600 µl/ml and (C, F) 1000 µl/ml.
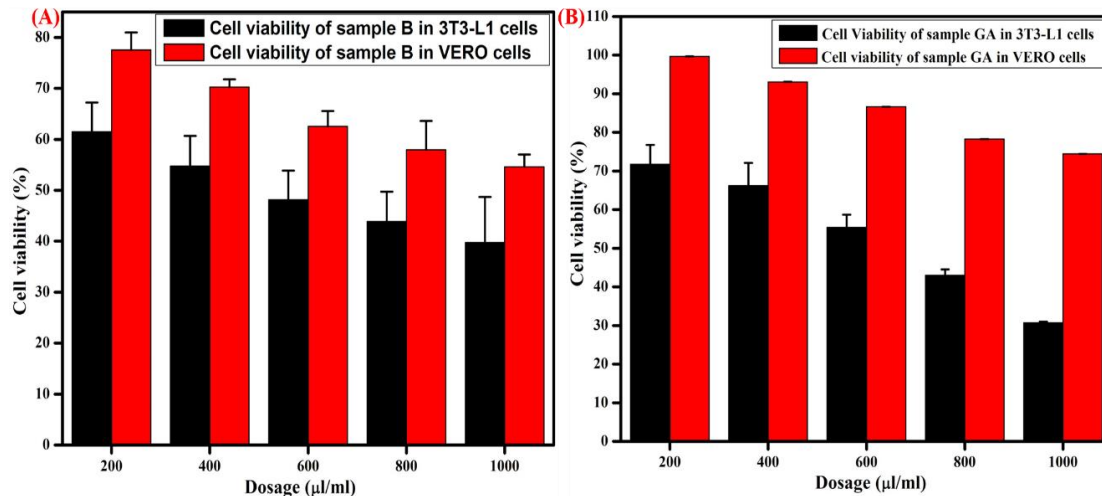
Figure 5.8: Comparative cell viability analysis after treating diabetic (3T3-L1) and non-diabetic (VERO) cell lines with sample B and GA

It can be noted from Appendix E3 that the viability of VERO cells is higher than 3T3-L1 cells after treating samples B and GA for 24 hours. The graph in Figure 5.8 shows the bar diagram, comparing viability of both cell lines after nanoparticle treatments. The IC_{50} of sample B towards VERO cells (Figure 5.8 a) was obtained at a higher dosage (1000 μl/ml), whereas with sample GA, the IC_{50} concentration (Figure 5.8 b) was not obtained even at a higher dosage. This shows that the selected MgO nanoparticles are less toxic to normal, non-diabetic cells than diabetic cells. The micrographs in Figure 5.7 show that the morphologies of VERO cells are not similar after treatment with low and high dosage of nanoparticles. The cells possess fibroblast morphology, which is the characteristic morphology of VERO cell, when low (200 μl/ml) dosage of nanoparticle is added as shown in Figure 5.7A. The cells slowly elongate with increasing nanoparticle dosage as shown in Figure 5.7B and the cells transform into enlarged fibroblastic morphology at high nanoparticle dosage (1000 μl/ml) which is the IC_{50} as shown in Figure 5.7C. Similar results were obtained when sample GA (Figure 5.7 D, E and F) was treated with VERO cells. This confirms that both chemical and green synthesized hexagonal shaped nanoparticles shows similar cytotoxic mechanism towards normal VERO cells. This can be attributed to the selective bioavailability of hexagonal shaped MgO nanoparticles which is comparatively high in diabetic cells than non-diabetic cells.

The cytotoxicity of various nanoparticles has been established through VERO cell lines in literatures. Chueh et al (2014) studied the cytotoxicity of commercially available gold nanoparticles using various cells including VERO and demonstrated concentration-dependent suppression of cell growth similar to the current study (Chueh et al., 2014). Similarly, VERO cells were utilized by Su et al (2007) to evaluate the cytotoxicity of gold nano-shells and reported that cell viability decreased 15% at 200 μg/ml after 24 hours of incubation (Su et al., 2007). Likewise, Sasidharan et al (2011) found that pristine coated non-biodegradable graphene is more toxic from 0 to 300 μg/ml towards VERO cells compared to functionalized graphene (Sasidharan et al., 2011). Balaji et al (2017) studied the cytotoxicity of 10 nm sized spherical shaped zirconia nanoparticles towards VERO cells and noted that higher concentrations of nanoparticles reduced VERO cell viability (Balaji et al., 2017). The cytotoxicity of iron oxide nanoparticles in VERO cells after short (4 h) and long-term (24 h) exposure were evaluated by Szalay et al (2011). The study showed negligible level of cytotoxicity after 4 hours of iron oxide nanoparticle exposure whereas cell viability reduced with increasing nanoparticle concentration (Szalay et al., 2012). All these reported findings show that the cell viability is inversely proportional to nanoparticle concentration in VERO cells and all the nanoparticles, except iron oxide, impact excess toxicity in VERO cells at higher concentrations. When comparing cell viability versus nanoparticle concentration (dosage) of the current study with literature, sample GA shows better cell viability as the IC_{50} concentration was not obtained and 75% of cells were viable even at higher concentrations. Even for sample B, the IC_{50} was obtained only at a higher concentration (1000 μl/ml or 40 μg/ml) after 24 hours of incubation. Thus, it was proven that the selected MgO nanoparticles were less toxic to non-diabetic cells.

The two-stage cytotoxicity testing was performed for MgO nanoparticle samples in order to evaluate their toxicity in both diabetic and non-diabetic cells. The cytotoxicity test using diabetic cell model helps to identify less toxic MgO nanoparticles dosage to be used for effective diabetes treatment. The cytotoxicity test in non-diabetic cell model was performed to avoid or minimize side-effects on normal cells during the usage of MgO nanoparticles for diabetic treatments. It can be noted that the IC_{50} of sample B in 3T3-L1 cell is 600 μl/ml and in VERO cell is 1000 μl/ml. Similarly, the IC_{50} of sample GA in

3T3-L1 cell is also 600 µl/ml and up to 1000 µl/ml. IC$_{50}$ dosage was not observed in VERO cell. It is evident that electrostatic forces of attraction between cells and nanoparticles, play a major role in the cytotoxicity mechanism of nanoparticles. The surface charge of VERO cells are negative (Van der Velden-de Groot, 1995; Maroudas, 1975). Thus, the surface charge of sample B (-7.21 mV) and sample GA (-3.21 mV) creates a repulsive force, acting as a barrier to nanoparticle-cell attraction and plays a major role in reducing toxicity towards VERO cells. The viability of 3T3-L1 cells were observed to be 54% at 400 µl/ml nanoparticles dosage which is above the IC$_{50}$ whereas at the same dosage, 71% cells were viable in VERO cells for sample B. Likewise, the viability of 3T3-L1 cells were observed to be 55% at 600 µl/ml nanoparticles dosage, which is above the IC$_{50}$, whereas at the same dosage 86% VERO cells were viable for sample GA. Hence, 400 µl/ml (0.016 mg/ml) dosage of sample B and 600 µl/ml (0.58 mg/ml) dosage of sample GA are more suitable dosages for further formulation and diabetes treatment from the two-stage cytotoxic analysis.

5.4. Proposed cytotoxicity mechanism of MgO nanoparticles
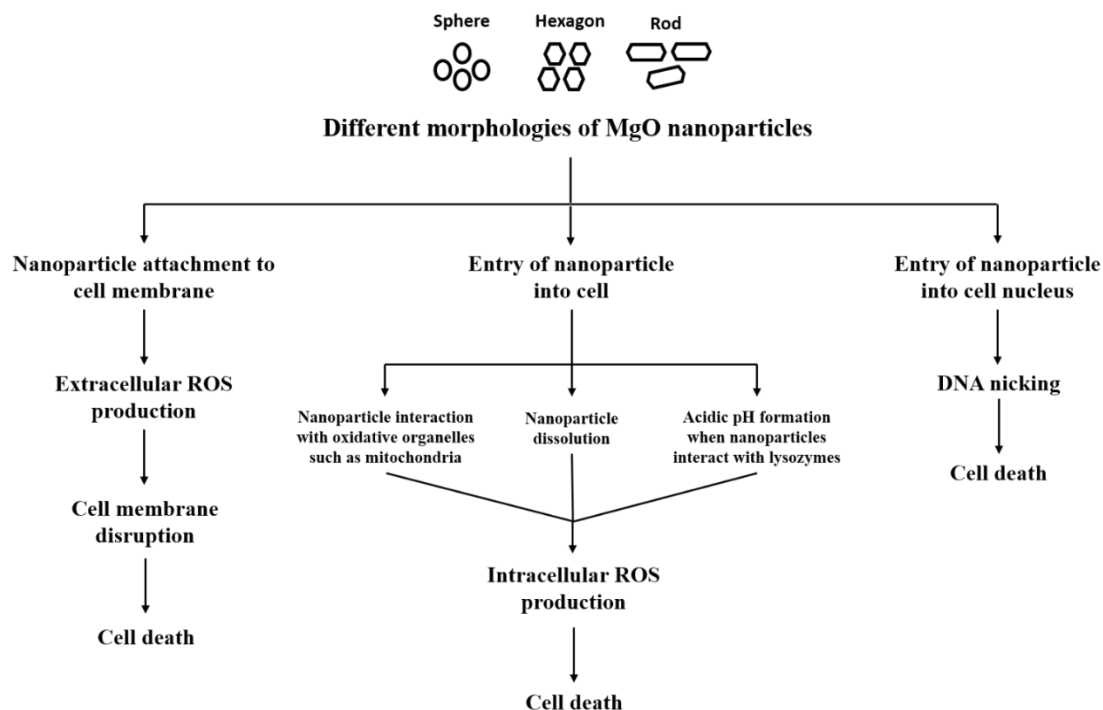
Figure 5.9: Proposed cytotoxicity mechanism of MgO nanoparticles

The probable mechanism of cytotoxicity by different MgO nanoparticles of different morphology has been depicted in Figure 5.9. Depending on the surface charge (Fröhlich, 2012), morphology (Andelman et al., 2010; Murgia et al., 2010) and size (Kim et al., 2012) of nanoparticles, there are three possible ways through which nanoparticles can induce toxic effect to cells. These involve attachment to the cell membrane, penetration into the cell and penetration into the nucleus. Nanoparticles may attach to the cell membrane depending on their surface charge, release reactive oxygen species (ROS) for the disruption of cell membrane, leading to cell mortality (Ryabchikova et al., 2010; Draeger et al., 2011; Wang et al., 2012; Mellgren, 2011). In the present work, the difference in the cytotoxicity of MgO nanoparticles in 3T3-L1 and VERO cells may be due to this mechanism. 3T3-L1 as an adipose cell possess positive surface charges which attract the negatively charged nanoparticles (Kohn et al., 1996). Whereas VERO cells contain negative surface charges (Ito et al., 2005) which regulate nanoparticle attraction towards cells due to repulsion. Moreover, the nanoparticles which are less electronegative and closer to neutral stability promote cellular bioavailability and cytotoxicity towards diabetic cells than non-diabetic cells. Attraction of nanoparticles towards cells may lead to penetration of nanoparticles into the cell to induce toxic effects. The nanoparticles interact with the mitochondria, dissolve and increase intracellular ionic content or react with lysozymes. The interaction of nanoparticles with mitochondria increases the intracellular ROS level and cause swelling of the mitochondria (Lovrić et al., 2005), which then results in cell disruption (Green et al., 2004; Tait et al., 2010). When nanoparticles dissolute inside cells, especially oxide materials, it alters the cellular equilibrium potential and increases cell membrane potential which leads to the disruption of cell membrane via oxidative stress (Annunziato et al., 2003; Fröhlich, 2012). Similarly, when nanoparticles interact with lysozymes, it decreases the acidity within the cell by forming intracellular ROS, which disrupts the cell metabolic pathway, thereby causing cell mortality (Soenen et al., 2011; Funnell et al., 2006; Asati et al., 2010). Smaller nanoparticles may also penetrate into the nucleus of the cells (AshaRani et al., 2008; Boyoglu et al., 2011) and may cause DNA nicking, leading to cell death (Zinchenko et al., 2007; Chen et al., 2005; Li et al., 2009). It was reported that nanoparticles smaller than 90 nm (Nitin et al., 2009) with neutral or close-to-neutral charge (Nabeshi et al.,

2011) can enter into the nucleus through nuclear pore (Peters, 2005). All these mechanisms are possible to induce cytotoxicity in the present study. However, further cytotoxicity test such as Lactose dehydrogenase (LDH) assay and microscopic studies are required to determine the exact mechanism of MgO nanoparticles that induces cytotoxicity in both cell lines. LDH assay will help to confirm the release of cytosolic LDH enzyme which is released into the culture medium upon cell death due to plasma membrane damage (Parboosing et al., 2017). Similarly, electron microscopic study will help to analyze the morphology of cells upon nanoparticle interaction (Leung et al., 2017).

5.5. Biological assay to analyze insulin resistance reversal ability of MgO nanoparticles

In the present study, three biological assays are conducted to study, analyze and confirm the insulin resistance reversal ability of MgO nanoparticles. DNS assay was performed to determine the amount of glucose present and converted in cells before and after incubating cells with nanoparticle for 24 hrs. This assay confirms the initial reversal of insulin resistance in diabetic cells. Western blot analysis then used to determine the reversal of insulin resistance as it studies the expression of GLUT 4 (glucose transporter protein) in plasma membrane, when insulin resistance is reversed (Favaretto et al., 2014; Cushman et al., 1980). Finally, fluorescent microscopy is used to confirm the mechanism of MgO nanoparticle interaction with the cells to in reverse insulin resistance in diabetic cells.

5.5.1. DNS based colorimetric glucose assay

A standard DNS graph was obtained from known glucose concentration, prior to the DNS assay experiment, to identify glucose quantity in cells. The data is found in Appendix C. The selected MgO nanoparticle samples (400 μl/ml dosage of sample B and 600 μl/ml dosage of sample GA) were added to the 3T3-L1 adipose cells and incubated for 25 hours. A positive control (cells with no nanoparticle treatment) was also incubated for 25 hours to analyze the quantity of glucose present in the normal diabetic cell. DNS based glucose experiment was sampled after every 5 hours to analyze the glucose present in the DMEM medium. After 25 hours, the cells were lysed and centrifuged to obtain the amount of glucose present inside the cells. The DNS based glucose assay was also performed using

127

the supernatant obtained after centrifugation to calculate the amount of intracellular glucose as stated in Table 5.2 and the raw data was included in Appendix E3. Figure 5.10 gives a clear insight on the reduction of glucose present in the medium and the kinetics of their reduction.

Table 5.2: **Concentration of extra and intracellular glucose sampled periodically during incubation.**

S.No.	Samples	0th hr OD	0th hr Conc (mg)	5th hr OD	5th hr Conc (mg)	10th hr OD	10th hr Conc (mg)	15th hr OD	15th hr Conc (mg)	20th hr OD	20th hr Conc (mg)	25th hr (In medium) OD	25th hr (In medium) Conc (mg)	25 hr (Inside cell) OD	25 hr (Inside cell) Conc (mg)
1	Control	1.8	**3.67**	1.723	3.47	1.66	3.35	1.608	3.25	1.525	3.07	0.209	**0.57**	0.045	**0.71**
2	Sample GA (600 µl/ml)	1.9	**3.67**	1.575	3.1	1.532	3	1.479	2.92	1.421	2.75	0.019	**0.09**	0.017	**0.17**
3	Sample B (400 µl/ml)	1.9	**3.67**	1.378	2.67	1.353	2.57	1.328	2.52	1.276	2.4	0.008	**0.04**	0.016	**0.15**
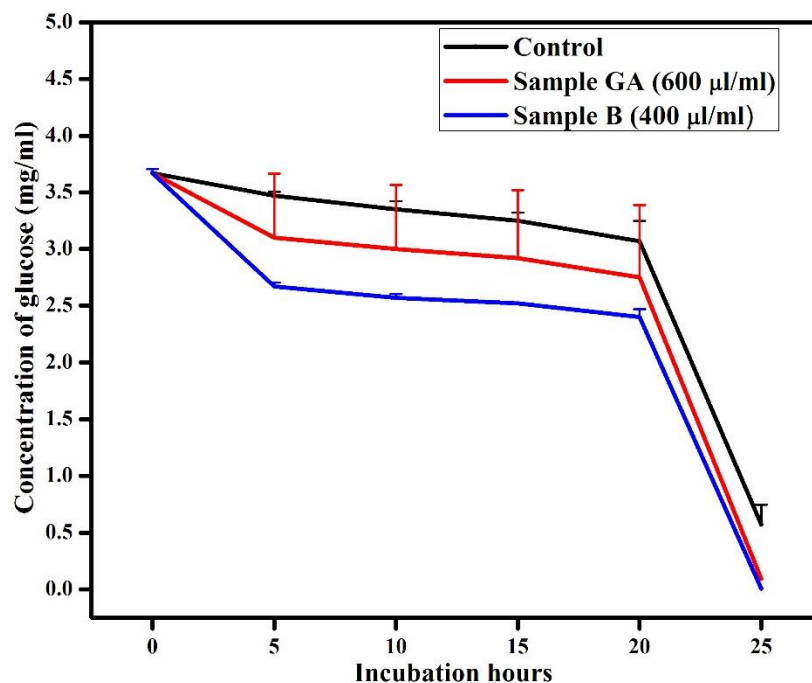
Figure 5.10: Time-dependent reduction of glucose in control and nanoparticles loaded cells

From Figure 5.10, it can be noted that ~3.7 μg/ml of glucose was present in DMEM medium. The cells slowly utilize glucose in the medium for their growth and development. It is noteworthy that the control (3T3-L1) utilizes certain amount of glucose depending on the percentage of insulin resistance in those cells (Houstis, 2007). Thus, the amount of intercellular glucose reduced to 0.57 mg/ml after 24 hours of incubation in the control. It is shown in Figure 5.10 that the nanoparticle loaded cells resulted in increasing glucose uptake and this resulted in reduced glucose concentration in the medium for cell growth than the control. Table 5.2 shows that 0.09 mg/ml and 0.04 mg/ml of intercellular glucose were present in the nanoparticle-loaded cells for sample GA and sample B respectively. The rate of intercellular glucose uptake is constant from 5-20 hours, and after 20 hours of incubation, a drastic uptake of glucose was observed, both in the control and the nanoparticle-loaded cells. This may be due to several factors such as activity of poly (ADP-Ribose) synthetase as mentioned in the literature (Pekala et al., 1981; Luo et al., 2017). The intracellular glucose was found to be 0.71mg/ml in the control cells and 0.017 mg/ml and 0.15 mg/ml for samples GA and sample B respectively.

Table 5.3: Total glucose and glucose uptake in the control and nanoparticle loaded cells

Sample	0 hrs mg/ml	After 24 hrs mg/ml		Total glucose (medium + inside cell glucose) mg/ml	Glucose utilization by cells after 24 hours (%)	Difference in glucose uptake compared to control cells (%)
		In medium	Inside cells			
Control	3.67	0.57	0.71	1.22	66.75%	-
Sample GA	3.67	0.09	0.17	0.26	92.9%	28.1%
Sample B	3.67	0.04	0.15	0.19	94.8%	29.5%

In the control cells, 66.75% of glucose was utilized by the cells in 24 hours as presented in Table 5.3. Also, the MgO nanoparticles loaded cells, reversed insulin resistance in the 3T3-L1 cells and resulted in glucose utilization of 92.9% and 94.8% in samples GA and B. This shows that the MgO nanoparticles loaded cells increased glucose uptake by 28.1% (for sample GA) and 29.5% (for sample B) compared to the control (Table 5.3). The reduction of glucose in the nanoparticle-loaded 3T3-L1 medium is due to MgO nanoparticle mediated activation of enzymes that reverses insulin resistance (Jeevanandam et al., 2015). The reversal of insulin resistance enables more insulin activity, leading to effective conversion of glucose into adenosine triphosphate (ATP) (Kahn et al., 2006). A similar observation is made for the control cells. 0.71 mg/ml of glucose was present inside the cells and for the MgO loaded samples only 0.17 mg/ml (for sample GA) and 0.15 mg/ml (for sample B) were present. The conversion process leads to a drastic reduction in the quantity of glucose present inside the cell and the medium after incubation with MgO nanoparticles for 24 hours compared to the control.

Literature strongly suggests that there is a relationship between magnesium level in the human body and cases of insulin resistance and type 2 diabetes. Kao et al (1999) found

that there is a significant inverse correlation between serum magnesium and the occurrence of type 2 diabetes (Kao et al., 1999). Similarly, many reported works have demonstrated that magnesium level is important to prevent diabetes as both serum and ionized magnesium are found to be low in diabetic patients (Mather et al., 1979; Garland, 1992; Sjogren et al., 1988b; Schnack et al., 1992; Vanroelen et al., 1985; Kurstjens et al., 2017). Even at the cellular level, type 2 diabetic patients showed reduced cytosolic free magnesium level compared to non-diabetic patients (Resnick et al., 1991; Barbagallo et al., 2000). Additionally, it was reported that magnesium directly regulates glucose metabolism at the cellular biochemical level by reversing insulin resistance due to its role in activating MgATP complex needed for rate-limiting glycolysis enzymes and the activity of all protein kinases (Barbagallo et al., 1996; Paolisso et al., 1997; Barbagallo et al., 2003). Thus, researchers have used magnesium supplement to reverse insulin resistance in diabetic rats and cells. Kandeel et al (1996) used adipocytes retrieved from male Sprague-Dawley rats and demonstrated that low ambient magnesium concentration (free Mg ion, 0.16 mM) caused insulin resistance.

It is quite evident, both in the present work and reported literature that, in the presence of magnesium, cellular glucose uptake increases as a result of insulin resistance reversal in diabetic cells. Moreover, the cytotoxicity analysis showed 55% of adipose cells were viable after treatment with MgO nanoparticles for 24 hours. This reduced cellular viability could also have an effect in glucose uptake. However, the MgO nanoparticles loaded cells showed increased glucose uptake compared to the control cells, indicating that the nanoparticles effectively reversed insulin resistance and reduce glucose level in the diabetic cells.

5.5.2. Western blot assay

Western blot assay was performed to detect the presence of GLUT4 (Glucose transporter) protein in the control and nanoparticles loaded cells. GLUT4 protein is a common protein that is present in the cytoplasm of adipose cells (Favaretto et al., 2014). Upon insulin binding to its substrate, GLUT4 protein is expressed in the plasma membrane, facilitating the entry of glucose into the cells and increasing glucose uptake from the extracellular

matrix (Cushman et al., 1980). Thus, there are two types of GLUT4 proteins; plasma membrane GLUT4 and cytoplasmic vesicular GLUT4. The protein from the intracellular region was obtained through centrifugation of insulin resistant adipose cells and western blot was performed using the supernatant solution. The present work analyses the presence of cytoplasmic GLUT4 protein via western blotting. GLUT4 in the plasma membrane binds with the lipid bilayer and eventually increases molecular weight, making it difficult for anti-GLUT4 antibody to detect at ~54 kDa (Stöckli et al., 2011; Martin et al., 2006).
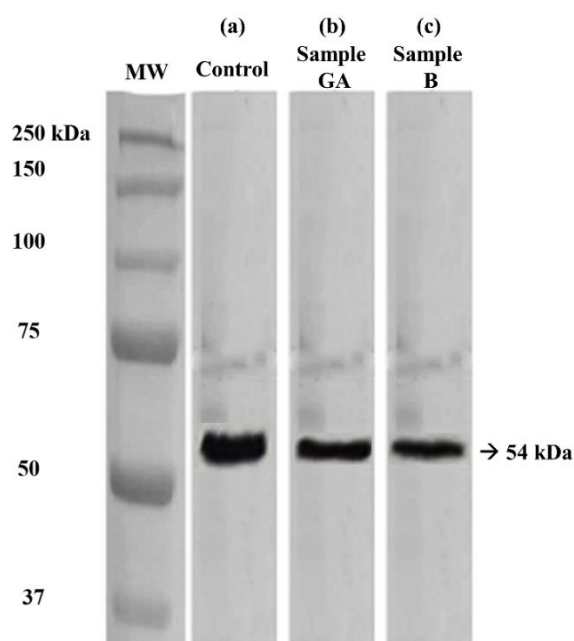
Figure 5.11: Western blot analysis of GLUT4 protein expression in (a) Control, (b) Sample GA and (c) Sample B

The blotting results as mentioned in Figure 5.11 shows a wide protein band in control cells and shorter bands in nanoparticles loaded cells. In insulin resistant adipose cells, the GLUT4 protein is located in the intracellular vesicles due to the inhibition of binding mechanism between insulin and their respective receptor. The western blot result also reveals that the control cells are insulin resistant as a wide protein band is obtained at 54kDa (Sylow et al., 2014; Sylow et al., 2013) as showed in Figure 5.11 (a). However, the width of protein band (54kDa) in the nanoparticle loaded cells is smaller compared to

the control cells, showing that insulin resistance is reversed due to MgO nanoparticles. When MgO nanoparticle are loaded to the cells, insulin resistance is reversed as discussed in the DNS glucose assay, which eventually increases the binding of insulin to their receptors. This induces the expression of GLUT4 protein from the intracellular vesicles to the plasma membrane. As the GLUT4 protein expressed in the plasma membrane to increase glucose uptake from extracellular matrix, the quantity of intracellular GLUT4 protein reduces (Martin et al., 2006; Etgen et al., 1993). Thus, Figure 5.11 (b) and (c) indicate that the quantity of intracellular GLUT4 protein is low compared to control cells, confirming the insulin resistance reversal ability of MgO nanoparticles. It can be noted that the intensity of the protein band is lower for sample B compared to sample GA. This is due to a higher insulin resistance reversal in sample B than sample GA, and the finding correlates well with the DNS glucose assay results. The reversal of insulin resistance leads to the binding of insulin to their substrate which assist the expression of cytoplasmic GLUT4 protein in the plasma membrane and eventually allows glucose signals to enter into the cell and increases glucose uptake. The increase in glucose uptake after MgO nanoparticles mediated reversal of insulin resistance is clearly evident in DNS glucose assay results (Section 5.5.1).

5.5.3. Fluorescent microscope studies

Two dyes namely propidium iodide and acridine orange were used to predict the possible mechanism of nanoparticle interaction with diabetic adipose cells. Propidium iodide (PI) is a membrane impermanent dye that generally gets excluded from viable cells and binds to double stranded DNA between their base pairs (Riccardi et al., 2006). This staining method gives information on the nanoparticle mediated cell membrane disruption and also whether the nanoparticle entered the cell to cause DNA nicking. On the other hand, Acridine orange (AO) is a cell permeable, nucleic acid selective dye that emits green fluorescence after binding with double stranded DNA. It emits a green colour after binding with live cells and emits an orange color when in contact with acidic cell organelles such as lysozyme during natural or induced cell apoptosis (Cousin et al., 1999). This staining method gives information on the entry of nanoparticles and the release of ROS inside the cell which eventually increases intracellular acidity and emits an orange

color. The fluorescent microscopy images of propidium iodide stained cells, incubated without nanoparticle (control) and with nanoparticle dosages (sample GA – 600μl/ml and sample B – 400 μl/ml) are shown in Figure 5.14. The yellow stains on the image represent non-viable cells due to membrane disruption. Usually, the propidium iodide stained cell images are red in color. However, the image was recolored to yellow with equivalent intensities using ImageJ software for better understanding. It can be noted that the nanoparticle loaded cells possess more yellow stains compared to the control cells. The non-viability of nanoparticle-loaded cells represented by the propidium iodide stains can be attributed to the cytotoxicity of MgO nanoparticle towards adipose cells as mentioned earlier in the cytotoxic (MTT) assay (Section 5.2). Similarly, the fluorescent microscope images of acridine orange stained cells, incubated without nanoparticle (control) and with nanoparticle dosages (sample GA – 600μl/ml and sample B – 400 μl/ml) is shown in Figure 5.15.
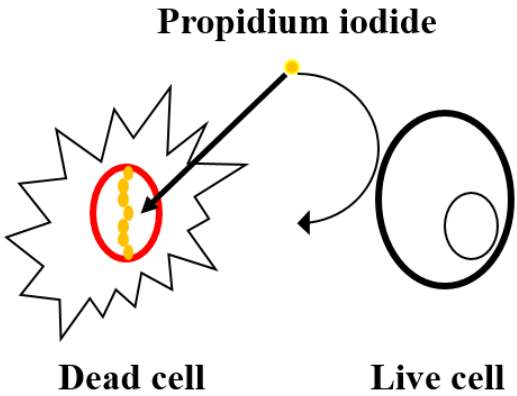
Figure 5.12: Mechanism of propidium iodide fluorescent microscopy image
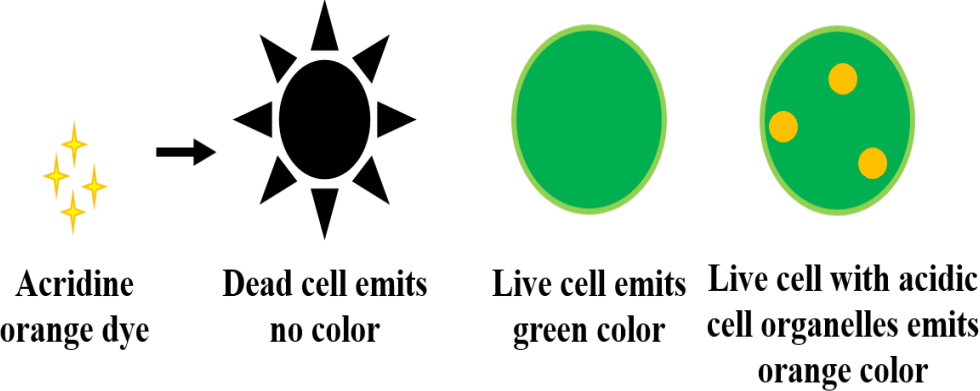
Figure 5.13: Mechanism of acridine orange fluorescent microscopy image
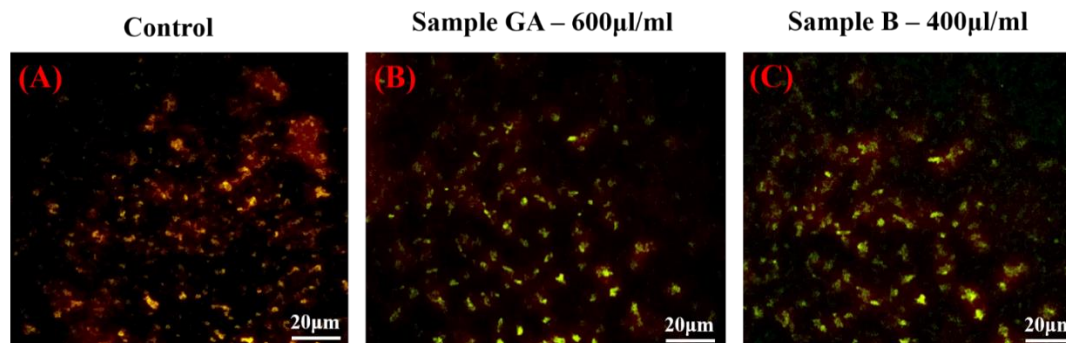
Figure 5.14: Fluorescent microscope images of propidium iodide stained 3T3-L1 cells after 24 hours (A) Control cells, (B) Sample GA – 600 μl/ml and (C) Sample B – 400 μl/ml
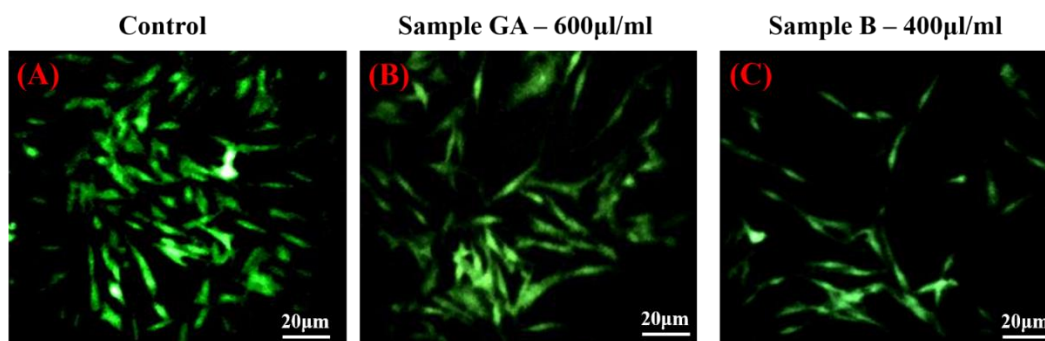
Figure 5.15: Fluorescent microscope images of acridine orange stained 3T3-L1 cells after 24 hours (A) Control cells, (B) Sample GA – 600 μl/ml and (C) Sample B – 400 μl/ml

The propidium iodide staining method clearly shows that the cytotoxicity of hexagonal shaped nanoparticle was due to the disruption of 3T3-L1 cell membrane. The cell membrane disruption may be due to two possible mechanism. The first mechanism is that the larger MgO nanoparticles (from chemical synthesis, < 40 nm) may attach to the cell membrane due to electrostatic forces of attraction (Nel et al., 2009). The nanoparticles after attachment disintegrate into its ionic states (Yameen et al., 2014) such as Mg^{2+} and O^{2-} based on their size. The magnesium ion passes through cellular ionic channels, enters into the cell and activates certain enzymes to reverse insulin resistance (Lansman et al., 1986; Monteilh-Zoller et al., 2003; White et al., 1989). The oxide ions act as reactive oxygen species and induce the formation of hydrogen peroxide which increases

136

extracellular oxidative stress and disrupts cell the membrane (Simon et al., 2000; Premanathan et al., 2011).

Another mechanism could be based on the mechanism of cell penetration by the nanoparticles. Smaller MgO nanoparticles from green synthesis (18-40 nm) may penetrate into the cells (Oh et al., 2014; Zhao et al., 2011) and disintegrate into their ionic states. Magnesium ions activate intracellular enzymes and reverse insulin resistance without ion channel transportation. The oxide ion increases intracellular oxidative stress and disrupts the cell. When correlating the glucose assay and western blot, both mechanisms are possible for MgO nanoparticles to reverse insulin resistance in adipose cells. The nanoparticles may enter or attach to the cell surface and release magnesium as well as oxide ions from 0-20 hours. The release of oxygen causes cell apoptosis and leads to cell death. After 20 hours, the release of oxygen ion from the nanoparticles is reduced. This increases the magnesium content in the cell and helps in activating certain enzymes, either intracellularly (through ion channel entry) or extracellularly, to reverse insulin resistance in the adipose cells. However, the second mechanism may not be the case according to the fluorescent microscope studies. The entry of nanoparticles into the adipose cell and reversing insulin resistance is not feasible because nanoparticle dissolution into its ionic state inside cells leads to intracellular oxidative stress which may disrupt cell organelles such as lysozyme, mitochondria, nucleus as well as cell membrane (Xia et al., 2008). It can be noted from the acridine orange stains image (Figure 5.15) that the cells are green, indicating live cells with no orange emission, indicating no fluctuation in intracellular pH (Chinni et al., 1999). Moreover, the fluorescence microscopy images reveal that the cytotoxicity of chemically synthesized MgO is higher compared to green synthesized MgO. It was shown from the propidium iodide staining analysis that only the cell membrane is disrupted but not the nucleus and DNA, as propidium iodide bind only with the DNA base pairs. It was then confirmed from the acridine orange staining method that the nanoparticles did not penetrate into the cells and released ROS to fluctuate intracellular pH and eventually cause cell apoptosis. Thus, it is clear that MgO nanoparticles attached to the cell via electrostatic force of attraction, disintegrated and released its ions into the growth medium. The oxygen ion species in the medium led to oxidative stress and disrupted the cell membrane whereas the Mg^{2+} ions activated

extracellular or intracellular (via ion channel) enzymes to reverse insulin resistance. The mechanism of MgO nanoparticles reverse insulin resistance in adipose cells is presented schematically in Figure 5.16.
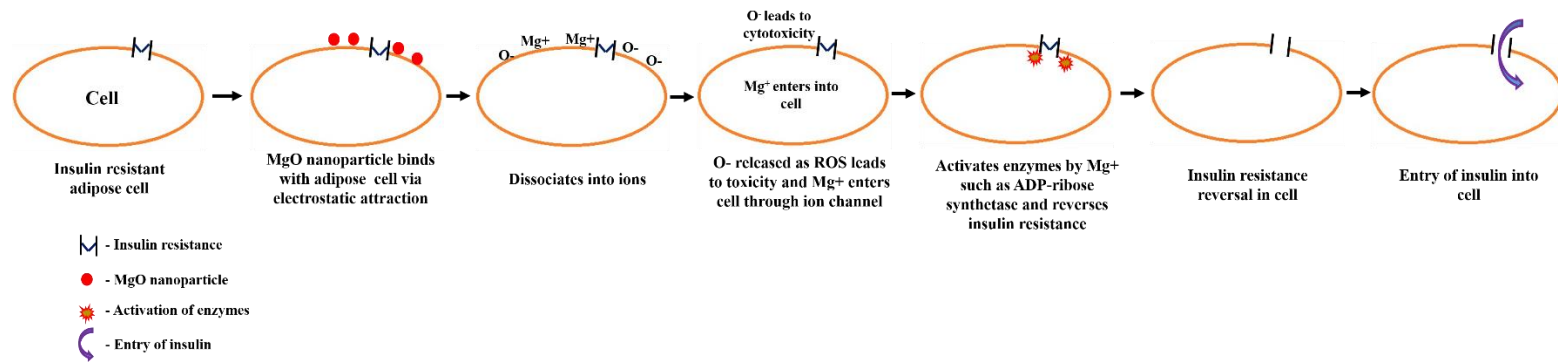
Figure 5.16: Mechanism of reversing insulin resistance using MgO nanoparticle as magnesium supplement

CHAPTER 6:

CONCLUSIONS AND RECOMMENDATIONS

The aim of the present work is to study the insulin resistant reversal ability of MgO nanoparticles and identify the morphology that enhances their insulin resistance reversibility. A chemical based sol-gel method has been employed to yield different morphologies of MgO nanoparticles, whereas plant leaf extract based green synthesis is used to yield different sizes of MgO nanoparticles. The current work articulates the evidences required to answer the research questions that emphasize the strategies important for triggering different morphology transformation through chemical method, potential of using green method for MgO nanoparticle synthesis and the efficacy level of MgO nanoparticles in insulin resistance reversibility. The primary objective of the current study is to investigate the efficiency of different shapes and sizes of MgO nanoparticles in reversing insulin resistance in diabetic cell model. The secondary objectives such as synthesizing, optimizing and characterizing MgO nanoparticles from chemical and green method as well as selecting their less toxic dosages in diabetic cell models helps in achieving the primary objectives. Both the primary and secondary objectives have been achieved in the present study, which gives a solution for all the research questions and furthermore, gives ample reasons to confirm the insulin resistance reversal ability.

The initial objective of the study is to synthesize, optimize and characterize MgO nanoparticles using different synthesis routes. The sol-gel method was used to synthesize different morphologies of MgO nanoparticles via chemical route as part of the first and second objective. Two types of magnesium precursors along with the combination of gelling agents were used for the sol-gel synthesis. The calcination temperature of the sol-gel product was selected from the melting transition temperature obtained from thermal analysis via TG-DSC. The results show that the sol-gel method yields different morphologies such as spherical (sample A), hexagonal (sample B) and rod (sample C) upon an increase in calcination temperature. The physicochemical and morphological characteristics of MgO nanoparticles were analyzed, which is evident as a solution for the

research question on the process strategies that are important to trigger different morphological transformations of MgO nanoparticles during sol-gel process.

The research question on the potential of synthesizing different sizes of MgO nanoparticles using plant leaf extracts, which is a part of initial objective, has been addressed by using three plant leaf extracts such as *A. tricolor*, *A. blitum* and *A. paniculata*. Six MgO nanoparticle samples were synthesized using plant leaf extracts along with two magnesium precursors. The physicochemical analysis of the nanoparticle samples revealed that the magnesium nitrate as precursor with lower molecular weight than magnesium acetate and leaf extract with higher flavonoid content, play a major role in defining the molecular features of MgO nanoparticles. The result shows that the particle sizes of the optimized samples were between 20 – 60 nm sizes and the green synthesized colloidal MgO nanoparticles are efficient in yielding nanoparticles with different sizes in a shorter time compared to chemical method. TEM micrograph of MgO nanoparticle sample synthesized using *A. tricolor* leaf extract and magnesium nitrate possess capability to yield a hexagon shape. Thus, this sample was selected for further optimization to yield hexagon shaped MgO nanoparticles via pH modifications which is a unique method, introduced in the present work, to transform colloidal nanoparticle morphology. The morphology of MgO nanoparticles synthesized using *A. tricolor* leaf extract and magnesium nitrate precursor was transformed from spherical to hexagon with 40 nm size in acidic pH 3. Six MgO nanoparticle samples with different sizes and shapes selected for further analysis to achieve initial objectives.

The cytotoxic analysis of MgO nanoparticles in diabetic and non-diabetic cells are identified via MTT assay to achieve the third objective of the study. MgO nanoparticles possess dosage dependent toxicity towards diabetic cells. However, MgO nanoparticles shows negligible toxicity even at higher concentrations for both diabetic and non-diabetic cells. It was found that hexagonal shaped nanoparticles are less toxic to cells compared to other morphologies. It was also confirmed that green synthesized MgO nanoparticles are less toxic to diabetic cells than chemical synthesized samples. 400 μl/ml dosage of 0.001M chemical synthesized (sample B) and 600 μl/ml dosage of 0.024M green synthesized (sample GA) MgO nanoparticles are selected for further bio-assays to study

their insulin resistance reversal ability. These results helps to achieve the third objective which reveals the cytotoxic specificity of MgO nanoparticles towards diabetic cell and their impacts in normal cells.

DNS glucose assay, western blot and fluorescent microscope studies were utilized to achieve the fourth objective of the study, which is to confirm the insulin resistance reversal efficacy of MgO nanoparticles. DNS glucose assays shows that the nanoparticle loaded adipose cells has ~30% more glucose uptake than control cells. However, the reversal of insulin resistance was confirmed by using anti-GLUT4 antibody in the western blot technique. The results showed a wide protein band of GLUT4 protein at 54kDa for control cells and the protein band is short for MgO nanoparticle loaded cells compared to control cells. This reveals the reduction of cytoplasmic GLUT4 protein quantity in MgO nanoparticle loaded cells compared to control cells. Hence, it is proven that MgO nanoparticles possess insulin resistance reversal ability. It is also noted that the reversal ability is higher in the chemical synthesized sample than green synthesized MgO nanoparticles. However, green synthesized samples are curated to be superior in insulin resistance reversing ability as they showcase less cytotoxicity at higher concentrations and dosages. The propidium iodide staining method in fluorescent microscope study shows that the cytotoxicity of MgO nanoparticles towards adipose cells is due to cell disruption and acridine orange staining method shows that the MgO nanoparticle does not enter into the cells. Thus, it is proposed from the biological studies that the MgO nanoparticles are attracted towards adipose cells via electrostatic attraction, disintegrate into ions where magnesium enters into cells through ion channels, activates intracellular enzymes and reverses insulin resistance. The fourth objective has been achieved through simple biological assays which helps in achieving the aim of the study and to quantify the efficacy of MgO nanoparticles for reversing insulin resistance in diabetic cell model.

These potential MgO nanoparticles will be highly impactful for type 2 diabetic patients where the cells are unable to utilize the insulin due to insulin resistance. However, the conditions such as the level of insulin resistance, magnesium content in cells and insulin secretion in patients also plays a major role in utilizing MgO nanoparticles as a magnesium supplement to reverse insulin resistance. Further, enhancements in the

morphology, formulation and surface charge will eventually increase the potentiality of MgO nanoparticles in reversing insulin resistance for the treatment of type 2 diabetes. Intense bio-assays and animal model studies will also help to understand and gain in-depth knowledge on the exact mechanism of MgO nanoparticles in exhibiting cytotoxic reaction and reversing insulin resistance in adipose cells.

The following recommendations are made for future studies to advance the development of MgO nanoparticles as active nanomedicines for effective insulin resistance reversal in type 2 diabetes treatment

- The current study focuses on investigating and revealing MgO nanoparticles as a potential drug material to be a magnesium supplement for reversing insulin resistance. However, nanoformulation of these nanoparticles will enhance the drug efficiency and efficacy by controlled targeted delivery. Thus, nanoformulation of these nanoparticles using several techniques will help to enhance their biocompatibility and insulin resistance reversal ability in future.

- The current study uses 3T3-L1 adipose cell lines for the investigation of insulin resistance reversal upon loading nanoparticles. The study can be extended to skeletal, kidney and liver cells to study the effect of MgO nanoparticles in reversing insulin resistance in various cells. Depending on the performance, the nanoformulated MgO nanoparticles have to be investigated on these cells to further develop them into a less toxic drug.

- In the present study, the uptake and conversion of glucose in insulin resistance and reversed adipose cells were investigated. Fructose is another form of simple sugar molecularly similar to glucose. Most of the fructose from one's diet will be converted into glucose through metabolism in liver. The inhibition of fructose metabolism will decrease glucose level in bloodstream and also reduces circulating insulin. Fructose (fructose metabolism) in the liver can also be enhanced via MgO nanoparticles as magnesium ion is a co-factor for many enzymes. Moreover, fructose was transported into liver cells by GLUT5. Thus, the effect of fructose in liver cells, its effect on insulin resistance, glucose levels, and the effect of MgO nanoparticles in regulating their mechanism can be studied. The current study emphasizes the expression of

cytoplasmic GLUT4 protein in adipose cells. The study can also be extended to GLUT1 which is also a glucose transporter protein that leads to glucose uptake in adipose cells.

- Finally, animal models such as zebrafish or mice have to be utilized to test the *in vivo* efficiency of the MgO nanoparticles in reversing insulin resistance. The bioavailability, circulation time and excretion of nanoparticles has to be further studied to design a superior nanoformulation to enhance the insulin resistant reversal ability and for the controlled, targeted delivery of MgO nanoparticles.

References

Abdullah N, Pesterfield C, Elleri D, and Dunger D B. 2014. "Management of insulin pump therapy in children with type 1 diabetes." *Archives of disease in childhood-Education & practice edition*:edpract-2013-304501.

Abdulmajeed I M, Chyad F A, Abbas M M, and Kareem H A. 2013. "Fabrication and Characterization of Ultrafine Crystalline MgO and ZnO Powders." *International Journal of Innovative Research in Science, Engineering and Technology* 2 (10):5101-5106.

Abraira C, Colwell J A, Nuttall F Q, Sawin C T, Nagel N J, Comstock J P, Emanuele N V, Levin S R, Henderson W, and Lee H S. 1995. "Veterans Affairs Cooperative Study on glycemic control and complications in type II diabetes (VA CSDM). Results of the feasibility trial. Veterans Affairs Cooperative Study in Type II Diabetes." *Diabetes Care* 18 (8):1113-23.

Achigan-Dako E G, Sogbohossou O E, and Maundu P. 2014. "Current knowledge on Amaranthus spp.: research avenues for improved nutritional value and yield in leafy amaranths in sub-Saharan Africa." *Euphytica* 197 (3):303-317.

Agarwal R, Singh V, Jurney P, Shi L, Sreenivasan S, and Roy K. 2013. "Mammalian cells preferentially internalize hydrogel nanodiscs over nanorods and use shape-specific uptake mechanisms." *Proceedings of the National Academy of Sciences* 110 (43):17247-17252.

Ahmad N, Sharma S, Alam M K, Singh V, Shamsi S, Mehta B, and Fatma A. 2010. "Rapid synthesis of silver nanoparticles using dried medicinal plant of basil." *Colloids Surf., B* 81 (1):81-86.

Ahn S, Kim K, Chun Y, and Yoon K. 2007. "Nucleation and growth of Cu (In, Ga) Se 2 nanoparticles in low temperature colloidal process." *Thin Solid Films* 515 (7):4036-4040.

Akbar S. 2011a. "Andrographis paniculata: a review of pharmacological activities and clinical effects." *Altern. Med Rev* 16 (1):66-77.

Akbar S. 2011b. "Andrographis paniculata: a review of pharmacological activities and clinical effects." *Alternative Medicine Review* 16 (1):66-77.

Akowuah G, Zhari I, and Mariam A. 2008. "Analysis of urinary andrographolides and antioxidant status after oral administration of Andrographis paniculata leaf extract in rats." *Food Chem. Toxicol.* 46 (12):3616-3620.

Alam M, and Janata E. 2006. "UV absorption spectrum, formation and disappearance of the oxide radical ion O− in aqueous solution: A pulse radiolysis study." *Chemical physics letters* 417 (4):363-366.

Albanese A, Tang P S, and Chan W C. 2012. "The effect of nanoparticle size, shape, and surface chemistry on biological systems." *Annual review of biomedical engineering* 14:1-16.

Alegbejo J O. 2014. "Nutritional Value and Utilization of Amaranthus (Amaranthus spp.)–A Review." *Bayero Journal of Pure and Applied Sciences* 6 (1):136-143.

Alexis F, Pridgen E, Molnar L K, and Farokhzad O C. 2008. "Factors affecting the clearance and biodistribution of polymeric nanoparticles." *Molecular pharmaceutics* 5 (4):505-515.

Ali A T, Ferris W F, Naran N H, and Crowther N J. 2011. "Insulin resistance in the control of body fat distribution: a new hypothesis." *Horm Metab Res* 43 (2):77-80. doi: 10.1055/s-0030-1269851.

Ali M E, Rahman M M, Sarkar S M, and Hamid S B A. 2014. "Heterogeneous Metal Catalysts for Oxidation Reactions." *Journal of Nanomaterials*.

Alighourchi H, and Barzegar M. 2009. "Some physicochemical characteristics and degradation kinetic of anthocyanin of reconstituted pomegranate juice during storage." *Journal of Food Engineering* 90 (2):179-185.

Alkaladi A, Abdelazim A M, and Afifi M. 2014. "Antidiabetic Activity of Zinc Oxide and Silver Nanoparticles on Streptozotocin-Induced Diabetic Rats." *International Journal of Molecular Sciences* 15 (2):2015-2023. doi: 10.3390/ijms15022015.

Alrobayi E M, Algubili A M, Aljeboree A M, Alkaim A F, and Hussein F H. 2017. "Investigation of photocatalytic removal and photonic efficiency of maxilon blue dye GRL in the presence of TiO2 nanoparticles." *Particulate Science and Technology* 35 (1):14-20.

Alwan R M, Kadhim Q A, Sahan K M, Ali R A, Mahdi R J, Kassim N A, and Jassim A N. 2015. "Synthesis of Zinc Oxide Nanoparticles via Sol–Gel Route and Their Characterization." *Nanoscience and Nanotechnology* 5 (1):1-6.

Alzaid A, Dinneen S, Moyer T, and Rizza R. 1995. "Effects of insulin on plasma magnesium in noninsulin-dependent diabetes mellitus: evidence for insulin resistance." *The Journal of Clinical Endocrinology & Metabolism* 80 (4):1376-1381.

Amin I, Norazaidah Y, and Hainida K E. 2006. "Antioxidant activity and phenolic content of raw and blanched Amaranthus species." *Food Chem.* 94 (1):47-52.

Amos A F, McCarty D J, and Zimmet P. 1997. "The rising global burden of diabetes and its complications: estimates and projections to the year 2010." *Diabet Med* 14 Suppl 5:S1-85.

Anastas P T, and Warner J C. 2000. *Green chemistry: theory and practice*: Oxford university press.

Andelman T, Gordonov S, Busto G, Moghe P V, and Riman R E. 2010. "Synthesis and cytotoxicity of Y2O3 nanoparticles of various morphologies." *Nanoscale research letters* 5 (2):263.

Annunziato L, Amoroso S, Pannaccione A, Cataldi M, Pignataro G, D'Alessio A, Sirabella R, Secondo A, Sibaud L, and Di Renzo G. 2003. "Apoptosis induced in neuronal cells by oxidative stress: role played by caspases and intracellular calcium ions." *Toxicology letters* 139 (2):125-133.

Ansari A A, Kaushik A, Solanki P R, and Malhotra B. 2010. "Nanostructured zinc oxide platform for mycotoxin detection." *Bioelectrochemistry* 77 (2):75-81.

Antony T, Peter M J, and Raj J Y. 2013. "Phytochemical Analysis of Stylosanthes fruticosa using UV-VIS, FTIR and GCMS." *Research Journal of Chemical Sciences* 3 (11):14-23.

áO'Brien R W. 1990. "Electroacoustic studies of moderately concentrated colloidal suspensions." *Faraday Discussions of the Chemical Society* 90:301-312.

Arefi M R, and Rezaei-Zarchi S. 2012. "Synthesis of Zinc Oxide Nanoparticles and Their Effect on the Compressive Strength and Setting Time of Self-Compacted Concrete

Paste as Cementitious Composites." *International journal of molecular sciences* 13 (4):4340-4350.

Armendariz V, Herrera I, Jose-yacaman M, Troiani H, Santiago P, and Gardea-Torresdey J L. 2004. "Size controlled gold nanoparticle formation by Avena sativa biomass: use of plants in nanobiotechnology." *Journal of Nanoparticle Research* 6 (4):377-382.

Asati A, Santra S, Kaittanis C, and Perez J M. 2010. "Surface-charge-dependent cell localization and cytotoxicity of cerium oxide nanoparticles." *ACS nano* 4 (9):5321-5331.

AshaRani P, Low Kah Mun G, Hande M P, and Valiyaveettil S. 2008. "Cytotoxicity and genotoxicity of silver nanoparticles in human cells." *ACS nano* 3 (2):279-290.

Association A D. 2016. "7. Approaches to glycemic treatment." *Diabetes care* 39 (Supplement 1):S52-S59.

Atalay S, Beskok A, and Qian S. 2014. "Surface Charge Properties of Nanoparticle: Size Dependency and Boundary Effect." Meeting Abstracts.

Athar T, Hakeem A, and Ahmed W. 2012. "Synthesis of MgO Nanopowder via Non Aqueous Sol–Gel Method." *Advanced Science Letters* 7 (1):27-29.

Atlas I D. 2015. "International Diabetes Federation, Brussels, 2015." *Available from:[Last accessed: 5 March 2014]*.

Awwad A, Albiss B, and Salem N. 2015. "Antibacterial Activity of synthesized Copper Oxide Nanoparticles using Malva sylvestris Leaf Extract." *SMU Medical Journal* 2 (1):91-100.

Ayyub P, Palkar V, Chattopadhyay S, and Multani M. 1995. "Effect of crystal size reduction on lattice symmetry and cooperative properties." *Physical Review B* 51 (9):6135.

Azevedo M, and Alla S. 2008. "Diabetes in sub-saharan Africa: kenya, mali, mozambique, Nigeria, South Africa and zambia." *Int J Diabetes Dev Ctries* 28 (4):101-8. doi: 10.4103/0973-3930.45268.

Badawy A M E, Luxton T P, Silva R G, Scheckel K G, Suidan M T, and Tolaymat T M. 2010. "Impact of environmental conditions (pH, ionic strength, and electrolyte

type) on the surface charge and aggregation of silver nanoparticles suspensions." *Environmental science & technology* 44 (4):1260-1266.

Baek M, Kim M, Cho H, Lee J, Yu J, Chung H, and Choi S. 2011. "Factors influencing the cytotoxicity of zinc oxide nanoparticles: particle size and surface charge." Journal of Physics: Conference Series.

Bala I, Hariharan S, and Kumar M N. 2004. "PLGA nanoparticles in drug delivery: the state of the art." *Crit Rev Ther Drug Carrier Syst* 21 (5):387-422.

Balaji S, Mandal B K, Ranjan S, Dasgupta N, and Chidambaram R. 2017. "Nano-zirconia–Evaluation of its antioxidant and anticancer activity." *Journal of Photochemistry and Photobiology B: Biology*.

Balasundaram G, Sato M, and Webster T J. 2006. "Using hydroxyapatite nanoparticles and decreased crystallinity to promote osteoblast adhesion similar to functionalizing with RGD." *Biomaterials* 27 (14):2798-2805. doi: https://doi.org/10.1016/j.biomaterials.2005.12.008.

Bangale M, Mitkare S, Gattani S, and Sakarkar D. 2012. "Recent nanotechnological aspects in cosmetics and dermatological preparations." *International Journal of Pharmacy & Pharmaceutical Sciences* 4 (2).

Bar H, Bhui D K, Sahoo G P, Sarkar P, De S P, and Misra A. 2009. "Green synthesis of silver nanoparticles using latex of Jatropha curcas." *Colloids and surfaces A: Physicochemical and engineering aspects* 339 (1):134-139.

Barbagallo M, Dominguez L J, Galioto A, Ferlisi A, Cani C, Malfa L, Pineo A, and Paolisso G. 2003. "Role of magnesium in insulin action, diabetes and cardio-metabolic syndrome X." *Molecular aspects of medicine* 24 (1):39-52.

Barbagallo M, Gupta R K, Dominguez L J, and Resnick L M. 2000. "Cellular ionic alterations with age: relation to hypertension and diabetes." *Journal of the American Geriatrics Society* 48 (9):1111-1116.

Barbagallo M, and Resnick L M. 1996. "Calcium and Magnesium in the regulation of smooth muscle function and blood pressure." In *Endocrinology of the Vasculature*, 283-300. Springer.

Barone P W, Parker R S, and Strano M S. 2005. "*In vivo* fluorescence detection of glucose using a single-walled carbon nanotube optical sensor: design, fluorophore

properties, advantages, and disadvantages." *Analytical chemistry* 77 (23):7556-7562.

Baskar G, Chandhuru J, Fahad K S, and Praveen A. 2013. "Mycological synthesis, characterization and antifungal activity of zinc oxide nanoparticles." *Asian Journal of Pharmacy and Technology* 3 (4):142-146.

Begon S, Pickering G, Eschalier A, Mazur A, Rayssiguier Y, and Dubray C. 2001. "Role of spinal NMDA receptors, protein kinase C and nitric oxide synthase in the hyperalgesia induced by magnesium deficiency in rats." *British journal of pharmacology* 134 (6):1227-1236.

Berg J M, Romoser A, Banerjee N, Zebda R, and Sayes C M. 2009. "The relationship between pH and zeta potential of~ 30 nm metal oxide nanoparticle suspensions relevant to *in vitro* toxicological evaluations." *Nanotoxicology* 3 (4):276-283.

Berne B J, and Pecora R. 2000. *Dynamic light scattering: with applications to chemistry, biology, and physics*: Courier Corporation.

Bertinetti L, Drouet C, Combes C, Rey C, Tampieri A, Coluccia S, and Martra G. 2009a. "Surface characteristics of nanocrystalline apatites: effect of mg surface enrichment on morphology, surface hydration species, and cationic environments." *Langmuir* 25 (10):5647-54. doi: 10.1021/la804230j.

Bertinetti L, Drouet C, Combes C, Rey C, Tampieri A, Coluccia S, and Martra G. 2009b. "Surface characteristics of nanocrystalline apatites: effect of Mg surface enrichment on morphology, surface hydration species, and cationic environments." *Langmuir* 25 (10):5647-5654.

Bhattacharyya D, Howden R M, Borrelli D C, and Gleason K K. 2012. "Vapor phase oxidative synthesis of conjugated polymers and applications." *Journal of Polymer Science Part B: Polymer Physics* 50 (19):1329-1351.

Bhattacharyya S, and Gedanken A. 2008. "A template-free, sonochemical route to porous ZnO nano-disks." *Microporous and Mesoporous Materials* 110 (2):553-559.

Blanco E, Shen H, and Ferrari M. 2015. "Principles of nanoparticle design for overcoming biological barriers to drug delivery." *Nature biotechnology* 33 (9):941-951.

Boeuf J. 2003. "Plasma display panels: physics, recent developments and key issues." *Journal of Physics D: Applied Physics* 36 (6):R53.

Bokhimi X, Morales A, Portilla M, and García-Ruiz A. 1999. "Hydroxides as precursors of nanocrystalline oxides." *Nanostructured Materials* 12 (1):589-592.

Bora T, Lakshman K K, Sarkar S, Makhal A, Sardar S, Pal S K, and Dutta J. 2013. "Modulation of defect-mediated energy transfer from ZnO nanoparticles for the photocatalytic degradation of bilirubin." *Beilstein journal of nanotechnology* 4 (1):714-725.

Borm P, Costa D, Castranova V, Donaldson K, Driscoll K, Dungworth D, Green F, Greim H, Harkema J, and Jarabek A. 2000. The relevance of the rat lung response to particle overload for human risk assessment: a workshop consensus report. Informa healthcare telephone house, 69-77 Paul street, London EC2A 4LQ, England.

Boyoglu C, Boyoglu-Barnum S, Soni S, He Q, Willing G, Miller M, and Singh S. 2011. "The intracellular co-localizations of different size of gold nanoparticles." *Nanotechnology*:489-492.

Braibanti A, Tiripicchio A, Camellini M, Lanfredi A, and Bigoli F. 1969. "The crystal structures of nitrates of divalent hexaaquocations. II. Hexaaquomagnesium nitrate." *Acta Crystallographica Section B: Structural Crystallography and Crystal Chemistry* 25 (2):354-361.

Buchanan T A, and Xiang A H. 2005. "Gestational diabetes mellitus." *Journal of Clinical Investigation* 115 (3):485.

Burkill I H. 1966. "A dictionary of the economic products of the Malay Peninsula." *A Dictionary of the Economic Products of the Malay Peninsula.* 2 (2nd edition).

Burmeister J S, Olivier L A, Reichert W, and Truskey G A. 1998. "Application of total internal reflection fluorescence microscopy to study cell adhesion to biomaterials." *Biomaterials* 19 (4-5):307-325.

Cao G. 2004. *Synthesis, properties and applications*: World Scientific.

Cao L, Ye J, Tong L, and Tang B. 2008. "A new route to the considerable enhancement of glucose oxidase (GOx) activity: the simple assembly of a complex from CdTe quantum dots and GOx, and its glucose sensing." *Chemistry-A European Journal* 14 (31):9633-9640.

Carella A M, Marinelli T, Melfitano A, Di Pumpo M, Conte M, and Benvenuto A. 2017. "Hypoglycemia by Ginseng in type 2 Diabetic Patient: Case Report."

Carino G P, and Mathiowitz E. 1999. "Oral insulin delivery." *Advanced drug delivery reviews* 35 (2):249-257.

Carmichael J, DeGraff W G, Gazdar A F, Minna J D, and Mitchell J B. 1987. "Evaluation of a tetrazolium-based semiautomated colorimetric assay: assessment of chemosensitivity testing." *Cancer Res* 47 (4):936-42.

Caro J F. 1991. "Clinical review 26: Insulin resistance in obese and nonobese man." *J Clin Endocrinol Metab* 73 (4):691-5. doi: 10.1210/jcem-73-4-691.

Cash K J, and Clark H A. 2010. "Nanosensors and nanomaterials for monitoring glucose in diabetes." *Trends in molecular medicine* 16 (12):584-593.

Chaari M, and Matoussi A. 2012. "Electrical conduction and dielectric studies of ZnO pellets." *Physica B: Condensed Matter* 407 (17):3441-3447.

Chadwick A V, Poplett I J, Maitland D T, and Smith M E. 1998. "Oxygen speciation in nanophase MgO from solid-state 17O NMR." *Chemistry of materials* 10 (3):864-870.

Chakraborti S, Chatterjee T, Joshi P, Poddar A, Bhattacharyya B, Singh S P, Gupta V, and Chakrabarti P. 2009. "Structure and activity of lysozyme on binding to ZnO nanoparticles." *Langmuir* 26 (5):3506-3513.

Chalkidou A, Simeonidis K, Angelakeris M, Samaras T, Martinez-Boubeta C, Balcells L, Papazisis K, Dendrinou-Samara C, and Kalogirou O. 2011. "*In vitro* application of Fe/MgO nanoparticles as magnetically mediated hyperthermia agents for cancer treatment." *Journal of Magnetism and Magnetic Materials* 323 (6):775-780.

Chan W C. 2017. "Nanomedicine 2.0." *Accounts of Chemical Research* 50 (3):627-632.

Chan Y, and Don M. 2011. "A Macro View of Bionanotechnology: Application and Implications in the Near Future." *Journal of Bionanoscience* 5 (2):97-106.

Chen M, and von Mikecz A. 2005. "Formation of nucleoplasmic protein aggregates impairs nuclear function in response to SiO 2 nanoparticles." *Experimental cell research* 305 (1):51-62.

Cheon J, Kang N-J, Lee S-M, Lee J-H, Yoon J-H, and Oh S J. 2004. "Shape evolution of single-crystalline iron oxide nanocrystals." *Journal of the American Chemical Society* 126 (7):1950-1951.

Chibac A L, Buruiana T, Melinte V, and Buruiana E C. 2017. "Photocatalysis applications of some hybrid polymeric composites incorporating TiO2 nanoparticles and their combinations with SiO2/Fe2O3." *Beilstein journal of nanotechnology* 8:272.

Chinni S R, and Shisheva A. 1999. "Arrest of endosome acidification by bafilomycin A1 mimics insulin action on GLUT4 translocation in 3T3-L1 adipocytes." *Biochemical Journal* 339 (3):599-606.

Chithrani B D, Ghazani A A, and Chan W C. 2006. "Determining the size and shape dependence of gold nanoparticle uptake into mammalian cells." *Nano letters* 6 (4):662-668.

Choudhary V, Rane V, and Gadre R. 1994. "Influence of precursors used in preparation of MgO on its surface properties and catalytic activity in oxidative coupling of methane." *Journal of Catalysis* 145 (2):300-311.

Chow E H, Strobridge F C, and Friščić T. 2010. "Mechanochemistry of magnesium oxide revisited: facile derivatisation of pharmaceuticals using coordination and supramolecular chemistry." *Chemical Communications* 46 (34):6368-6370.

Chowdhury A H, Chowdhury I H, and Naskar M K. 2015. "A facile synthesis of grainy rod-like porous MgO." *Materials Letters* 158:190-193.

Chrastina A, Massey K A, and Schnitzer J E. 2011. "Overcoming *in vivo* barriers to targeted nanodelivery." *Wiley Interdisciplinary Reviews: Nanomedicine and Nanobiotechnology* 3 (4):421-437.

Chueh P J, Liang R-Y, Lee Y-H, Zeng Z-M, and Chuang S-M. 2014. "Differential cytotoxic effects of gold nanoparticles in different mammalian cell lines." *Journal of hazardous materials* 264:303-312.

Chung T-H, Wu S-H, Yao M, Lu C-W, Lin Y-S, Hung Y, Mou C-Y, Chen Y-C, and Huang D-M. 2007. "The effect of surface charge on the uptake and biological function of mesoporous silica nanoparticles in 3T3-L1 cells and human mesenchymal stem cells." *Biomaterials* 28 (19):2959-2966.

Cichosz S L, Lundby-Christensen L, Johansen M D, Tarnow L, Almdal T P, Hejlesen O
K, and Group T C. 2017. "Prediction of excessive weight gain in insulin treated
patients with type 2 diabetes." *Journal of diabetes* 9 (4):325-331.

Cines D B, Pollak E S, Buck C A, Loscalzo J, Zimmerman G A, McEver R P, Pober J S,
Wick T M, Konkle B A, and Schwartz B S. 1998. "Endothelial cells in physiology
and in the pathophysiology of vascular disorders." *Blood* 91 (10):3527-3561.

Clark J H, and Macquarrie D J. 2008. *Handbook of green chemistry and technology*: John
Wiley & Sons.

Cochran E, and Gorden P. 2008. "Use of U-500 insulin in the treatment of severe insulin
resistance." *Insulin* 3 (4):211-218.

Colditz G A, Willett W C, Stampfer M J, Manson J E, Hennekens C H, Arky R A, and
Speizer F E. 1990. "Weight as a risk factor for clinical diabetes in women." *Am J
Epidemiol* 132 (3):501-13.

Cork S J, and Krockenberger A K. 1991. "Methods and pitfalls of extracting condensed
tannins and other phenolics from plants: Insights from investigations
onEucalyptus leaves." *Journal of Chemical Ecology* 17 (1):123-134.

Cosentino I, Muccillo E, Muccillo R, and Vichi F. 2006. "Low-temperature sol-gel
synthesis of single-phase ZrTiO4 nanoparticles." *Journal of sol-gel science and
technology* 37 (1):31-37.

Cousin B, Munoz O, André M, Fontanilles A, Dani C, Cousin J, Laharrague P, Casteilla
L, and Enicaud L. 1999. "A role for preadipocytes as macrophage-like cells." *The
FASEB Journal* 13 (2):305-312.

Cryer PE F J, Shamoon H. 1994. "Hypoglycemia (Technical review)." *Diabetes Care*
17:734 -755.

Cunningham D P, and Lundie L. 1993. "Precipitation of cadmium by Clostridium
thermoaceticum." *Applied and Environmental Microbiology* 59 (1):7-14.

Cushman S, and Wardzala L. 1980. "Potential mechanism of insulin action on glucose
transport in the isolated rat adipose cell. Apparent translocation of intracellular
transport systems to the plasma membrane." *Journal of Biological Chemistry* 255
(10):4758-4762.

D'Eliseo P, Blaauw J, Milicevic Z, Wyatt J, Ignaut D A, and Malone J K. 2000. "Patient acceptability of a new 3.0 ml pre-filled insulin pen." *Curr Med Res Opin* 16 (2):125-33.

Daniel S K, Vinothini G, Subramanian N, Nehru K, and Sivakumar M. 2013. "Biosynthesis of Cu, ZVI, and Ag nanoparticles using Dodonaea viscosa extract for antibacterial activity against human pathogens." *Journal of nanoparticle research* 15 (1):1-10.

Das S K, and Elbein S C. 2006. "The Genetic Basis of Type 2 Diabetes." *Cellscience* 2 (4):100-131. doi: 10.1901/jaba.2006.2-100.

Davini P, and Tartarelli R. 1985. "Emissions from the combustion of heavy oils: effect of granulometry and surface area of MgO additive." *Fuel* 64 (3):380-383.

Davis M E, and Shin D M. 2008. "Nanoparticle therapeutics: an emerging treatment modality for cancer." *Nature reviews Drug discovery* 7 (9):771-782.

Davis T, and Edelman S V. 2004. "Insulin therapy in type 2 diabetes." *Med Clin North Am* 88 (4):865-95, x. doi: 10.1016/j.mcna.2004.04.005.

de la Hoz A, Diaz-Ortiz A, and Moreno A. 2005. "Microwaves in organic synthesis. Thermal and non-thermal microwave effects." *Chemical Society Reviews* 34 (2):164-178.

De Volder M F, Tawfick S H, Baughman R H, and Hart A J. 2013. "Carbon nanotubes: present and future commercial applications." *Science* 339 (6119):535-539.

DeFronzo R A. 1992. "Insulin resistance, hyperinsulinemia, and coronary artery disease: a complex metabolic web." *J Cardiovasc Pharmacol* 20 Suppl 11:S1-16.

DeFronzo R A. 1999. "Pharmacologic Therapy for Type 2 Diabetes Mellitus." *Annals of Internal Medicine* 131 (4):281-303. doi: 10.7326/0003-4819-131-4-199908170-00008.

Demir M M, Gulgun M A, Menceloglu Y Z, Erman B, Abramchuk S S, Makhaeva E E, Khokhlov A R, Matveeva V G, and Sulman M G. 2004. "Palladium nanoparticles by electrospinning from poly (acrylonitrile-co-acrylic acid)-PdCl2 solutions. Relations between preparation conditions, particle size, and catalytic activity." *Macromolecules* 37 (5):1787-1792.

Devaux S, Adrian M, Laurant P, Berthelot A, and Quignard-Boulangé A. 2016. "Dietary magnesium intake alters age-related changes in rat adipose tissue cellularity." *Magnesium Research* 29 (4):175-183.

Devi R S, and Gayathri R. 2014. "Green Synthesis of Zinc Oxide Nanoparticles by using Hibiscus rosa-sinensis." *International Journal of Current Engineering and Technology* 4 (4):2444-2446.

DeWitt D E, and Hirsch I B. 2003. "Outpatient insulin therapy in type 1 and type 2 diabetes mellitus: scientific review." *Jama* 289 (17):2254-64.

Di D-R, He Z-Z, Sun Z-Q, and Liu J. 2012. "A new nano-cryosurgical modality for tumor treatment using biodegradable MgO nanoparticles." *Nanomedicine: Nanotechnology, Biology and Medicine* 8 (8):1233-1241.

DiSanto R M, Subramanian V, and Gu Z. 2015. "Recent advances in nanotechnology for diabetes treatment." *Wiley Interdisciplinary Reviews: Nanomedicine and Nanobiotechnology* 7 (4):548-564.

Doreswamy B, Mahendra M, Sridhar M, Prasad J S, Varughese P, George J, and Varghese G. 2005. "A novel three-dimensional polymeric structure of crystalline neodymium malonate hydrate." *Materials Letters* 59 (10):1206-1213.

Dou M, Ma Y, Ma A-G, Han L, Song M-M, Wang Y-G, Yao M-X, Sun X-F, Li Y, and Gao S. 2016. "Combined chromium and magnesium decreases insulin resistance more effectively than either alone." *Asia Pacific journal of clinical nutrition* 25 (4):747-753.

Draeger A, Monastyrskaya K, and Babiychuk E B. 2011. "Plasma membrane repair and cellular damage control: the annexin survival kit." *Biochemical pharmacology* 81 (6):703-712.

Drbohlavova J, Adam V, Kizek R, and Hubalek J. 2009. "Quantum dots—characterization, preparation and usage in biological systems." *International journal of molecular sciences* 10 (2):656-673.

Dreaden E C, Austin L A, Mackey M A, and El-Sayed M A. 2012. "Size matters: gold nanoparticles in targeted cancer drug delivery." *Ther Deliv* 3 (4):457-78.

Duan J, Yu Y, Li Y, Yu Y, Li Y, Zhou X, Huang P, and Sun Z. 2013. "Toxic effect of silica nanoparticles on endothelial cells through DNA damage response via Chk1-dependent G2/M checkpoint." *PloS one* 8 (4):e62087.

Duyar O, and Durusoy H Z. 2004. "Design and preparation of antireflection and reflection optical coatings." *Turk. J. Phys* 28:139-144.

Eatemadi A, Daraee H, Karimkhanloo H, Kouhi M, Zarghami N, Akbarzadeh A, Abasi M, Hanifehpour Y, and Joo S W. 2014. "Carbon nanotubes: properties, synthesis, purification, and medical applications." *Nanoscale Res Lett* 9 (1):393.

Ee W C, and Cheong K Y. 2008. "Effects of annealing temperature on ultra-low dielectric constant SiO 2 thin films derived from sol–gel spin-on-coating." *Physica B: Condensed Matter* 403 (4):611-615.

Eibl N L, Kopp H-P, Nowak H R, Schnack C J, Hopmeier P G, and Schernthaner G. 1995. "Hypomagnesemia in type II diabetes: effect of a 3-month replacement therapy." *Diabetes Care* 18 (2):188-192.

Elam M B, Ginsberg H N, Lovato L C, Corson M, Largay J, Leiter L A, Lopez C, O'Connor P J, Sweeney M E, and Weiss D. 2017. "Association of fenofibrate therapy with long-term cardiovascular risk in statin-treated patients with type 2 diabetes." *Jama cardiology* 2 (4):370-380.

Elsayed E M, and Elsaman S I. 2017. "Synthesis of smart medical socks for diabetic foot ulcers patients." *Fibers and Polymers* 18 (4):811-815.

Ensafi A A, Khoddami E, Nabiyan A, and Rezaei B. 2017. "Study the role of poly (diethyl aminoethyl methacrylate) as a modified and grafted shell for TiO 2 and ZnO nanoparticles, application in flutamide delivery." *Reactive and Functional Polymers*.

Epstein F H, and Ross R. 1999. "Atherosclerosis—an inflammatory disease." *New England journal of medicine* 340 (2):115-126.

Etgen G, Memon A, Thompson G, and Ivy J. 1993. "Insulin-and contraction-stimulated translocation of GTP-binding proteins and GLUT4 protein in skeletal muscle." *Journal of Biological Chemistry* 268 (27):20164-20169.

Fabian E, Landsiedel R, Ma-Hock L, Wiench K, Wohlleben W, and Van Ravenzwaay B. 2008. "Tissue distribution and toxicity of intravenously administered titanium dioxide nanoparticles in rats." *Archives of toxicology* 82 (3):151-157.

Fagot-Campagna A, Balkau B, Simon D, Warnet J M, Claude J R, Ducimetiere P, and Eschwege E. 1998. "High free fatty acid concentration: an independent risk factor for hypertension in the Paris Prospective Study." *Int J Epidemiol* 27 (5):808-13.

Farokhzad O C, and Langer R. 2009. "Impact of nanotechnology on drug delivery." *ACS nano* 3 (1):16-20.

Favaretto F, Milan G, Collin G B, Marshall J D, Stasi F, Maffei P, Vettor R, and Naggert J K. 2014. "GLUT4 defects in adipose tissue are early signs of metabolic alterations in Alms1GT/GT, a mouse model for obesity and insulin resistance." *PloS one* 9 (10):e109540.

Fawcett W, Haxby E, and Male D. 1999. "Magnesium: physiology and pharmacology." *British Journal of Anaesthesia* 83 (2):302-320.

Ferancová A, and Labuda J. 2008. "DNA biosensors based on nanostructured materials." *Nanostructured Materials in Electrochemistry*:409-434.

Fernando T, and Bean G. 1984. "Fatty acids and sterols of Amaranthus tricolor L." *Food Chem.* 15 (3):233-237.

Fierro J L G. 2005. *Metal Oxides: chemistry and applications*: CRC press.

Finnegan M P, Zhang H, and Banfield J F. 2007. "Phase stability and transformation in titania nanoparticles in aqueous solutions dominated by surface energy." *The Journal of Physical Chemistry C* 111 (5):1962-1968.

Fleming T E, and Mansmann Jr H C. 1999. Methods and compositions for the prevention and treatment of diabetes mellitus. Google Patents.

Förster H. 2004. "UV/vis spectroscopy." In *Characterization I*, 337-426. Springer.

Frayn K N. 2000. "Visceral fat and insulin resistance — causative or correlative?" *British Journal of Nutrition* 83 (SupplementS1):S71-S77. doi: doi:10.1017/S0007114500000982.

Frayn KN W C, Arner P. 1996. "Are increased plasma non-esterified fatty acid concentrations a risk marker for coronary heart disease and other chronic diseases? ." *ClinSci* 90:243 - 253.

Freitas R A. 2005a. "Current status of nanomedicine and medical nanorobotics." *Journal of Computational and Theoretical Nanoscience* 2 (1):1-25.

Freitas R A, Jr. 2005b. "What is nanomedicine?" *Nanomedicine* 1 (1):2-9. doi: 10.1016/j.nano.2004.11.003.

Friese M A, and Banerjee S. 1995. *FT-IR spectroscopy*: CRC Press: Boca Raton, FL.

Fröhlich E. 2012. "The role of surface charge in cellular uptake and cytotoxicity of medical nanoparticles." *Int J Nanomedicine* 7 (1):5577-91.

Fu S, Lin Y, Ping P, Luo L, and Ye P. 2017. "Overall obesity had similar ability to identify the insulin resistance and pancreatic β-cell function compared with abdominal obesity in Chinese community-dwelling population without type 2 diabetes." *International Journal of Clinical & Experimental Medicine* 10 (3).

Fujita-Becker S, Dürrwang U, Erent M, Clark R J, Geeves M A, and Manstein D J. 2005. "Changes in Mg2+ ion concentration and heavy chain phosphorylation regulate the motor activity of a class I myosin." *Journal of Biological Chemistry* 280 (7):6064-6071.

Funnell W R J, and Maysinger D. 2006. "Three-dimensional reconstruction of cell nuclei, internalized quantum dots and sites of lipid peroxidation." *Journal of nanobiotechnology* 4 (1):10.

Ganapathi A P, Devaki R, Thuniki N R, Manna J, Tirumuru B, Gopu C R, Deepthi S B, Trivedi R, Rana R K, and Hasan A. 2017. "*In vitro* assessment of Ag and TiO2 nanoparticles cytotoxicity." *International Journal of Research in Medical Sciences* 2 (4):1360-1367.

Gardea-Torresdey J, Tiemann K, Parsons J, Gamez G, and Yacaman M J. 2002. "Characterization of trace level Au (III) binding to alfalfa biomass (Medicago sativa) by GFAAS." *Advances in Environmental Research* 6 (3):313-323.

Garland H. 1992. "New experimental data on the relationship between diabetes mellitus and magnesium." *Magnesium research* 5 (3):193-202.

Gaumet M, Vargas A, Gurny R, and Delie F. 2008. "Nanoparticles for drug delivery: the need for precision in reporting particle size parameters." *European journal of pharmaceutics and biopharmaceutics* 69 (1):1-9.

Ge S, Wang G, Shen Y, Zhang Q, Jia D, Wang H, Dong Q, and Yin T. 2011. "Cytotoxic effects of MgO nanoparticles on human umbilical vein endothelial cells *in vitro*." *IET nanobiotechnology* 5 (2):36-40.

Genuth S. 1990. "Insulin use in NIDDM." *Diabetes Care* 13 (12):1240-64.

Ghodake G, Deshpande N, Lee Y, and Jin E. 2010. "Pear fruit extract-assisted room-temperature biosynthesis of gold nanoplates." *Colloids and Surfaces B: Biointerfaces* 75 (2):584-589.

Ghorbani H R, Safekordi A A, Attar H, and Sorkhabadi S. 2011. "Biological and non-biological methods for silver nanoparticles synthesis." *Chemical and Biochemical Engineering Quarterly* 25 (3):317-326.

Gibson R S. 2005. *Principles of nutritional assessment*: Oxford university press.

Giri N, Natarajan R, Gunasekaran S, and Shreemathi S. 2011. "13C NMR and FTIR spectroscopic study of blend behavior of PVP and nano silver particles." *Archives of Applied Science Research* 3 (5):624-30.

Gnanasangeetha D a D S. 2013. "Biogenic production of zinc oxide nanoparticles using *Acalypha indica*." *Journal of Chemical Biological and Physical Sciences* 4 (1):238-246.

Golberg D, Bando Y, Fushimi K, Mitome M, Bourgeois L, and Tang C-C. 2003. "Nanoscale oxygen generators: MgO2-based fillings of BN nanotubes." *The Journal of Physical Chemistry B* 107 (34):8726-8729.

Golovchenko J A, Batterman B W, and Brown W L. 1974. "Observation of internal X-ray wave fields during Bragg diffraction with an application to impurity lattice location." *Physical Review B* 10 (10):4239.

Gordon K, and Balasubramanian S. 1999. "Solid phase synthesis–designer linkers for combinatorial chemistry: a review." *Journal of Chemical Technology and Biotechnology* 74 (9):835-851.

Gratton S E, Ropp P A, Pohlhaus P D, Luft J C, Madden V J, Napier M E, and DeSimone J M. 2008. "The effect of particle design on cellular internalization pathways." *Proceedings of the National Academy of Sciences* 105 (33):11613-11618.

Green D R, and Kroemer G. 2004. "The pathophysiology of mitochondrial cell death." *Science* 305 (5684):626-629.

Green H, and Kehinde O. 1975. "An established preadipose cell line and its differentiation in culture II. Factors affecting the adipose conversion." *Cell* 5 (1):19-27.

Greenstreet J, and Norris K. 1957. "The existence of differences between the infra-red absorption spectra of bacteria." *Spectrochimica acta* 9 (3):177-198.

Greenwood R, and Kendall K. 1999. "Electroacoustic studies of moderately concentrated colloidal suspensions." *Journal of the European Ceramic Society* 19 (4):479-488.

Gu Y, Chen D, Jiao X, and Liu F. 2007. "LiCoO 2–MgO coaxial fibers: co-electrospun fabrication, characterization and electrochemical properties." *Journal of Materials Chemistry* 17 (18):1769-1776.

Guinier A. 1994. *X-ray diffraction in crystals, imperfect crystals, and amorphous bodies*: Courier Corporation.

Gunalan S, Sivaraj R, and Rajendran V. 2012a. "Green synthesized ZnO nanoparticles against bacterial and fungal pathogens." *Progress in Natural Science: Materials International* 22 (6):693-700.

Gunalan S, Sivaraj R, and Venckatesh R. 2012b. "Aloe barbadensis Miller mediated green synthesis of mono-disperse copper oxide nanoparticles: optical properties." *Spectrochimica Acta Part A: Molecular and Biomolecular Spectroscopy* 97:1140-1144.

Guo X, and Wang W. 2017. "Challenges and recent advances in the subcutaneous delivery of insulin." *Expert Opinion on Drug Delivery* 14 (6):727-734. doi: 10.1080/17425247.2016.1232247.

Gupta A K, and Curtis A S. 2004. "Surface modified superparamagnetic nanoparticles for drug delivery: interaction studies with human fibroblasts in culture." *Journal of Materials Science: Materials in Medicine* 15 (4):493-496.

Gupta K, Singh R, Pandey A, and Pandey A. 2013. "Photocatalytic antibacterial performance of TiO2 and Ag-doped TiO2 against S. aureus. P. aeruginosa and E. coli." *Beilstein journal of nanotechnology* 4 (1):345-351.

Gupta K, Taneja S, Dhar K, and Atal C. 1983. "Flavonoids of Andrographis paniculata." *Phytochemistry* 22 (1):314-315.

Hackenberg S, Scherzed A, Technau A, Kessler M, Froelich K, Ginzkey C, Koehler C, Burghartz M, Hagen R, and Kleinsasser N. 2011. "Cytotoxic, genotoxic and pro-

inflammatory effects of zinc oxide nanoparticles in human nasal mucosa cells *in vitro*." *Toxicology in vitro* 25 (3):657-663.

Haines P J. 2012. *Thermal methods of analysis: principles, applications and problems*: Springer Science & Business Media.

Haiss W, Thanh N T, Aveyard J, and Fernig D G. 2007. "Determination of size and concentration of gold nanoparticles from UV-vis spectra." *Analytical chemistry* 79 (11):4215-4221.

Hales C, and Barker D. 2013. "Type 2 (non-insulin-dependent) diabetes mellitus: the thrifty phenotype hypothesis." *International journal of epidemiology* 42 (5):1215-1222.

Halliwell B. 1994. "Antioxidants: Sense or Speculation?" *Nutrition today* 29 (6):15-19.

Hamet J, Mercey B, Hervieu M, Poullain G, and Raveau B. 1992. "*a*-Axis oriented superconductive YBCO thin films: Growth mechanism on MgO substrate." *Physica C: Superconductivity* 198 (3):293-302.

Hanaor D, Michelazzi M, Leonelli C, and Sorrell C C. 2012. "The effects of carboxylic acids on the aqueous dispersion and electrophoretic deposition of ZrO 2." *Journal of the European Ceramic Society* 32 (1):235-244.

Hanazaki K, Nosé Y, and Brunicardi F C. 2001. "Artificial endocrine pancreas." *Journal of the American College of Surgeons* 193 (3):310-322.

Haraguchi F, Inoue K-i, Toshima N, Kobayashi S, and Takatoh K. 2007. "Reduction of the threshold voltages of nematic liquid crystal electrooptical devices by doping inorganic nanoparticles." *Japanese journal of applied physics* 46 (9L):L796.

Harris M I. 1996. "Medical care for patients with diabetes. Epidemiologic aspects." *Ann Intern Med* 124 (1 Pt 2):117-22.

Harris P J, and Harris P J F. 2009. *Carbon nanotube science: synthesis, properties and applications*: Cambridge University Press.

Haruta M, Yamada N, Kobayashi T, and Iijima S. 1989. "Gold catalysts prepared by coprecipitation for low-temperature oxidation of hydrogen and of carbon monoxide." *Journal of catalysis* 115 (2):301-309.

Hasanein P, Parviz M, Keshavarz M, Javanmardi K, Allahtavakoli M, and Ghaseminejad M. 2007. "Modulation of cholestasis-induced antinociception in rats by two

NMDA receptor antagonists: MK-801 and magnesium sulfate." *European journal of pharmacology* 554 (2):123-127.

Hassan S, Bhat A, R Bhonde R, and A Lone M. 2016. "Fighting diabetes: lessons from xenotransplantation and nanomedicine." *Current pharmaceutical design* 22 (11):1494-1505.

Hayashi H, and Hakuta Y. 2010. "Hydrothermal synthesis of metal oxide nanoparticles in supercritical water." *Materials* 3 (7):3794-3817.

Hayashi T, Boyko E J, McNeely M J, Leonetti D L, Kahn S E, and Fujimoto W Y. 2008. "Visceral adiposity, not abdominal subcutaneous fat area, is associated with an increase in future insulin resistance in Japanese Americans." *Diabetes* 57 (5):1269-75. doi: 10.2337/db07-1378.

Hayward R A, Manning W G, Kaplan S H, Wagner E H, and Greenfield S. 1997. "Starting insulin therapy in patients with type 2 diabetes: effectiveness, complications, and resource utilization." *Jama* 278 (20):1663-9.

He A, Zhu L, Gupta N, Chang Y, and Fang F. 2007. "Overexpression of micro ribonucleic acid 29, highly up-regulated in diabetic rats, leads to insulin resistance in 3T3-L1 adipocytes." *Molecular endocrinology* 21 (11):2785-2794.

Heaton F W. 1990. "Role of magnesium in enzyme systems." *Metal ions in biological systems* 26:119-133.

Helfrich A, Brüchert W, and Bettmer J. 2006. "Size characterisation of Au nanoparticles by ICP-MS coupling techniques." *Journal of Analytical Atomic Spectrometry* 21 (4):431-434.

Helveg S, Lauritsen J V, Lægsgaard E, Stensgaard I, Nørskov J K, Clausen B, Topsøe H, and Besenbacher F. 2000. "Atomic-scale structure of single-layer MoS 2 nanoclusters." *Physical review letters* 84 (5):951.

Henry R R, Gumbiner B, Ditzler T, Wallace P, Lyon R, and Glauber H S. 1993. "Intensive conventional insulin therapy for type II diabetes. Metabolic effects during a 6-mo outpatient trial." *Diabetes Care* 16 (1):21-31.

Hirsch I B. 2005. "Insulin analogues." *N Engl J Med* 352 (2):174-83. doi: 10.1056/NEJMra040832.

Hoag G E, Collins J B, Holcomb J L, Hoag J R, Nadagouda M N, and Varma R S. 2009. "Degradation of bromothymol blue by 'greener'nano-scale zero-valent iron synthesized using tea polyphenols." *Journal of Materials Chemistry* 19 (45):8671-8677.

Hossain M S, Urbi Z, Sule A, and Rahman K. 2014. "Andrographis paniculata (Burm. f.) Wall. ex Nees: A Review of Ethnobotany, Phytochemistry, and Pharmacology." *Sci. World J.* 2014.

Houstis N E. 2007. "Reactive oxygen species play a causal role in multiple forms of insulin resistance." Massachusetts Institute of Technology.

Huang C-C, Aronstam R S, Chen D-R, and Huang Y-W. 2010. "Oxidative stress, calcium homeostasis, and altered gene expression in human lung epithelial cells exposed to ZnO nanoparticles." *Toxicology in vitro* 24 (1):45-55.

Huang D-M, Hung Y, Ko B-S, Hsu S-C, Chen W-H, Chien C-L, Tsai C-P, Kuo C-T, Kang J-C, and Yang C-S. 2005. "Highly efficient cellular labeling of mesoporous nanoparticles in human mesenchymal stem cells: implication for stem cell tracking." *The FASEB journal* 19 (14):2014-2016.

Huang J, Zhan G, Zheng B, Sun D, Lu F, Lin Y, Chen H, Zheng Z, Zheng Y, and Li Q. 2011. "Biogenic silver nanoparticles by Cacumen platycladi extract: synthesis, formation mechanism, and antibacterial activity." *Industrial & Engineering Chemistry Research* 50 (15):9095-9106.

Hudlikar M, Joglekar S, Dhaygude M, and Kodam K. 2012. "Green synthesis of TiO 2 nanoparticles by using aqueous extract of Jatropha curcas L. latex." *Materials Letters* 75:196-199.

Huerta M G, Roemmich J N, Kington M L, Bovbjerg V E, Weltman A L, Holmes V F, Patrie J T, Rogol A D, and Nadler J L. 2005. "Magnesium deficiency is associated with insulin resistance in obese children." *Diabetes care* 28 (5):1175-1181.

Hussain A H M Z I, Claussen B, Asghar S. 2010. "Type 2 Diabetes and obesity: A review." *Journal of Diabetology* 2 (1).

Hussain S, Hess K, Gearhart J, Geiss K, and Schlager J. 2005. "*In vitro* toxicity of nanoparticles in BRL 3A rat liver cells." *Toxicology in vitro* 19 (7):975-983.

Hwang P T, Shah D K, Garcia J A, Bae C Y, Lim D-J, Huiszoon R C, Alexander G C, and Jun H-W. 2016. "Progress and challenges of the bioartificial pancreas." *Nano Convergence* 3 (1):28.

Hyun J W, Kim S Y, Lee S, Park H, Pyee J, and Kim S. 2003. "A novel sol-gel method to produce the poly-L-lysine coated plate as a platform for protein chips." *Bulletin-Korean Chemical Society* 24 (4):411-412.

Ibrahim N. 2010. "Synthesis and characterization of MgO nanopowders by sol-gel method incorporated reflux approach." Universiti Teknologi MARA.

Iijima S. 1991. "Helical microtubules of graphitic carbon." *nature* 354 (6348):56-58.

Instruments M. 2004. "Zetasizer nano series user manual." *MAN0317* (1.1).

Iravani S. 2011. "Green synthesis of metal nanoparticles using plants." *Green Chemistry* 13 (10):2638-2650.

Iravani S. 2017. "EMR of Metallic Nanoparticles." In *EMR/ESR/EPR Spectroscopy for Characterization of Nanomaterials*, 79-90. Springer.

IS C. 2008. "Nanopharmacology: experimental and clinical aspect." *Lik Sprava* 3 (4):104 - 109.

ISO13321 I. 1996. "Methods for determination of particle size distribution part 8: Photon correlation spectroscopy." *International Organisation for Standardisation (ISO)*.

Itatani K, Yasuda R, Howell F S, and Kishioka A. 1997. "Effect of starting particle size on hot-pressing of magnesium oxide powder prepared by vapour-phase oxidation process." *Journal of materials science* 32 (11):2977-2984.

Ito A, Shinkai M, Honda H, and Kobayashi T. 2005. "Medical application of functionalized magnetic nanoparticles." *Journal of bioscience and bioengineering* 100 (1):1-11.

Jahangiri L, Kesmati M, and Najafzadeh H. 2013. "Evaluation of analgesic and anti-inflammatory effect of nanoparticles of magnesium oxide in mice with and without ketamine." *Eur Rev Med Pharmacol Sci* 17 (20):2706-2710.

Jahangiri L, Kesmati M, and Najafzadeh H. 2014a. "Evaluation of anticonvulsive effect of magnesium oxide nanoparticles in comparison with conventional MgO in diabetic and non-diabetic male mice." *Basic and clinical neuroscience* 5 (2):156.

Jahangiri L, Kesmati M, and Najafzadeh H. 2014b. "Evaluation of Anticonvulsive Effect of Magnesium Oxide Nanoparticles in Comparison with Conventional MgO in Diabetic and Non-diabetic Male Mice." *Basic and Clinical Neuroscience* 5 (2):156-161.

Jain P K, Huang X, El-Sayed I H, and El-Sayed M A. 2007. "Review of some interesting surface plasmon resonance-enhanced properties of noble metal nanoparticles and their applications to biosystems." *Plasmonics* 2 (3):107-118.

Jaison J, Balakumar S, and Chan Y. 2015. "Sol–Gel synthesis and characterization of magnesium peroxide nanoparticles." IOP Conference Series: Materials Science and Engineering.

Jarukamjorn K, and Nemoto N. 2008. "Pharmacological aspects of Andrographis paniculata on health and its major diterpenoid constituent andrographolide." *J. Health Sci.* 54 (4):370-381.

Jayaraman S M T, Rajendran K, Suthakaran P K, Nair L D V, Rajaram L, Gnanasekar R, and Karuthodiyil R. 2017. "Study on serum magnesium levels and glycemic status in newly detected type 2 diabetes patients." *International Journal of Advances in Medicine* 3 (1):11-14.

Jeevanandam J, Chan Y S, and Danquah M K. 2016a. "Biosynthesis of Metal and Metal Oxide Nanoparticles." *ChemBioEng Rev.* 3 (2):55-67.

Jeevanandam J, Chan Y S, and Danquah M K. 2016b. "Nano-formulations of drugs: Recent developments, impact and challenges." *Biochimie* 128-129 (Supplement C):99-112. doi: https://doi.org/10.1016/j.biochi.2016.07.008.

Jeevanandam J, Chan Y S, and Danquah M K. 2017. "Biosynthesis and characterization of MgO nanoparticles from plant extracts via induced molecular nucleation." *New Journal of Chemistry* 41:2800-2814.

Jeevanandam J, K Danquah M, Debnath S, S Meka V, and S Chan Y. 2015. "Opportunities for nano-formulations in type 2 diabetes mellitus treatments." *Current pharmaceutical biotechnology* 16 (10):853-870.

Jeevanandam J, San Chan Y, and Danquah M K. 2016c. "Nano-formulations of drugs: recent developments, impact and challenges." *Biochimie* 128:99-112.

Jeevanandam P, and Klabunde K J. 2002. "A study on adsorption of surfactant molecules on magnesium oxide nanocrystals prepared by an aerogel route." *Langmuir* 18 (13):5309-5313.

Jennings A M, Lewis K S, Murdoch S, Talbot J F, Bradley C, and Ward J D. 1991. "Randomized trial comparing continuous subcutaneous insulin infusion and conventional insulin therapy in type II diabetic patients poorly controlled with sulfonylureas." *Diabetes Care* 14 (8):738-44.

Jiang C, Guo Z, Zhu Y, Liu H, Wan M, and Jiang L. 2015. "Shewanella-mediated Biosynthesis of Manganese Oxide Micro-/Nanocubes as Efficient Electrocatalysts for the Oxygen Reduction Reaction." *ChemSusChem* 8 (1):158-163.

Jiang J, Oberdörster G, and Biswas P. 2009. "Characterization of size, surface charge, and agglomeration state of nanoparticle dispersions for toxicological studies." *Journal of Nanoparticle Research* 11 (1):77-89.

Jiu J, Kurumada K-i, Tanigaki M, Adachi M, and Yoshikawa S. 2004. "Preparation of nanoporous MgO using gel as structure-direct template." *Materials Letters* 58 (1):44-47.

John Ł, and Sobota P. 2010. "Alkoxide molecular precursors for nanomaterials: a one step strategy for oxide ceramics." *Ceramic Materials*:69À86.

Jones M R, Macfarlane R J, Prigodich A E, Patel P C, and Mirkin C A. 2011. "Nanoparticle shape anisotropy dictates the collective behavior of surface-bound ligands." *Journal of the American Chemical Society* 133 (46):18865-18869.

Ju-Nam Y, and Lead J R. 2008. "Manufactured nanoparticles: an overview of their chemistry, interactions and potential environmental implications." *Science of the total environment* 400 (1):396-414.

Kahn S E, Hull R L, and Utzschneider K M. 2006. "Mechanisms linking obesity to insulin resistance and type 2 diabetes." *Nature* 444 (7121):840.

Kakkar R, Kapoor P N, and Klabunde K J. 2004. "Theoretical study of the adsorption of formaldehyde on magnesium oxide nanosurfaces: Size effects and the role of low-coordinated and defect sites." *The Journal of Physical Chemistry B* 108 (47):18140-18148.

Kanade K, Kale B, Aiyer R, and Das B. 2006. "Effect of solvents on the synthesis of nano-size zinc oxide and its properties." *Materials Research Bulletin* 41 (3):590-600.

Kandeel F R, Balon E, Scott S, and Nadler J L. 1996. "Magnesium deficiency and glucose metabolism in rat adipocytes." *Metabolism* 45 (7):838-843.

Kang T, Guan R, Chen X, Song Y, Jiang H, and Zhao J. 2013. "*In vitro* toxicity of different-sized ZnO nanoparticles in Caco-2 cells." *Nanoscale Res Lett* 8 (1):496. doi: 10.1186/1556-276x-8-496.

Kao W L, Folsom A R, Nieto F J, Mo J-P, Watson R L, and Brancati F L. 1999. "Serum and dietary magnesium and the risk for type 2 diabetes mellitus: the Atherosclerosis Risk in Communities Study." *Archives of Internal Medicine* 159 (18):2151-2159.

Kappe C O, Stadler A, and Dallinger D. 2012. *Microwaves in organic and medicinal chemistry*: John Wiley & Sons.

Kareiva A, Karppinen M, and Niinistö L. 1994. "Sol–gel synthesis of superconducting YBa 2 Cu 4 O 8 using acetate and tartrate precursors." *Journal of Materials Chemistry* 4 (8):1267-1270.

Karosanidze T. 2014. "Magnesium–so underappreciated." *Practical Gastroenterology*.

Karthik K, Dhanuskodi S, Gobinath C, and Sivaramakrishnan S. 2017. "Microwave Assisted Green Synthesis of MgO Nanorods and Their Antibacterial and Anti-breast Cancer Activities." *Materials Letters*.

Kawaguchi Y. 2000. "Luminescence spectra at bending fracture of single crystal MgO." *Solid State Communications* 117 (1):17-20. doi: http://dx.doi.org/10.1016/S0038-1098(00)00413-0.

Keely W, and Maynor H W. 1963. "Thermal Studies of Nickel, Cobalt, Iron and Copper Oxides and Nitrates." *Journal of Chemical and Engineering Data* 8 (3):297-300.

Kelly K L, Coronado E, Zhao L L, and Schatz G C. 2003. "The optical properties of metal nanoparticles: the influence of size, shape, and dielectric environment." *The Journal of Physical Chemistry B* 107 (3):668-677.

Kesavadev J. 2011. "Continuous insulin infusion systems in type 2 diabetes." *J Assoc Physicians India* 59:41-43.

Khlebtsov B, and Khlebtsov N. 2011. "On the measurement of gold nanoparticle sizes by the dynamic light scattering method." *Colloid Journal* 73 (1):118-127.

Kim D J, Hahn S H, Oh S H, and Kim E J. 2002. "Influence of calcination temperature on structural and optical properties of TiO 2 thin films prepared by sol–gel dip coating." *Materials Letters* 57 (2):355-360.

Kim T H, Kim M, Park H S, Shin U S, Gong M S, and Kim H W. 2012. "Size-dependent cellular toxicity of silver nanoparticles." *Journal of Biomedical Materials Research Part A* 100 (4):1033-1043.

King H, Aubert R E, and Herman W H. 1998. "Global burden of diabetes, 1995-2025: prevalence, numerical estimates, and projections." *Diabetes Care* 21 (9):1414-31.

Kittitheeranun P, Sajomsang W, Phanpee S, Treetong A, Wutikhun T, Suktham K, Puttipipatkhachorn S, and Ruktanonchai U R. 2015. "Layer-by-layer engineered nanocapsules of curcumin with improved cell activity." *International journal of pharmaceutics* 492 (1):92-102.

Klaas J, Schulz-Ekloff G, and Jaeger N I. 1997. "UV-visible diffuse reflectance spectroscopy of zeolite-hosted mononuclear titanium oxide species." *The Journal of Physical Chemistry B* 101 (8):1305-1311.

Klabunde K J, Stark J, Koper O, Mohs C, Park D G, Decker S, Jiang Y, Lagadic I, and Zhang D. 1996. "Nanocrystals as stoichiometric reagents with unique surface chemistry." *The Journal of Physical Chemistry* 100 (30):12142-12153.

Kluson P, Drobek M, Bartkova H, and Budil I. 2007. "Welcome in the Nanoworld." *CHEMICKE LISTY* 101 (4):262-272.

Kohn A D, Summers S A, Birnbaum M J, and Roth R A. 1996. "Expression of a constitutively active Akt Ser/Thr kinase in 3T3-L1 adipocytes stimulates glucose uptake and glucose transporter 4 translocation." *Journal of Biological Chemistry* 271 (49):31372-31378.

Kolhar P, Anselmo A C, Gupta V, Pant K, Prabhakarpandian B, Ruoslahti E, and Mitragotri S. 2013. "Using shape effects to target antibody-coated nanoparticles to lung and brain endothelium." *Proceedings of the National Academy of Sciences* 110 (26):10753-10758.

Kołodziejczak-Radzimska A, and Jesionowski T. 2014. "Zinc Oxide—From Synthesis to Application: A Review." *Materials* 7 (4):2833-2881.

Koper O B, Klabunde J S, Marchin G L, Klabunde K J, Stoimenov P, and Bohra L. 2002. "Nanoscale powders and formulations with biocidal activity toward spores and vegetative cells of bacillus species, viruses, and toxins." *Current Microbiology* 44 (1):49-55.

Kral V, Sotola J, Neuwirth P, Kejik Z, Zaruba K, and Martasek P. 2006. "Nanomedicine-Current status and perspectives: A big potential or just a catchword?" *Chemicke Listy* 100 (1):4-9.

Krishnamoorthy K, Moon J Y, Hyun H B, Cho S K, and Kim S-J. 2012. "Mechanistic investigation on the toxicity of MgO nanoparticles toward cancer cells." *Journal of Materials Chemistry* 22 (47):24610-24617.

Krishnaraj C, Jagan E, Rajasekar S, Selvakumar P, Kalaichelvan P, and Mohan N. 2010. "Synthesis of silver nanoparticles using Acalypha indica leaf extracts and its antibacterial activity against water borne pathogens." *Colloids and Surfaces B: Biointerfaces* 76 (1):50-56.

Kuku G, and Culha M. 2017. "Investigating the Origins of Toxic Response in TiO2 Nanoparticle-Treated Cells." *Nanomaterials* 7 (4):83.

Kulkarni H P. 2008. *Synthesis and applications of titania nanotubes: Drug delivery and ionomer composites*: ProQuest.

Kumar A, and Kumar J. 2008. "On the synthesis and optical absorption studies of nano-size magnesium oxide powder." *Journal of Physics and Chemistry of Solids* 69 (11):2764-2772.

Kumar A A, Jaison J, Prabakaran K, Nagarajan R, and Chan Y. 2016. "Water quality monitoring: A comparative case study of municipal and Curtin Sarawak's lake samples." IOP Conference Series: Materials Science and Engineering.

Kurstjens S, de Baaij J H, Bouras H, Bindels R J, Tack C J, and Hoenderop J G. 2017. "Determinants of hypomagnesemia in patients with type 2 diabetes mellitus." *European journal of endocrinology* 176 (1):11-19.

Lai J C, Lai M B, Jandhyam S, Dukhande V V, Bhushan A, Daniels C K, and Leung S W. 2008. "Exposure to titanium dioxide and other metallic oxide nanoparticles

induces cytotoxicity on human neural cells and fibroblasts." *International journal of nanomedicine* 3 (4):533.

Langer R, and Tirrell D A. 2004. "Designing materials for biology and medicine." *Nature* 428 (6982):487-492.

Lanje A S, Sharma S J, Pode R B, and Ningthoujam R S. 2010. "Synthesis and optical characterization of copper oxide nanoparticles." *Advances in Applied Science Research* 1 (2):36-40.

Lansman J B, Hess P, and Tsien R W. 1986. "Blockade of current through single calcium channels by Cd2+, Mg2+, and Ca2+. Voltage and concentration dependence of calcium entry into the pore." *The Journal of General Physiology* 88 (3):321-347.

Laughlin M R, and Thompson D. 1996. "The regulatory role for magnesium in glycolytic flux of the human erythrocyte." *Journal of Biological Chemistry* 271 (46):28977-28983.

Law C-y, and Lam C-w. 2017. "Urine 'total triglyceride'for diagnosis of a rare cause of hypoglycemia: a novel, rapid and simple test." *Pathology* 49:S105.

Le Parlouër P. 1987. "Simultaneous TG-DSC: a new technique for thermal analysis." *Thermochimica acta* 121:307-322.

Lee K-S, and El-Sayed M A. 2006. "Gold and silver nanoparticles in sensing and imaging: sensitivity of plasmon response to size, shape, and metal composition." *The Journal of Physical Chemistry B* 110 (39):19220-19225.

Lee K, Trochimowicz H, and Reinhardt C. 1985. "Pulmonary response of rats exposed to titanium dioxide (TiO< sub> 2</sub>) by inhalation for two years." *Toxicology and applied pharmacology* 79 (2):179-192.

Leung Y H, Guo M Y, Ma A P, Ng A M, Djurišić A B, Degger N, and Leung F C. 2017. "Transmission electron microscopy artifacts in characterization of the nanomaterial-cell interactions." *Applied Microbiology and Biotechnology*:1-11.

Li N, Ma L, Wang J, Zheng L, Liu J, Duan Y, Liu H, Zhao X, Wang S, and Wang H. 2009. "Interaction between nano-anatase TiO 2 and liver DNA from mice *in vivo*." *Nanoscale research letters* 5 (1):108.

Li Y-F, Liu Z-M, Liu Y-L, Yang Y-H, Shen G-L, and Yu R-Q. 2006. "A mediator-free phenol biosensor based on immobilizing tyrosinase to ZnO nanoparticles." *Analytical biochemistry* 349 (1):33-40.

LI Z, Liu Y, GONG P, and ZHAI Y. 2007. "Preparation of chain copper oxide nanoparticles by microwave." *Rare Metals* 26 (5):476-481.

Liang S H, and Gay I D. 1985. "Adsorption and thermal decomposition of methanol on magnesium oxide. Carbon-13 NMR studies." *Langmuir* 1 (5):593-599.

Lide D, and Haynes W. 2009. *CRC handbook of chemistry and physics: a ready-reference book of chemical and physical data-/editor-in-chief, David R. Lide; ass. ed. WM" Mickey" Haunes*: Boca Raton, Fla: CRC.

Lifton R P, Gharavi A G, and Geller D S. 2001. "Molecular mechanisms of human hypertension." *Cell* 104 (4):545-556.

Lim J, Yeap S P, Che H X, and Low S C. 2013. "Characterization of magnetic nanoparticle by dynamic light scattering." *Nanoscale research letters* 8 (1):1-14.

Lima R, Seabra A B, and Durán N. 2012. "Silver nanoparticles: a brief review of cytotoxicity and genotoxicity of chemically and biogenically synthesized nanoparticles." *Journal of Applied Toxicology* 32 (11):867-879.

Lin L, Mawatari K, Morikawa K, Pihosh Y, Yoshizaki A, and Kitamori T. 2017. "Micro/extended-nano sampling interface from a living single cell." *Analyst*.

Lin Y-S, Tsai C-P, Huang H-Y, Kuo C-T, Hung Y, Huang D-M, Chen Y-C, and Mou C-Y. 2005. "Well-ordered mesoporous silica nanoparticles as cell markers." *Chemistry of Materials* 17 (18):4570-4573.

Lin Y, and Sun Z. 2010. "Current views on type 2 diabetes." *J Endocrinol* 204 (1):1-11. doi: 10.1677/joe-09-0260.

Lind C, Gates S D, Pedoussaut N M, and Baiz T I. 2010. "Novel materials through non-hydrolytic sol-gel processing: Negative thermal expansion oxides and beyond." *Materials* 3 (4):2567-2587.

Liu B, and Zeng H C. 2004. "Mesoscale organization of CuO nanoribbons: formation of "dandelions"." *Journal of the American Chemical Society* 126 (26):8124-8125.

Liu H, Yang D, Yang H, Zhang H, Zhang W, Fang Y, Lin Z, Tian L, Lin B, and Yan J. 2013. "Comparative study of respiratory tract immune toxicity induced by three

sterilisation nanoparticles: silver, zinc oxide and titanium dioxide." *Journal of hazardous materials* 248:478-486.

Liu J-H, Ma X, Xu Y, Tang H, Yang S-T, Yang Y-F, Kang D-D, Wang H, and Liu Y. 2017. "Low toxicity and accumulation of zinc oxide nanoparticles in mice after 270-day consecutive dietary supplementation." *Toxicology Research*.

Liu S, Weaver J, Yuan Z, Donner W, Chen C, Jiang J, Meletis E, Chang W, Kirchoefer S, and Horwitz J. 2005. "Ferroelectric (Pb, Sr) TiO 3 epitaxial thin films on (001) MgO for room temperature high-frequency tunable microwave elements." *Applied Physics Letters* 87 (14):142905-142905-3.

Liu X, Atwater M, Wang J, and Huo Q. 2007. "Extinction coefficient of gold nanoparticles with different sizes and different capping ligands." *Colloids and Surfaces B: Biointerfaces* 58 (1):3-7.

LM T. 2002. *Current Medical Diagnosis and Treatment*. New York: Lange Medical Books/Mcgraw-Hill.

Long T C, Tajuba J, Sama P, Saleh N, Swartz C, Parker J, Hester S, Lowry G V, and Veronesi B. 2007. "Nanosize titanium dioxide stimulates reactive oxygen species in brain microglia and damages neurons *in vitro*." *Environmental Health Perspectives*:1631-1637.

López-Moreno M L, de la Rosa G, Hernández-Viezcas J Á, Castillo-Michel H, Botez C E, Peralta-Videa J R, and Gardea-Torresdey J L. 2010. "Evidence of the differential biotransformation and genotoxicity of ZnO and CeO2 nanoparticles on soybean (Glycine max) plants." *Environmental science & technology* 44 (19):7315-7320.

Lostroh A, and Krahl M. 1973. "Accumulation *in vitro* of magnesium and potassium in rat uterus ion pump activity." *Bioch Bioph Acta* 291:260-268.

Lou X. 1991. "Development of ZnO series ceramic semiconductor gas sensors." *J. Sens. Trans. Technol* 3 (1).

Loupy A. 2006. "Microwaves in organic synthesis."

Lovrić J, Cho S J, Winnik F M, and Maysinger D. 2005. "Unmodified cadmium telluride quantum dots induce reactive oxygen species formation leading to multiple organelle damage and cell death." *Chemistry & biology* 12 (11):1227-1234.

Lu F, Wu S H, Hung Y, and Mou C Y. 2009. "Size effect on cell uptake in well-suspended, uniform mesoporous silica nanoparticles." *Small* 5 (12):1408-1413.

Lu L, Zhang L, Zhang X, Wu Z, Huan S, Shen G, and Yu R. 2010. "A MgO Nanoparticles Composite Matrix-Based Electrochemical Biosensor for Hydrogen Peroxide with High Sensitivity." *Electroanalysis* 22 (4):471-477.

Ludi B, and Niederberger M. 2013. "Zinc oxide nanoparticles: chemical mechanisms and classical and non-classical crystallization." *Dalton Transactions* 42 (35):12554-12568.

Luo X, Ryu K W, Kim D-S, Nandu T, Medina C J, Gupte R, Gibson B A, Soccio R E, Yu Y, and Gupta R K. 2017. "PARP-1 controls the adipogenic transcriptional program by PARylating C/EBPβ and modulating its transcriptional activity." *Molecular cell* 65 (2):260-271.

Lv J, Qiu L, and Qu B. 2004. "Controlled growth of three morphological structures of magnesium hydroxide nanoparticles by wet precipitation method." *Journal of Crystal Growth* 267 (3):676-684.

Ly T T, Nicholas J A, Retterath A, Lim E M, Davis E A, and Jones T W. 2013. "Effect of sensor-augmented insulin pump therapy and automated insulin suspension vs standard insulin pump therapy on hypoglycemia in patients with type 1 diabetes: a randomized clinical trial." *Jama* 310 (12):1240-1247.

Machado S, Stawiński W, Slonina P, Pinto A, Grosso J, Nouws H, Albergaria J T, and Delerue-Matos C. 2013. "Application of green zero-valent iron nanoparticles to the remediation of soils contaminated with ibuprofen." *Science of the Total Environment* 461:323-329.

Madhava Chetty K, Sivaji K, and Tulasi Rao K. 2008. "Flowering plants of chittoor district." *Andhra Pradesh, India* 169:201.

Madhavi V, Prasad T, Reddy A V B, Reddy B R, and Madhavi G. 2013. "Application of phytogenic zerovalent iron nanoparticles in the adsorption of hexavalent chromium." *Spectrochimica Acta Part A: Molecular and Biomolecular Spectroscopy* 116:17-25.

Mahl D, Diendorf J, Meyer-Zaika W, and Epple M. 2011. "Possibilities and limitations of different analytical methods for the size determination of a bimodal dispersion

of metallic nanoparticles." *Colloids and Surfaces A: Physicochemical and Engineering Aspects* 377 (1):386-392.

Mahmood T, and Yang P-C. 2012. "Western Blot: Technique, Theory, and Trouble Shooting." *North American Journal of Medical Sciences* 4 (9):429-434. doi: 10.4103/1947-2714.100998.

Mahmoud A, Ezgi Ö, Merve A, and Özhan G. 2016. "*In vitro* toxicological assessment of magnesium oxide nanoparticle exposure in several mammalian cell types." *International journal of toxicology* 35 (4):429-437.

Maia C S, Mehnert W, and Schafer-Korting M. 2000. "Solid lipid nanoparticles as drug carriers for topical glucocorticoids." *Int J Pharm* 196 (2):165-7.

Maier J A, Malpuech-Brugère C, Zimowska W, Rayssiguier Y, and Mazur A. 2004. "Low magnesium promotes endothelial cell dysfunction: implications for atherosclerosis, inflammation and thrombosis." *Biochimica et Biophysica Acta (BBA)-Molecular Basis of Disease* 1689 (1):13-21.

Makaram P, Owens D, and Aceros J. 2014. "Trends in Nanomaterial-Based Non-Invasive Diabetes Sensing Technologies." *Diagnostics* 4 (2):27-46.

Makarov V, Love A, Sinitsyna O, Makarova S, Yaminsky I, Taliansky M, and Kalinina N. 2014. ""Green" nanotechnologies: synthesis of metal nanoparticles using plants." *Acta Naturae (англоязычная версия)* 6 (1 (20)).

Makhluf S, Dror R, Nitzan Y, Abramovich Y, Jelinek R, and Gedanken A. 2005. "Microwave-Assisted Synthesis of Nanocrystalline MgO and Its Use as a Bacteriocide." *Advanced Functional Materials* 15 (10):1708-1715.

Mal J, Veneman W J, Nancharaiah Y, van Hullebusch E D, Peijnenburg W J, Vijver M G, and Lens P N. 2017. "A comparison of fate and toxicity of selenite, biogenically, and chemically synthesized selenium nanoparticles to zebrafish (Danio rerio) embryogenesis." *Nanotoxicology* 11 (1):87-97.

Malik P, Shankar R, Malik V, Sharma N, and Mukherjee T K. 2014. "Green Chemistry Based Benign Routes for Nanoparticle Synthesis." *Journal of Nanoparticles* 2014:1-14. doi: 10.1155/2014/302429.

Mangalampalli B, Dumala N, and Grover P. 2017. "Acute oral toxicity study of magnesium oxide nanoparticles and microparticles in female albino Wistar rats." *Regulatory Toxicology and Pharmacology*.

Mann S. 1985. "Structure, morphology, and crystal growth of bacterial magnetite." In *Magnetite Biomineralization and Magnetoreception in Organisms*, 311-332. Springer.

Mao Z, Xu B, Ji X, Zhou K, Zhang X, Chen M, Han X, Tang Q, Wang X, and Xia Y. 2015. "Titanium dioxide nanoparticles alter cellular morphology via disturbing the microtubule dynamics." *Nanoscale* 7 (18):8466-8475.

Maria d L L, Cruz T, Pousada J C, Rodrigues L E, Barbosa K, and Canguçu V. 1998. "The effect of magnesium supplementation in increasing doses on the control of type 2 diabetes." *Diabetes care* 21 (5):682-686.

Maroudas N. 1975. "Adhesion and spreading of cells on charged surfaces." *Journal of theoretical biology* 49 (1):417-424.

Marshall M J, Beliaev A S, Dohnalkova A C, Kennedy D W, Shi L, Wang Z, Boyanov M I, Lai B, Kemner K M, and McLean J S. 2006. "c-Type cytochrome-dependent formation of U (IV) nanoparticles by Shewanella oneidensis." *PLoS Biol* 4 (8):e268.

Martin O J, Lee A, and McGraw T E. 2006. "GLUT4 distribution between the plasma membrane and the intracellular compartments is maintained by an insulin-modulated bipartite dynamic mechanism." *Journal of Biological Chemistry* 281 (1):484-490.

Martinez-Boubeta C, Balcells L, Cristofol R, Sanfeliu C, Rodriguez E, Weissleder R, Lope-Piedrafita S, Simeonidis K, Angelakeris M, Sandiumenge F, Calleja A, Casas L, Monty C, and Martinez B. 2010. "Self-assembled multifunctional Fe/MgO nanospheres for magnetic resonance imaging and hyperthermia." *Nanomedicine* 6 (2):362-70. doi: 10.1016/j.nano.2009.09.003.

Martins I J. 2016. "Type 3 diabetes with links to NAFLD and Other Chronic Diseases in the Western World."

Mastuli M S, Ansari N S, Nawawi M A, and Mahat A M. 2012. "Effects of cationic surfactant in sol-gel synthesis of nano sized magnesium oxide." *APCBEE Procedia* 3:93-98.

Mastuli M S, Kamarulzaman N, Nawawi M A, Mahat A M, Rusdi R, and Kamarudin N. 2014. "Growth mechanisms of MgO nanocrystals via a sol-gel synthesis using different complexing agents." *Nanoscale research letters* 9 (1):1.

Mather H, Nisbet J A, Burton G, Poston G, Bland J, Bailey P A, and Pilkington T. 1979. "Hypomagnesaemia in diabetes." *Clinica Chimica Acta* 95 (2):235-242.

Mathers C D, and Loncar D. 2006. "Projections of Global Mortality and Burden of Disease from 2002 to 2030." *PLoS Med* 3 (11):e442. doi: 10.1371/journal.pmed.0030442.

Mattevi C, Kim H, and Chhowalla M. 2011. "A review of chemical vapour deposition of graphene on copper." *Journal of Materials Chemistry* 21 (10):3324-3334.

Mclaren A, Valdes-Solis T, Li G, and Tsang S C. 2009. "Shape and size effects of ZnO nanocrystals on photocatalytic activity." *Journal of the American Chemical Society* 131 (35):12540-12541.

Mellgren R L. 2011. "A new twist on plasma membrane repair." *Communicative & integrative biology* 4 (2):198-200.

Merino-Ibarra E, Artieda M, Cenarro A, Goicoechea J, Calvo L, Guallar A, and Civeira F. 2005. "Ultrasonography for the evaluation of visceral fat and the metabolic syndrome." *Metabolism* 54 (9):1230-5. doi: 10.1016/j.metabol.2005.04.009.

Meshkani F, and Rezaei M. 2009. "Facile synthesis of nanocrystalline magnesium oxide with high surface area." *Powder Technology* 196 (1):85-88.

Michailova A P, Belik M E, and McCulloch A D. 2004. "Effects of magnesium on cardiac excitation-contraction coupling." *J Am Coll Nutr* 23 (5):514s-517s.

Miller G L. 1959. "Use of dinitrosalicylic acid reagent for determination of reducing sugar." *Analytical chemistry* 31 (3):426-428.

Mirhosseini M. 2016. "Evaluation of antibacterial effect of magnesium oxide nanoparticles with nisin and heat in milk." *Nanomedicine Journal* 3 (2):135-142.

Mirhosseini M, and Firouzabadi F B. 2013. "Antibacterial activity of zinc oxide nanoparticle suspensions on food-borne pathogens." *International Journal of Dairy Technology* 66 (2):291-295.

Mirzaei H, and Darroudi M. 2017. "Zinc oxide nanoparticles: Biological synthesis and biomedical applications." *Ceramics International* 43 (1):907-914.

Mirzaei H, and Davoodnia A. 2012. "Microwave assisted sol-gel synthesis of MgO nanoparticles and their catalytic activity in the synthesis of hantzsch 1, 4-dihydropyridines." *Chinese journal of catalysis* 33 (9):1502-1507.

Mitropoulos K A, Miller G J, Watts G F, and Durrington P N. 1992. "Lipolysis of triglyceride-rich lipoproteins activates coagulant factor XII: a study in familial lipoprotein-lipase deficiency." *Atherosclerosis* 95 (2-3):119-25.

Moghimi S M, Hunter A C, and Murray J C. 2005. "Nanomedicine: current status and future prospects." *The FASEB Journal* 19 (3):311-330.

Mohamed S A, Al-Malki A L, and Kumosani T A. 2009. "Partial purification and characterization of five α-amylases from a wheat local variety (Balady) during germination." *Aust J Basic Appl Sci* 3:1740-8.

Mohanpuria P, Rana N K, and Yadav S K. 2008. "Biosynthesis of nanoparticles: technological concepts and future applications." *Journal of Nanoparticle Research* 10 (3):507-517.

Montazer M, Behzadnia A, Pakdel E, Rahimi M K, and Moghadam M B. 2011. "Photo induced silver on nano titanium dioxide as an enhanced antimicrobial agent for wool." *Journal of Photochemistry and Photobiology B: Biology* 103 (3):207-214.

Monteilh-Zoller M K, Hermosura M C, Nadler M J, Scharenberg A M, Penner R, and Fleig A. 2003. "TRPM7 provides an ion channel mechanism for cellular entry of trace metal ions." *The Journal of general physiology* 121 (1):49-60.

Moon J Y, Mosaddik A, Kim H, Cho M, Choi H-K, Kim Y S, and Cho S K. 2011. "The chloroform fraction of guava (Psidium cattleianum sabine) leaf extract inhibits human gastric cancer cell proliferation via induction of apoptosis." *Food chemistry* 125 (2):369-375.

Mooren F C, Stoll R, Spyrou E, Beil W, and Domschke W. 1994. "Stimulus-Secretion Coupling in Rat Parietal-Cells Is Affected by Extracellular Magnesium." *Biochemical and biophysical research communications* 204 (2):512-518.

Morais J B S, Severo J S, de Alencar G R R, de Oliveira A R S, Cruz K J C, Marreiro D d N, Freitas B d J e S d A, de Carvalho C M R, Martins M d C d C e, and Frota K d M G. 2017. "Effect of magnesium supplementation on insulin resistance in humans: A systematic review." *Nutrition* 38:54-60. doi: http://dx.doi.org/10.1016/j.nut.2017.01.009.

Morales A, Lopez T, and Gomez R. 1995. "Crystalline structure of MgO prepared by the sol-gel technique with different hydrolysis catalysts." *Journal of solid state chemistry* 115 (2):411-415.

Morales A E, Mora E S, and Pal U. 2007. "Use of diffuse reflectance spectroscopy for optical characterization of un-supported nanostructures." *Revista Mexicana de Fisica S* 53 (5):18.

Moreno-Navarrete J M, and Fernández-Real J M. 2017. "Adipocyte differentiation." In *Adipose tissue biology*, 69-90. Springer.

Moreno-Vega A-I, Gomez-Quintero T, Nunez-Anita R-E, Acosta-Torres L-S, and Castaño V. 2012. "Polymeric and ceramic nanoparticles in biomedical applications." *Journal of Nanotechnology* 2012.

Morris R M, and Klabunde K J. 1983. "Formation of paramagnetic adsorbed molecules on thermally activated magnesium and calcium oxides. Characteristics of the active surface sites." *Inorganic Chemistry* 22 (4):682-687.

Mosmann T. 1983. "Rapid colorimetric assay for cellular growth and survival: application to proliferation and cytotoxicity assays." *Journal of immunological methods* 65 (1-2):55-63.

Mourdikoudis S, Altantzis T, Liz-Marzán L M, Bals S, Pastoriza-Santos I, and Pérez-Juste J. 2016. "Hydrophilic Pt nanoflowers: synthesis, crystallographic analysis and catalytic performance." *CrystEngComm* 18 (19):3422-3427.

Mudaliar S, and Edelman S V. 2001. "Insulin therapy in type 2 diabetes." *Endocrinol Metab Clin North Am* 30 (4):935-82.

Murgia S, Falchi A M, Mano M, Lampis S, Angius R, Carnerup A M, Schmidt J, Diaz G, Giacca M, and Talmon Y. 2010. "Nanoparticles from lipid-based liquid crystals: emulsifier influence on morphology and cytotoxicity." *The Journal of Physical Chemistry B* 114 (10):3518-3525.

Myagkov V G e, Bayukov O A, Bykova L E e, Zhigalov V S, and Bondarenko G N. 2004. "Solid-state synthesis in Ni/Fe/MgO (001) epitaxial thin films." *Journal of Experimental and Theoretical Physics Letters* 80 (7):487-490.

Nabeshi H, Yoshikawa T, Arimori A, Yoshida T, Tochigi S, Hirai T, Akase T, Nagano K, Abe Y, and Kamada H. 2011. "Effect of surface properties of silica nanoparticles on their cytotoxicity and cellular distribution in murine macrophages." *Nanoscale research letters* 6 (1):1-6.

Nadler J L, Buchanan T, Natarajan R, Antonipillai I, Bergman R, and Rude R. 1993. "Magnesium deficiency produces insulin resistance and increased thromboxane synthesis." *Hypertension* 21 (6 Pt 2):1024-9. doi: 10.1161/01.hyp.21.6.1024.

Naik N S, Lamani S, and Devarmani S S. 2017. "The role of serum magnesium level in type 2 diabetes mellitus." *International Journal of Research in Medical Sciences* 3 (3):556-559.

Najim N, Rusdi R, Hamzah A S, Shaameri Z, Mat Zain M, and Kamarulzaman N. 2014. "Effects of the Absorption Behaviour of ZnO Nanoparticles on Cytotoxicity Measurements." *Journal of Nanomaterials* 2014.

Narayanan S, Sathy B N, Mony U, Koyakutty M, Nair S V, and Menon D. 2011. "Biocompatible magnetite/gold nanohybrid contrast agents via green chemistry for MRI and CT bioimaging." *ACS applied materials & interfaces* 4 (1):251-260.

Nasir A. 2010. "Nanodermatology: a bright glimpse just beyond the horizon—part I." *Skin Therapy Lett* 15 (8):1-4.

Nathan D M, Buse J B, Davidson M B, Ferrannini E, Holman R R, Sherwin R, and Zinman B. 2009. "Medical management of hyperglycemia in type 2 diabetes: a consensus algorithm for the initiation and adjustment of therapy: a consensus statement of the American Diabetes Association and the European Association for the Study of Diabetes." *Diabetes Care* 32 (1):193-203. doi: 10.2337/dc08-9025.

Nel A E, Mädler L, Velegol D, Xia T, Hoek E M, Somasundaran P, Klaessig F, Castranova V, and Thompson M. 2009. "Understanding biophysicochemical interactions at the nano-bio interface." *Nature materials* 8 (7):543.

Ng C T, Yong L Q, Hande M P, Ong C N, Yu L E, Bay B H, and Baeg G H. 2017. "Zinc oxide nanoparticles exhibit cytotoxicity and genotoxicity through oxidative stress responses in human lung fibroblasts and Drosophila melanogaster." *International Journal of Nanomedicine* 12:1621.

Nicollian E H, Brews J R, and Nicollian E H. 1982. *MOS (metal oxide semiconductor) physics and technology*. Vol. 1987: Wiley New York et al.

Niederberger M. 2007. "Nonaqueous sol–gel routes to metal oxide nanoparticles." *Accounts of chemical research* 40 (9):793-800.

Nishiyama N. 2007. "Nanomedicine: nanocarriers shape up for long life." *Nature nanotechnology* 2 (4):203-204.

Nitin N, LaConte L, Rhee W J, and Bao G. 2009. "Tat peptide is capable of importing large nanoparticles across nuclear membrane in digitonin permeabilized cells." *Annals of biomedical engineering* 37 (10):2018-2027.

Njagi E C, Huang H, Stafford L, Genuino H, Galindo H M, Collins J B, Hoag G E, and Suib S L. 2010. "Biosynthesis of iron and silver nanoparticles at room temperature using aqueous sorghum bran extracts." *Langmuir* 27 (1):264-271.

Noori M, Talebi M, and Nasiri Z. 2015. "Seven Amaranthus L.(Amaranthaceae) Taxa Flavonoid Compounds from Tehran Province, Iran." *International Journal of Modern Botany* 5 (1):9-17.

Nune S K, Chanda N, Shukla R, Katti K, Kulkarni R R, Thilakavathy S, Mekapothula S, Kannan R, and Katti K V. 2009. "Green nanotechnology from tea: phytochemicals in tea as building blocks for production of biocompatible gold nanoparticles." *Journal of materials chemistry* 19 (19):2912-2920.

Oberdörster G. 2000. "Pulmonary effects of inhaled ultrafine particles." *International archives of occupational and environmental health* 74 (1):1-8.

Oberdörster G, Ferin J, and Lehnert B E. 1994. "Correlation between particle size, *in vivo* particle persistence, and lung injury." *Environmental health perspectives* 102 (Suppl 5):173.

181

Oh N, and Park J-H. 2014. "Endocytosis and exocytosis of nanoparticles in mammalian cells." *International journal of nanomedicine* 9 (Suppl 1):51.

Olin J L, and Harris K B. 2017. "Expanded Basal Insulin Options for Type 2 Diabetes Mellitus." *The Journal for Nurse Practitioners* 13 (3):210-215. doi: https://doi.org/10.1016/j.nurpra.2016.07.011.

Ollila M-M, West S, Keinänen-Kiukaanniemi S, Jokelainen J, Auvinen J, Puukka K, Ruokonen A, Järvelin M-R, Tapanainen J, and Franks S. 2016. "Overweight and obese but not normal weight women with PCOS are at increased risk of Type 2 diabetes mellitus—a prospective, population-based cohort study." *Human Reproduction*.

Oluwafemi O S, Mohan S, Olubomehin O, Osibote O A, and Songca S P. 2016. "Size tunable synthesis of HDA and TOPO capped ZnSe nanoparticles via a facile aqueous/thermolysis hybrid solution route." *Journal of Materials Science: Materials in Electronics* 27 (4):3880-3887.

ORTLIEB M. 2010. "White Giant or White Dwarf?: Particle Size Distribution Measurements of TiO2." *GIT laboratory journal Europe* 14 (9-10):42-43.

Ouraipryvan P, Sreethawong T, and Chavadej S. 2009. "Synthesis of crystalline MgO nanoparticle with mesoporous-assembled structure via a surfactant-modified sol–gel process." *Materials Letters* 63 (21):1862-1865.

Ozkan S, Nguyen N T, Hwang I, Mazare A, and Schmuki P. 2017. "Highly Conducting Spaced TiO2 Nanotubes Enable Defined Conformal Coating with Nanocrystalline Nb2O5 and High Performance Supercapacitor Applications." *Small* 13 (14).

Painter N A, Morello C M, Singh R F, and McBane S E. 2013. "An evidence-based and practical approach to using Bydureon™ in patients with type 2 diabetes." *The Journal of the American Board of Family Medicine* 26 (2):203-210.

Palanikumar L, Ramasamy S, Hariharan G, and Balachandran C. 2013. "Influence of particle size of nano zinc oxide on the controlled delivery of Amoxicillin." *Applied Nanoscience* 3 (5):441-451.

Panariti A, Miserocchi G, and Rivolta I. 2012. "The effect of nanoparticle uptake on cellular behavior: disrupting or enabling functions?" *Nanotechnology, science and applications* 5:87.

Pandurangan M, Veerappan M, and Kim D H. 2015. "Cytotoxicity of zinc oxide nanoparticles on antioxidant enzyme activities and mRNA expression in the cocultured C2C12 and 3T3-L1 cells." *Applied biochemistry and biotechnology* 175 (3):1270-1280.

Paolisso G, and Barbagallo M. 1997. "Hypertension, diabetes mellitus, and insulin resistance: the role of intracellular magnesium." *American journal of hypertension* 10 (3):346-355.

Paolisso G, Passariello N, Pizza G, Marrazzo G, Giunta R, Sgambato S, Varricchio M, and D'Onofrio F. 1989. "Dietary magnesium supplements improve B-cell response to glucose and arginine in elderly non-insulin dependent diabetic subjects." *Acta endocrinologica* 121 (1):16-20.

Paolisso G, Scheen A, d'Onofrio F, and Lefèbvre P. 1990. "Magnesium and glucose homeostasis." *Diabetologia* 33 (9):511-514.

Paolisso G, Sgambato S, Gambardella A, Pizza G, Tesauro P, Varricchio M, and d'Onofrio F. 1992. "Daily magnesium supplements improve glucose handling in elderly subjects." *The American journal of clinical nutrition* 55 (6):1161-1167.

Paolisso G, Sgambato S, Passariello N, Giughano D, Scheen A, and Lefèbvre P. 1986. "Insulin induces opposite changes in plasma and erythrocyte magnesium concentrations in normal man." *Diabetologia* 29 (9):644-647.

Parak W J, Gerion D, Pellegrino T, Zanchet D, Micheel C, Williams S C, Boudreau R, Gros M A L, Larabell C A, and Alivisatos A P. 2003. "Biological applications of colloidal nanocrystals." *Nanotechnology* 14 (7):R15.

Parboosing R, Mzobe G, Chonco L, and Moodley I. 2017. "Cell-based Assays for Assessing Toxicity: A Basic Guide." *Medicinal Chemistry* 13 (1):13-21.

Pareta R, McQuilling J P, Farney A, and Opara E C. 2012. "Bioartificial pancreas: evaluation of crucial barriers to clinical application." *Organ Donation and Transplantation-Public Policy and Clinical Perspectives*.

Park Y-S, Hong Y, Weyers A, Kim Y S, and Linhardt R. 2011. "Polysaccharides and phytochemicals: a natural reservoir for the green synthesis of gold and silver nanoparticles." *Nanobiotechnology, IET* 5 (3):69-78.

Parmar A, Mishra A, and Pathak A. 2015. "Preparation and evaluation of mucoadhesive microspheres of repaglinide for treatment of diabetes mellitus type II." *International Journal of Advances in Pharmaceutics* 4 (5):72-82.

Pasupuleti V R, Prasad T, Shiekh R A, Balam S K, Narasimhulu G, Reddy C S, Ab Rahman I, and Gan S H. 2013. "Biogenic silver nanoparticles using Rhinacanthus nasutus leaf extract: synthesis, spectral analysis, and antimicrobial studies." *International journal of nanomedicine* 8:3355.

Patil S, Sandberg A, Heckert E, Self W, and Seal S. 2007. "Protein adsorption and cellular uptake of cerium oxide nanoparticles as a function of zeta potential." *Biomaterials* 28 (31):4600-4607.

Peer D, Karp J M, Hong S, Farokhzad O C, Margalit R, and Langer R. 2007. "Nanocarriers as an emerging platform for cancer therapy." *Nature nanotechnology* 2 (12):751-760.

Pekala P, Lane M D, Watkins P A, and Moss J. 1981. "On the mechanism of preadipocyte differentiation. Masking of poly (ADP-ribose) synthetase activity during differentiation of 3T3-L1 preadipocytes." *Journal of Biological Chemistry* 256 (10):4871-4876.

Peters R. 2005. "Translocation through the nuclear pore complex: selectivity and speed by reduction-of-dimensionality." *Traffic* 6 (5):421-427.

Petrak F, Herpertz S, Albus C, Hermanns N, Hiemke C, Hiller W, Kronfeld K, Kruse J, Kulzer B, and Ruckes C. 2013. "Study protocol of the Diabetes and Depression Study (DAD): a multi-center randomized controlled trial to compare the efficacy of a diabetes-specific cognitive behavioral group therapy versus sertraline in patients with major depression and poorly controlled diabetes mellitus." *BMC psychiatry* 13 (1):206.

Philip D. 2010. "Green synthesis of gold and silver nanoparticles using Hibiscus rosa sinensis." *Physica E: Low-Dimensional Systems and Nanostructures* 42 (5):1417-1424.

Philipse A P, and Maas D. 2002. "Magnetic colloids from magnetotactic bacteria: chain formation and colloidal stability." *Langmuir* 18 (25):9977-9984.

Phillips J M. 1996. "Substrate selection for high-temperature superconducting thin films." *Journal of Applied Physics* 79 (4):1829-1848.

Piattelli M, De Nicola M G, and Castrogiovanni V. 1969. "Photocontrol of amaranthin synthesis in Amaranthus tricolor." *Phytochemistry* 8 (4):731-736.

Pickup J C, Zhi Z L, Khan F, Saxl T, and Birch D J. 2008. "Nanomedicine and its potential in diabetes research and practice." *Diabetes/metabolism research and reviews* 24 (8):604-610.

Ponder S W, Brouhard B H, and Travis L B. 1990. "Hyperphosphaturia and hypermagnesuria in children with IDDM." *Diabetes Care* 13 (4):437-441.

Präbst K, Engelhardt H, Ringgeler S, and Hübner H. 2017. "Basic Colorimetric Proliferation Assays: MTT, WST, and Resazurin." *Cell Viability Assays: Methods and Protocols*:1-17.

Premanathan M, Karthikeyan K, Jeyasubramanian K, and Manivannan G. 2011. "Selective toxicity of ZnO nanoparticles toward Gram-positive bacteria and cancer cells by apoptosis through lipid peroxidation." *Nanomedicine: Nanotechnology, Biology and Medicine* 7 (2):184-192.

Pudukudy M, Yaakob Z, Mazuki M Z, Takriff M S, and Jahaya S S. 2017. "One-pot sol-gel synthesis of MgO nanoparticles supported nickel and iron catalysts for undiluted methane decomposition into COx free hydrogen and nanocarbon." *Applied Catalysis B: Environmental*.

Qian S. 2014. "Surface Charge Properties of Nanoparticle: Size Dependency and Boundary Effect." 2014 ECS and SMEQ Joint International Meeting (October 5-9, 2014).

Qiao Q, and Nyamdorj R. 2010. "Is the association of type II diabetes with waist circumference or waist-to-hip ratio stronger than that with body mass index?" *Eur J Clin Nutr* 64 (1):30-4. doi: 10.1038/ejcn.2009.93.

Qingwen L, Hao Y, Yan C, Jin Z, and Zhongfan L. 2002. "A scalable CVD synthesis of high-purity single-walled carbon nanotubes with porous MgO as support material." *J. Mater. Chem.* 12 (4):1179-1183.

Quaresma S, André V, Fernandes A, and Duarte M T. 2017. "Mechanochemistry – A green synthetic methodology leading to metallodrugs, metallopharmaceuticals

and bio-inspired metal-organic frameworks." *Inorganica Chimica Acta* 455, Part 2:309-318. doi: https://doi.org/10.1016/j.ica.2016.09.033.

Rahaman M H, and Kemp B A. 2017. "A study of plasmonic field enhancement in bimetallic and active core-shell nanoparticles/nanorods." SoutheastCon, 2017.

Rahiman S, and Tantry B A. 2012a. "Nanomedicine & Nanotechnology." *Journal of Nanomedicine & Nanotechnology* (3):137.

Rahiman S, and Tantry B A. 2012b. "Nanomedicine current trends in diabetes management." *J Nanomed Nanotechol* 3:5.

Rajagopalan S, Koper O, Decker S, and Klabunde K J. 2002. "Nanocrystalline metal oxides as destructive adsorbents for organophosphorus compounds at ambient temperatures." *Chemistry-A European Journal* 8 (11):2602-2607.

Rajakumar G, Rahuman A A, Priyamvada B, Khanna V G, Kumar D K, and Sujin P. 2012. "Eclipta prostrata leaf aqueous extract mediated synthesis of titanium dioxide nanoparticles." *Materials Letters* 68:115-117.

Raliya R, Biswas P, and Tarafdar J. 2015. "TiO 2 nanoparticle biosynthesis and its physiological effect on mung bean (Vigna radiata L.)." *Biotechnology Reports* 5:22-26.

Ramchandani N, and Heptulla R A. 2012. "New technologies for diabetes: a review of the present and the future." *Int J Pediatr Endocrinol* 1:28.

Ramiya V K, Maraist M, Arfors K E, Schatz D A, Peck A B, and Cornelius J G. 2000. "Reversal of insulin-dependent diabetes using islets generated *in vitro* from pancreatic stem cells." *Nature medicine* 6 (3):278-282.

Rao A, Bankar A, Kumar A R, Gosavi S, and Zinjarde S. 2013. "Removal of hexavalent chromium ions by Yarrowia lipolytica cells modified with phyto-inspired Fe 0/Fe 3 O 4 nanoparticles." *Journal of contaminant hydrology* 146:63-73.

Rao K N, Padhy S K, Dinakaran S K, Banji D, Madireddy S, and Avasarala H. 2010. "Study of pharmacognostic, phytochemical, antimicrobial and antioxidant activities of Amaranthus tricolor Linn. leavs extract." *Iran. J. Pharm. Sci.* 6:289-99.

rao Pasupuleti V. 2013. "Biogenic silver nanoparticles using Rhinacanthus nasutus leaf extract: synthesis, spectral analysis, and antimicrobial studies." *International journal of nanomedicine* 8:3355-3364.

Raskin P, Bode B W, Marks J B, Hirsch I B, Weinstein R L, McGill J B, Peterson G E, Mudaliar S R, and Reinhardt R R. 2003. "Continuous subcutaneous insulin infusion and multiple daily injection therapy are equally effective in type 2 diabetes: a randomized, parallel-group, 24-week study." *Diabetes Care* 26 (9):2598-603.

Rašović I. 2017. "Water-soluble fullerenes for medical applications." *Materials Science and Technology* 33 (7):777-794.

Ravishankar Rai V, and Jamuna Bai A. 2011. "Nanoparticles and their potential application as antimicrobials." *Science against microbial pathogens: Communicating current research and technological advances, A. Méndez-Vilas (Ed.)*:197-209.

Reaven G M. 1995. "Pathophysiology of insulin resistance in human disease." *Physiol Rev* 75 (3):473-86.

Relier C, Dubreuil M, Lozano Garcìa O, Cordelli E, Mejia J, Eleuteri P, Robidel F, Loret T, Pacchierotti F, and Lucas S. 2017. "Study of TiO2 P25 Nanoparticles Genotoxicity on Lung, Blood, and Liver Cells in Lung Overload and Non-Overload Conditions After Repeated Respiratory Exposure in Rats." *Toxicological Sciences* 156 (2):527-537.

report C. 1992. "Threshold limit values and biological exposure indices for 1992 -1993." American Conference of governmental industrial hygienists (ACGIH), Cincinnati, Ohio.

Report W. 2013. "Nanotechnology for diabetes treatment. Pvt. Ltd http://www.AZoM.com. ." http://www.AZoM.com. .

Resch-Genger U, Grabolle M, Cavaliere-Jaricot S, Nitschke R, and Nann T. 2008. "Quantum dots versus organic dyes as fluorescent labels." *Nature methods* 5 (9):763-775.

Resnick L M. 1997. "Magnesium in the pathophysiology and treatment of hypertension and diabetes mellitus: where are we in 1997?" *American journal of hypertension* 10 (3):368.

Resnick L M, Gupta R K, Bhargava K K, Gruenspan H, Alderman M H, and Laragh J H. 1991. "Cellular ions in hypertension, diabetes, and obesity. A nuclear magnetic resonance spectroscopic study." *Hypertension* 17 (6 Pt 2):951-957.

Rezaei M, Khajenoori M, and Nematollahi B. 2011. "Synthesis of high surface area nanocrystalline MgO by pluronic P123 triblock copolymer surfactant." *Powder technology* 205 (1):112-116.

Riccardi C, and Nicoletti I. 2006. "Analysis of apoptosis by propidium iodide staining and flow cytometry." *Nature protocols* 1 (3):1458.

Rivers D B, Gracheck S J, Woodford L C, and Emert G H. 1984. "Limitations of the DNS assay for reducing sugars from saccharified lignocellulosics." *Biotechnology and bioengineering* 26 (7):800-802.

Rodríguez-Morán M, and Guerrero-Romero F. 2003. "Oral magnesium supplementation improves insulin sensitivity and metabolic control in type 2 diabetic subjects." *Diabetes care* 26 (4):1147-1152.

Rodríguez J A, and Fernández-García M. 2007. *Synthesis, properties, and applications of oxide nanomaterials*: John Wiley & Sons.

Ropp R C. 2012. *Encyclopedia of the alkaline earth compounds*: Newnes.

Rosenbloom A L, Joe J R, Young R S, and Winter W E. 1999. "Emerging epidemic of type 2 diabetes in youth." *Diabetes care* 22 (2):345-354.

Rossi A, Zoppini G, Benfari G, Geremia G, Bonapace S, Bonora E, Vassanelli C, Enriquez-Sarano M, and Targher G. 2017. "Mitral Regurgitation and Increased Risk of All-Cause and Cardiovascular Mortality in Patients with Type 2 Diabetes." *The American Journal of Medicine* 130 (1):70-76. e1.

Ryabchikova E I, Mazurkova N A, Shikina N V, and Ismagilov Z R. 2010. "The crystalline forms of titanium dioxide nanoparticles affect their interactions with individual cells." *Journal of Medical Chemical, Biological and Radiological Defense* 8.

Ryan M, Livingstone M B, Ducluzeau P H, Salle A, Genaitay M, and Ritz P. 2008. "Is a failure to recognize an increase in food intake a key to understanding insulin-induced weight gain?" *Diabetes Care* 31 (3):448-50. doi: 10.2337/dc07-1171.

S Rahiman B A T. 2012a. "Nanomedicine current trends in diabetes management." *J Nanomed Nanotechol* 3 (5).

S Rahiman B A T. 2012b. "Nanomedicine current trends in diabetes management." 4th International Conference on Nanostructures (ICNS4).

Sager T M, Kommineni C, and Castranova V. 2008. "Pulmonary response to intratracheal instillation of ultrafine versus fine titanium dioxide: role of particle surface area." *Part Fibre Toxicol* 5:17.

Sahaya S S, Janakiraman N, and Johnson M. 2012. "Phytochemical analysis of Vitex altissima L. using UV-Vis, FTIR and GC-MS." *Int J Pharm Sci Drug Res* 4 (1):56-62.

Sahil K, Akanksha M, Premjeet S, Bilandi A, and Kapoor B. 2011. "Microsphere: a review." *International journal of research in pharmacy and chemistry* 1 (4):1184-1198.

Sales C H, dos Santos A R, Cintra D E C, and Colli C. 2014. "Magnesium-deficient high-fat diet: Effects on adiposity, lipid profile and insulin sensitivity in growing rats." *Clinical Nutrition* 33 (5):879-888.

Sanna V, Pala N, and Sechi M. 2014. "Targeted therapy using nanotechnology: focus on cancer." *International journal of nanomedicine* 9:467.

Sanne G. Swinnen J B H, J. Hans DeVries. 2009. "Insulin Therapy fpr Type 2 Diabetes." *Diabetes Care* 32 (2):S253 - S259.

Sanui H, and Rubin A H. 1978. "Membrane bound and cellular cationic changes associated with insulin stimulation of cultured cells." *Journal of cellular physiology* 96 (3):265-278.

Sasank K S, Musunuru G, Koushik N K, Rao R V, and Nadendla R. 2016. "NANO TECHNOLOGY: A NEW THERAPEUTIC APPROACH FOR DIABETES." *INDO AMERICAN JOURNAL OF PHARMACEUTICAL SCIENCES* 3 (12):1488-1491.

Sasidharan A, Panchakarla L, Chandran P, Menon D, Nair S, Rao C, and Koyakutty M. 2011. "Differential nano-bio interactions and toxicity effects of pristine versus functionalized graphene." *Nanoscale* 3 (6):2461-2464.

Sato N, Quitain A T, Kang K, Daimon H, and Fujie K. 2004. "Reaction kinetics of amino acid decomposition in high-temperature and high-pressure water." *Industrial & Engineering Chemistry Research* 43 (13):3217-3222.

Saudek C D, Duckworth W C, Giobbie-Hurder A, Henderson W G, Henry R R, Kelley D E, Edelman S V, Zieve F J, Adler R A, Anderson J W, Anderson R J, Hamilton B P, Donner T W, Kirkman M S, and Morgan N A. 1996. "Implantable insulin pump vs multiple-dose insulin for non-insulin-dependent diabetes mellitus: a randomized clinical trial. Department of Veterans Affairs Implantable Insulin Pump Study Group." *Jama* 276 (16):1322-7.

Saudek C D, Selam J-L, Pitt H A, Waxman K, Rubio M, Jeandidier N, Turner D, Fischell R E, and Charles M A. 1989. "A preliminary trial of the programmable implantable medication system for insulin delivery." *New England Journal of Medicine* 321 (9):574-579.

Sawai J, and Yoshikawa T. 2004. "Quantitative evaluation of antifungal activity of metallic oxide powders (MgO, CaO and ZnO) by an indirect conductimetric assay." *Journal of applied microbiology* 96 (4):803-809.

SBU. 2009. Intensive Glucose-Lowering Therapy in Diabetes (Summary and Conclusions) Systematic Review. edited by Swedish Council on Technology Assessment in Health Care (SBU).

Schkroeder H, Balassa J, and Tipton I. 1963. "Abnormal trace metals in man: titanium." *Journal of chronic diseases* 16:55.

Schnack C, Bauer I, Pregant P, Hopmeier P, and Schernthaner G. 1992. "Hypomagnesaemia in type 2 (non-insulin-dependent) diabetes mellitus is not corrected by improvement of long-term metabolic control." *Diabetologia* 35 (1):77-79.

Schönberger U, and Aryasetiawan F. 1995. "Bulk and surface electronic structures of MgO." *Physical Review B* 52 (12):8788.

Segets D, Gradl J, Taylor R K, Vassilev V, and Peukert W. 2009. "Analysis of optical absorbance spectra for the determination of ZnO nanoparticle size distribution, solubility, and surface energy." *Acs Nano* 3 (7):1703-1710.

Selam J-L, and Charles M A. 1990. "Devices for insulin administration." *Diabetes care* 13 (9):955-979.

Senarathna U, Fernando S, Gunasekara T, Weerasekera M, Hewageegana H, Arachchi N, Siriwardena H, and Jayaweera P. 2017. "Enhanced antibacterial activity of TiO2 nanoparticle surface modified with Garcinia zeylanica extract." *Chemistry Central Journal* 11 (1):7.

Senthil A, Sivakumar T, and Narayanaswamy V. 2011. "Mucoadhesive microspheres of oral anti diabetic drug-Glipizide using different polymers." *Pharm Lett 2011; 3 (2): 496* 506.

Senthil M, and Ramesh C. 2012. "Biogenic synthesis of Fe 3 O 4 nanoparticles using *Tridax procumbens* leaf extract and its antibacterial activity on *Pseudomonas aeroginosa*." *Digest Journal of Nanomaterials & Biostructures (DJNB)* 7 (4).

Senthilkumar S, and Sivakumar T. 2014. "Green tea (Camellia sinensis) mediated synthesis of zinc oxide (ZNO) nanoparticles and studies on their antimicrobial activities." *Int J Pharm Pharm Sci* 6:461-465.

Shaban S M, Aiad I, El-Sukkary M M, Soliman E, and El-Awady M Y. 2014. "One step green synthesis of hexagonal silver nanoparticles and their biological activity." *Journal of Industrial and Engineering Chemistry* 20 (6):4473-4481.

Shahwan T, Sirriah S A, Nairat M, Boyacı E, Eroğlu A E, Scott T B, and Hallam K R. 2011. "Green synthesis of iron nanoparticles and their application as a Fenton-like catalyst for the degradation of aqueous cationic and anionic dyes." *Chemical Engineering Journal* 172 (1):258-266.

Shand M A. 2006. *The chemistry and technology of magnesia*: John Wiley & Sons.

Shang L, Wang Y, Jiang J, and Dong S. 2007. "pH-dependent protein conformational changes in albumin: gold nanoparticle bioconjugates: a spectroscopic study." *Langmuir* 23 (5):2714-2721.

Shankar S S, Rai A, Ahmad A, and Sastry M. 2005. "Controlling the optical properties of lemongrass extract synthesized gold nanotriangles and potential application in infrared-absorbing optical coatings." *Chemistry of Materials* 17 (3):566-572.

Shapiro A J, Pokrywczynska M, and Ricordi C. 2017. "Clinical pancreatic islet transplantation." *Nature Reviews Endocrinology* 13 (5):268-277.

Shapiro A M J, Lakey J R T, Ryan E A, Korbutt G S, Toth E, Warnock G L, Kneteman N M, and Rajotte R V. 2000. "Islet transplantation in seven patients with type 1 diabetes mellitus using a glucocorticoid-free immunosuppressive regimen." *New England Journal of Medicine* 343 (4):230-238.

Sharma G, Soni R, and Jasuja N D. 2017. "Phytoassisted synthesis of magnesium oxide nanoparticles with Swertia chirayaita." *Journal of Taibah University for Science* 11 (3):471-477. doi: https://doi.org/10.1016/j.jtusci.2016.09.004.

Sharma V, Shukla R K, Saxena N, Parmar D, Das M, and Dhawan A. 2009. "DNA damaging potential of zinc oxide nanoparticles in human epidermal cells." *Toxicology letters* 185 (3):211-218.

Shehab M, Ebrahim S, and Soliman M. 2017. "Graphene quantum dots prepared from glucose as optical sensor for glucose." *Journal of Luminescence* 184:110-116. doi: https://doi.org/10.1016/j.jlumin.2016.12.006.

Sheikhpour M, Barani L, and Kasaeian A. 2017. "Biomimetics in drug delivery systems: A critical review." *Journal of Controlled Release*.

Shen J, Zhu Y, Yang X, and Li C. 2012. "Graphene quantum dots: emergent nanolights for bioimaging, sensors, catalysis and photovoltaic devices." *Chemical Communications* 48 (31):3686-3699.

Shen S, Chow P S, Chen F, and Tan R B H. 2007. "Submicron particles of SBA-15 modified with MgO as carriers for controlled drug delivery." *Chemical and pharmaceutical bulletin* 55 (7):985-991.

Shi H, Magaye R, Castranova V, and Zhao J. 2013a. "Titanium dioxide nanoparticles: a review of current toxicological data." *Particle and Fibre Toxicology* 10:15-15. doi: 10.1186/1743-8977-10-15.

Shi H, Magaye R, Castranova V, and Zhao J. 2013b. "Titanium dioxide nanoparticles: a review of current toxicological data." *Part Fibre Toxicol* 10 (1):15.

Shi L, Zhu J, Yang P, Tang X, Yu W, Pan C, Shen M, Zhu D, Cheng J, and Ye X. 2017. "Comparison of exenatide and acarbose on intra-abdominal fat content in patients with obesity and type-2 diabetes: A randomized controlled trial." *Obesity Research & Clinical Practice*.

Shilpa Hiremath V C, M A Lourdu Antonyraj, Chandraprabha M N, and S S. 2014. "Green Synthesis of Tio2nanoparticles By Using Neem Leaf Extract." *International Review of Applied Biotechnology and Biochemistry* 2 (1):11-17.

Shimkunas R A, Robinson E, Lam R, Lu S, Xu X, Zhang X-Q, Huang H, Osawa E, and Ho D. 2009. "Nanodiamond–insulin complexes as pH-dependent protein delivery vehicles." *Biomaterials* 30 (29):5720-5728.

Shukla S, Parashar G, Mishra A, Misra P, Yadav B, Shukla R, Bali L, and Dubey G. 2004. "Nano-like magnesium oxide films and its significance in optical fiber humidity sensor." *Sensors and Actuators B: Chemical* 98 (1):5-11.

Simon H-U, Haj-Yehia A, and Levi-Schaffer F. 2000. "Role of reactive oxygen species (ROS) in apoptosis induction." *Apoptosis* 5 (5):415-418.

Simonsen O, Mogelmosea M-L H, and Courb A I. 1999. "Crystal Structures of the Reaction Product from Ethyl Acetoacetate and Hydroxylamine, C8H8N203'H201." *Acta Chemica Scandinavica* 53:432-435.

Siripong P, Kongkathip B, Preechanukool K, Picha P, Tunsuwan K, and Taylor W. 1992. "Cytotoxic diterpenoid constituents from Andrographis paniculata Nees leaves." *J. Sci. Soc. Thailand* 18 (4):187-194.

Sjogren A, Floren C H, and Nilsson Å. 1988a. "Magnesium, potassium and zinc deficiency in subjects with type II diabetes mellitus." *Acta Medica Scandinavica* 224 (5):461-466.

Sjogren A, Floren C H, and Nilsson Å. 1988b. "Magnesium, potassium and zinc deficiency in subjects with type II diabetes mellitus." *Journal of Internal Medicine* 224 (5):461-466.

Slot J W, Geuze H J, Gigengack S, James D E, and Lienhard G E. 1991. "Translocation of the glucose transporter GLUT4 in cardiac myocytes of the rat." *Proceedings of the National Academy of Sciences* 88 (17):7815-7819.

Soenen S J, Rivera-Gil P, Montenegro J-M, Parak W J, De Smedt S C, and Braeckmans K. 2011. "Cellular toxicity of inorganic nanoparticles: common aspects and guidelines for improved nanotoxicity evaluation." *Nano Today* 6 (5):446-465.

Sōmiya S, and Roy R. 2000. "Hydrothermal synthesis of fine oxide powders." *Bulletin of Materials Science* 23 (6):453-460.

Song G, Ma S, Tang G, and Wang X. 2010. "Ultrasonic-assisted synthesis of hydrophobic magnesium hydroxide nanoparticles." *Colloids and Surfaces A: Physicochemical and Engineering Aspects* 364 (1):99-104.

Song Y, He K, Levitan E, Manson J, and Liu S. 2006. "Effects of oral magnesium supplementation on glycaemic control in Type 2 diabetes: a meta-analysis of randomized double-blind controlled trials." *Diabetic Medicine* 23 (10):1050-1056.

Stang J, and Story M. 2005. "Guidelines for Adolescent Nutrition Services (2005)." *Center for Leadership, Education and Training in Maternal and Child Nutrition, Division of Epidemiology and Community Health, School of Public Health, University of Minnesota: Minneapolis*.

Stark J V, and Klabunde K J. 1996. "Nanoscale metal oxide particles/clusters as chemical reagents. Adsorption of hydrogen halides, nitric oxide, and sulfur trioxide on magnesium oxide nanocrystals and compared with microcrystals." *Chemistry of materials* 8 (8):1913-1918.

Štengl V, Bakardjieva S, Marıková M, Bezdicka P, and Šubrt J. 2003. "Magnesium oxide nanoparticles prepared by ultrasound enhanced hydrolysis of Mg-alkoxides." *Materials Letters* 57 (24):3998-4003.

Stöckli J, Fazakerley D J, and James D E. 2011. "GLUT4 exocytosis." *J Cell Sci* 124 (24):4147-4159.

Stoimenov P K, Klinger R L, Marchin G L, and Klabunde K J. 2002. "Metal oxide nanoparticles as bactericidal agents." *Langmuir* 18 (17):6679-6686.

Strauss C R, and Trainor R W. 1995. "Developments in microwave-assisted organic chemistry." *Australian Journal of Chemistry* 48 (10):1665-1692.

Stumvoll M, Goldstein B J, and van Haeften T W. 2005. "Type 2 diabetes: principles of pathogenesis and therapy." *The Lancet* 365 (9467):1333-1346.

Su C-H, Sheu H-S, Lin C-Y, Huang C-C, Lo Y-W, Pu Y-C, Weng J-C, Shieh D-B, Chen J-H, and Yeh C-S. 2007. "Nanoshell magnetic resonance imaging contrast agents." *Journal of the American Chemical Society* 129 (7):2139-2146.

Su Y, Wei H, Zhou Z, Yang Z, Wei L, and Zhang Y. 2011. "Rapid synthesis and characterization of magnesium oxide nanocubes via DC arc discharge." *Materials Letters* 65 (1):100-103.

Subramani K, Pathak S, and Hosseinkhani H. 2012. "Recent trends in diabetes treatment using nanotechnology." *Dig J Nanomat Biostructures* 7 (1):85-95.

Subramania A, Kumar G V, Priya A S, and Vasudevan T. 2007. "Polyol-mediated thermolysis process for the synthesis of MgO nanoparticles and nanowires." *Nanotechnology* 18 (22):225601.

Sudhagar S, Sathya S, Pandian K, and Lakshmi B S. 2011. "Targeting and sensing cancer cells with ZnO nanoprobes *in vitro*." *Biotechnology letters* 33 (9):1891-1896.

Sun J, Wang S, Zhao D, Hun F H, Weng L, and Liu H. 2011. "Cytotoxicity, permeability, and inflammation of metal oxide nanoparticles in human cardiac microvascular endothelial cells." *Cell biology and toxicology* 27 (5):333-342.

Sundrarajan M, Suresh J, and Gandhi R R. 2012a. "A comparative study on antibacterial properties of MgO nanoparticles prepared under different calcination temperature." *Digest J Nanomaterials Biostructures* 7 (3):983-989.

Sundrarajan M, Suresh J, and Gandhi R R. 2012b. "A comparative study on antibacterial properties of MgO nanoparticles prepared under different calcination temperature." *Digest Journal of Nanomaterials and Biostructures* 7 (3):983-989.

Suresh J, Yuvakkumar R, Sundrarajan M, and Hong S I. 2014. "Green Synthesis of Magnesium Oxide Nanoparticles." Advanced Materials Research.

Suresh S. 2014. "Investigations on synthesis, structural and electrical properties of MgO nanoparticles by sol-gel method." *Journal of Ovonic Research Vol* 10 (6):205-210.

Surugue L. 2016. "World Health Day 2016: 422 million people live with diabetes worldwide." International Business Times.

Swaminathan R. 2003. "Magnesium Metabolism and its Disorders." *The Clinical Biochemist Reviews* 24 (2):47-66.

Swihart M T. 2003. "Vapor-phase synthesis of nanoparticles." *Current Opinion in Colloid & Interface Science* 8 (1):127-133.

Sylow L, Jensen T E, Kleinert M, Højlund K, Kiens B, Wojtaszewski J, Prats C, Schjerling P, and Richter E A. 2013. "Rac1 signaling is required for insulin-stimulated glucose uptake and is dysregulated in insulin-resistant murine and human skeletal muscle." *Diabetes* 62 (6):1865-1875.

Sylow L, Kleinert M, Pehmøller C, Prats C, Chiu T T, Klip A, Richter E A, and Jensen T E. 2014. "Akt and Rac1 signaling are jointly required for insulin-stimulated glucose uptake in skeletal muscle and downregulated in insulin resistance." *Cellular signalling* 26 (2):323-331.

Szacilowski K, Macyk W, Drzewiecka-Matuszek A, Brindell M, and Stochel G. 2005. "Bioinorganic photochemistry: frontiers and mechanisms." *Chemical reviews* 105 (6):2647-2694.

Szalay B, Tátrai E, Nyírő G, Vezér T, and Dura G. 2012. "Potential toxic effects of iron oxide nanoparticles in *in vivo* and *in vitro* experiments." *Journal of Applied Toxicology* 32 (6):446-453.

Tait S W, and Green D R. 2010. "Mitochondria and cell death: outer membrane permeabilization and beyond." *Nature reviews Molecular cell biology* 11 (9):621-632.

Tamilselvi P, Yelilarasi A, Hema M, and Anbarasan R. 2013. "Synthesis of hierarchical structured MgO by sol-gel method." *Nano Bulletin* 2 (1):130106.

Tanaka K, Capule M F, and Hisanaga T. 1991. "Effect of crystallinity of TiO 2 on its photocatalytic action." *Chemical Physics Letters* 187 (1):73-76.

Tang B, Cao L, Xu K, Zhuo L, Ge J, Li Q, and Yu L. 2008. "A new nanobiosensor for glucose with high sensitivity and selectivity in serum based on fluorescence resonance energy transfer (FRET) between CdTe quantum dots and Au nanoparticles." *Chemistry-a European Journal* 14 (12):3637-3644.

Tang Z-X, Fang X-J, Zhang Z-L, Zhou T, Zhang X-Y, and Shi L-E. 2012. "Nanosize MgO as antibacterial agent: preparation and characteristics." *Brazilian Journal of Chemical Engineering* 29 (4):775-781.

Terenteva E, Apyari V, Dmitrienko S, and Zolotov Y A. 2015. "Formation of plasmonic silver nanoparticles by flavonoid reduction: A comparative study and application for determination of these substances." *Spectrochimica Acta Part A: Molecular and Biomolecular Spectroscopy* 151:89-95.

Thabit H, Hartnell S, Allen J M, Lake A, Malgor-Zata E, Evans M L, Coll A P, and Hovorka R. 2016. "Automated Artificial Pancreas System in Type 2 Diabetes in the General Ward: A Randomized, Controlled, Parallel-Design Study." DIABETES.

Thakur S, and Karak N. 2014. "One-step approach to prepare magnetic iron oxide/reduced graphene oxide nanohybrid for efficient organic and inorganic pollutants removal." *Materials Chemistry and Physics* 144 (3):425-432.

Thirunakaran R, Kim K-T, Kang Y-M, and Young-Lee J. 2005. "Cr 3+ modified LiMn 2 O 4 spinel intercalation cathodes through oxalic acid assisted sol–gel method for lithium rechargeable batteries." *Materials research bulletin* 40 (1):177-186.

Thorsen T, Maerkl S J, and Quake S R. 2002. "Microfluidic large-scale integration." *Science* 298 (5593):580-584.

Toprak O, Kurt H, Sarı Y, Şarkış C, Us H, and Kırık A. 2017. "Magnesium replacement improves the metabolic profile in obese and pre-diabetic patients with mild-to-moderate chronic kidney disease: a 3-month, randomised, double-blind, placebo-controlled study." *Kidney and Blood Pressure Research* 42 (1):33-42.

Torchilin V P. 2012. "Multifunctional nanocarriers." *Advanced drug delivery reviews* 64:302-315.

Tso C-p, Zhung C-m, Shih Y-h, Tseng Y-M, Wu S-c, and Doong R-a. 2010. "Stability of metal oxide nanoparticles in aqueous solutions." *Water science and technology* 61 (1):127-133.

Tsuji J S, Maynard A D, Howard P C, James J T, Lam C-w, Warheit D B, and Santamaria A B. 2006. "Research strategies for safety evaluation of nanomaterials, part IV: risk assessment of nanoparticles." *Toxicological sciences* 89 (1):42-50.

Uboldi C, Giudetti G, Broggi F, Gilliland D, Ponti J, and Rossi F. 2012. "Amorphous silica nanoparticles do not induce cytotoxicity, cell transformation or genotoxicity

in Balb/3T3 mouse fibroblasts." *Mutation Research/Genetic Toxicology and Environmental Mutagenesis* 745 (1):11-20.

Uddin I, Adyanthaya S, Syed A, Selvaraj K, Ahmad A, and Poddar P. 2008. "Structure and microbial synthesis of sub-10 nm Bi2O3 nanocrystals." *Journal of nanoscience and nanotechnology* 8 (8):3909-3913.

Umar A A, Rahman M Y A, Taslim R, Salleh M M, and Oyama M. 2011. "A simple route to vertical array of quasi-1D ZnO nanofilms on FTO surfaces: 1D-crystal growth of nanoseeds under ammonia-assisted hydrolysis process." *Nanoscale research letters* 6 (1):1-12.

Umrani R D, and Paknikar K M. 2014. "Zinc oxide nanoparticles show antidiabetic activity in streptozotocin-induced Type 1 and 2 diabetic rats." *Nanomedicine* 9 (1):89-104.

Utamapanya S, Klabunde K J, and Schlup J R. 1991. "Nanoscale metal oxide particles/clusters as chemical reagents. Synthesis and properties of ultrahigh surface area magnesium hydroxide and magnesium oxide." *Chemistry of Materials* 3 (1):175-181.

Van der Velden-de Groot C. 1995. "Microcarrier technology, present status and perspective." *Cytotechnology* 18 (1-2):51-56.

Van Hardeveld R, and Hartog F. 1969. "The statistics of surface atoms and surface sites on metal crystals." *Surface Science* 15 (2):189-230.

van Meerloo J, Kaspers G J, and Cloos J. 2011. "Cell sensitivity assays: the MTT assay." *Cancer cell culture: methods and protocols*:237-245.

Vanroelen W F, Van Gaal L F, Van Rooy P E, and de Leeuw I H. 1985. "Serum and erythrocyte magnesium levels in type I and type II diabetics." *Acta Diabetologica* 22 (3):185-190.

Velayutharaj A, Saraswathi R, Shivakumar R, Saha S, Niranjan G, Ramesh R, and Sreenivasan A. 2016. "Association of serum magnesium with glycemic control and insulin resistance in patients with type 2 diabetes mellitus." *International Journal of Current Research and Review* 8 (13):17.

Venekamp W J, Kerr L, Dowsett S A, Johnson P A, Wimberley D, McKenzie C, Malone J, and Milicevic Z. 2006. "Functionality and acceptability of a new electronic

insulin injection pen with a memory feature." *Current medical research and opinion* 22 (2):315-325.

Venkateswarlu S, Rao Y S, Balaji T, Prathima B, and Jyothi N. 2013. "Biogenic synthesis of Fe 3 O 4 magnetic nanoparticles using plantain peel extract." *Materials Letters* 100:241-244.

Verma A, and Stellacci F. 2010. "Effect of surface properties on nanoparticle–cell interactions." *Small* 6 (1):12-21.

Vieira P, Cameron J, Rahikkala E, Keski-Filppula R, Zhang L-H, Santra S, Matthews A, Myllynen P, Nuutinen M, and Moilanen J S. 2017. "Novel homozygous PCK1 mutation causing cytosolic phosphoenolpyruvate carboxykinase deficiency presenting as childhood hypoglycemia, an abnormal pattern of urine metabolites and liver dysfunction." *Molecular Genetics and Metabolism* 120 (4):337-341.

Vignesh Subramanian I B, Pranav R. and Rajendran N. 2015. "Phytochemical screening and functional group analysis of four medicinally important plants." *Journal of Chemical and Pharmaceutical Research* 7 (1):116-123.

Vignesh Subramanian. I B, Pranav R. and Rajendran N. 2015. "Phytochemical screening and functional group analysis of four medicinally important plants." *Journal of Chemical and Pharmaceutical Research* 7 (1):116-123.

Walshaw S. 2005. "Plant Resources of Tropical Africa 2. Vegetables." *Econ. Bot.* 59 (4):401-402.

Wang Q, Huang J-Y, Li H-Q, Zhao A Z-J, Wang Y, Zhang K-Q, Sun H-T, and Lai Y-K. 2017. "Recent advances on smart TiO2 nanotube platforms for sustainable drug delivery applications." *International Journal of Nanomedicine* 12:151.

Wang R, Geiger C, Chen L, Swanson B, and Whitten D G. 2000. "Direct observation of sol-gel conversion: the role of the solvent in organogel formation." *Journal of the American Chemical Society* 122 (10):2399-2400.

Wang T, Bai J, Jiang X, and Nienhaus G U. 2012. "Cellular uptake of nanoparticles by membrane penetration: a study combining confocal microscopy with FTIR spectroelectrochemistry." *ACS nano* 6 (2):1251-1259.

Wang Z. 2013. "Iron complex nanoparticles synthesized by eucalyptus leaves." *ACS Sustainable Chemistry & Engineering* 1 (12):1551-1554.

Wang Z, Bentley J, Kenik E, Horton L, and McKee R A. 1992. "In-situ formation of MgO2 thin films on MgO single-crystal surfaces at high temperatures." *Surface science* 273 (1-2):88-108.

Wang Z, Fang C, and Megharaj M. 2014. "Characterization of Iron–Polyphenol Nanoparticles Synthesized by Three Plant Extracts and Their Fenton Oxidation of Azo Dye." *ACS Sustainable Chemistry & Engineering* 2 (4):1022-1025.

Wang Z L. 2008. "Splendid one-dimensional nanostructures of zinc oxide: a new nanomaterial family for nanotechnology." *Acs Nano* 2 (10):1987-1992.

Warren B E. 1969. *X-ray Diffraction*: Courier Corporation.

Were P S W W, Ozwara H S, Kutima H L. 2015. "Phytochemical analysis of Warburgia ugandensis sparague using Fourier Transform Infra-Red (FT-IR) spectroscopy." *International Journal of Pharmacognosy and Phytochemical Research* 7 (2):201-205.

Weyer C, Bogardus C, Mott D M, and Pratley R E. 1999. "The natural history of insulin secretory dysfunction and insulin resistance in the pathogenesis of type 2 diabetes mellitus." *The Journal of Clinical Investigation* 104 (6):787-794. doi: 10.1172/JCI7231.

White R E, and Hartzell H C. 1989. "Magnesium ions in cardiac function: regulator of ion channels and second messengers." *Biochemical pharmacology* 38 (6):859-867.

WHO W H O. 2016. *Global report on diabetes*: World Health Organization.

Wiesenthal A, Hunter L, Wang S, Wickliffe J, and Wilkerson M. 2011. "Nanoparticles: small and mighty." *International journal of dermatology* 50 (3):247-254.

Williams D B, and Carter C B. 1996. *The transmission electron microscope*: Springer.

Woldu M A, and Lenjisa J L. 2014. "Nanoparticles and the new era in diabetes management." *International Journal of Basic & Clinical Pharmacology* 3 (2):277-284.

Wriedt H. 1987. "The Mg− O (magnesium-oxygen) system." *Bulletin of Alloy Phase Diagrams* 8 (3):227-233.

Xia T, Kovochich M, Liong M, Mädler L, Gilbert B, Shi H, Yeh J I, Zink J I, and Nel A E. 2008. "Comparison of the mechanism of toxicity of zinc oxide and cerium oxide

nanoparticles based on dissolution and oxidative stress properties." *ACS nano* 2 (10):2121-2134.

Xiao K, Li Y, Luo J, Lee J S, Xiao W, Gonik A M, Agarwal R G, and Lam K S. 2011. "The effect of surface charge on *in vivo* biodistribution of PEG-oligocholic acid based micellar nanoparticles." *Biomaterials* 32 (13):3435-3446.

Xiong H-M. 2010. "Photoluminescent ZnO nanoparticles modified by polymers." *Journal of Materials Chemistry* 20 (21):4251-4262.

Xu X, Ho W, Zhang X, Bertrand N, and Farokhzad O. 2015. "Cancer Nanomedicine: From Targeted Delivery to Combination Therapy." *Trends in molecular medicine* 21 (4):223-232. doi: 10.1016/j.molmed.2015.01.001.

Xu Z P, Niebert M, Porazik K, Walker T L, Cooper H M, Middelberg A P, Gray P P, Bartlett P F, and Lu G Q M. 2008. "Subcellular compartment targeting of layered double hydroxide nanoparticles." *Journal of Controlled Release* 130 (1):86-94.

Yadavalli T, and Shukla D. 2017. "Role of metal and metal oxide nanoparticles as diagnostic and therapeutic tools for highly prevalent viral infections." *Nanomedicine: Nanotechnology, Biology and Medicine* 13 (1):219-230.

Yamamoto Y, Nagasaki Y, Kato Y, Sugiyama Y, and Kataoka K. 2001. "Long-circulating poly (ethylene glycol)–poly (d, l-lactide) block copolymer micelles with modulated surface charge." *Journal of Controlled Release* 77 (1):27-38.

Yameen B, Choi W I, Vilos C, Swami A, Shi J, and Farokhzad O C. 2014. "Insight into nanoparticle cellular uptake and intracellular targeting." *Journal of Controlled Release* 190:485-499.

Yanagisawa R, Takano H, Inoue K-i, Koike E, Kamachi T, Sadakane K, and Ichinose T. 2009. "Titanium dioxide nanoparticles aggravate atopic dermatitis-like skin lesions in NC/Nga mice." *Experimental Biology and Medicine* 234 (3):314-322.

Yaturu S. 2011. "Obesity and type 2 diabetes." *Journal of diabetes mellitus* 1 (4):79 - 95.

Yaturu S. 2013. "Insulin therapies: current and future trends at dawn." *World journal of diabetes* 4 (1):1.

Yin H, Casey P S, McCall M J, and Fenech M. 2010. "Effects of surface chemistry on cytotoxicity, genotoxicity, and the generation of reactive oxygen species induced by ZnO nanoparticles." *Langmuir* 26 (19):15399-15408.

Yki-Jarvinen H. 2001. "Combination therapies with insulin in type 2 diabetes." *Diabetes Care* 24 (4):758-67.

Yoshimura M, and Sōmiya S. 1999. "Hydrothermal synthesis of crystallized nano-particles of rare earth-doped zirconia and hafnia." *Materials Chemistry and Physics* 61 (1):1-8.

Yu H-F, and Liu P-C. 2006. "Effects of pH and calcination temperatures on the formation of citrate-derived hexagonal barium ferrite particles." *Journal of alloys and compounds* 416 (1):222-227.

Yu J-G, Yu H-G, Cheng B, Zhao X-J, Yu J C, and Ho W-K. 2003. "The effect of calcination temperature on the surface microstructure and photocatalytic activity of TiO2 thin films prepared by liquid phase deposition." *The Journal of Physical Chemistry B* 107 (50):13871-13879.

Yu J, Shan C-X, Qiao Q, Xie X-H, Wang S-P, Zhang Z-Z, and Shen D-Z. 2012. "Enhanced responsivity of photodetectors realized via impact ionization." *Sensors* 12 (2):1280-1287.

Yubao L, Klein C, De Wijn J, Van De Meer S, and De Groot K. 1994. "Shape change and phase transition of needle-like non-stoichiometric apatite crystals." *Journal of Materials Science: Materials in Medicine* 5 (5):263-268.

Zang J, Li C M, Cui X, Wang J, Sun X, Dong H, and Sun C Q. 2007. "Tailoring zinc oxide nanowires for high performance amperometric glucose sensor." *Electroanalysis* 19 (9):1008-1014.

Zhan J, Bando Y, Hu J, and Golberg D. 2004. "Bulk synthesis of single-crystalline magnesium oxide nanotubes." *Inorganic chemistry* 43 (8):2462-2464.

Zhang H-J, and Xiong H-M. 2013. "Biological applications of ZnO nanoparticles." *Current Molecular Imaging* 2 (2):177-192.

Zhang H, Chen B, Jiang H, Wang C, Wang H, and Wang X. 2011. "A strategy for ZnO nanorod mediated multi-mode cancer treatment." *Biomaterials* 32 (7):1906-1914.

Zhang J-j, Ning J-w, Liu X-j, Pan Y-b, and Huang L-p. 2003. "Synthesis of ultrafine YAG: Tb phosphor by nitrate–citrate sol–gel combustion process." *Materials research bulletin* 38 (7):1249-1256.

Zhang J, Pan F, Hao W, and Wang T. 2006. "Effect of MgO doping on the luminescent properties of ZnO." *Materials Science and Engineering: B* 129 (1):93-95.

Zhang R, and Gao L. 2002. "Preparation of nanosized titania by hydrolysis of alkoxide titanium in micelles." *Materials research bulletin* 37 (9):1659-1666.

Zhang W-x, Wang Y-z, and Sun C-f. 2007. "Characterization on oxidative stabilization of polyacrylonitrile nanofibers prepared by electrospinning." *Journal of Polymer Research* 14 (6):467-474.

Zhang Y, Chen Y, Westerhoff P, Hristovski K, and Crittenden J C. 2008. "Stability of commercial metal oxide nanoparticles in water." *Water research* 42 (8):2204-2212.

Zhao F, Zhao Y, Liu Y, Chang X, Chen C, and Zhao Y. 2011. "Cellular uptake, intracellular trafficking, and cytotoxicity of nanomaterials." *Small* 7 (10):1322-1337.

Zhao J, Bowman L, Zhang X, Vallyathan V, Young S-H, Castranova V, and Ding M. 2009. "Titanium dioxide (TiO2) nanoparticles induce JB6 cell apoptosis through activation of the caspase-8/Bid and mitochondrial pathways." *Journal of Toxicology and Environmental Health, Part A* 72 (19):1141-1149.

Zhou Z, Xie S, Wan D, Liu D, Gao Y, Yan X, Yuan H, Wang J, Song L, and Liu L. 2004. "Multidimensional magnesium oxide nanostructures with cone-shaped branching." *Solid state communications* 131 (7):485-488.

Zhu Q, Oganov A R, and Lyakhov A O. 2013. "Novel stable compounds in the Mg–O system under high pressure." *Physical Chemistry Chemical Physics* 15 (20):7696-7700.

Zimmet P. 2000. "Globalization, coca-colonization and the chronic disease epidemic: can the Doomsday scenario be averted?" *J Intern Med* 247 (3):301-10.

Zinchenko A A, Luckel F, and Yoshikawa K. 2007. "Transcription of giant DNA complexed with cationic nanoparticles as a simple model of chromatin." *Biophysical journal* 92 (4):1318-1325.

Zuas O, Hamim N, and Sampora Y. 2014. "Bio-synthesis of silver nanoparticles using water extract of Myrmecodia pendan (Sarang Semut plant)." *Materials Letters* 123:156-159.

Zuo P, Jiang L, Li X, Li B, Xu Y, Shi X, Ran P, Ma T, Li D, and Qu L. 2017. "Shape-Controllable Gold Nanoparticle–MoS2 Hybrids Prepared by Tuning Edge-Active Sites and Surface Structures of MoS2 via Temporally Shaped Femtosecond Pulses." *ACS Applied Materials & Interfaces* 9 (8):7447-7455.

Every reasonable effort has been made to acknowledge the owners of copyright material. I would be pleased to hear from any copyright owner who has been omitted or incorrectly acknowledges.

Appendix

Appendix A: Plates showing characterization instruments
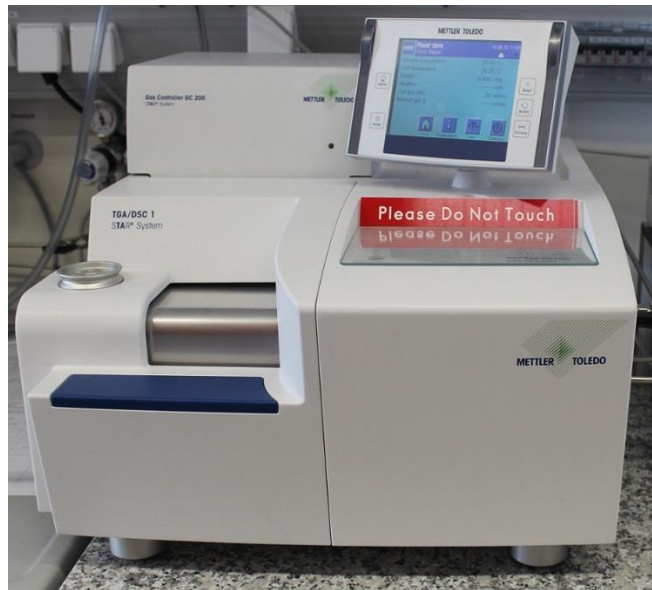
Plate A.1: Thermogravimetry-Differential Scanning Calorimeter

Plate A.2: Zeta sizer using Dynamic Light Scattering

Plate A.3: UV-Visible spectrophotometer

Plate A.4: X-ray Diffractometer

Plate A.5: Fourier Transform Infrared spectroscopy
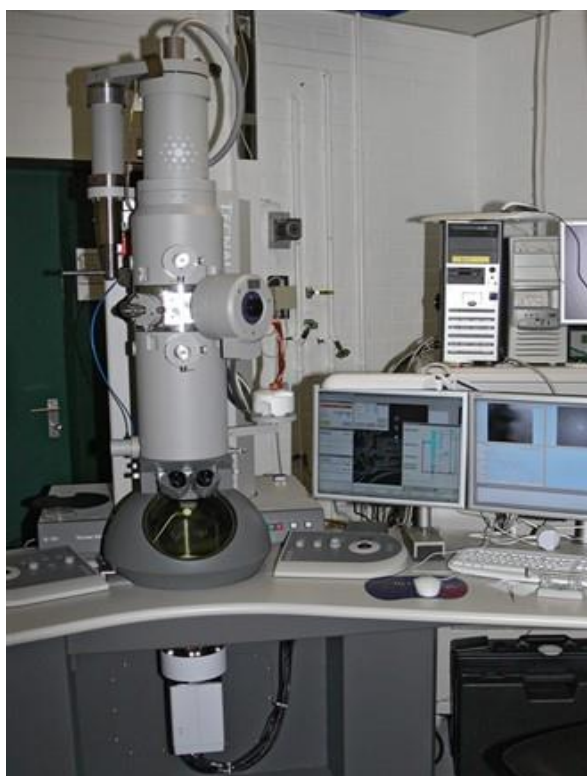
Plate A.6: Transmission Electron Microscope

Appendix B: MgO nanoparticles concentration in green synthesized samples

When analyzing the cytotoxicity of nanoparticles, their dosages to be added are more important. Since, green synthesized MgO nanoparticles are colloidal in nature, their yield is calculated by using absorbance of sample A from chemical synthesis at 322 nm. The chemical synthesized samples are analyzed and are found to be pure MgO crystals. Thus, sample A which is spherical shaped MgO nanoparticle was used to obtain linear fit graph of MgO nanoparticle concentration which was mentioned in Figure B.1. The linear fit graph of MgO nanoparticle was obtained by suspending sample A which is chemical synthesized, spherical shaped MgO nanoparticle in distilled water at different concentrations. The absorbance at 322 nm for each concentration of MgO nanoparticles leads to a standard linear fit graph for MgO nanoparticles. The slope of the linear straight line is identified to be $Y = 0.3784x + 0.0511$. By substituting the absorbance of green synthesized MgO nanoparticles in the equation, the concentration can be identified. The concentration of MgO nanoparticles in mg/ml from green synthesis that are selected for cytotoxic analysis are mentioned in Table B.1. 1 mg/ml = 1000 microgram. Hence, Sample GA, Sample GB and Sample GC contains 980, 1080, 820 µg/mL of nanoparticles respectively.
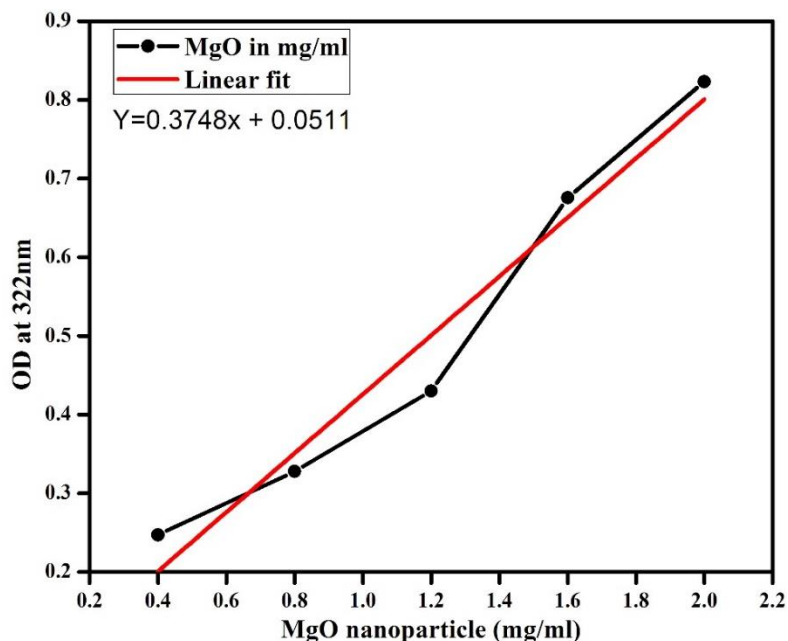
Figure B.1: Linear fit graph of MgO nanoparticles

Table B.1: Concentration of selected green synthesized MgO nanoparticles

Sample	New sample name	Absorbance @ 322 nm	Concentration (mg/ml)	Concentration (M)
Sample NT @ pH3	Sample GA	0.37	0.98	0.024
Sample NB	Sample GB	0.39	1.08	0.026
Sample NP	Sample GC	0.33	0.82	0.02

Appendix C: Standard DNS graph for known glucose concentration

The standard graph of known concentration of glucose using DNS reagent was obtained according to literature (Mohamed et al., 2009) and Table C.1 denotes the amount of glucose used and intensity of color change (measured at 570 nm using calorimeter) after incubation, to obtain the standard DNS graph. The color of the solution changes from yellow to red depending on the glucose concentration in the mixture as mentioned in Figure C.1 and the standard DNS graph with straight line equation was depicted in the Figure C.2.

Table C.1.: Reagents to be added for DNS assay and OD at 540 nm to plot standard DNS graph

S.No	Test tubes	Standard glucose solution	Amount of glucose in mg	Distilled water (ml)	DNS (ml)		Distilled water (ml)	OD at 540nm
1	Blank	0	0	2	1	Incubate for 5min in boiling water bath	9	0
2	0.2	0.2	0.9	1.8	1		9	0.468
3	0.4	0.4	1.8	1.6	1		9	0.829
4	0.6	0.6	2.7	1.4	1		9	1.362
5	0.8	0.8	3.6	1.2	1		9	1.647
6	1	1	4.5	1	1		9	2.013

Standard (before incubation)

Standard (After incubation)
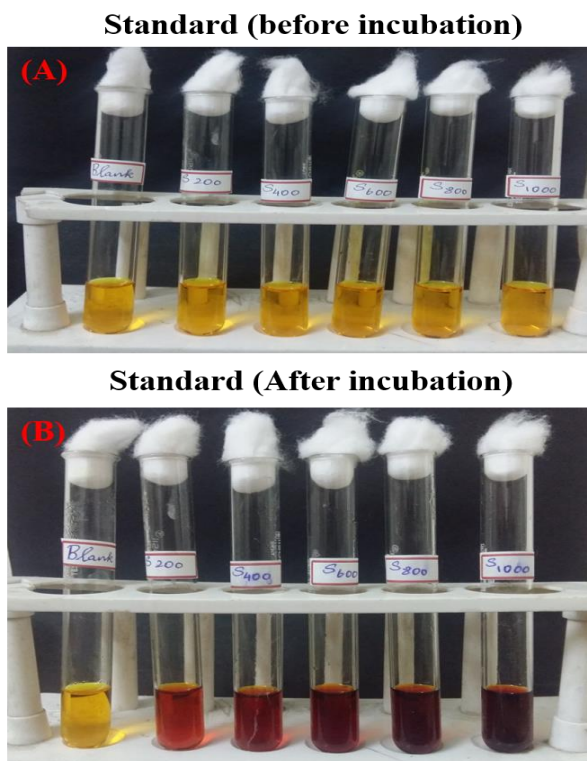
Figure C.1: Color of the DNS and glucose mixture before and after incubation

**Figure C.2: Standard DNS graph for known glucose concentration**
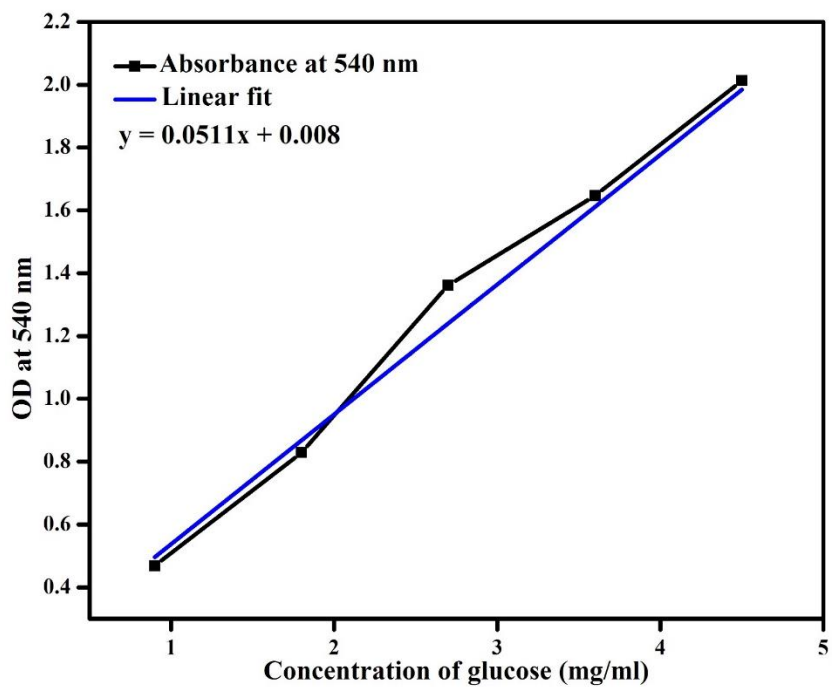
Appendix D: Particle size distribution and zeta potential of optimized MgO nanoparticles

Appendix D1: Particle size distribution and zeta potential of sample A (chemical synthesized)

Size Distribution by Number

47.95nm
PDI − 0.706

Record 5: MgO ace +T A 500C size dual2 1

Zeta Potential Distribution

-7.01mV

Record 7: MgO ace +T A 500C zeta 1
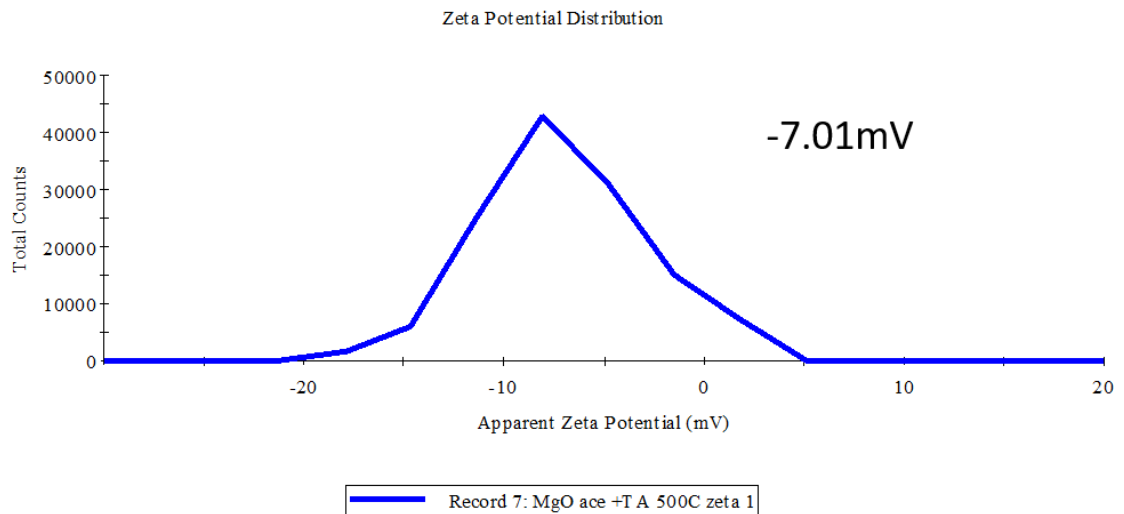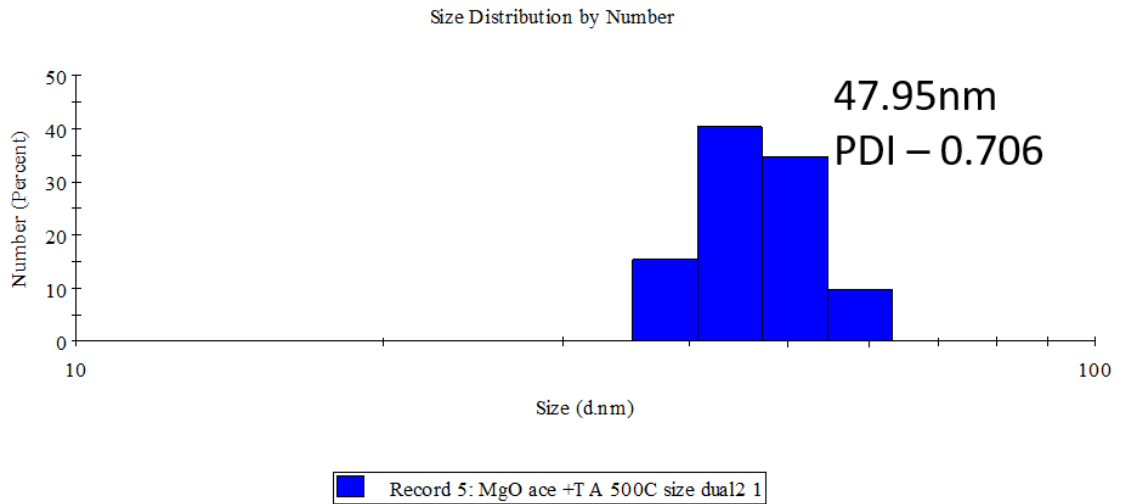
Appendix D2: Particle size distribution and zeta potential of sample B (chemical synthesized)

Size Distribution by Number

43.82nm
PDI - 0.615

Record 6: MgO ace + CA 650C 1

Zeta Potential Distribution

-7.12mV

Record 8: MgO ace + CA 650C zeta 1
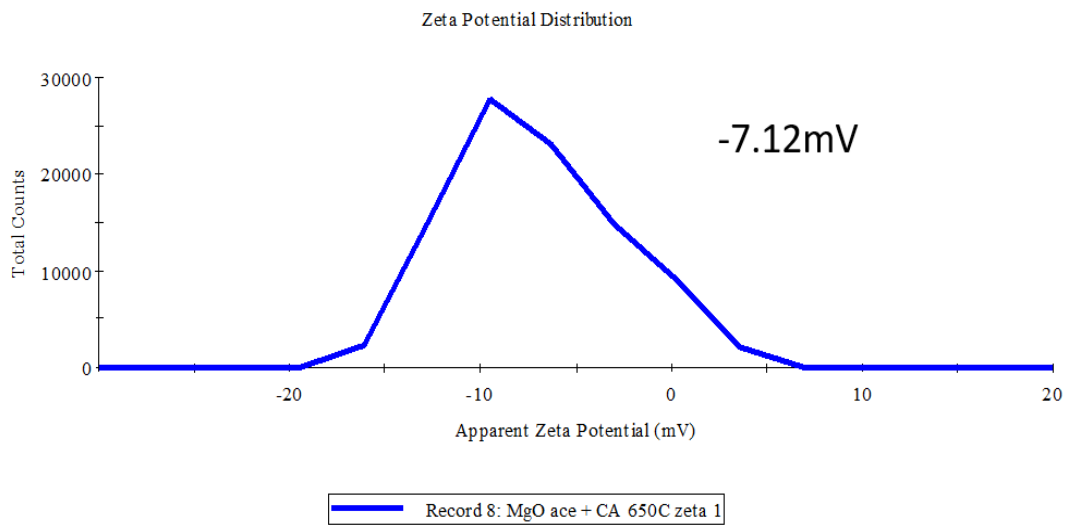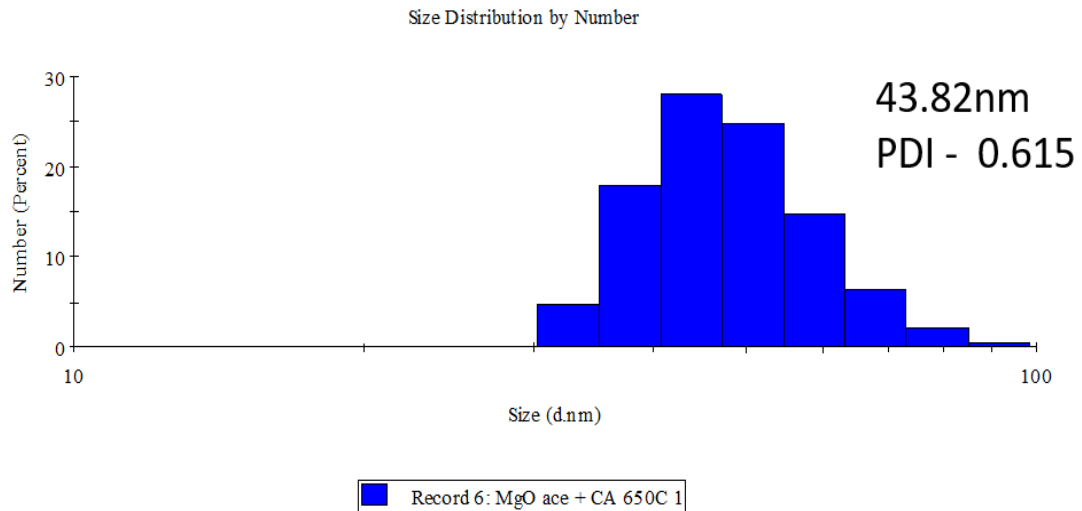
Appendix D3: Particle size distribution and zeta potential of sample C (chemical synthesized)

Size Distribution by Number

91.28nm
PDI - 0.547

■ Record 12: MgO ace + CA 750C 1

Zeta Potential Distribution

-9.83mV

—— Record 10: MgO ace + CA 750C zeta 1
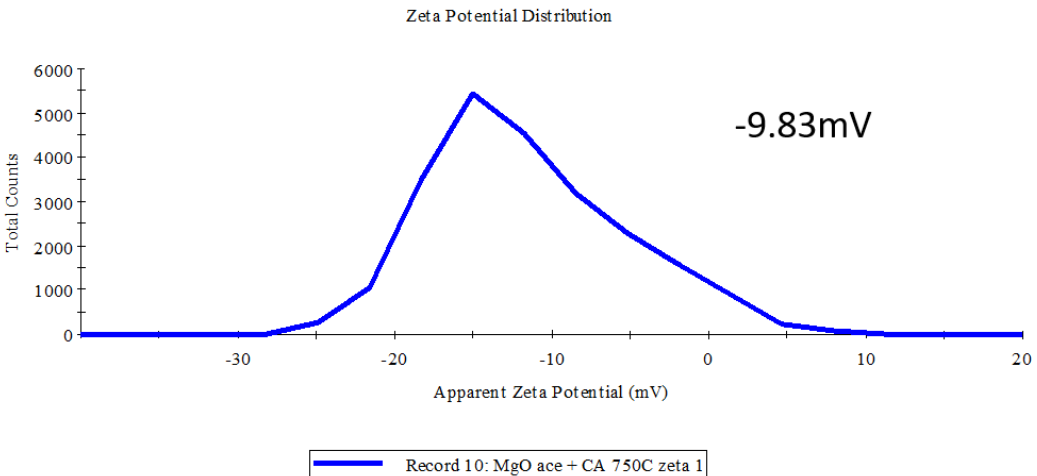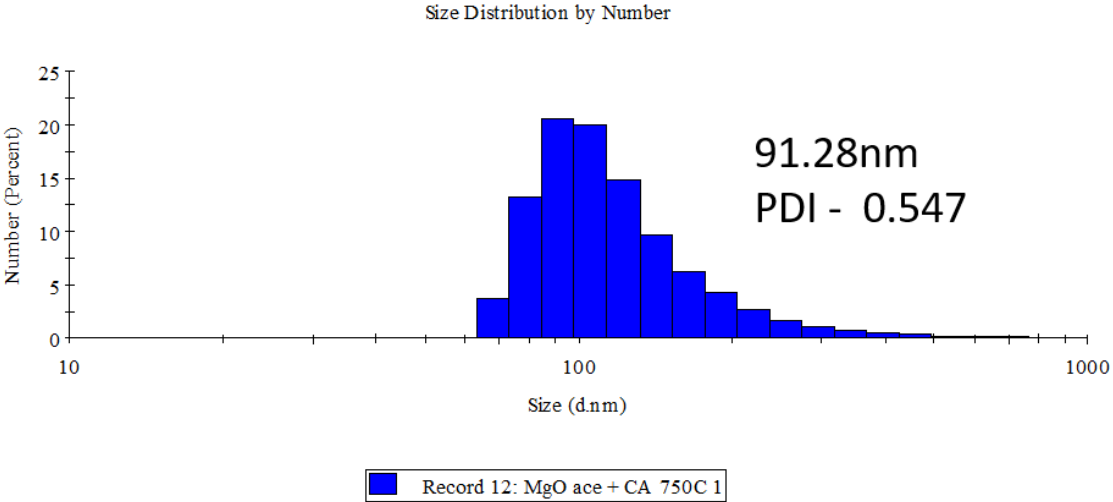
Appendix D4: Particle size distribution and zeta potential of sample GA (green synthesized)

Size Distribution by Number

43.82 nm

Record 4: MgO pH 3 1

Zeta Potential Distribution

-3.39 mV

Record 5: MgO pH 3 1
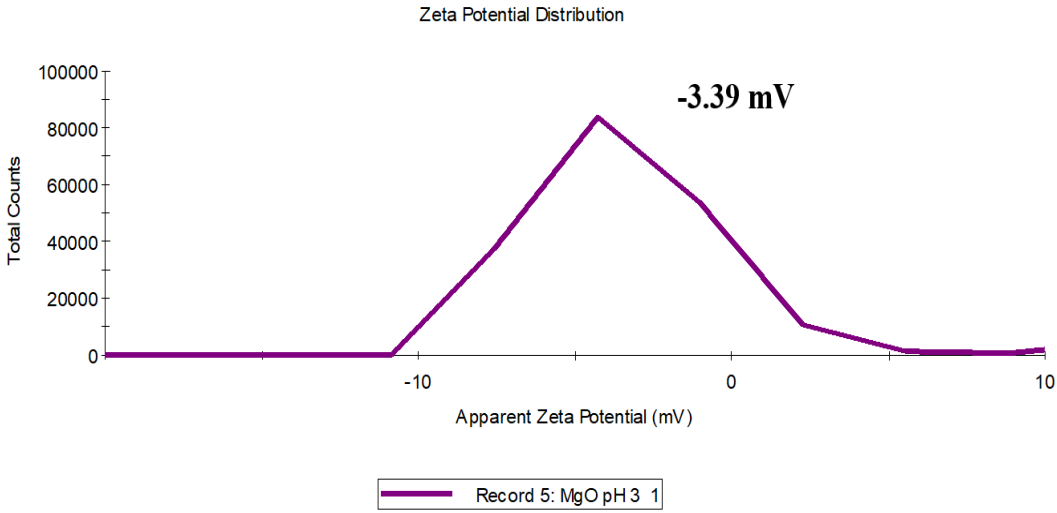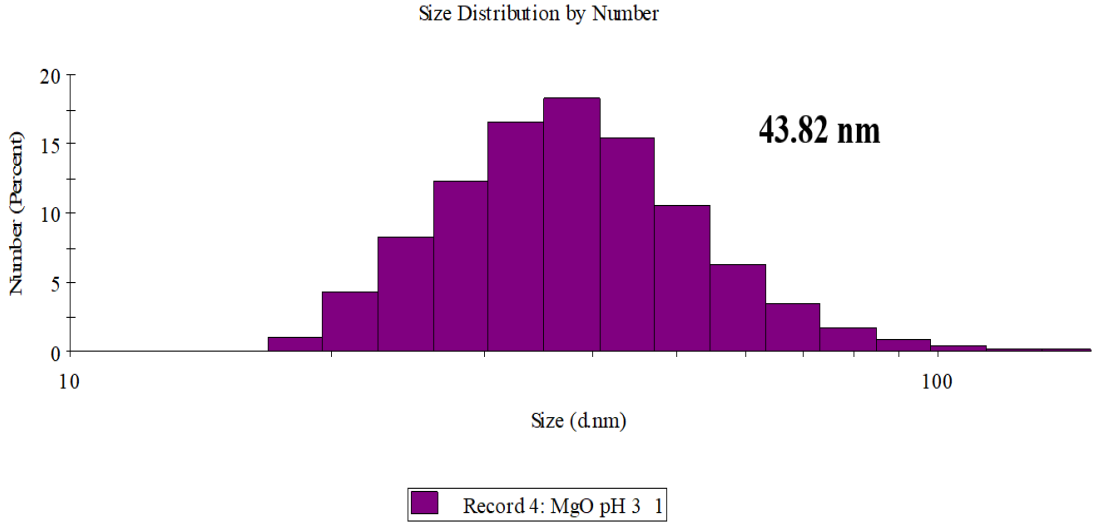
Appendix D5: Particle size distribution and zeta potential of sample GB (green synthesized)

Size Distribution by Number
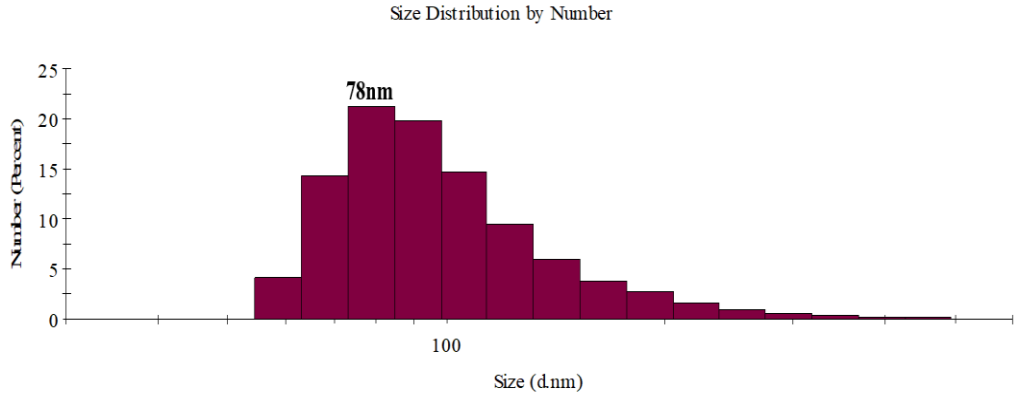
Record 4: MgO nanoparticle with 5ml A. blitium extract

Zeta Potential Distribution
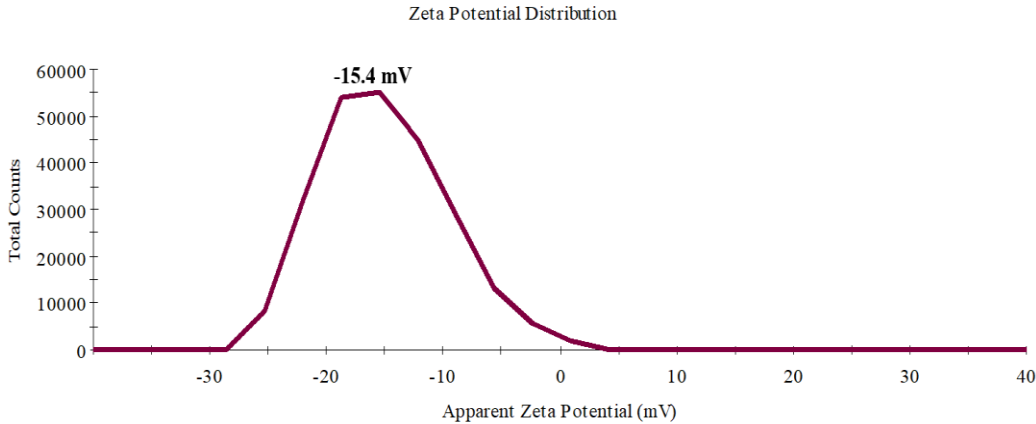
Record 8: MgO nanoparticle with 5ml A. blitium extract

Appendix D6: Particle size distribution and zeta potential of sample GC (green synthesized)

Size Distribution by Number
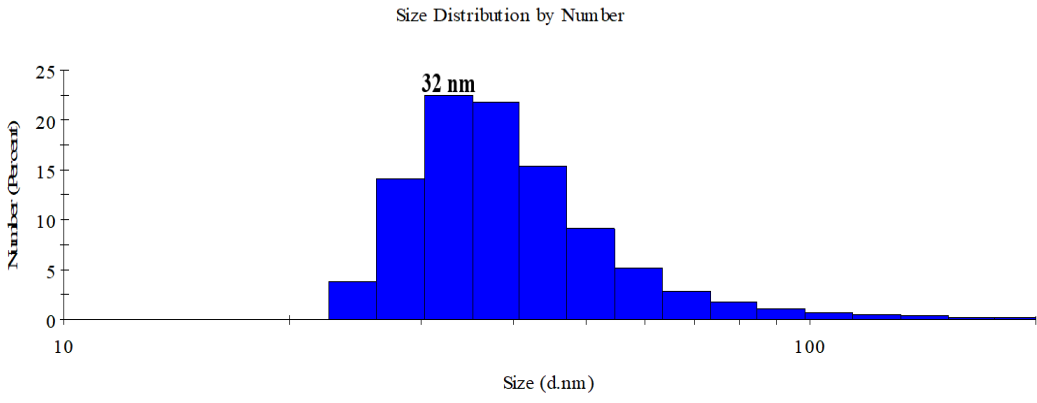
Record 7: MgO nanoparticle with 10ml A. paniculata extract

Zeta Potential Distribution
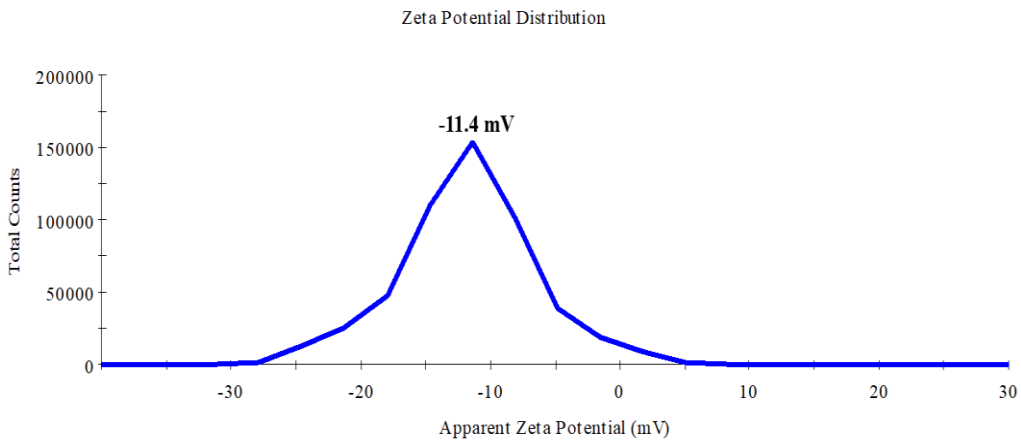
Record 15: MgO nanoparticle with 10ml A. paniculata extract

Appendix E:

Appendix E1: Percentage of viable cells at different dosages of chemical synthesized MgO nanoparticle treatment

Dosages (µl/ml)	% Cell viability Sample A	% Cell viability Sample B	% Cell viability Sample C
Control	100	100	100
200	64.13	61.47	53.07
400	56.96	54.71	45.69
600	49.38	48.15	38.93
800	37.09	43.85	32.17
1000	28.27	39.75	22.13

Appendix E2: Percentage of viable cells after different dosages of nanoparticle treatment

Concentration (µl/ml)	% Cell viability Sample GA	% Cell viability Sample GB	% Cell viability Sample GC
Control	100	100	100
200	71.72	67.97	61.73
400	66.19	61.81	54.54
600	55.39	50.44	49.19
800	42.99	43.57	40.69
1000	30.68	31.08	31.31

Table E3: Comparative percentage viability of 3T3-L1 and VERO cells after MgO nanoparticles treatment

Dosage (µl/ml)	% 3T3-L1 cell viability Sample B	% VERO cell viability Sample B	% 3T3-L1 cell viability Sample GA	% VERO cell viability Sample GA
Control	100	100	100	100
200	61.47	77.52	71.72	99.64
400	54.71	70.96	66.19	93.08
600	48.15	62.54	55.39	86.62
800	43.85	57.93	42.99	78.26
1000	39.75	54.61	30.68	74.45

Appendix E4: Raw data of Concentration of extra and intracellular glucose sampled periodically during incubation.

S.No.	Samples	0th hr OD	Conc (mg)	5th hr OD	Conc (mg)	10th hr OD	Conc (mg)	15th hr OD	Conc (mg)	20th hr OD	Conc (mg)	25th hr (In medium) OD	Conc (mg)	25 hr (Inside cell) OD	Conc (mg)
1	Control	1.970	3.70	1.744	3.50	1.694	3.40	1.628	3.30	1.558	3.20	0.297	0.70	0.043	0.68
2	Control	1.828	3.65	1.702	3.45	1.635	3.30	1.588	3.20	1.492	2.95	0.121	0.45	0.047	0.75
3	Sample GA (600 µl/ml)	1.974	3.70	1.410	2.70	1.363	2.60	1.315	2.50	1.243	2.30	0.018	0.09	0.016	0.16
4	Sample GA (600 µl/ml)	1.826	3.65	1.740	3.50	1.701	3.40	1.644	3.35	1.599	3.20	0.021	0.09	0.018	0.18
5	Sample B (400 µl/ml)	1.978	3.70	1.363	2.65	1.345	2.55	1.319	2.50	1.255	2.35	0.009	0.04	0.018	0.19
6	Sample B (400 µl/ml)	1.823	3.65	1.394	2.70	1.362	2.60	1.337	2.55	1.298	2.45	0.008	0.04	0.015	0.14

Appendix F: Copyright

Appendix F1. Copyright from Current Pharmaceutical Biotechnology journal

Copyright
Clearance
Center

Note: Copyright.com supplies permissions but not the copyrighted content itself.

1	2	3
PAYMENT	REVIEW	CONFIRMATION

Step 3: Order Confirmation

Thank you for your order! A confirmation for your order will be sent to your account email address. If you have questions about your order, you can call us 24 hrs/day, M-F at +1.855.239.3415 Toll Free, or write to us at info@copyright.com. This is not an invoice.

Confirmation Number: 11681691
Order Date: 11/16/2017

If you paid by credit card, your order will be finalized and your card will be charged within 24 hours. If you choose to be invoiced, you can change or cancel your order until the invoice is generated.

Payment Information

Jaison Jeevanandam
jaison.jeevanandam@postgrad.curtin.edu.my
+91 601125073546
Payment Method: n/a

Order Details

Current pharmaceutical biotechnology

Order detail ID:	70793709
Order License Id:	4230610671989
ISSN:	1389-2010
Publication Type:	e-Journal
Volume:	
Issue:	
Start page:	
Publisher:	Bentham Science Publishers Ltd.

Permission Status: ✓ Granted

Permission type:	Republish or display content
Type of use:	Thesis/Dissertation

Requestor type	Author of requested content
Format	Print, Electronic
Portion	chapter/article
The requesting person/organization	Jaison Jeevanandam/Curtin University
Title or numeric reference of the portion(s)	Chapter 1 and chapter 2. Figure 1.1.
Title of the article or chapter the portion is from	Introduction and Literature review
Editor of portion(s)	Jaison Jeevanandam
Author of portion(s)	Jaison Jeevanandam

Appendix F2. Copyright from ChemBioEng Reviews journal

Curtin University
Malaysia

JAISON JEEVANANDAM <jaison.jeevanandam@postgrad.curtin.edu.my>

Regarding copyright to reuse a manuscript in thesis

Rights DE <RIGHTS-and-LICENCES@wiley-vch.de>   Thu, Nov 16, 2017 at 5:59 PM
To: "jaison.jeevanandam@postgrad.curtin.edu.my" <jaison.jeevanandam@postgrad.curtin.edu.my>

Dear J. Jaison,

We hereby grant permission for the requested use expected that due credit is given to the original source.

If material appears within our work with credit to another source, authorisation from that source must be obtained.

Credit must include the following components:

- Journals: Author(s) Name(s): Title of the Article. Name of the Journal. Publication year. Volume. Page(s). Copyright Wiley-VCH Verlag GmbH & Co. KGaA. Reproduced with permission.

If you also wish to publish your thesis in electronic format, you may use the article according to the Copyright transfer agreement:

3. Final Published Version.

Wiley-VCH hereby licenses back to the Contributor the following rights with respect to the final published version of the Contribution:

a. [...]

b. Re-use in other publications. The right to re-use the final Contribution or parts thereof for any publication authored or edited by the Contributor (excluding journal articles) where such re-used material constitutes less

than half of the total material in such publication. In such case, any modifications should be accurately noted.

Kind regards

Bettina Loycke

Senior Rights Manager

Rights & Licenses

Appendix F3. Copyright from New Journal of Chemistry

Curtin University
Malaysia

JAISON JEEVANANDAM <jaison.jeevanandam@postgrad.curtin.edu.my>

Regarding copyright to reuse a manuscript in thesis

CONTRACTS-COPYRIGHT (shared) <Contracts-Copyright@rsc.org>   Fri, Nov 17, 2017 at 4:12 PM
To: JAISON JEEVANANDAM <jaison.jeevanandam@postgrad.curtin.edu.my>

Dear Jaison

The Royal Society of Chemistry (RSC) hereby grants permission for the use of your paper(s) specified below in the printed and microfilm version of your thesis. You may also make available the PDF version of your paper(s) that the RSC sent to the corresponding author(s) of your paper(s) upon publication of the paper(s) in the following ways: in your thesis via any website that your university may have for the deposition of theses, via your university's Intranet or via your own personal website. We are however unable to grant you permission to include the PDF version of the paper(s) on its own in your institutional repository. The Royal Society of Chemistry is a signatory to the STM Guidelines on Permissions (available on request).

Please note that if the material specified below or any part of it appears with credit or acknowledgement to a third party then you must also secure permission from that third party before reproducing that material.

Please ensure that the thesis states the following:

Reproduced by permission of The Royal Society of Chemistry

and include a link to the paper on the Royal Society of Chemistry's website.

Please ensure that your co-authors are aware that you are including the paper in your thesis.

Regards

Gill Cockhead

Publishing Contracts & Copyright Executive

Gill Cockhead

Publishing Contracts & Copyright Executive

Royal Society of Chemistry,

Thomas Graham House,

Science Park, Milton Road,

Cambridge, CB4 0WF, UK

Tel +44 (0) 1223 432134

Appendix F4. Copyright from Chemistry select